The Dissertation Committee for Manish Saggar

certifies that this is the approved version of the following dissertation:

Computational Analysis of Meditation

Committee:

Risto Miikkulainen, Supervisor

Clifford D. Saron, Co-Supervisor

David M. Schnyer

Dana H. Ballard

Pradeep Ravikumar

Computational Analysis of Meditation

by

Manish Saggar, B.Tech., M.S.

Dissertation

Presented to the Faculty of the Graduate School of

The University of Texas at Austin

in Partial Fulfillment

of the Requirements

for the Degree of

Doctor of Philosophy

The University of Texas at Austin

August 2011

To my Gurus.

Acknowledgments

I owe my deepest gratitude to my advisors: Risto Miikkulainen and Clifford D. Saron, without their guidance, support, and patience this dissertation would not have been possible. They have always showed tremendous interest in my research and helped me bring out the best in my work. I would also like to thank my dissertation committee members: David M. Schnyer, Dana H. Ballard, and Pradeep Ravikumar, for all their time and effort. Their thoughtful feedback and unique perspectives enriched this dissertation.

I am thankful to the Shamatha Project team for the experimental implementation, data collection and analysis, and support; with special attention to those who collected the EEG data: Stephen Aichele, David Bridwell, Tonya Jacobs, Brandon King, Katherine MacLean, and Anthony Zanesco.

I am forever indebted to my parents who always encouraged me to settle for nothing but the best, to my brother who epitomizes determination and taught me persistence, and to my colleagues who kept me sane all these years.

The most special thanks to my wife, Megha, for all her sacrifices, unrelenting understanding, selfless love, encouragement, and companionship throughout this journey. This dissertation is as much hers as it is mine.

Finally and most of all, I thank my spiritual teacher, H. H. Sant Rajinder Singh, who has been the greatest role model and source of inspiration throughout my life.

This research was supported by Francisco J. Varela Research Award (Mind and Life Institute), Fetzer Institute grant (#2191), and NIH 1R01 MH089626-01 grant. Data

collection and non-EEG analysis was supported by Fetzer Institute grant (#2191) and gifts from the Hershey Family, Tan Teo, Baumann, Yoga Research and Education, Mental Insight Foundations, the Santa Barbara Institute for Consciousness Studies, Grant Couch and Louise Pearson, Carolyn Zecca-Ferris, and other individual and anonymous donors, all to Clifford D. Saron; a National Science Foundation predoctoral fellowship to Katherine MacLean; and a postdoctoral fellowship from the Social Sciences and Humanities Research Council of Canada to Baljinder Sahdra.

MANISH SAGGAR

The University of Texas at Austin

August 2011

Computational Analysis of Meditation

Publication No. _____

Manish Saggar, Ph.D.
The University of Texas at Austin, 2011

Supervisor: Risto Miikkulainen
Co-supervisor: Clifford D. Saron

Meditation training has been shown to improve attention and emotion regulation. However, the mechanisms responsible for these effects are largely unknown. In order to make further progress, a rigorous interdisciplinary approach that combines both empirical and theoretical experiments is required.

This dissertation uses such an approach to analyze electroencephalogram (EEG) data collected during two three-month long intensive meditation retreats in four steps. First, novel tools were developed for preprocessing the EEG data. These tools helped remove ocular artifacts, muscular artifacts, and interference from power lines in a semi-automatic fashion.

Second, in order to identify the cortical correlates of meditation, longitudinal changes in the cortical activity were measured using spectral analysis. Three main longitudinal changes were observed in the retreat participants: (1) reduced individual alpha frequency after training, similar reduction has been consistently found in experienced meditators; (2) reduced alpha-band power in the midline frontal region, which correlated with improved vigilance performance; and (3) reduced beta-band power in the parietal-occipital regions,

which correlated with daily time spent in meditation and enhanced self-reported psychological well-being.

Third, a formal computational model was developed to provide a concrete and testable theory about the underlying mechanisms. Four theoretical experiments were run, which showed, (1) reduced intrathalamic gain after training, suggesting enhanced alertness; (2) increased cortico-thalamic delay, which strongly correlated with the reduction in individual alpha frequency (found during spectral analysis); (3) reduction in intrathalamic gain provided increased stability to the brain; and (4) anterior-posterior division in the modeled reticular nucleus of the thalamus (TRN) layer and increased connectivity in the posterior region of TRN after training.

Fourth, correlation analysis was performed to ground the changes in cortical activity and model parameters into changes in behavior and self-reported psychological functions.

Through these four steps, a concrete theory of the mechanisms underlying focused-attention meditation was constructed. This theory provides both mechanistic and teleological reasoning behind the changes observed during meditation training. The theory further leads to several predictions, including the possibility that customized meditation techniques can be used to treat patients suffering from neurodevelopmental disorders and epilepsy. Lastly, the dissertation attempts to link the theory to the long-held views that meditation improves awareness, attention, stability, and psychological well-being.

Contents

List of Tables

List of Figures

Chapter 1

Introduction

Imagine being asked to "think of nothing" for two minutes, or yet more difficult, imagine being asked "not to think of a pink elephant" for two minutes. Both of these tasks might appear simple at first, but they are actually dauntingly difficult. Cognitive control of thought, attention, and emotion is a challenging problem. It is, however, an important one. Understanding the neural dynamics of such control can provide insight into the cognitive system as a whole. Further, studies on several neurodevelopmental disorders (e.g., ADHD (Vaidya et al., 2005), autism (Dichter and Belger, 2007), and schizophrenia (Lesh et al., 2010)) suggest that alterations to the networks underlying cognitive control contribute to the behavioral symptoms.

Broadly speaking, cognitive (or executive) control refers to the ability to process task-related information despite distractions (O'Reilly et al., 2010). For example, when reading a lengthy technical article, one has to exercise cognitive control to keep processing the information in the article while keeping the distractions, such as time pressure, anxiety, environmental noise, boredom, etc., at bay. More demanding examples include situations where an operator of a nuclear power plant (or a pilot of an airplane) must attend and respond to continuous regular stimuli while concurrently looking for warnings or threats, and take appropriate action when such threats arise. Thus, in order to perform both day-to-

day activities and complex tasks, cognitive control is essential.

Starting from the color-naming task (Stroop, 1935), remarkable progress has been made in understanding cognitive control by breaking it into components and analyzing them separately (Posner, 2004; Verbruggen and Logan, 2008; Posner and Cohen, 1984; Posner and Petersen, 1990; Posner and Fan, 2005; Robertson et al., 1997). Typically such components include response inhibition, attentional bias, performance/conflict monitoring, response priming, task shifting/setting, working memory maintenance and update, and supervising through attention (Cooper, 2010). However, the following issues need to be addressed to push this research forward: (1) How do these individual components emerge or recess during a task, and more importantly, how do they interact and influence each other?; (2) How can such control abilities be improved in healthy populations, and more crucially, how can they be recovered in patient populations?; and (3) How can cognitive control theories formulated in limited lab settings be applied to real-world situations?

One potentially powerful way to approach these issues is to study meditation. Meditation involves regulation of thought, attention, and emotion (Cahn and Polich, 2006; Slagter et al., 2011). Typically, such regulation is made possible by focusing one's attention on an object or a phenomenon. Repeated practice of focusing attention on a chosen object has been shown to improve cognitive control components, for example, to improve inhibition of undesired responses (Sahdra et al., 2011), enrich perceptual discrimination (MacLean et al., 2010), enhance sustained attention (MacLean et al., 2010), increase attentional stability (Lutz et al., 2009; MacLean et al., 2010), improve handling of brain resources (Slagter et al., 2007), and so on. Further, sustained attention during meditation involves interaction among several control components (such as response inhibition, performance monitoring, task setting, and a supervising attentional system; Lutz et al. (2006)). Thus, understanding the mechanisms underlying meditation can dramatically further our knowledge of cognitive control, since it (1) involves interaction among several control functions, (2) alters high-level cognitive processes for enhanced cognitive control, and (3)

provides not just state but also trait changes in behavior (Cahn and Polich, 2006).

How does meditation affect the brain? In the last 55 years or so, this question has been asked several hundred times (Cahn and Polich, 2006). Various neuroimaging modalities have been used to answer it, ranging from EEG (e.g., Cahn and Polich, 2006; Anand et al., 1961; Wallace, 1970; Banquet, 1973; Lutz et al., 2004; Aftanas and Golosheikin, 2003; Cahn et al., 2010), fMRI (e.g., Lazar et al., 2000; Khushu et al., 2000; Short et al., 2010; Raffone et al., 2007; Brefczynski-Lewis et al., 2007; Ritskes et al., 2004), PET (e.g., Herzog et al., 1990; Lou et al., 1999; Kjaer et al., 2002), SPECT (e.g., Newberg et al., 2001; Khalsa and Newberg, 2007), and others. Several different tasks have also been used in these studies, e.g., attentional blink (Slagter et al., 2007), sustained attention (MacLean et al., 2010), and response inhibition (Sahdra et al., 2011). Numerous different meditation techniques have been evaluated, such as, Kriya Yoga (Das and Gastaut, 1955), Raj Yoga (Anand et al., 1961), Zen (e.g., Kasamatsu and Hirai, 1966; Ritskes et al., 2004; Austin, 1999), Transcendental Meditation (e.g., Travis and Wallace, 1999; Travis, 1991; Pagano et al., 1983), Tibetan Buddhist (e.g., Lutz et al., 2004; Lehmann et al., 2001; Raffone et al., 2007; Benson et al., 1990; Kabat-Zinn, 1993) and many others (see Cahn and Polich, 2006, for details). Yet, we still know very little about how practicing meditation enhances attention and emotion regulation. This lack of understanding can be attributed to the huge variability in results.

Three main factors can be held responsible for such variance: (1) multiplicity of meditation techniques that have been assessed; (2) lack of matched control groups to compare the data with; and (3) use of relatively less sophisticated methods for measuring brain activation. Presently, there is some evidence of heightened activation in attention-related cortical areas (Cahn and Polich, 2006). Recent studies have advanced the field using high density EEG (e.g., Lutz et al., 2004) and fMRI (e.g., Brefczynski-Lewis et al., 2007; Farb et al., 2007) with well-characterized practices, expert practitioners, and modern methods. These studies, however, did not examine changes longitudinally nor used control partici-

pants matched to those who had undergone training. Further, in neuroimaging studies, the regions found to be active during meditation were also active during many other psychological tasks. Thus, by just knowing which areas are active it is not possible to understand how the involved networks manifest, evolve, and interact during meditation. None of the previous work focused on formalizing a theory of meditation either. Instead, theories were limited to verbal formulations that form a weak base for future research and applications. Further, a formal theory could also help in generalizing the results (from previous work) and in turn reducing the variability in findings.

Thus, this dissertation aims to understand the mechanisms underlying meditation using rigorous empirical and theoretical experiments. The meditation technique analyzed was focused-attention meditation (or $\acute{s}amatha$), where participants attend, primarily, to breath sensations. The EEG data was collected as part of a larger project (the Shamatha project; Shamatha-Project, 2007), during two three-month retreats in a randomized wait-list design using matched control and training groups that examined both trait and state variables during intensive practice of focused-attention meditation (MacLean et al., 2010; Sahdra et al., 2011; Jacobs et al., 2010; Shamatha-Project, 2007). Chapter 2 provides background knowledge about the Shamatha project along with other key concepts.

The research consists of four steps. First, blind source separation methods were used to pre-process the EEG data. A novel semi-automatic tool was constructed for identifying and removing noisy sources. Further, other advanced signal processing steps, such as scalp current density estimation, were implemented to assure high quality and high signal-to-noise ratio in the EEG data. Chapter 3 presents this approach in detail.

Second, to identify the cortical correlates of intensive meditation training, longitudinal changes in cortical activity were analyzed using spectral analysis. This empirical approach provides a unique opportunity to understand how the networks underlying meditation change with training. Such an understanding has applications in a wide range of research areas, from building better brain-computer interaction systems to treating neu-

rodevelopmental disorders. Chapter 4 presents the methods of that analysis, along with results. Briefly, three main longitudinal changes were observed in the retreat participants; no such change was observed in the control group: (1) reduced individual alpha frequency after training, similar reduction is consistently found in experienced meditators (Cahn and Polich, 2006); (2) reduced alpha-band power in the midline frontal region, which correlated with improved vigilance performance; and (3) reduced beta-band power in the parietal-occipital regions, which correlated with daily time spent in meditation and enhanced self-reported psychological well-being.

Third, to understand the changes observed in cortical activity and to develop a theoretical account for them, computational modeling was employed. Modeling is a powerful tool in cognitive science for three reasons: It makes it possible (1) to compare and evaluate existing verbal theories; (2) to make novel predictions; and (3) to generate highly detailed simulations of human performance. Further, these simulations occur over time, and hence, provide the opportunity to understand the dynamics of the hypothesized underlying processes, which is currently impossible to do otherwise. Previously, modeling has been successfully applied to many other cognitive processes ranging from single-neuron modeling and sensory processing (e.g., Hodgkin and Huxley, 1952; Neilson and Neilson, 1987), to memory and learning (e.g., Chklovskii et al., 2004; Saggar et al., 2007, 2010; Moll and Miikkulainen, 1997; O'Reilly et al., 1999), language (e.g., Miikkulainen, 1993; Koskenniemi, 1984), and even to visual attention and consciousness (e.g., Itti and Koch, 2001; Tsotsos, 1995; Crick and Koch, 2003). Chapter 5 presents the model architecture and the results from four computational experiments. Briefly, these experiments showed, (1) reduced intrathalamic gain after training, suggesting enhanced alertness (Steriade, 2000); (2) increased corticothalamic delay, which strongly correlated with the reduction in individual alpha frequency (found during spectral analysis); (3) reduction in intrathalamic gain provided increased stability to the brain; and (4) anterior-posterior division in the TRN layer and increased connectivity in the posterior region of TRN after training.

Fourth, in order to test the efficacy of time-series analysis and modeling, the results from these approaches were correlated with the data recorded from other behavioral measures and self-reported psychological functions. These correlations provide twofold benefits: (1) They help ground the findings into trait changes in behavior, and (2) They help understand the cortical changes observed during training. The relations that were found, during this analysis, are presented in chapters 4 and 5.

The discussion, Chapter 6, connects the dots and provides a theoretical account for the mechanisms underlying focused-attention meditation. It also links these empirical and theoretical results with the long-held views that meditation improves awareness, attention, stability, and psychological well-being. In the end, the chapter discusses broader implications of this work, for example, in medicine, by creating customized meditations for treating patients with neurodevelopmental disorders and epilepsy.

Thus, using a tight interaction between empirical and theoretical approaches, the dissertation formalizes the verbal descriptions of meditation effects and makes testable predictions, forming a foundation for future research and applications in the area of meditation research.

Chapter 2

Background

In this chapter, a brief introduction to the key concepts and techniques is provided, including meditation, neuroimaging, data acquisition, time-series analysis, and computational modeling. Each section also provides advantages and limitations of each technique.

2.1 Meditation

The term meditation refers to a broad variety of practices, ranging from health exercises to exercises that are performed for achieving a heightened sense of wellbeing (Davidson and Lutz, 2008). In Buddhist traditions, two fundamental kinds of meditation practices exist: focused-attention and insight meditation (Lutz et al., 2006).

The focused-attention meditation is more widely-practiced and is aimed at improving concentration, such that ultimately the meditator can focus on an object or a phenomenon for an unlimited amount of time (a.k.a. the state of $\acute{s}amatha$) (Lutz et al., 2006; Wallace, 2006). From the Buddhist point of view, in focused-attention meditation, the practitioner uses two faculties of mind - $smr\underline{i}ti$ (to keep focused on the intended object) and $samprajanya$ (to check whether the focus is maintained or not). Thus, the second faculty provides the role of meta-awareness (Lutz et al., 2006; Wallace, 1999, 2006). Figure

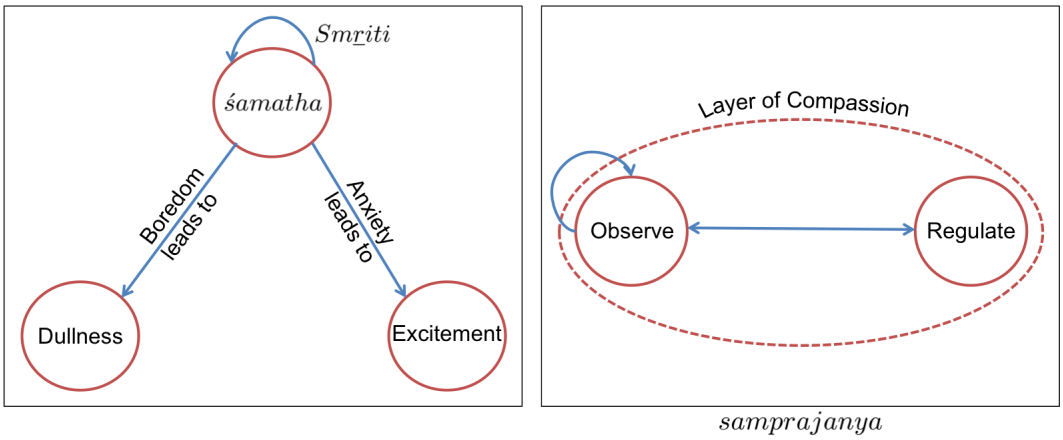

Figure 2.1: The two faculties involved in meditation. (a) $Smṛiti$, literally means 'memory' in Sanskrit, is the faculty of mind that allows a continuous focus on an object or a phenomenon (a.k.a. the state of $śamatha$). To continue focusing on the object, one needs stability (i.e. avoiding anxiety that leads to excitement) and clarity (i.e. avoiding boredom that leads to dullness) (Wallace, 2006). (b) $Samprajanya$ is the faculty of meta-awareness (Wallace, 2006; Lutz et al., 2006). It checks to make sure that the focus is on the object (of meditation), and if not, it regulates the focus to bring it back upon the object. It is important to note that there is also a layer of compassion, shown here as engulfing the $samprajanya$, which makes sure that one is compassionate towards himself or herself when a distraction (dullness or excitement) is detected. This layer of compassion is crucial, since it makes sure that the meta-awareness itself does not become source of distraction (as one berates himself or herself due to mind wandering, especially in beginners; Kabat-Zinn, 1994).

2.1 visualizes the relationship of these two faculties and Figure 2.2 shows the interaction between the faculties during focused-attention meditation. Additionally, in Buddhist traditions, cultivation of compassion towards all living beings (including oneself) is given equal importance as in all other styles of meditation. Compassion meditation provides the emotional balance, which in turn helps bypass several other obstacles in achieving focused attention (Wallace, 2006).

The second fundamental type of Buddhist practice is insight meditation (or more commonly, $vipaśyanā$). In this practice, the practitioner works on the meta-awareness (or $samprajanya$) and the goal is to reach a state of reflexive awareness, i.e. beyond objectivity and subjectivity (Lutz et al., 2006). It is believed that the practitioners need a

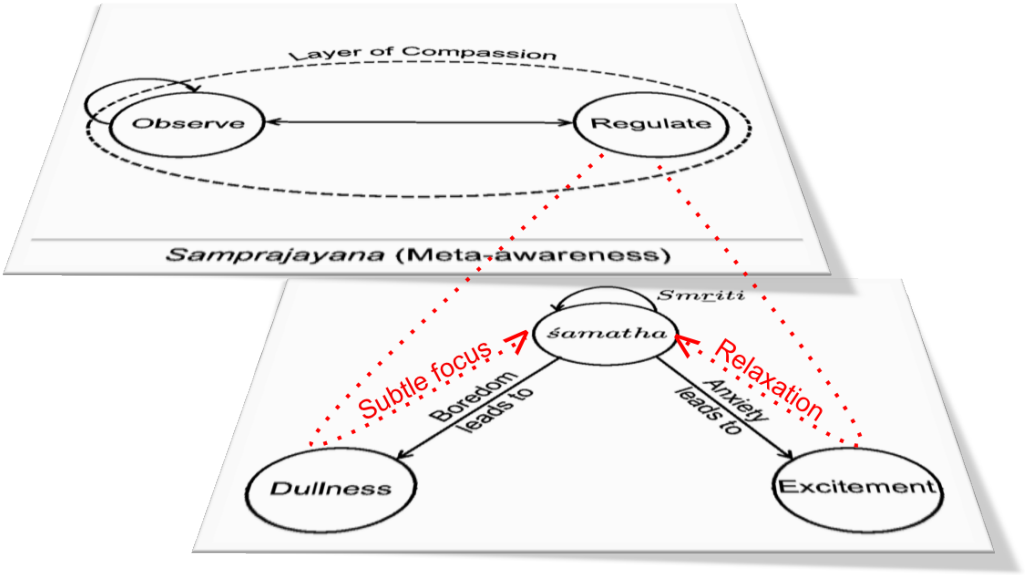

Figure 2.2: Interaction between faculties during focused-attention meditation. $Samprajanya$, or meta-awareness, constantly monitors whether the $smṛiti$ is focussed on the object of meditation or not. If any distraction is detected, the attention can be regulated to bring it back on the object of meditation. For example, as described in Wallace (2006), if dullness is detected then one should try to focus on even subtler objects. This increase in task difficulty, could lead one back to $śamatha$. Similarly, if excitement is detected then one can try relaxing for a while and begin again. Both clarity (less dullness) and stability (less excitement) are required for progress in meditation (Wallace, 2006).

unison between $vipaśyanā$ and $śamatha$ in order to progress further (Lutz et al., 2006).

Apart from these two fundamental types of practices, ethical discipline is also deemed essential in Buddhist traditions. Over the course of meditation training, the idea is to develop strong ethical foundations to be able to distinguish between wholesome and unwholesome momentary mental states (and processes), so that unwholesome states can be avoided (Wallace, 2006; Olendzki, 2011).

Although meditation is often described in mystic terms, its effects are real and

can be studied scientifically (Slagter et al., 2011; Jacobs et al., 2010; Sahdra et al., 2011; MacLean et al., 2010). Various kinds of meditation techniques help the practitioner to regulate attention, impulses, and emotions (Chambers et al., 2009). Further, practicing meditation has been shown to enhance one or more cognitive control components. Thus, meditation provides a fascinating window into cognitive functioning as a whole, and into cognitive control in particular. Keeping these applications of meditation in mind, this dissertation applies a quantitative approach to focused-attention meditation in order to understand how the brain and its processes change during intensive meditation training.

2.2 Methods of neuroimaging

Neuroimaging consists of various direct or indirect methods that are used to measure structural, functional, or pharmacological aspects of the brain. The field can be divided into two broad categories: structural and functional imaging. Structural neuroimaging provides an anatomical view of the brain with ways to measure volume of different brain regions. It is used to diagnose gross intracranial diseases, like tumors and injury, as well as to characterize development, individual variability in brain structures, and to provide anatomical anchors for other functional brain measures. Functional imaging, on the other hand, provides a way to visualize how information is processed in different brain areas during a particular task (or in the absence of a task, e.g. "default state"). Such processing causes the involved areas to increase metabolism and "light up" (i.e., activate) in the image.

There are several modalities of neuroimaging, among which a choice can be made based on the experimental question at hand (Figure 2.3). A brief introduction to the most relevant methods is given below.

2.2.1 Electroencephalography (EEG)

EEG is the recording of electrical activity at the scalp produced by synchronized firing of cortical neurons (Pizzagalli, 2007). It measures the difference between the potential at the

Method	Measures	Advantages	Limitations
EEG	Neuronal source currents	Temporal resolution Sensitive to deep sources Low cost	Sensitive to artifacts Inverse problem not unique
MEG	Neuronal source currents	Temporal resolution	Blind to radial dipoles Inverse problem not unique
PET	Blood flow metabolism Receptor density	Measures physiological parameters	Radiation Low temporal resolution High cost
fMRI	Blood oxygenation Blood flow Blood volume	Excellent spatial resolution	Temporal resolution limited by hemodynamic response
SPECT	Blood flow Receptor density	Sensitive to picomole concentrations	Poor spatial and temporal resolution
NIRS	Local concentration of oxy- and de-oxygenated hemoglobin	Measures both oxy- and de-oxygenated hemoglobin Higher temporal resolution	Limited to superficial cortex

Figure 2.3: Comparison between different types of neuroimaging techniques. There is no single best method. Thus, one should choose a technique that can most accurately answer the experimental question at hand. For this dissertation high temporal resolution was important and hence EEG was chosen.

location of interest (sensor) and at a reference point. By measuring the electrical activity of neural assemblies with sub-millisecond temporal resolution, EEG offers the possibility of studying brain functions in real time (Pizzagalli, 2007). On the other hand, the spatial resolution provided by EEG is limited; due to volume conduction, low signal-to-noise ratio, and limited spatial sampling (number of electrodes). These factors, however, can be mitigated (to some extent) by sound physiological and anatomical assumptions and by utilizing laws of electrodynamics (Baillet et al., 2001; Michel et al., 2004).

2.2.2 Magnetoencephalography (MEG)

MEG measures the magnetic field produced by the electrical activity in the brain via extremely sensitive sensors such as superconducting quantum inference devices (SQUIDs). Thus, MEG provides a direct measurement of electrical activity of neural assemblies with high signal-to-noise ratio and temporal resolution. The spatial resolution of MEG was said to be better than EEG, however recent work has shown otherwise (Malmivuo and Suihko, 2004), and this aspect remains controversial.

2.2.3 Positron emission tomography (PET)

PET scans require an injection of a radioactive material in to the participant. Although no surgery is involved, PET is still considered an invasive procedure. The injected substance (a.k.a. tracers; e.g., FDG, O-15, etc.) collects in the neurons that are more active, and thus highlights areas of the brain that are used for a particular function under study. The greatest benefit of PET is that different compounds can show blood flow, oxygen, and glucose metabolism in the tissues of the working brain. In addition to its high cost and exposure to radiation, a third drawback with PET is that the resultanting scans do not include any anatomical information. Hence, PET needs to be combined with CAT or MRI scans to localize the activity (Davis, 2003). Another crucial drawback is that the radioactivity decays rapidly (in case of moderately expensive tracers), and as a result, the technique is limited to monitoring short tasks (Nilsson and Markowitsch, 1999).

2.2.4 Functional magnetic resonance imaging (fMRI)

The paramagnetic properties of oxy- and de-oxygenated hemoglobin is harnessed in fMRI to create images of change in blood flow. Such changes are then associated with the neural activity in the brain regions (Logothetis, 2008). This technique allows images to be generated that reflect the brain structures activated during performance of different functional tasks. The spatial resolution of fMRI is two-three millimeters, however its temporal reso-

lution is limited to the hemodynamic response (approximately two-five seconds). Further, a baseline state is required in the experimental design, so that the neural activity during a task can be measured (by subtracting the baseline activity from it).

2.2.5 Single photon emission computed tomography (SPECT)

SPECT is similar to PET and uses gamma emitting radioisotopes and a gamma camera to record the data. Like PET, an injection of radioactive tracer is given to the participant before scanning. The uptake of this agent is nearly 100% within 30-60 seconds. SPECT provides a snapshot of cerebral blood flow, but its resolution is not as good as that of fMRI (about one centimeter). One advantage of SPECT over PET is that it can make use of tracers with much longer half-lives (hence allowing longer experiments) and as a result it is more widely used than PET.

2.2.6 Near infrared spectroscopy (NIRS)

NIRS can measure changes in concentration of oxygenated and deoxygenated hemoglobin in the blood. The signal measured by NIRS is highly correlated with the BOLD signal measured in fMRI (Cui et al., 2010). The spatial resolution of NIRS, however, is limited and it can only measure changes related to the cerebral blood. However, the temporal resolution of NIRS is better than fMRI and is approximately at the rate of 10Hz.

The goal of this dissertation is to analyze and understand the dynamics behind meditation. A high temporal resolution is required to analyze the oscillatory dynamics and therefore, high-density EEG was chosen for this work.

2.3 The Shamatha project research setting

Over the past 55 years many studies have attempted to characterize the brain activity patterns that occur during meditation (Cahn and Polich, 2006). Such patterns may reflect the

effects of contemplative training that are ultimately expressed as characteristic changes in behavior. However, a large variability exists in the findings of these studies. There could be several reasons for this variability, including assessment of a large number of meditation techniques, lack of adequate controls matched to the experimental group of participants, and relative lack of sophisticated methods that results in an inability to generalize results across studies. The most reliable conclusion is best characterized as some evidence of activation in attention-related cortical areas (Cahn and Polich, 2006).

More recent studies have advanced the field using high density EEG (Lutz et al., 2004) and fMRI (Brefczynski-Lewis et al., 2007) with well characterized practices, expert practitioners, and modern methods. These studies, however, did not examine the changes longitudinally (with time) nor used the control participants matched to those who had undergone training.

In contrast, this dissertation aims to understand the longitudinal aspects of focused-attention meditation using sophisticated empirical and theoretical experiments, while controlling for group differences. Thus, the dissertation is based on a high-quality corpus of EEG data, collected during two three-month retreats using matched control and training groups. It was collected by a team of neuroscientists lead by Dr. Clifford Saron from UC Davis, over a period of nine months from 60 participants. This very large longitudinal study of meditation is also known as the Shamatha Project (Shamatha-Project, 2007). Dr. Alan Wallace initiated this project and was the meditation teacher for both the retreats. The Shamatha project was lead by a team of 16 members and 24 consulting scientists, and the data acquisition was completed in 2007. This longitudinal study will provide a unique opportunity to understand the temporal evolution of mechanisms underlying focused-attention meditation. Such an insight should prove useful for applying meditation to neurodevelopmental disorders in the future (as will be discussed in section 6.4).

Following subsections briefly discuss the design of the Shamatha project.

2.3.1 Participants

The participants in the Shamatha project were recruited by advertising in various Buddhist magazines (Figure 2.4). Sixty participants were selected (out of 142 applications) based on age, availability, medical and neuropsychiatric evaluation, and previous retreat experience. The participants were then matched and assigned to either an initial training group (n=30; RG1) or a waitlist control group (n=30; CG). The groups were matched on age (M = 48 years, range = 22-69), sex (28 men, 32 women), and years of meditation experience (M = 13). Additionally the groups did not differ in mean education level, marital status, or household income (see Shamatha-Project, 2007; MacLean et al., 2010; Sahdra et al., 2011; Jacobs et al., 2010 for more details). Retreat participants stayed at a remote mountain resort (Shambhala Mountain Center, CO) during the three months of training. Control group participants were flown to the retreat center, only for testing, during Retreat1, and later comprised as participants for Retreat2 (RG2). Thus, data from the control group in Retreat1 served as a control for retreat group in Retreat1, and as a control for themselves in Retreat2. This design provides an interesting set of comparisons, as shown in Figure 2.4. EEG from twenty-two participants in RG1, CG, and RG2 (same set of participants as in CG) was found usable and hence included in the dissertation. See Table 2.1 for details about the participants.

2.3.2 Training

The participants in this project practiced meditation under the guidance of Dr. Alan Wallace. The goal was to build strong ethical foundations in addition to improving the faculty of attention. Each participant practiced focused-attention meditation for 6 hours each day (on average) and compassion meditation for 1 hour each day (on average). The training was based on Buddhist teachings and constituted the following seven practices (Wallace, 2006): (1) focus on breath sensations, (2) observing mental events, (3) observing the nature of consciousness, (4) loving-kindness, (5) compassion, (6) empathetic joy, and (7) equa-

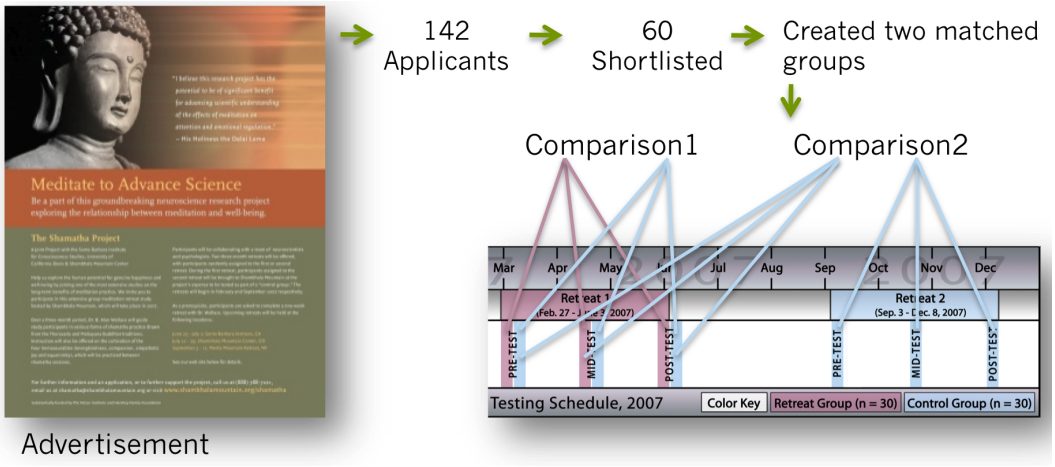

Figure 2.4: Recruitment of participants for the Shamatha project. The project had two three-month retreats. Thus, as shown above, there can be two major comparisons. First, a between-group comparison between control and retreat participants of Retreat1. Second, a within-subjects comparison for control group of Retreat1 and the same group when they were the retreat group in Retreat2. This design makes the second comparison strongly controlled, as the same group of people acts as controls for themselves.

nimity. Participants were encouraged to spend most of their time in practicing one or two of the first three techniques. These techniques were specifically designed to improve sustained attention and attention regulation. They were also asked to spend some time in the day on the remaining practices. These practices (4-7) were designed to generate positive and balanced aspirations for their own and others' well-being. In addition to practicing alone, participants spent two half-hour sessions with Dr. Wallace, as a group, for guided meditation. Table 2.1 provides details about number of hours spent in meditation daily.

2.3.3 Task

The participants were assessed on a number of self-report, cognitive and affective tasks, at three time points (beginning, middle, and end of the retreat). Additionally, the participants were assessed on two kinds of meditation techniques: focused-attention ($\acute{s}amatha$) and compassion meditation, on two different days. Focused-attention meditation involved

	Mean age (S.D.)	Gender	Lifetime meditation (in hrs.)		Daily time spent in meditation during retreat (in mins.)	
			Min	Max	Shamatha	Compassion
RG1	49.45 (13.49)	10 M, 12 F	250.00	9500.00	339.79 (87.35)	52.94 (24.15)
CG	44.18 (15.76)	11 M, 11 F	200.00	10000.00	-	-
RG2	44.18 (15.76)	11 M, 11 F	200.00	10000.00	319.82 (87.80)	61.20 (27.86)

Table 2.1: Description of participants in the Shamatha Project. The groups in Retreat1 (RG1 (n=22) and CG (n=22)) and Retreat2 (when CG becomes RG2) had similar age, division of gender, and lifetime hours of meditation. Further, on average, both retreat groups spent most of their daily time in Shamatha meditation (focusing primarily on breath sensations). The time spent in compassion meditation is the sum of compassion meditation itself and meditation on four immeasurables (4-7; see Wallace (2006) for more details about these meditation techniques).

attentional focus, primarily, on breath sensations (Wallace, 2006). During compassion meditation, participants imagined their loved ones, people who they had difficulties with, and all the others to be free from suffering and the causes of suffering (Wallace and Houshmand, 2004). This dissertation, however, focuses on the task where the participants practiced eyes-closed focused-attention meditation. In this task participants were asked to rest for one min both before and after the 12 minutes of focused-attention meditation. The audio instruction for resting state was, "For the next sixty seconds, please sit quietly with your eyes closed". For meditation, the audio instructions were

> During the next 12 minutes, engage in the practice of mindfulness of breathing, focusing your attention on the tactile sensations at the apertures of your nostrils or just above your upper lip. With each inhalation arouse your attention and focus clearly on these tactile sensations. With each out-breath continue to maintain your attention upon the tactical sensations, while relaxing your body and mind, releasing any involuntary thoughts that may arise. So in this way maintain an ongoing flow of mindfulness arousing with each in-breath, relaxing with each out-breath.

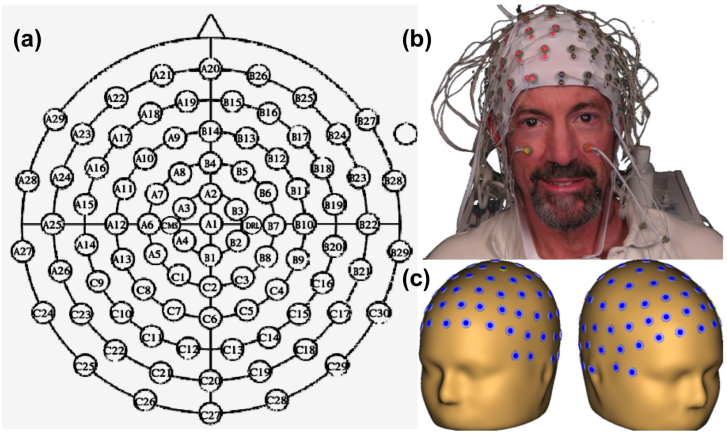

Figure 2.5: EEG montage and 3D locations of electrodes. (a) Eighty-eight channel montage of the EEG cap. (b) A subject during data collection, with the cap and polygraph channels hooked on. (c) The 3D digitized locations for scalp channels. This digitization was done separately before each recording. Such high-density electrode cap and 3D digitization will provide better source localization.

EEG was recorded during the entire session. Pre-meditation resting time will allow for the measurement of baseline brain activity.

2.3.4 Data

A high-density EEG cap was used in this project, with 88 equidistant scalp electrodes. The 3D locations of the electrodes on each participant was determined with a magnetic digitizer (Figure 2.5). The data was collected using the Biosemi Active2 system (BIOSEMI, 2006), at a sampling rate of 2,048 Hz. The sub-millisecond temporal resolution and the high-density electrode array provides a unique window to understand meditation.

2.4 Time-series analysis of oscillatory activity in the brain

A time series consists of a sequence of data points. Time-series analysis methods are employed to either understand the underlying generators or to make predictions about the

sequence. Such methods have been used widely in many domains, ranging from financial markets to brain data. This subsection will briefly review some of the commonly used approaches in brain imaging. Chapter 4 will describe those actually used in this dissertation in more detail.

2.4.1 Spectral analysis

The oscillatory activity in any time series can be represented using a linear sum of different sinusoidal waves with distinct frequencies and coefficients (Pizzagalli, 2007). Thus, the goal of spectral analysis is to estimate the contribution of various frequencies on the measured EEG data. The most common approach is to compute estimates of power (the square of amplitude) for a set of functionally mappable frequencies (e.g., alpha band 8-12 Hz). There are many issues that should be considered in this seemingly simple analysis. First, EEG is not a stationary signal for durations longer than 3.5 secs (Gasser and Molinari, 1996), thus the segments analyzed should be smaller than this limit. Second, due to low signal-to-noise ratio, averaging over such segments is essential. About 60 secs of total data should be used for reliable spectral analysis (Nuwer et al., 1999b). Third, convolution with the Hanning (or similar) taper should be used to avoid leakage at the beginning and at the end of each segment (Dumermuth and Molinari, 1987). Some of the advanced issues include taking into account individual differences in defining frequency bands (Klimesch, 1999), scalp current density estimation, and transforming data to approximate Gaussian distribution to get statistical power (Davidson et al., 2000). These are explained in more detail in later chapters (Chapters 3 and 4). The dissertation used spectral analysis to understand the longitudinal changes in cortical activity associated with meditation training (see Chapter 4).

2.4.2 Asymmetry metrics

Asymmetry metrics provide a possible method for analyzing hemispheric differences. Among many such approaches, the alpha-power asymmetry index has been the most commonly used (Pivik et al., 1993). This index is derived by subtracting natural logarithm of the left hemisphere alpha power from that of right hemisphere $(\ln\alpha_R - \ln\alpha_L)$. Because alpha-power is inversely correlated with activity (Pizzagalli, 2007), positive number on this index means low activity in the right hemisphere, and vice-versa. Several studies have previously examined the role of this metric to study emotion, motivation, and psychopathology (Coan and Allen, 2004). An important aspect of it is that laterality effect is legitimate only if *Group (or Condition)* x *Hemisphere* interaction is also significant (Davidson et al., 2000). The dissertation did not use this method, but in future it could be used to relate the findings from this work and data from EEG studies of emotion regulation in meditators.

2.4.3 Time-frequency analysis

Spectral and asymmetry analyses are important for many reasons, but they do not provide information on temporal changes in frequency. EEG is a dynamic phenomenon and it is therefore necessary to investigate its transient nature over time. Thus, various methods of time-frequency analysis have been developed. Two commonly used ones are (1) short-time Fourier transform (STFT) for computation of FFT-based time-dependent spectrum (or spectrogram); and (2) wavelet analysis, which allows more flexible temporal resolution based on the frequency under consideration. For example, for faster frequencies a smaller segment can be used as compared to slower frequencies (Samar et al., 1999). Time-frequency analysis is commonly used to understand the temporal evolution of frequencies before, during, and after a cognitive task. This information is useful in mapping changes in frequency of activation to cognitive processes. The dissertation did not use this method, since it requires a task with large number of trials for each condition.

2.4.4 Topographical analysis

EEG mapping, or topographical analysis, considers the value at each electrode and through interpolation, displays the field distribution of brain electric activity over the whole scalp (or its 2D projections). It considers all electrodes at once and provides a global picture of activation at the scalp. However, it does not provide any additional mathematical or experimental information about the generating sources underlying the scalp (Pizzagalli, 2007; Pivik et al., 1993). Nonetheless it is a very useful method to visualize the results and the dissertation used this method in association with a nonparametric cluster-based statistical approach to find longitudinal changes in cortical activity.

Altogether, time-series analysis provides a toolbox that can be used to understand various cortical dynamics measured on the scalp. However, one should choose approaches based on the particular hypothesis at hand. In this dissertation spectral and topographical mapping were used to identify cortical correlates of meditation training (see Chapter 4). These analyses provide critical information for building an accurate computational model, as will be discussed next.

2.5 Computational modeling of EEG data

Computational modeling based on physiological and anatomical assumptions can provide an important method for understanding the complexity of human brain and behavior (O'Reilly and Munakata, 2000). It is possible to explore the underlying mechanisms of complex phenomena by implementing, testing, and manipulating them on a computer, in order to ultimately understand them. This subsection will introduce some of the computational approaches used previously to model EEG data.

Since 1875, when Caton first discovered macroscopic brain potentials, much progress has been made in EEG recording and analysis (Pizzagalli, 2007). Currently, it is one of the most widely used technique in cognitive science to study the physiological correlates of sen-

sory processing, perception, and information processing in the brain (Handy, 2005; Luck, 2005). However, even after many years of progress, issues such as understanding the origins of EEG and how to optimally retrieve useful quantities from EEG are still unresolved. Recent advances in signal processing and computational modeling can provide solutions to these issues (Handy, 2009; Robinson et al., 2003). As a way of providing context for the current work, a brief overview of previous modeling approaches to EEG data is useful.

The modeling work of EEG data can be classified into three main categories: (1) phenomenological models; (2) neuron and network models; and (3) analytical models (Rennie, 2006). Phenomenological modeling describes the dynamics purely formally or mathematically, that is, the dynamics can be motivated biologically but are not explicitly stated in terms of physiological and anatomical details (Biswas and Guha, 2010; Isaksson et al., 1981). These models provide a straightforward approach of measuring the noticeable features in the data and correlating the findings with behavior. Examples from these models include estimation of latency in an event related potential (ERP) and its relation to other measures or behavior. However, the measured quantities are not based on physiology and anatomy and hence it is hard to construct a clear and formal account of the underlying mechanisms (Rennie, 2006).

Another approach is to model the activity of a single neuron or a network of neurons as a stepping stone to ultimately model data from EEGs. Notable attempts to model mesoscale neural networks include those of Traub et al. (1997); Wilson and Bower (1992); Lagerlund and Sharbrough (1989) and Lumer et al. (1997). The value of these models lies in expressing a reasonable amount of neuroanatomical and physiological detail. However, such detail comes at an expense of having to provide correct values for a myriad of parameters and could result in a combinatorial explosion while fitting.

The third approach to modeling EEG data is to use analytical models. The idea is to simulate a large-scale phenomena, without violating physiological and anatomical constraints of structure involved (Rennie, 2006). The basic approach is to develop a continuum

(or mean field) equation that describes the average properties of the system at hand. This approach is justified in that the diameter of each electrode in the EEG cap is several orders of magnitude larger than the single neuron and that the area of an electrode covers thousands of neurons (Baillet et al., 2001). In previous studies continuum models were used to show steady state and limit cycle behavior in visual cortex (Wilson and Cowan, 1972, 1973), to explain alpha rhythms (Lopes da Silva et al., 1974), to model olfactory tract (Freeman, 1972, 1987), and even to model 'global theory' of EEG (Nunez, 1974a,b).

Among the three approaches mentioned above, the analytical approach suits modeling meditation and resting state EEG the best. The starting point for the dissertation was therefore based on an analytical model, more specifically the one developed by Robinson et al. (2003). This model was further extended as presented in Chapter 5.

2.6 Conclusion

Altogether, a brief overview is provided about the concept of meditation, the Shamatha project, and the methods used for EEG analysis. But, before using EEG data for any analysis, preprocessing is essential. The next chapter describes the preprocessing process developed in this dissertation.

Chapter 3

Preprocessing

Data that captures the transient nature of brain activity is required to understand the dynamics of brain networks during focused-attention meditation. The 88-channel high-resolution EEG measurements, collected during the Shamatha project, provide such data. This chapter describes how this data was pre-processed for all the later analyses.

3.1 Motivation

Preprocessing is usually the first crucial step in analyzing any dataset. It includes several stages for preparing the data so that other analyses can be run on it. For any analysis to be successful, the data should be clean, i.e. it should originate purely from the neural sources. However, EEG signals are almost always contaminated by various sources of artifacts (signals that are not of neural or cerebral origin) and noise (Figure 3.1). Most common types of artifacts derive from subjects' muscular movements (EMG), eye blinks, heartbeat, and sweating. Further, channels can also get affected by non-biological sources of artifacts, like interference from power lines (50/60Hz), poor grounding, and poor electrode contact with the scalp. These biological and non-biological sources of non-neural activity need to be removed before any analysis can be run, so that precise inferences can be made about the

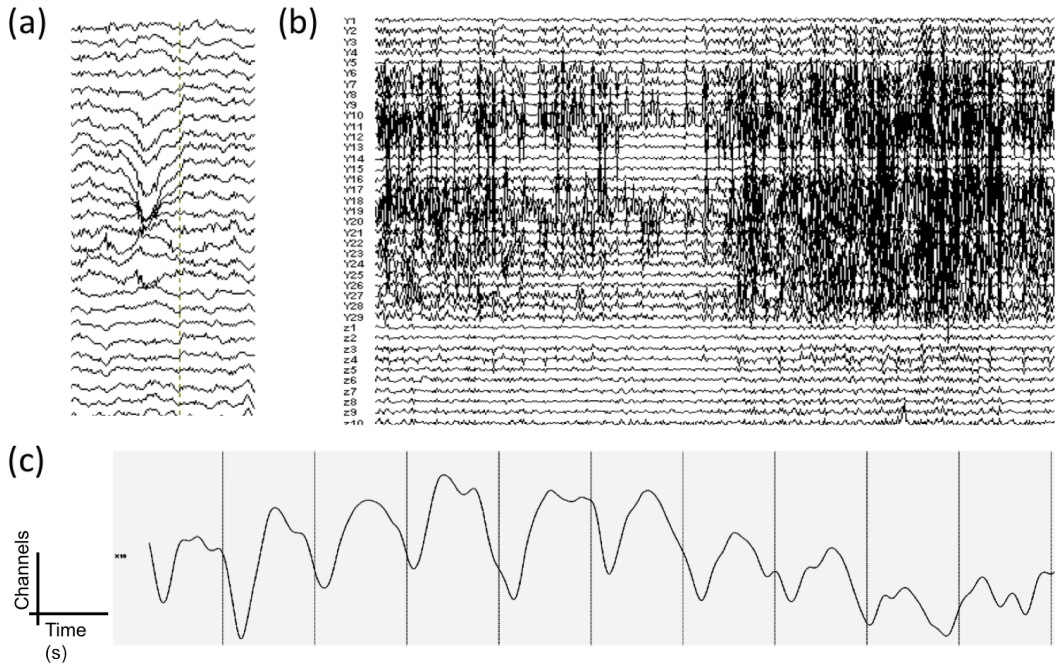

Figure 3.1: Artifacts in EEG data. Showing time on x-axis and different channels (as rows) on y-axis. (a) Ocular artifact due to eye blink resulted in huge dip in the activity (of frontal channels). (b) Muscular (EMG) artifact due to movements in face or other parts of body resulted in large amount of noise across a long period of time. (c) Heartbeat or ECG artifact oscillating at about 1Hz. The hardest artifact to identify and remove is EMG, mainly because the frequencies in EMG overlap significantly with cognitive range of frequencies in EEG. Thus, EMG can drastically confound the findings (Pizzagalli, 2007; Nunez and Srinivasan, 2010; McMenamin et al., 2010). Hence, the preprocessing phase is crucial and should be done rigorously before any analyses can be performed. In current work blind source separation is used to remove these artifacts.

data.

Traditionally, filtering and manual artifact correction and rejection is performed on the data in order to get rid of artifacts. However, there are three main disadvantages of this approach: (1) significant amount of data may get lost; (2) this process is very time consuming; and (3) the quality of preprocessing depends on the expertise of the operator. The first limitation can be overcome by using blind source separation (BSS) for separating sources

of activity. If the sources of artifact are removed, the neural data for those time points can be used (Makeig et al., 1996; Thakor and Tong, 2004; Joyce et al., 2004). However, the second and third limitations are still major issues for large data sets, since it can be quite laborious to identify artifact components correctly. Further, there is always a risk of misclassifying neural sources as artifacts and vice versa.

To counter such issues, a novel Semi-autoMated Artifact Removal Tool (SMART) was developed. This tool takes the already separated components from BSS and extracts features from each of these components to classify them as an artifact or a neural source. It then creates an interactive web page to show the results of the classification and lets the user overrule any classification. This novel integration of BSS and SMART provides the user an accurate and quick way to identify artifact sources. The methods section, next, explains this preprocessing pipeline in detail, starting from data acquisition all the way to scalp current density. It is followed by the results section, where the effects of preprocessing pipeline are shown on the raw data.

3.2 Methods

Starting from the raw EEG, a series of steps were developed to clean and prepare the data for later analyses (Figure 3.2). Following subsections provide details about each step.

3.2.1 Data Acquisition and filtering

The 88-channel EEG was acquired using BioSemi ActiveTwo system (BIOSEMI, 2006), during meditation and resting states, at a sampling rate of 2,048 Hz. The data was first filtered (zero-phase; roll-off: 12db for low-pass and 24db for high-pass), to allow only the 0.1 - 200 Hz frequencies. The filtering was followed by referencing to the average of all channels, to provide full common-mode rejection ratio (CMRR) and to avoid spatial bias. The next step was to use blind source separation for segregating artifactual and neuronal sources.

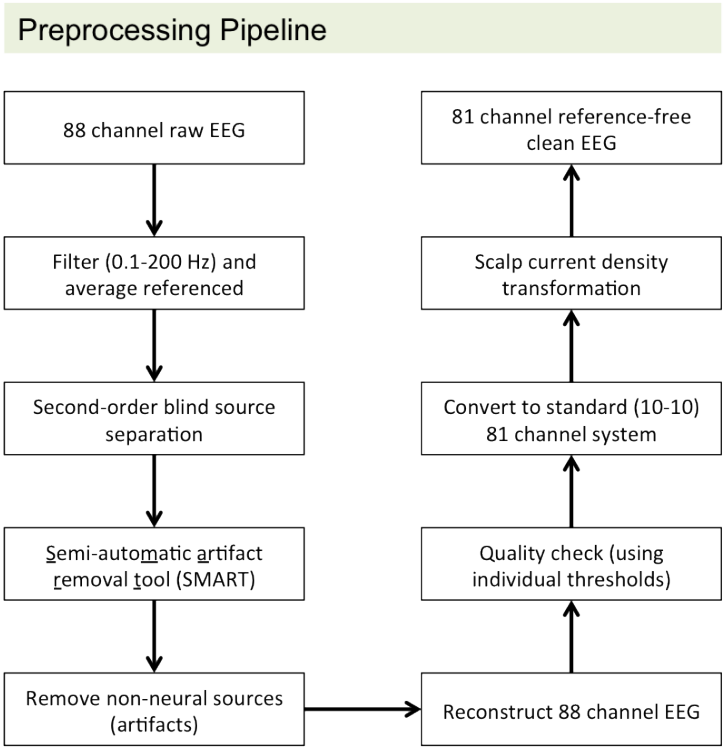

Figure 3.2: The preprocessing pipeline. The pipeline lists the steps, starting from 88-channel raw EEG all the way to 81-channel reference-free EEG, required for obtaining clean and rich dataset for this dissertation.

3.2.2 Blind source separation (SOBI)

Separating unobserved sources without any a priori information about the mixture is commonly known as blind source (or signal) separation (BSS) (Hyvärinen et al., 2001). In order to successfully separate sources, the underlying assumptions for the BSS algorithm should be in line with the physical properties of the problem at hand. This is essential since the direct validation of separation is not possible in case of EEG (Joyce et al., 2004).

One commonly used BSS approach is independent component analysis (ICA; Hyvärinen et al., 2001; Makeig et al., 1996; Thakor and Tong, 2004). ICA algorithms assume that the components (or underlying sources) are statistically independent at each time point. As

a result, ICA uses higher order statistical moments of the data. However, given the extensive feedforward and feedback connections in the brain, the statistical assumption of independence is unlikely to hold in neuroimaging data. Further, ICA does not utilize temporal information in the data, which can be very useful for source separation (Belouchrani et al., 1993; Belouchrani and Amin, 1998; Muller et al., 2004; Ziehe and Muller, 1998). Third, the use of higher-order instantaneous statistics makes ICA vulnerable to outliers. A fourth problem is that it cannot separate more than one Gaussian or near-Gaussian source (Hyvärinen et al., 2001).

Second-order blind source separation (SOBI), on the other hand, assumes that the underlying sources are uncorrelated (as opposed to independent). SOBI was recently introduced for preprocessing of EEG data (Belouchrani et al., 1993; Joyce et al., 2004; Tang et al., 2005). Unlike ICA, SOBI separates signals by minimizing cross-correlations across multiple time delays. SOBI uses average statistics across time, which makes it less vulnerable to noise and outliers. Further, second order statistics can be reliably estimated using fewer data points (Joyce et al., 2004). This property is helpful in the case of EEG, where the signals are not guaranteed to be stationary over periods of time longer than 3.5 sec (Pizzagalli, 2007). Furthermore, SOBI can even separate Gaussian sources, thus no assumptions about the underlying distribution are required.

Considering all the points above, SOBI was chosen to be the BSS algorithm for this dissertation. The algorithm was originally developed by Belouchrani et al. (1997) and it was implemented as it is (Algorithm 1), with minor modifications to handle the huge dataset. The results of applying it to the 88-channel EEG data separation are shown in Figure 3.3. The next subsection describes how the separated sources were classified as neural or artifact.

Algorithm 1 Second-order blind source separation (SOBI). Adapted from Belouchrani et al. (1997).

Given multi-dimensional time series data $\mathbf{X}(\mathbf{t})$, which is a $\{m, T\}$ matrix with m sensors and T time points,

1. Calculate the instantaneous $\{m, m\}$ correlation matrix $\mathbf{R_{XX}}(\mathbf{0})$.

2. Using $\mathbf{R_{XY}}(\mathbf{0})$, calculate presphering matrix $\mathbf{B}$ such that

$$\mathbf{B} = [(\lambda_1 - \sigma^2)^{-\left(\frac{1}{2}\right)}\mathbf{h_1}, \ldots, (\lambda_n - \sigma^2)^{-\left(\frac{1}{2}\right)}\mathbf{h_n}]^H,$$

   where $\lambda_1, \ldots \lambda_n$ denote the n largest eigenvalues and $\mathbf{h_1}, \ldots \mathbf{h_n}$ the corresponding eigenvectors of $\mathbf{R_{XX}}(\mathbf{0})$. Under the white noise assumption, σ^2 denotes the estimate of the noise variance.

3. Form sample estimates $\mathbf{R_{XX}}(\tau)$ by computing the sample covariance matrices of X(t) for a fixed set of time lags, $\tau \in \{\tau_j \mid j = 1, \ldots, K\}$.

4. Whiten the $\mathbf{R_{XX}}(\tau)$ matrices to get $\hat{\mathbf{R}}_{\mathbf{XX}}(\tau)$, using presphering matrix $\mathbf{B}$.

5. Joint diagonalize (JD) the set of matrices $\hat{\mathbf{R}}_{\mathbf{XX}}(\tau)$ using the JD criterion

$$C(M, \mathbf{V}) \doteq \sum_{k=1,\ldots,K} \mathbf{off}\left(\mathbf{V}^H \mathbf{M_k} \mathbf{V}\right),$$

   where the "off" of an $\{n, n\}$ matrix $\mathbf{M}$ with entries M_{ij} is

$$\mathbf{off}(\mathbf{M}) \doteq \sum_{1 \le i \ne j \le n} |M_{ij}|^2,$$

   to get the joint diagonalizer unitary matrix $\hat{\mathbf{U}}$, where $\hat{\mathbf{U}} \doteq V \; if \; \mathbf{off}\left(\mathbf{V}^H \mathbf{M} \mathbf{V}\right) = 0$.

6. Estimate the source signals as

$$\hat{\mathbf{S}} = \hat{\mathbf{U}}^H \mathbf{B} \mathbf{X},$$

   and the mixing matrix $\mathbf{A}$ as

$$\hat{\mathbf{A}} = \mathbf{B}' \hat{\mathbf{U}}.$$

3.2.3 Semi-automatic artifact removal tool (SMART)

Once the components are retrieved from SOBI, the next step is to identify those that are artifactual. This might seem like an easy task at first, however the amount of data makes it impossible to do it manually. Since SOBI was run separately on each minute of data (for a total of 14 minutes per subject per test-point) for about 90 subject files, three test-points (beginning, middle, and end of retreat), and 88 components (due to 88-channels), the total number of components comes out to be 332,640.

One solution could be to completely automate the process of artifact identification, based on some quantitative features. However, it would be difficult to guarantee that the results are correct, and wrong classifications could lead to unwanted conclusions in later analyses. Thus, a novel semi-automated artifact removal tool (SMART) was constructed to make sure that only the artifactual components are rejected and the neural components are retained.

After running SOBI on each one minute window of data, SMART extracts spatio-temporal features from each component: topography, auto-correlation, power spectrum, time-series, and effective power spectrum (after removing that particular component and keeping everything else). These features provide SMART the ability to classify the components in an automated fashion (Figure 3.3). However, human intervention is still required in the end, for quality assurance. To make it efficient, SMART generates a web page for the user to confirm its classification (of artifacts and neural components). This web page is interactive, and provides the user with an option to change the classification for any source that he/she may think as more appropriate. SMART provides all features at a glance, so that the user can see why SMART did what it did (Figure 3.4). Using an automatically generated web page, with all the information required in one place, the user can thus quickly and efficiently decide whether there are any discrepancies in the classification.

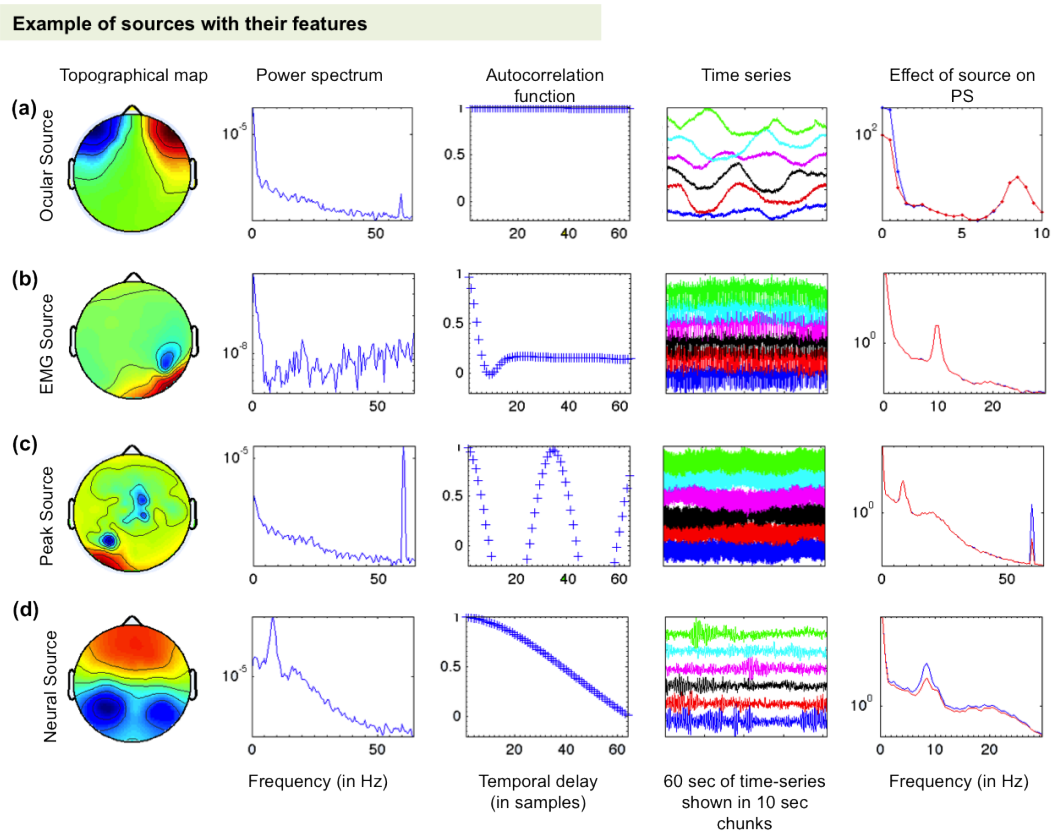

Figure 3.3: Components (rows) retrieved through blind source separation and their features (columns) extracted using SMART (Color figure). (a) An ocular source, located at front. The topographical maps and time-series (shows 60 seconds of data, where each wave is 10 seconds long) were used by SMART to identify this source as an ocular one. (b) An EMG component. The flat power spectrum and immediate drop in autocorrelation (within 10-20 samples) indicate noisy EMG source. (c) A peak component, due to interference from power lines (60Hz). The huge peak at 60 Hz and effect of taking out this source (which only affects the power spectrum at 60 Hz) suggests that this was indeed a power line source. (d) Example neural source, with occipital activity and a peak at 10 Hz. These neural sources were retained in the data. Overall, several features were used by SMART to identify the sources as neural or artifactual. Thus, the source identification can be done efficiently and reliably.

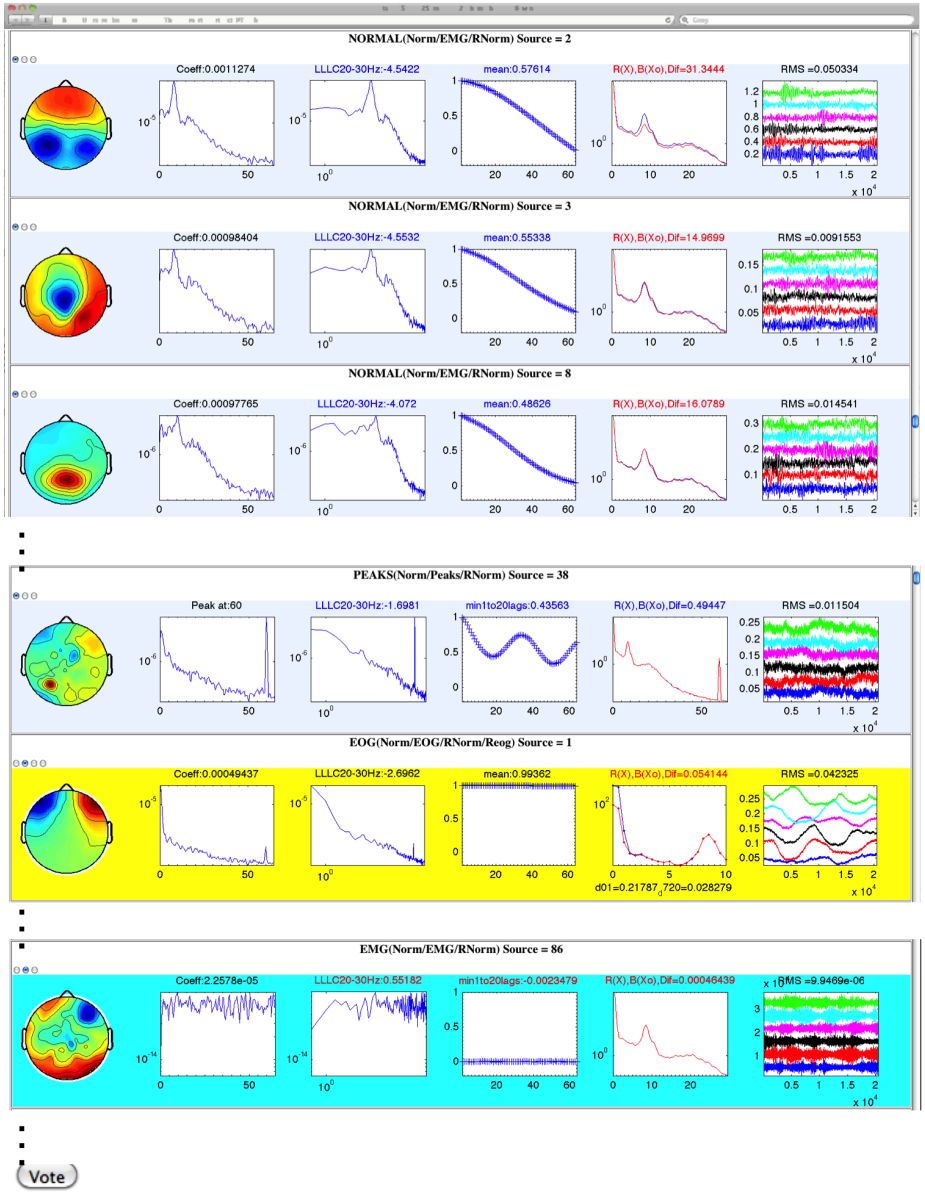

Figure 3.4: A screenshot of the web page created by SMART (Color figure). It displays all sources (in rows) and their features (in columns). The radio buttons above each source (on left), indicate the classification for that source. The user can change the classification by clicking on some other radio button. In the end, the user clicks on "Vote" button at the bottom and SMART records the user's input and then uses it to reconstruct the EEG data. The web interface provides an efficient way to double check and change SMART's classification of sources.

3.2.4 Reconstruction, quality check, and converting to standard space

After identifying the artifactual components, they were removed and the original configuration (88-channel EEG) was reconstructed:

$$\hat{X} = [A]_{88\times(88-N_a)}\,[S]_{(88-N_a)\times L}\,, \tag{3.1}$$

where N_a corresponds to the number of artifact components rejected using SMART. It is important to note that as long as sources were separated cleanly, removing purely artifactual components does not affect the reconstruction of neural components.

The reconstructed 88-channel EEG was then inspected for leftover noise in the data, especially in segments of data where there was no neural information to begin with. For example, there were cases where a participant had a sudden movement and all channels for that short time-period had a lot of noise. In such cases application of even SOBI and SMART cannot restore neural data: it was either not there to begin with, or the signal-to-noise ratio was so low that it could not be restored. Thus, a final quality check was done on each reconstructed data file to make sure only clean segments go forward for later analyses. This check involved extracting both amplitude and gradient thresholds for each subject (and at each test-point). The thresholds were then used to identify whether the data segment in question were to be rejected or kept.

Finally, the 88-channel EEG data was transformed into the standard 81-channel montage of the international 10-10 system (Chatrian, 1985; using spherical spline interpolation (Perrin et al., 1989) as implemented in Brain Electrical Source Analysis (BESA) software package; Version 5.3, http://www.besa.de), so that all participants have a similar number of channels and the channel locations are normalized. Figure 3.5 shows the 88-channel configuration and the 81-channel configuration overlaid on top. Due to lack of coverage, eight frontal channels were removed from the new 81-channel transform, and thus finally 73-channel EEG was used for later analyses.

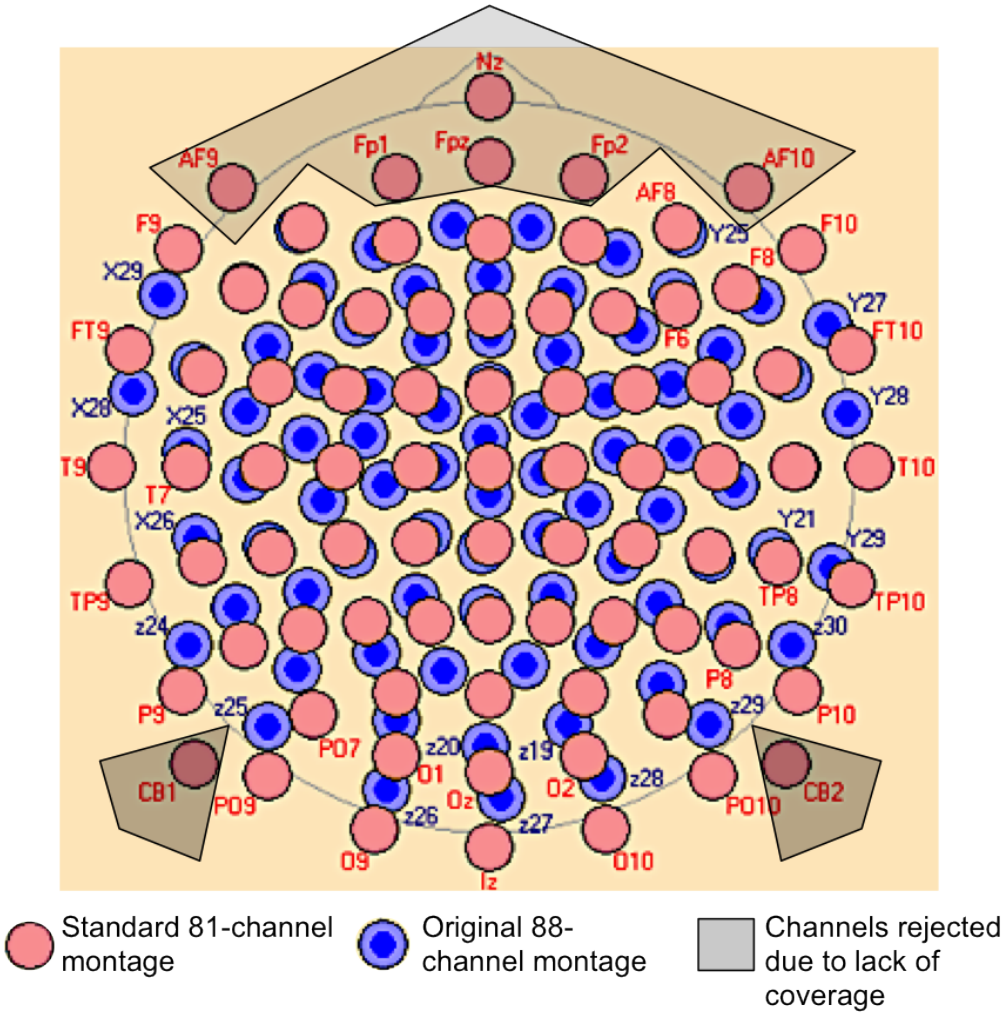

Figure 3.5: Converting to 81-channel standard space. The 81-channel montage is overlaid on the 88-channel montage used for data collection. Eight channels (Nz, AF9, Fp1, FPz, Fp2, AF10, CB1, and CB2) were not used from the 81-channel montage, since these locations were not covered by the original 88-channel montage in most participants. This transformation would provide equal treatment to all participants.

3.2.5 Estimating scalp current density

EEG measures the potential at each sensor location with respect to some reference. This reference should ideally be electrically inactive, thereby allowing measurement of true EEG waveforms (Pizzagalli, 2007). However, in practice such an inactive reference is not available. Thus, the choice of reference is important and does affect the results of EEG analysis (with few exceptions, like source localization; Lehmann, 1987; Dien, 1998). Further, if the reference sensor itself has noise in it, measuring all the other sensors with respect to the reference sensor will induce noise in all the sensors. Thus, one has to be very careful when selecting the reference.

In this work, the problem of selecting the correct reference electrode(s) was completely avoided by using a reference-free estimation of EEG waveforms. Scalp surface Laplacian (or scalp current density), estimated as a second derivative of the voltage surface, was used to transform EEG waveforms such that reference-free estimates were calculated. The CSDToolbox (Kayser, 2009; Kayser and Tenke, 2006) was used for this transformation.

3.3 Results

Blind source separation and a novel semi-automated tool (SMART) were employed for reconstructing clean EEG after removing artifactual components. This section presents the overall results of preprocessing and also provides supportive evidence that the excluded components were indeed artifacts.

3.3.1 Overall results

Preprocessing was done on the EEG collected from all three groups (RG1, CG, and RG2), three test-points (beginning, middle, and end of retreat), and three states (pre-meditation rest, meditation, and post-meditation rest). Table 3.1 presents the number of artifactual components rejected in each case. This number was similar across conditions and groups,

	T1			T2			T3		
	R1	M	R2	R1	M	R2	R1	M	R2
RG1	31.27	31.55	34.64	29.41	30.09	32.68	35.55	31.95	33.27
CG	29.91	29.63	31.45	27.00	25.31	27.95	27.77	27.61	30.45
RG2	30.27	29.30	30.55	30.41	28.77	31.41	30.14	29.17	31.23

Table 3.1: Mean number of artifactual components in each group (RG1, CG, and RG2), test-point (beginning (T1), middle (T2), and end (T3) of retreat), and state (pre-meditation (R1), meditation (M), and post-meditation rest (R2)). Overall, similar number of artifacts were rejected across conditions and groups.

suggesting that preprocessing was unbiased towards conditions and groups.

Log of temporal power spectral density (of neuronal EEG) has been shown to decrease in a near-linear fashion with increasing log of frequency (Freeman et al., 2003). However, in case of EMG, the power spectral density concave upwards with increase in frequency, especially in higher frequency ranges (e.g. gamma; Freeman et al., 2003). Thus, a clear departure from near-linear drop in power with frequency indicates EMG in the data. On the other hand, this observation also provides a straightforward way to judge the accuracy of preprocessing (especially for EMG), i.e., if the near-linear drop in power (with frequency) is restored for higher frequencies, without affecting power in lower frequencies, then the preprocessing step can be termed successful. For other artifacts, like interference from power lines, the reduced peaks at 60Hz (without affecting other frequencies) in the power spectral density can provide a good estimation of the success of preprocessing.

Figure 3.6, 3.7, and 3.8 provides the temporal power spectral densities before and after preprocessing. The raw data had EMG in it, visible as nonlinearities for higher frequency range ($>$20Hz). But after preprocessing, the neural signature of near-linear drop in power was restored and without affecting power in lower frequencies (same spectral power structure in frequency $<$20Hz). Furthermore, the interference from power line sources was greatly reduced (although not completely diminished) by preprocessing.

Next, features of artifactual sources was extracted and averaged across group, to

provide evidence that only the noise was removed and neural behavior of EEG was untouched.

3.3.2 Artifacts

In any kind of preprocessing methodology, the ideal result is to just remove the artifacts and nothing else. However, it is difficult to do, since the artifacts and neural signals sometime overlap. To confirm the success of preprocessing pipeline the average and standard error (over the participants in each group) of extracted features, which were used by SMART to decide whether to remove a component as an artifact, are presented in Figures 3.9, 3.10, and 3.11.

Starting with the EMG artifactual components, Figure 3.9 shows the average autocorrelation function and power spectrum of these removed sources for each group. As evident, the autocorrelation drops immediately to very low values, indicating the characteristic behavior of noise. Further, the power spectrum is concave upwards with no structure for low frequencies, strongly representing the EMG activity (Freeman et al., 2003). Altogether, these features show essential traits of EMG noise and lack of any neural structure (for low frequencies), thereby suggesting that SMART removed EMG activity without affecting neural content.

Although the EEG data presented in this dissertation was collected when participants had their eyes closed, ocular artifacts are still present due to horizontal saccadic activity. These ocular artifacts are known to affect low frequency bands, especially the delta and theta band (Pizzagalli, 2007). Topography, auto-correlation, and time-series of components were used by SMART to decide whether they are ocular artifacts (Figure 3.10). Topographically, the ocular artifacts lie in anterior frontal regions and are very easy to catch. Further, their temporal activity is very slow and hence, the auto-correlation is quite constant and close to one. Third, time-series itself can also be used to decide whether they are ocular artifacts or not, especially in case of high amplitude eye blinks and saccades (see Figure

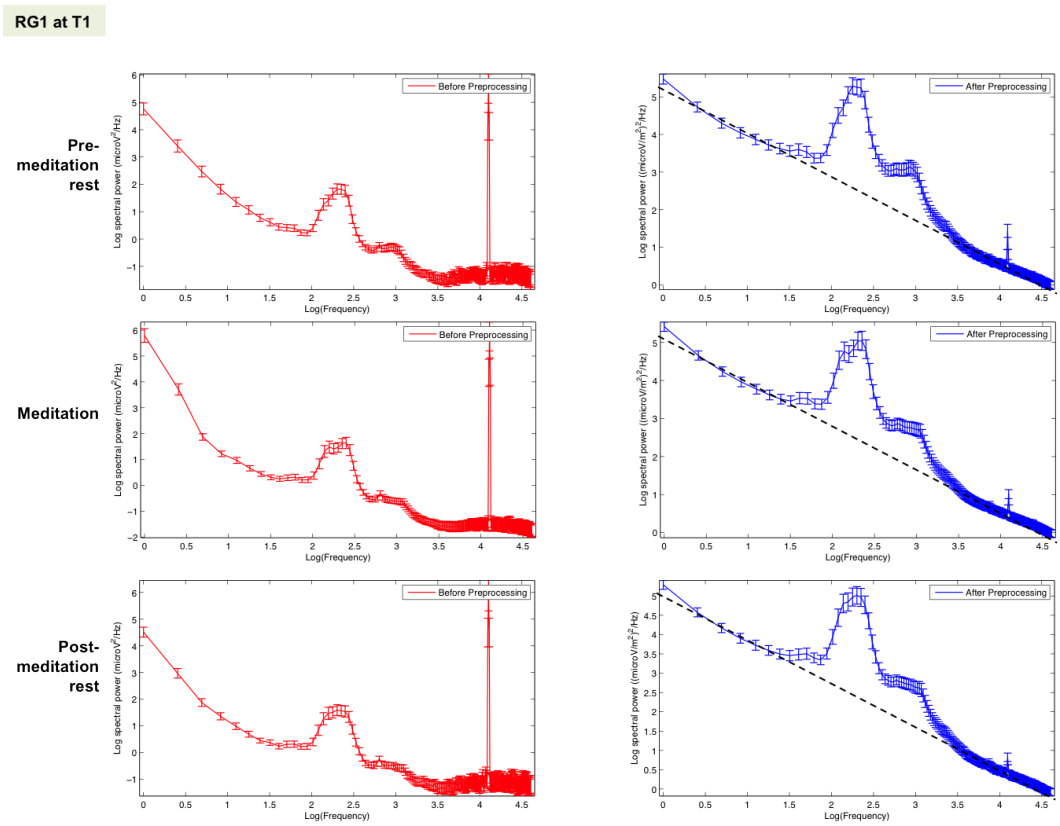

Figure 3.6: The effect of preprocessing on power spectrum in RG1. The left column shows mean log-log power spectrum (with error-bars showing standard error of the mean, across participants) for each state (rows) before preprocessing. The right column shows log-log power spectrum (computed from SCD transform, hence different scale) for each state (rows) after preprocessing. Dashed line was overlaid to show restored linear drop in power, especially for higher frequencies. Only the first test-point is shown, due to space, but all the test-points have similar results. The shape of the spectrum for lower frequencies ($<$20 Hz) is preserved as is, but the flat power spectrum (due to EMG) is removed. Also the noise in the spectrum due to interference from power lines is greatly diminished. Altogether, preprocessing pipeline removed artifacts, without touching lower frequencies.

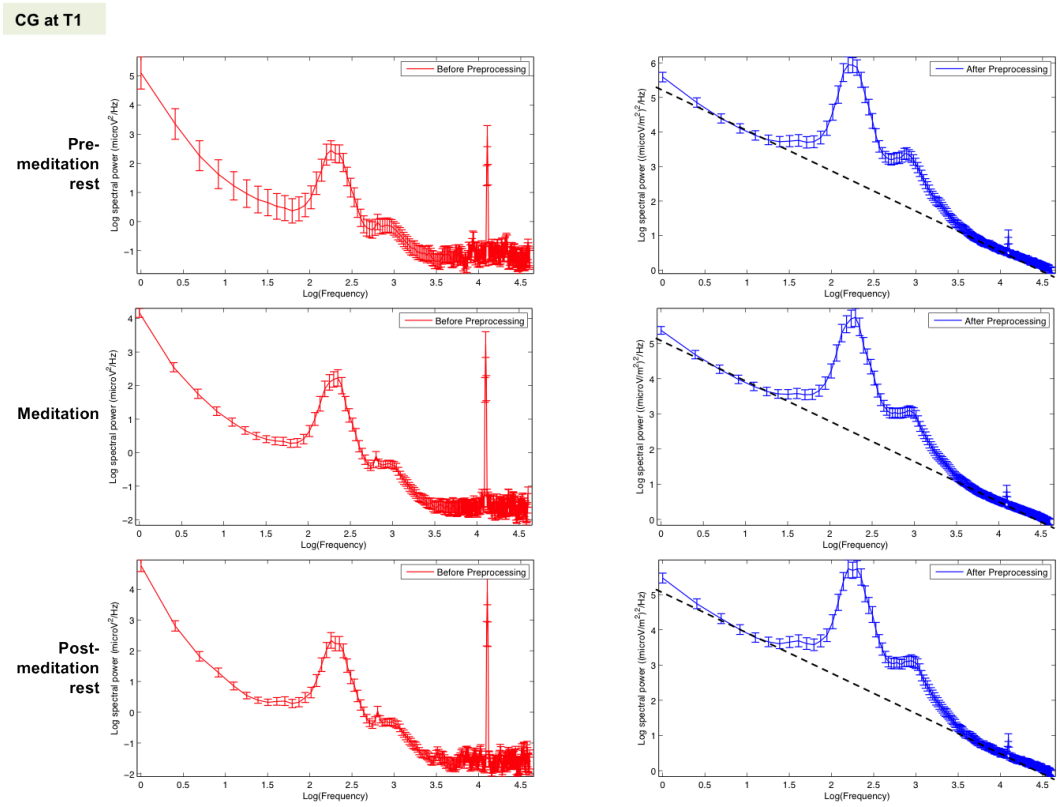

Figure 3.7: The effect of preprocessing on power spectrum in CG.

3.1). Altogether, only noise was removed by SMART.

Third, artifacts due to interference from nearby electrical sources, like power line (60 Hz) and skin-conductance equipment (16 Hz) were easy to identify based on topography and power spectrum. Having sudden spikes in the power spectrum (at 60 Hz or 16 Hz) and spatial locations limited to isolated channels clearly indicated non-neuronal activity. Figure 3.11 shows averaged power-spectrum and autocorrelation function for such components, as evident only interference from electrical equipment was removed and no neural content was touched.

In sum, artifactual components were successfully separated, identified, and removed

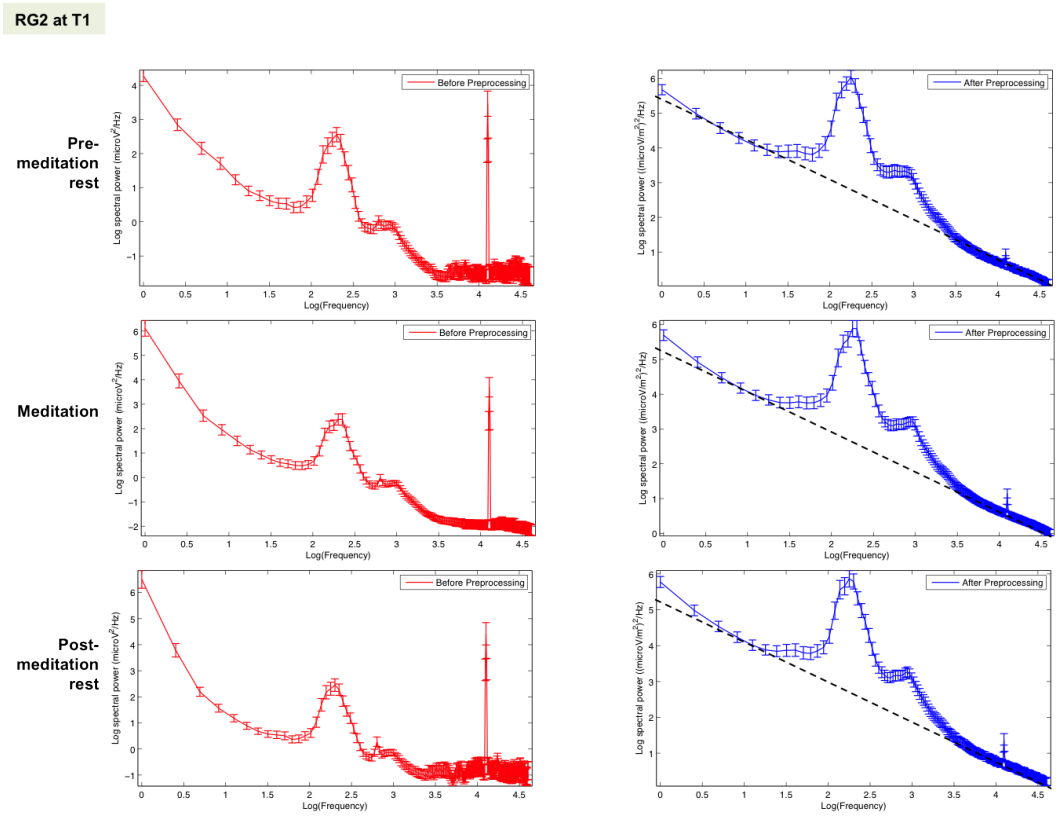

Figure 3.8: The effect of preprocessing on power spectrum in RG2.

using SOBI and SMART. Such a rejection of artifactual components, in turn, did not induce secondary artifacts in the data.

3.4 Discussion

Scalp-recorded EEG can easily get contaminated with a number of encephalic (muscular, ocular) and non-encephalic (power lines) sources of activity. Thus, a rigorous sequence of preprocessing steps is essential to eliminate the noise, while keeping the neural information intact. This chapter presented such a process, combining blind source separation and a novel

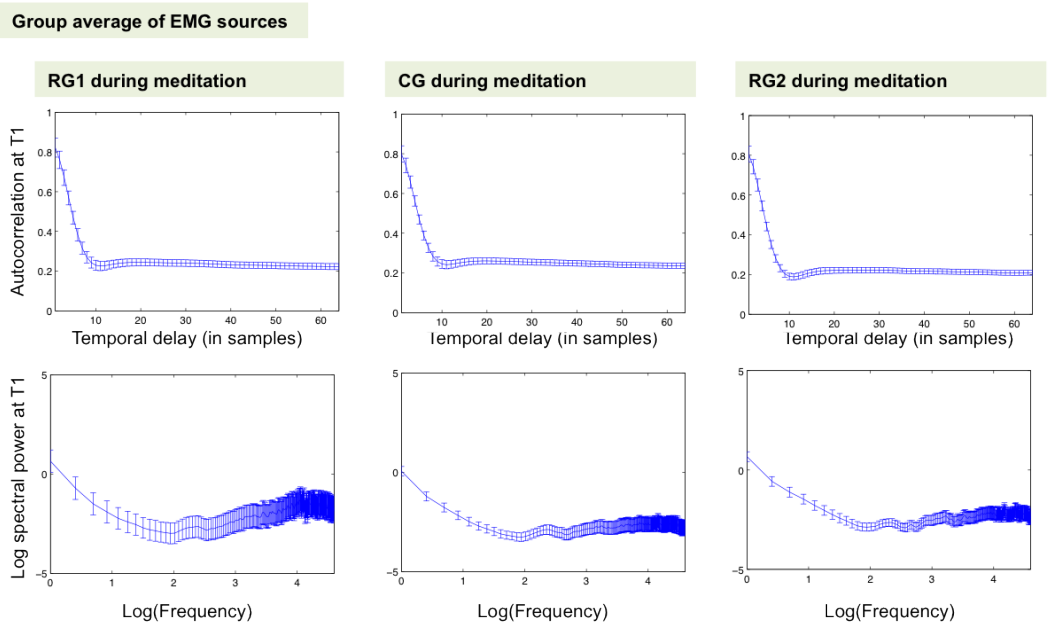

Figure 3.9: Group average of extracted features for EMG artifacts. Both autocorrelation function (sudden drop and stays low) and power spectrum (concave upwards) indicate that the sources are nothing but noise (Freeman et al., 2003). Mean values are drawn as a line and the error bars indicate standard error of the mean across participants. Only the first test-point and meditation state is shown here; to avoid redundancy and to save space.

semi-automatic noise source identification tool (SMART). The combination successfully eliminated noisy sources of activity without corrupting the neural data.

Application of SOBI and SMART on other datasets The successful integration of SOBI and SMART led to its application in other datasets at Saron Lab in UC Davis. In its new avatar it successfully preprocesses event related potentials (ERPs) recorded from healthy and autistic children (Saron et al., 2008). This application is crucial, because EEG collected from children in general is filled with muscular and ocular artifacts. Thus, SOBI and SMART can save a lot of data from getting rejected and at the same time it can even help reduce the duration of experiments. In the future, blind source separation and SMART

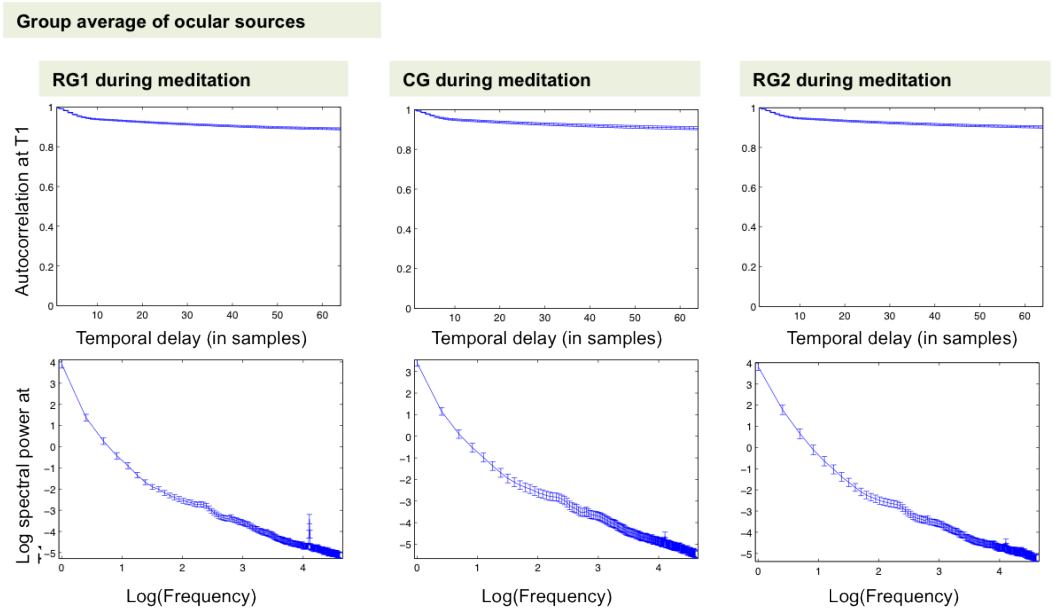

Figure 3.10: Group average of extracted features for ocular artifacts. Both autocorrelation function (constant and close to one) and power spectrum (no features) indicate that these sources have slow temporal properties. Topographic plots were used in addition to these two features, by SMART to identify them.

will be tested on other neuroimaging modalities, like near-infrared spectroscopy (NIRS; Villringer et al., 1993).

Dependent artifactual sources Although muscular and ocular sources of activity are considered as artifacts in the EEG data, it is important to ask whether these sources of activity are really independent of the task structure itself. Consider a case where the participant's response (clicking or punching a key) is followed by an eye-blink or a head movement. In this case, the associated ocular or muscular activity is not independent to the participant's neural activity (related to the response). Thus, source separation techniques that assume independence among sources of activity, for proper separation, could fail. Due to this reason, a second-order blind source separation (SOBI) was used in this dissertation; such a tech-

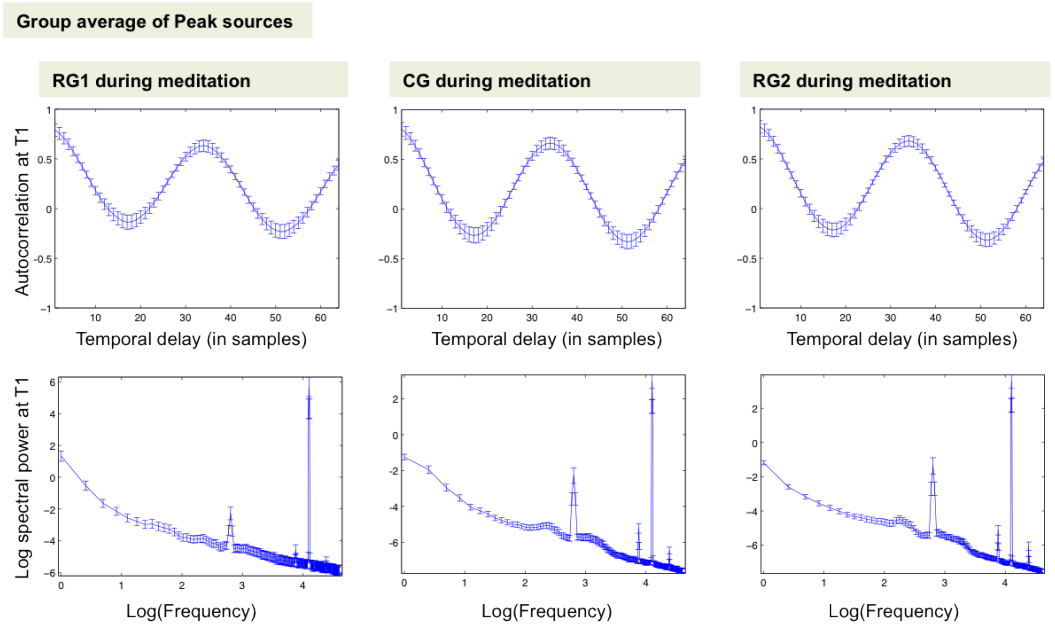

Figure 3.11: Group average of extracted features for interference from power line (60 Hz) and skin conductance equipment (16 Hz). Both autocorrelation function (vibrating at 60 Hz) and power spectrum (nothing but huge peaks at 16 and its harmonics and at 60 Hz) indicate that the sources are nothing but noise.

nique only assumes lack of correlation (on average over several temporal lags) and hence has a lesser chance of failure in removing dependent artifacts.

Number of components Usually, the number of sources separated by BSS algorithms is equal to the number of channels (or sensors) in the dataset on which the algorithm was run. However, more sophisticated algorithms (e.g. information theory) can be utilized to figure out how many sources should be separated, in order to avoid unnecessary leakage of artifactual sources on each other (Li et al., 2007; Sawada et al., 2004). However, reducing the number of sources can cause the problem of under-fitting (Li et al., 2007). In the current work, the number of sources was same as the number of EEG sensors. In future work, however, a comparison can be done to evaluate the optimal number of sources for separating

EEG data.

Manual vs. fully automated approach A lot of work has been done in dealing with artifactual sources of activity in EEG, ranging from basic visual inspection to completely automatic methods (Pizzagalli, 2007; McMenamin et al., 2010). In small experiments, with lesser data, manual inspection of each EEG segment is still possible. However, with huge datasets, like the current one, this approach cannot work. On the other hand, at least currently, complete automation of the process of detecting and rejecting artifacts is also not conceivable or advisable. Thus, in the current work, a semi-automated approach was taken, which also allows for quick and efficient quality check on top of automated first pass.

3.5 Conclusion

Altogether, a comprehensive preprocessing pipeline for continuous EEG data was developed for removing artifacts, estimating reference-free EEG, and projecting data into standard space. Such an approach is necessary to enhance signal-to-noise ratio in EEG studies. The next chapter takes this clean EEG data and analyzes longitudinal change in cortical activity associated with meditation training.

Chapter 4

Spectral Analysis

To measure the change in oscillatory activity of the brain due to intensive meditation training spectral analysis was employed. This chapter presents the methodology and the results from such analysis. In this chapter, first, an introduction is provided about the motivation, the challenges, and the approach used. Second, the methodological pipeline for the analysis is presented. Third, the results from three empirical experiments are furnished. Fourth, the interpretation of these results and their broader impact is discussed.

4.1 Introduction

A quick overview of what spectral analysis is and how it is used in neuroimaging is provided below. Followed by the motivation for using it to understand meditation and an overview of previous findings. Lastly, the challenges faced by previous studies and the approach used by this dissertation is presented along with an outline to the chapter.

4.1.1 What is spectral analysis and how is it used in neuroimaging?

Time-series data contain oscillatory activity, i.e., the signal changes with time. These changes can be rhythmic (e.g. 60Hz oscillations in power lines) or arrhythmic (e.g. ran-

domly varying white noise). To study the underlying mechanisms (or the generator) of these rhythms, one first needs to determine what kinds of rhythms are being generated. In some cases, the rhythm is quite obviously visible, e.g. shopping expenses go up during the holiday season every year. However, in other cases, e.g. in a mixture of rhythms (Figure 4.1d), it is hard to determine the rhythm by just looking at it. Brain-imaging data measured at the scalp, especially EEG, is similarly a mixture of different rhythms. These rhythms are very complex in nature, mainly because they are generated by various cortical, sub-cortical, and cortico-subcortical dynamics (Baillet et al., 2001; Speckmann and Altrup, 1993; Steriade et al., 1993; Buzsaki and Draguhn, 2004). Thus, to understand the brain-imaging data collected during a task (or otherwise), a sophisticated method is first required to untangle different rhythms out of the measured mixture. Once separated, different rhythms and their dynamics can be mapped to different functional roles (Pizzagalli, 2007) and thereby advance our understanding of information processing in the brain.

One such method to estimate the contribution of various frequencies to the measured data (EEG in this case) is spectral analysis. The most common approach to do this is to use Fourier transform to convert the time-series data into the frequency domain, followed by estimating the power of each frequency or range of frequencies (a.k.a. bands) to determine their contribution to the measured signal. Based on previous research, different frequency bands have been assigned different putative functional roles (Pizzagalli, 2007). Hence, when the contribution of certain frequency band increases (or decreases) in a particular experimental condition, the researchers can make claims about the functional roles based on the manipulation of those conditions. A brief review of the functional roles of these frequency bands is given below.

The lowest frequency band, delta (1-4Hz), is typically associated with sleep (Niedermeyer, 1993) and brain pathologies (Gilmore and Brenner, 1981; Fernandez-Bouzas et al., 1999) and, hence, it is considered as an inhibitory rhythm. The next band - theta (4-8Hz), is also dominant during sleep. However, during the awake state two different types of

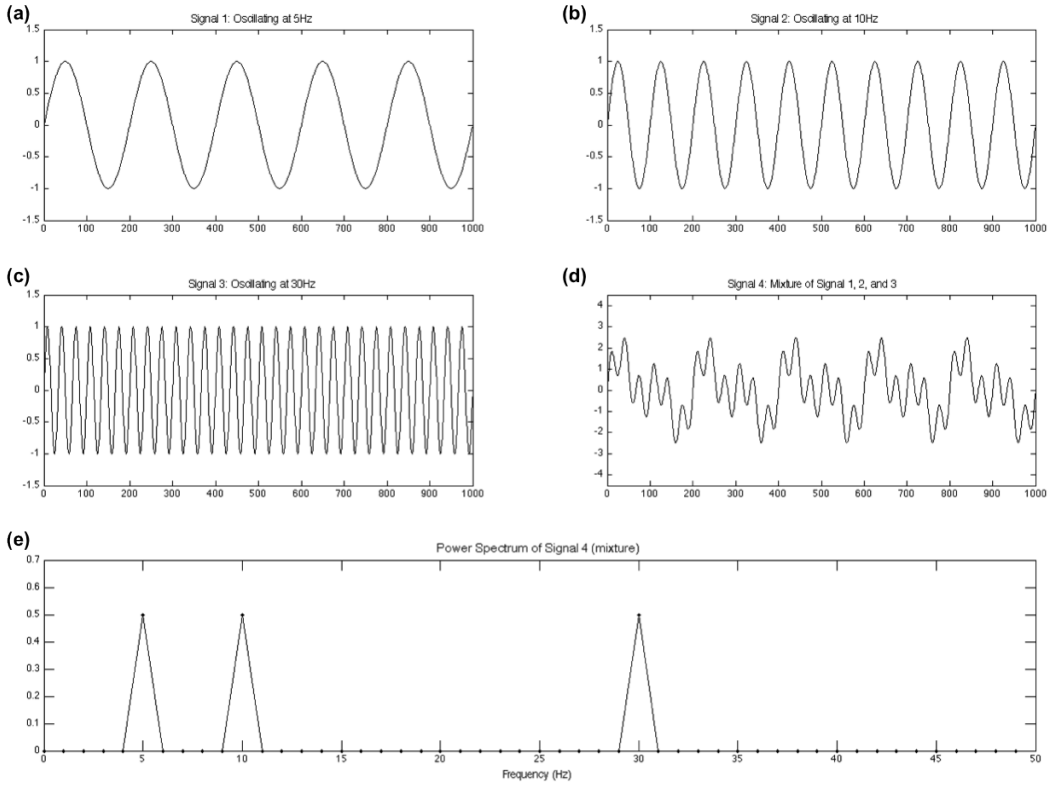

Figure 4.1: Spectral analysis of oscillations. By just looking at Signals 1, 2, and 3, one can find their frequency of oscillation. However, when these three signals (oscillating at 5, 10, and 30 Hz) are mixed (e.g. Signal-4, simply by linear summation with equal weights) it is hard even to determine the frequency content of the mixture let alone the weights of each of the contributing signals. Thus, spectral analysis (using Fourier transform, followed by power estimation) is done to determine the contributing frequencies and their weights, as shown in the last row for Signal-4.

theta rhythms can be seen. One of them has a large distribution over the scalp and has been linked with drowsiness and impaired information processing (Schacter, 1977). The other type of theta rhythms are topographically distributed over the frontal-midline areas of the scalp (hence these rhythms are also known as Fmθ) and have been linked with increased memory load and attention (Jensen and Tesche, 2002; Sauseng et al., 2007). Anterior cingulate gyrus is considered to be the generator for the second kind of theta band oscillations (Asada et al., 1999; Luu et al., 2003; Onton et al., 2005).

Next up is the alpha band (8-13Hz). Alpha rhythms can be easily seen over the parietal-occipital regions while resting with eyes closed. They immediately diminish by opening the eyes or with mental concentration (Pizzagalli, 2007). Due to this behavior they have been long considered as "idling-rhythms" (Pfurtscheller et al., 1996). However, recent studies have characterized a new form of alpha rhythm over the anterior-frontal-midline areas, whose amplitude (or power) increases with increased concentration and information processing. This relatively newer version is also known as paradoxical alpha (Cooper et al., 2003; Klimesch et al., 1999). Further, new evidence has come to light about the alpha sub-bands (α_1:8-10Hz, α_2:10-12Hz, and α_3:12-13Hz) and their functional dissociation with increasing task demands (Klimesch, 1999).

The next frequency band is the beta band (13-30Hz). Earlier studies have shown symmetric fronto-central distribution of beta rhythm, which increases with increasing attentional and vigilance task demands (Murthy and Fetz, 1992). More recent M/EEG studies in conjunction with fMRI, have shown negative correlation of alpha and beta activity with blood-oxygen-level-dependence (BOLD) signal (Goldman et al., 2002; Laufs et al., 2003; Yuan et al., 2010; Ritter et al., 2009; Scheeringa et al., 2011), indicating that decrease in beta activity implies increased cortical activation. These negative correlations were found in somatosensory/motor cortical areas. It has also been proposed that the beta-band activity could be responsible for binding distributed somatosensory and motor cortical areas into a functional network (Brovelli et al., 2004).

The last frequency band is the gamma band (30-50Hz). Activity in this band has been linked to visual binding (Tallon et al., 1995; Csibra et al., 2000; Gruber et al., 2006; Engel and Singer, 2001), attention (Jensen et al., 2007; Bichot et al., 2005; Fries et al., 2001; Lakatos et al., 2008), arousal (Balconi and Lucchiari, 2008; M$\ddot{u}$ller et al., 1999), learning and memory (Medendorp et al., 2007; Jokisch and Jensen, 2007; Gruber et al., 2004), and even consciousness (Engel et al., 1999; Melloni et al., 2007; Singer, 2001). Further, the hemodynamic response in fMRI has also been shown to positively correlate

with the activity in gamma band and this activity has been shown to explain the variance in the BOLD signal (Scheeringa et al., 2011).

Based on these and myriad of other studies on gamma band activity (after the paradigm shifting study of "binding-by-synchrony" (Singer, 1993)), it may seem that gamma band is behind everything our brain does. However, it is important to note that the interpretation of high-frequency activity from the scalp-recorded EEG is difficult (Menon et al., 1996; Nunez and Srinivasan, 2010), since such an activity is almost always accompanied by muscular (Whitham et al., 2007), saccadic (Yuval-Greenberg et al., 2008 also see Schwartzman and Kranczioch, 2010), and other artifacts. To add to the interpretation issues, gamma band (and other higher frequencies) have been shown to provide different cognitive functions in different experimental settings (Tallon-Baudry, 2009). Further complexifying the issue is the fact that multiple frequency bands (e.g. theta and gamma) can interact to provide completely different set of cognitive functions than the usual "binding" (Tallon-Baudry, 2009). Hence, extreme care should be taken and all the factors should be considered, in order to safely interpret spectral analysis results for high-frequency bands.

Given the studies defining functional roles for each band, it seems possible (at least to some extent) to decipher the mechanisms underlying the experiment at hand, based on spectral analysis. It is especially useful in experimental designs where the data are continuous in nature, i.e. without any events/trials (such as resting state or meditation data).

4.1.2 Why spectral analysis of meditation?

Focused-attention meditation involves sustaining focus on an object or a phenomenon (Wallace, 2006). Previous studies have shown that the participants take a while to reach such a meditative state (Baijal and Srinivasan, 2010). Hence, to understand the mechanisms underlying meditation, most studies use continuous data collection strategy (Cahn and Polich, 2006), thereby not disrupting the meditation process every now and then with trials. But, no trials means that the event related measures (e.g. ERP) could not be used to under-

stand the temporal dynamics of the task. However, in such cases spectral analysis can be used to determine the changes in oscillatory cortical activity (in the frequency domain) and these changes can be mapped to different functional brain states, which in concert with the task structure at hand (and other observations) may reflect the recruitment of brain resources (Pizzagalli, 2007). Further, using a dense EEG sensor array, detailed spatio-spectral changes can also be assessed using spectral analysis.

4.1.3 What do we already know about oscillations in meditation?

There is an increasing recognition that meditation can play an important role in the cultivation of attention and emotion regulation in both normative and clinical contexts (Lutz et al., 2008a; Slagter et al., 2011). Over the past 55 years many studies have attempted to characterize the brain activity patterns that occur during meditation. Such patterns may reflect effects of contemplative training that are ultimately expressed as trait changes in behavior. Following is a very brief overview of some of the continuous EEG studies done on meditation (for detailed review see Cahn and Polich, 2006).

Starting with the early results on meditation, increased global alpha-band power was often observed in meditators when meditation was compared with rest (or other control conditions; Cahn and Polich, 2006; Aftanas and Golocheikine, 2001; Deepak et al., 1994; Wallace, 1970; Taneli and Krahne, 1987; Dunn et al., 1999). Further, even during rest the alpha-band power was found to be higher in meditators as compared to control participants (Cahn and Polich, 2006; Travis, 1991; Aftanas and Golocheikine, 2001; Deepak et al., 1994), thereby indicating both state and trait changes in long-term meditators. It is important to note, however, that the trait changes associated with alpha-band power were later suggested to be due to the individual differences, i.e. perhaps long-term meditators had more relaxed personality to begin with (Cahn and Polich, 2006). Further, recent studies on meditation do not show an increase (some rather show a decrease) of alpha-band power even during meditation, especially when counterbalanced controlled relaxation conditions

are used for comparison (Cahn and Polich, 2006; Benson et al., 1990; Travis and Wallace, 1999; Jacobs and Lubar, 1989; Pagano et al., 1983). As opposed to alpha-band power, alpha frequency has been repeatedly shown to be reduced during meditation (Cahn and Polich, 2006; Banquet, 1973; Taneli and Krahne, 1987; Deepak et al., 1994) and rest (Cahn and Polich, 2006; Aftanas and Golocheikine, 2001; Stigsby et al., 1981) in experienced meditators.

Theta band activity, mainly the frontal-midline theta ($Fm\theta$) (Baijal and Srinivasan, 2010; Aftanas and Golocheikine, 2001; Hebert and Lehmann, 1977), has also been found to increase especially during concentration meditation (Jacobs and Lubar, 1989; Baijal and Srinivasan, 2010; Aftanas and Golocheikine, 2001; Banquet, 1973; Pagano et al., 1983). However, this effect could not be reproduced in some studies (Dunn et al., 1999), rather they showed an opposite effect - more frontal theta for mindfulness meditation than the concentrative kind.

Gamma band activity has also been associated with meditation training. Early studies on meditation have shown widespread increase in high-frequency activity (20-40Hz) during meditation (Cahn et al., 2010; Banquet, 1973; Anand et al., 1961; Das and Gastaut, 1955). The gamma band activity has also been used to dissociate between advanced and novice meditation practitioners and to define deep meditation states in experienced meditators (Banquet, 1973; Das and Gastaut, 1955). More recent a study by Lehmann et al. (2001) showed that activity in gamma band can reliably distinguish between different meditative states (in a single individual). Another recent study showed that long-term Buddhist meditation practitioners had a markedly increased gamma-band power (as compared to baseline rest) after engaging in compassion meditation (Lutz et al., 2004). Lastly, a very recent work by Cahn et al. (2010) showed increased occipital gamma-band power, during meditation as compared to rest, in long-term Vipassana meditators. Although meditation seems to affect high frequencies, it is also important to note that the gamma-band activity has always been marked as the hardest one to be measured using scalp-recorded EEG, due to muscular

artifacts and other issues (Nunez and Srinivasan, 2010). Furthermore, these self-induced high-frequency oscillations have also been a center of debate (Lansky and St Louis, 2006) regarding whether meditation is an epileptogenic (Jaseja, 2005, 2006) or an antiepileptic process (Orme-Johnson, 2006; Fehr, 2006).

Altogether, it is difficult to come to consensus about how meditation does what it does. The overall pattern, however, is that meditation influences oscillatory activity in the brain, especially in alpha, theta, and gamma bands (Cahn and Polich, 2006).

4.1.4 Why is there so much variability in the findings?

Several factors contribute to the large variability in results. First, several different meditation techniques were assessed. Even though meditation techniques can be classified as "mindfulness" or "concentrative" (Cahn and Polich, 2006; Davidson and Goleman, 1977; Lutz et al., 2008a) [1]. It is not a binary classification and the techniques actually fall into a spectrum between the two extreme ends of maintaining open-monitoring and one-pointed focus (Cahn and Polich, 2006; Wallace, 1999; Andresen, 2000). Further, this classification is done based only upon one factor - "how attention processes are directed" (Davidson and Goleman, 1977). There could be several other factors to consider, e.g., based on the benefits of meditation (such as stress reduction, emotion regulation, etc.) rather than the technique itself (Cahn and Polich, 2006). Lastly, it is also important to consider whether these two extreme types of meditation really are that different from each other or are there any common factors that can be used to unite all these findings. As per Buddhist literature, both open-monitoring and one-pointed focus need $samprajanya$ (the faculty of "meta" awareness (Lutz et al., 2006)) to make sure that the goal is being met. Hence, some kind of theoretical dimensional reduction analysis (like PCA in signal processing) is required to reduce the variance in these findings.

[1] Some researchers feel that there should be a third class for transcendental meditation (TM®; Travis and Shear, 2010). Currently TM® is considered as to be a concentrative type of meditation (although effortless concentration; Cahn and Polich, 2006)

Second, the individual participants enrolled in these studies differ greatly in terms of degree of meditation practiced, age, gender, socio-economic factors, and so on. For example, it is known that aging affects neurophysiological measures (especially scalp recorded EEG; Polich, 1997). Thus, care should be taken while comparing studies of elderly meditators with studies of young meditators. Another related point is to make sure that the control participants are adequately matched with meditators, to avoid making wrong claims about effects of meditation practices. Further, it has also been shown that long-term meditators have reduced alpha frequency (Cahn and Polich, 2006; Aftanas and Golocheikine, 2001). Hence, if individual alpha frequencies are not measured before analysis and each frequency band is not defined based on the individual alpha differences, then one might wrongly attribute changes in alpha-band to that of theta. According to Cahn and Polich (2006) only one study (Aftanas and Golocheikine, 2001) had taken these differences into account.

Third, early studies did not employ sophisticated measures and as a result their findings and analysis do not generalize (Cahn and Polich, 2006). Hence, extreme care should be taken while comparing and hypothesizing based on very early studies of meditation.

Fourth, even though recent advanced studies on meditation (Lutz et al., 2004; Cahn et al., 2010) have well characterized practices, expert practitioners, and modern methods they still did not examine the longitudinal changes in brain activation associated with meditation. Such an examination is crucial to properly understand the evolution of oscillations with meditation training. Further, it can also help in defining the spectrum of cortical activity results starting from beginners on one end to intermediate practitioners to more advanced adepts at the other end.

Fifth, in future studies the variability in meditation results can be reduced by applying systematic correlation analysis between cortical activity findings and other measures (e.g. self-reported measures and behavioral data on attention- and emotion-related tasks). These correlations will not only help ground the findings as neuronal, by providing more credibility to them, but will also help weed out the findings that might be artifactual.

Altogether, comprehensive empirical and theoretical studies are required to advance our understanding about what mechanisms underlying meditation and how they provide enhanced cognitive control.

4.1.5 Approach

In the present study two three-month meditation retreats were conducted in a randomized wait-list design using matched control and training groups that examined both trait (MacLean et al., 2010; Sahdra et al., 2011; Jacobs et al., 2010) and state variables during intensive practice of focused-attention meditation (Shamatha-Project, 2007). See section 2.3 for complete details.

Individual differences were kept in check by matching the training and control groups on age, sex, gender, socio-economic, educational and other features (Shamatha-Project, 2007). Further, individual alpha frequency was estimated (during rest) to define the frequency bands separately for each participant, thereby controlling for the individual neurophysiological differences (see section 4.2.2 for more details). A drop in individual alpha frequency was found in training groups; the results are presented in Experiment-1.

Longitudinal testing was done using nonparametric cluster-based permutation approach to understand the evolution of cortical changes across the retreat. Both spatial (73-channel EEG) and spectral dimensions were tested longitudinally. Reduced alpha- and beta-band power was found in both the training groups; the results are presented in Experiment-2.

Third, relations were found using systematic correlation analysis between longitudinal changes in cortical activity and participants' performance in other attention-related tasks. Experiment-3 provides results based on this analysis.

Altogether, a comprehensive empirical analysis was done to explore the cortical correlates of intensive meditation training. Section 4.4, discusses the implications of this research and provides future directions for it.

4.2 Methods

In this section the spectral analysis pipeline is described in details, along with brief information about data, participants, task, and meditation training (see Chapter 2 for more details).

4.2.1 Data acquisition and preparation

A high-density EEG cap was used with 88 equidistant scalp locations (later converted to standard normalized 10-10 system of 81-channels (Chatrian, 1985) for analysis). However, eight channels from the 10-10 montage were rejected because the original 88-channel cap did not cover the scalp locations of these eight channels; hence, finally only 73-channels were used in the final setup. Three dimensional (3D) location of the electrodes on each participant was determined with a magnetic digitizer. The data was collected using the Biosemi Active Two system (BIOSEMI, 2006), at a sampling rate of 2048 Hz.

Data preprocessing was done using second-order blind source separation (Belouchrani et al., 1997) and semi-automatic meticulous artifact removal tool (SMART; developed in this dissertation). Using SMART components related to muscular activity, ocular activity, and interference from power lines were removed, without loosing the neural components, as discussed in detail in Chapter 3.

4.2.2 Spectral analysis pipeline

After data acquisition and preprocessing, 73-channel EEG data during meditation and rest (pre- and post-meditation) was analyzed using the six-step spectral analysis pipeline shown in Figure 4.2(a). Each step is described below in detail.

Scalp current density estimation

Scalp-recorded EEG data is measured as a voltage difference between a given electrode and the recording reference. The choice of reference has a large effect on the EEG wave-

forms (Lehmann, 1987; Dien, 1998). Thus, a reference-free transformation is required to avoid choosing a single or multiple electrodes as reference. Re-referencing is an important methodological consideration that is still not often recognized in the EEG literature (Pizzagalli, 2007). In this dissertation, scalp-current density (SCD, also known as surface Laplacian) was computed using the CSDToolbox (Kayser and Tenke, 2006; Kayser, 2009) for Matlab (MATLAB, 2010), as the second derivative of the voltage surface to transform the data to a reference-free representation (Figure 4.2(b)). SCD helps in visualizing the focal patterns of occipital activity by acting as a spatial filter (Nunez and Pilgreen, 1991). SCD transformation also helps reduce the effects of volume conduction (Pizzagalli, 2007; Winter et al., 2007).

Power spectrum estimation

The EEG signal is assumed to be stationary[2] for up to 3.5 seconds (Gasser and Molinari, 1996). Thus, the power spectrum should be calculated on segments shorter than 3.5 seconds. Further, at least one minute of data are required to get stable power spectrum estimation (Nuwer et al., 1999a). Thus, the data (six-minutes during meditation and one-minute for each rest condition) was divided into segments of two-seconds duration with 75% overlap, thereby providing approximately 119 segments for every one-minute of data. Power spectra were then calculated for each of these segments using multi-tapered power spectral density estimation method (Mitra and Pesaran, 1999; Oostenveld et al., 2011). Later, averaged power spectrum was calculated over these segments for each condition. It is important to note that before calculating the power spectra, a quality check was implemented (as part of the preprocessing step) to weed out segments with leftover artifacts (e.g. rare signal jump etc.) using individually calculated amplitude and gradient thresholds (see Chapter 3 for more details).

[2] A time-series is stationary if its statistical properties (e.g., mean, variance) do not change over time.

IAF calculation and individual frequency bands

Individual alpha frequency (IAF) is the frequency at which the alpha-band power peaks (usually seen clearly in an eyes-closed state; Klimesch, 1999). Estimating IAF is crucial, since the alpha frequency shows large inter-individual (Klimesch, 1999) and intra-individual differences (Cahn and Polich, 2006; Aftanas and Golocheikine, 2001; Klimesch, 1999). If fixed-range frequency bands are used, one can wrongly attribute changes in alpha-band power to that in theta (and vice-versa) (Figure 4.2(c); Cahn and Polich, 2006). Thus, lower frequency bands were individualized by taking IAF as an anchor. IAF can be estimated using a center of gravity method between certain frequency range $f_1 - f_2$Hz (Klimesch, 1999),

$$\alpha_{IAF} = \frac{\sum_{i=f_1}^{f_2}(a(f_i) * f_i)}{\sum_{i=f_1}^{f_2} a(f_i)}, \tag{4.1}$$

where power-spectral estimates at f_i are denoted by $a(f_i)$. Also f_1 was set to 7 Hz and f_2 to 14 Hz. The α_{IAF} values were calculated for each channel and then were collapsed across all channels to get a single IAF value per subject for statistical analysis. IAF values during baseline resting state (or pre-meditation rest) were used to define individualized frequency bands (Table 4.1) separately for each participant and at each test-point.

Nonparametric cluster-based permutation testing

The dissertation is aimed at finding the longitudinal changes in cortical activity associated with intensive meditation training. However, finding such changes in a rich spatio-temporal dataset is statistically hard due to the multiple comparisons problem (MCP). For example, to assess changes in any one frequency-band power for all the 73 channels and at all three test-points (beginning, middle, and end of the retreat) would require $73 \times 3 = 219$ multiple comparisons. Now, for a predefined critical alpha level (e.g. $p = 0.05$), one needs to calculate a corrected critical alpha level to account for 219 multiple comparisons. A simple method to correct for MCP, without taking into account any spatial information, would be to

	Frequency range for bands	
	Fixed width	IAF based
Delta	$1-4$ Hz	$2-0.4\times\alpha_{IAF}$ Hz
Theta	$4-8$ Hz	$0.4\times\alpha_{IAF}-0.6\times\alpha_{IAF}$ Hz
Alpha	$8-14$ Hz	$0.6\times\alpha_{IAF}-1.2\times\alpha_{IAF}$ Hz
Alpha1	$8-10$ Hz	$0.6\times\alpha_{IAF}-0.8\times\alpha_{IAF}$ Hz
Alpha2	$10-12$ Hz	$0.8\times\alpha_{IAF}-1.0\times\alpha_{IAF}$ Hz
Alpha3	$12-14$ Hz	$1.0\times\alpha_{IAF}-1.2\times\alpha_{IAF}$ Hz
Beta	$14-30$ Hz	$1.2\times\alpha_{IAF}-30$ Hz
Gamma	$30-50$ Hz	$30-50$ Hz

Table 4.1: Frequency band definitions: fixed-width and IAF-based bands. In total, eight bands were analyzed in this study. The bands were defined for each individual and at each test-point.

use Bonferroni correction. But Bonferroni is an overly conservative approach, and it would bring down the critical alpha value to $p = 0.05/219 = 0.00023$, and sensitivity would be lost.

Thus, to avoid being overly conservative and at the same time include spatial information, nonparametric cluster-based permutation testing (Maris and Oostenveld, 2007) was used to find out spatio-temporal changes in spectral band power. In contrast to parametric testing, nonparametric testing can solve the MCP in a simple way (Maris and Oostenveld, 2007). Nonparametric testing is powerful for two reasons: (a) validity of these tests is not dependent on the distribution of the data; and (b) any test statistic can be used to base the statistical inference (t- or F-statistic or any other). The later reason allows us to use a cluster-based (to avoid spatial MCP) F-statistic (to avoid temporal MCP) with multiple comparisons. Further, this approach is better than the traditional method of dividing the scalp channel into various regions and calculating parametric statistics based on an average value from all those regions. As opposed to a priori division of scalp into regions, it considers clusters of channels across scalp that are significantly different in conditions under consideration. Thus, if an effect takes place between two traditional regions (Figure

4.2(d)), the cluster approach will provide more power, and it is not necessary to divide the scalp into an optimized set of regions. Furthermore, dividing scalp channels into regions and then calculating average spectral power over regions to do the parametric analysis defeats the purpose of having high-density EEG cap in the first place.

This non-parametric cluster-based approach is becoming standard in MEG and EEG (M/EEG) analysis (Capilla et al., 2011; Jung et al., 2011; Altmann et al., 2009; Grützner et al., 2010) and has been shown to work for analyzing changes in power spectra (Maris and Oostenveld, 2007) and coherence (Maris et al., 2007) in M/EEG data. The algorithm for finding changes in spectral band power is presented in Algorithm 2 and 3, based on previous work by Maris et al. (2007). Fieldtrip (Oostenveld et al., 2011), the open-source toolbox for Matlab®(MATLAB, 2010), was used to do these statistical tests.

Algorithm 2 Group-level nonparametric statistical test for each frequency band f_i

Null Hypothesis(H_0): Spectral power in f_i does not differ across the three test-points

1. Collect the spectral power in f_i for all the 73-channels and all the subjects, during the three test-point in a single super-set.
2. Randomly partition the super-set to three equal sets.
3. Calculate the cluster-based test-statistic (using Algorithm 3).
4. Repeat steps 2 and 3 a large number of times (e.g. 10,000) and construct a histogram of the test statistics.
5. Using the actually observed test-statistic and the histogram from step 4, estimate the proportion of random partitions that resulted in larger test-statistic than the observed. This proportion is the p-value.
6. If the p-value is less than the critical alpha-level, then conclude that the null hypothesis H_0 is rejected and that the power in f_i band is different across test points.

Algorithm 3 Cluster-based test statistic

1. For every channel, compare the spectral power in f_i band across the three test-points, using a F-statistic.
2. Select all channels, with F-statistic value larger than some threshold.
3. Cluster the selected channels in connected sets on the basis of spatial adjacency.
4. Calculate the cluster-level F-statistic, by taking a sum over all F-values within a cluster.
5. Output the largest of the cluster-level statistic.

Parametric testing of clusters

Although non-parametric cluster-based permutation approach works well with M/EEG data, it cannot handle more than one independent variable in the experimental design. This is because it is not possible to construct an exact permutation test for interactions, due to lack of exchangeable units to permute. The current work has at least two independent variables - Group (training vs. control) and Test-points (beginning, middle, and end of retreat). The previous subsection illustrated how non-parametric approach can be used to handle the second independent variable (Test-points). False discovery rate (FDR; Benjamini and Hochberg, 1995) is used after finding clusters to control for testing each group, frequency band, and state (rest or meditation) individually.

However, it is also important to explore the interactions between independent variables. Especially between group and test-points (for Retreat 1) and between retreat and test-points (for Retreat 2). In order to find such interactions a hybrid approach was created. Once the clusters were found and were corrected using FDR-based correction, the average spectral power for that cluster was extracted and log-transformed (to get normal distribution (Pizzagalli, 2007; Davidson et al., 2000)). Later this log-transformed spectral power was used to calculate interaction between group/retreat and test-points using parametric analysis

of variance approach (ANOVA) [3].

Thus, using this hybrid approach the best of both approaches (non-parametric and parametric) was achieved.

4.2.3 Subjects

Thirty participants in the retreat group (RG1), and another thirty in the wait-list control group (CG) were matched on age, sex, handedness, psychological measures, attention performance, and previous meditation experience (see Chapter 2 for more details). Retreat participants stayed at a remote mountain retreat center (Shambhala Mountain Center, CO) during the three months of training. Control group participants were flown to the retreat center for testing during Retreat-1, and later comprised as participants for Retreat-2 (RG2). Thus, data from the control group in Retreat-1 would act as a control for retreat group in Retreat-1, and as a control for themselves in Retreat-2. Due to technical difficulties (unusable data, missing EEG files, etc.), data is analyzed only for twenty-two subjects in each group (RG1, CG, and RG2).

4.2.4 Task

The participants were assessed at several psychological tasks, at the three test-points (beginning, middle, and end) during the retreats. The spectral analysis, however, is done on the task where participants practiced eyes-closed focused-attention meditation (twelve minutes) and rest (one minute before and after meditation). Please refer to Chapter 2 for details about the task structure. Due to technical difficulties only first six minutes of EEG data was recorded during meditation. Hence, the analysis was based on three eyes-closed states: one-minute of pre-meditation rest, six-minutes of focused-attention meditation, and one-minute of post-meditation rest.

[3] Parametric approaches are well suited to analyze datasets with multiple independent variables (Tabachnick et al., 2001)

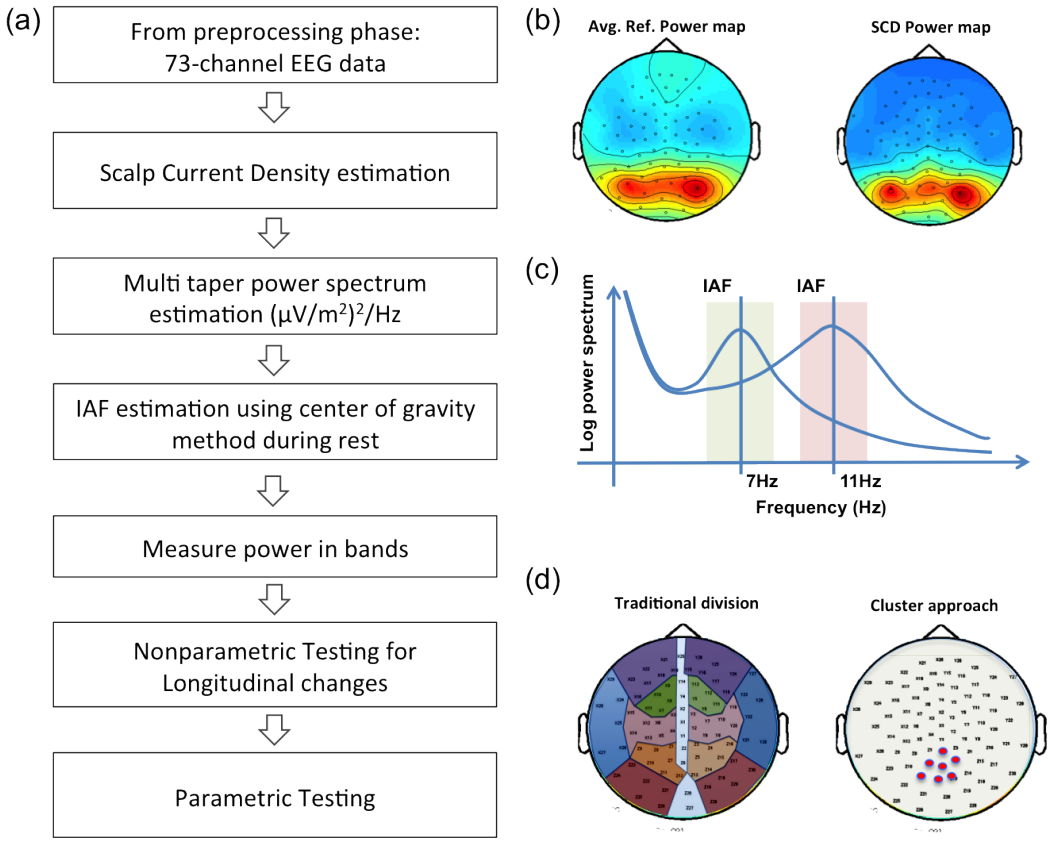

Figure 4.2: Spectral analysis of oscillatory activity (Color figure). (a) After preprocessing, there is a six-step pipeline for spectral analysis. These steps were implemented to make sure the data was as free of interference by artifacts as possible. (b) This image illustrates why scalp current density (SCD) estimation is important. During eyes-closed conditions, huge alpha activity can be seen in the occipital regions. Thus, when the average reference is subtracted from each channel, artifactual negative dips (as seen in central regions on left topographical map) can result. However, such artifacts are avoided in SCD and a reference-free estimation is achieved (right topographical map). (c) This plot shows why individual alpha frequency (IAF) estimation is important. With age, the alpha peak frequency (or IAF) varies, it increases during development and then decreases with aging (Klimesch, 1999). Thus, in studies like current one, where the participants' age varies from 22-69 years, it is important to estimate IAF and define frequency bands based on IAF as an anchor. Otherwise, the changes in spectral power in one band (e.g. alpha) can be wrongly attributed to other frequency band (e.g. theta; Cahn and Polich, 2006). (d) This image shows why non-parametric cluster-based approach (on right) is better than traditional division into regions (on left). Assuming there is an effect in the highlighted channels (colored red, on right), the traditional approach will have less statistical power, after division into regions, than the cluster-based approach.

4.2.5 Meditation Training

The participants practiced meditation under the guidance of Dr. Alan Wallace. Each participant practiced for several hours each day. Training consisted of sustaining attention to breath, mental events, or awareness (on average six hrs/day combined) and generating beneficial aspirations (on average one hr/day) (Wallace, 2006). Please refer to Chapter 2 for details about the training.

4.3 Results

To understand how cortical oscillations change with intensive meditation training, over the period of three months, a set of three experiments were run. First, changes in IAF during rest and meditation were measured to test the hypothesis that alpha frequency reduces with meditation training. Second, longitudinal changes in cortical activity of participants and controls were analyzed using nonparametric cluster-based permutation testing. The clusters retrieved from this approach were then log-transformed and analyzed parametrically to explore the group/retreat by test-point (three month period) interactions. The hypothesis here was that given the nature of the meditation practice, increased activation should be found in attention-related areas. Further, the intense practice (on average 6 hrs/day) should induce changes in cortical activity even during rest (a.k.a. trait changes). Third, the cortical activity changes observed in the first two experiments were systematically correlated with psychological function and performance during attention-related tasks. The goal for this experiment was to ground changes in cortical activity into behavioral interpretations.

4.3.1 Experiment 1: Longitudinal changes in individual alpha frequency

One of the consistent findings in meditation research literature is that of reduced alpha frequency in meditators (Cahn and Polich, 2006). Thus, the hypothesis for this experiment was that similar reductions (in IAF) should also be seen in the retreat groups (RG1 and

RG2) due to training. IAF values were calculated for each of the three states: pre-meditation rest, meditation, and post-meditation rest. Average values (and standard deviations), across participants, in each group, state, and test-point are presented in Table 4.2.

For the first retreat, repeated-measures ANOVA with between-subjects factors revealed an effect of state ($F(2, 84) = 10.9, p < 0.001$), test-point ($F(2, 84) = 29.121, p < 0.001$), and an interaction between group and test-points ($F(2, 84) = 10.753, p < 0.001$). The interaction was further explored using post-hoc analysis (Student's t-test, Bonferroni-corrected for nine tests). Collapsed across states, RG1 showed a drop in IAF value at the middle and end test-points (as compared to the beginning of the retreat). CG showed no difference in IAF across test-points. However, when CG became RG2, a similar drop as in RG1 was revealed in IAF values (Figure 4.3).

Altogether, the reduction previously seen only in long-term meditators was also found with just three months of intensive meditation training. Further, the reduction in IAF did not correlate with the meditation experience prior to the retreat and it was replicated in both the retreats. Correlation analysis (section 4.3.3) will shed some light on the relation between this reduction and the behavioral and self-reported measures. The next experiment was setup to explore the longitudinal changes in cortical activity associated with training, as described below.

4.3.2 Experiment 2: Longitudinal changes in spectral power

Changes in cortical activity, during rest and meditation, were assessed by measuring longitudinal changes in spectral power across all the channels. Given the focused-attention style of meditation (during training and assessment), increased activity in attention-related networks due to training was predicted. Further, provided the intense nature of practice (on average 6 hrs/day), changes in cortical activity even during rest states (both pre- and post-meditation) was also predicted. This change in trait itself will be a strong effect than the previously shown short-term carry over effects of meditation (Lutz et al., 2004).

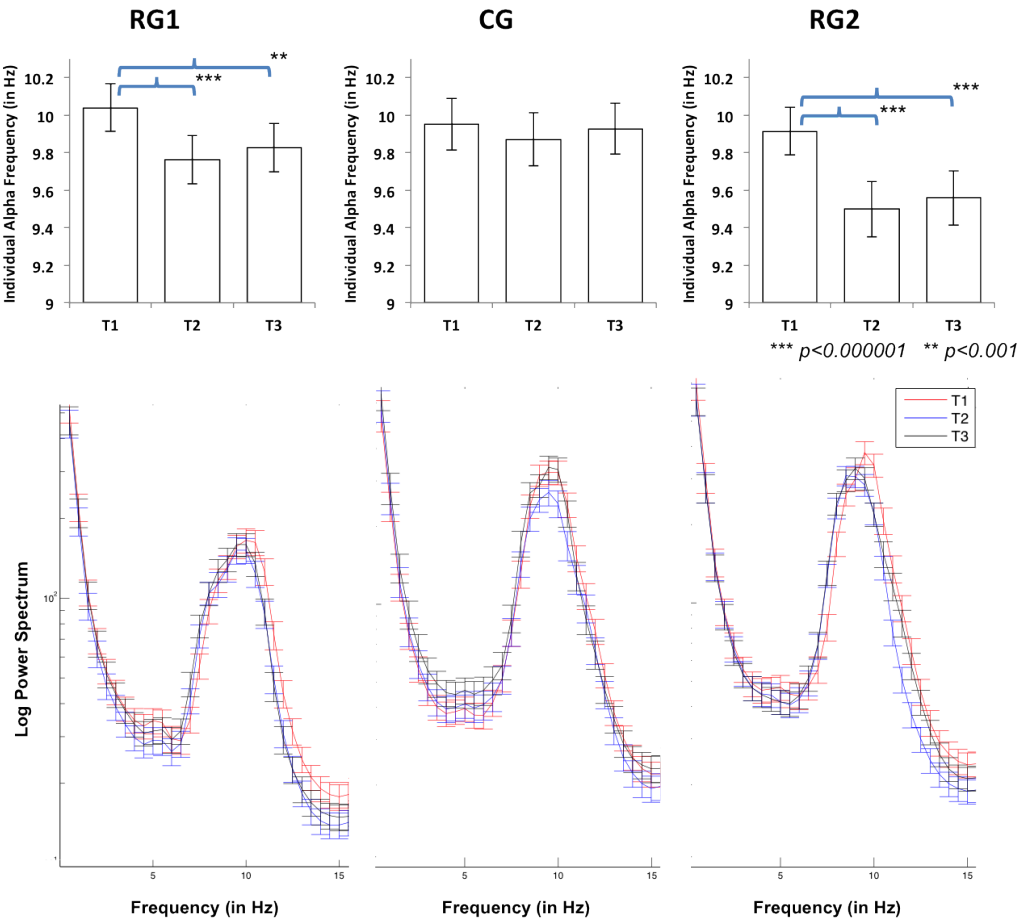

Figure 4.3: Change in Individual Alpha Frequency (IAF), across test-points (Color figure). Top row: shows IAF values, averaged across participants and states, in each group and at each test-point. Error bars are standard errors of the mean. Significant reductions in IAF were found in both retreat groups at T2 and T3 (as compared to T1). No change was found in the CG. Bottom row: Power spectrum, averaged over across participants and states, in each group and at each test-point. Close up at around 10 Hz to see the change in IAF in RG1 and RG2 at T2 and T3 (as compared to T1). No such change is evident in CG. Thus, even though a small effect (in terms of value) in IAF was found, it was a strong effect (in terms of statistical power). Although consistent effect in experienced meditators, its biological basis are unknown. Computational modeling will be employed in Chapter 5 to better understand its basis.

		RG1		CG		RG2	
		Mean	Std. Dev.	Mean	Std. Dev.	Mean	Std. Dev.
R1	T1	10.012	0.630	9.848	0.650	9.803	0.593
	T2	9.734	0.603	9.790	0.660	9.439	0.676
	T3	9.794	0.629	9.842	0.626	9.512	0.656
M	T1	10.058	0.554	10.010	0.645	9.949	0.610
	T2	9.785	0.595	9.916	0.671	9.531	0.685
	T3	9.845	0.592	9.959	0.634	9.614	0.740
R2	T1	10.049	0.621	9.998	0.680	9.993	0.609
	T2	9.767	0.634	9.905	0.669	9.524	0.723
	T3	9.843	0.648	9.982	0.694	9.550	0.670

Table 4.2: Mean and standard deviation values of IAF for each state (pre-meditation rest (R1), meditation (M), and post-meditation rest (R2)), test-point (beginning (T1), middle (T2), and end of retreat (T3)), and group. Drop in IAF can be seen for each state in the retreat groups, across test-points.

These longitudinal changes were assessed using a hybrid approach (Figure 4.4). In this way, first a non-parametric cluster-based permutation testing was performed to find spatio-spectro-temporal clusters that change significantly due to training, in each group separately. Second, a parametric approach was employed on the log-transformed spectral power extracted from the clusters to measure the main effects and interactions (between group/retreat and test-points). Two different parametric methods were used for each retreat: (1) a repeated-measures ANOVA with between-subject factors to compare spectral band power in RG1 and CG; and (2) a repeated-measures ANOVA with within-subject factors to compare spectral-band power in CG and RG2.

Results from this hybrid approach are shown in Figures 4.5, 4.6, 4.7, 4.8, 4.9, and 4.10. Results from each state are discussed below.

Pre-meditation rest During the eyes-closed pre-meditation rest state, changes in spectral power (across test-points) were found in both the retreat groups. No cluster was found in the control group. The changes were found in two frequency bands: alpha3 and beta band.

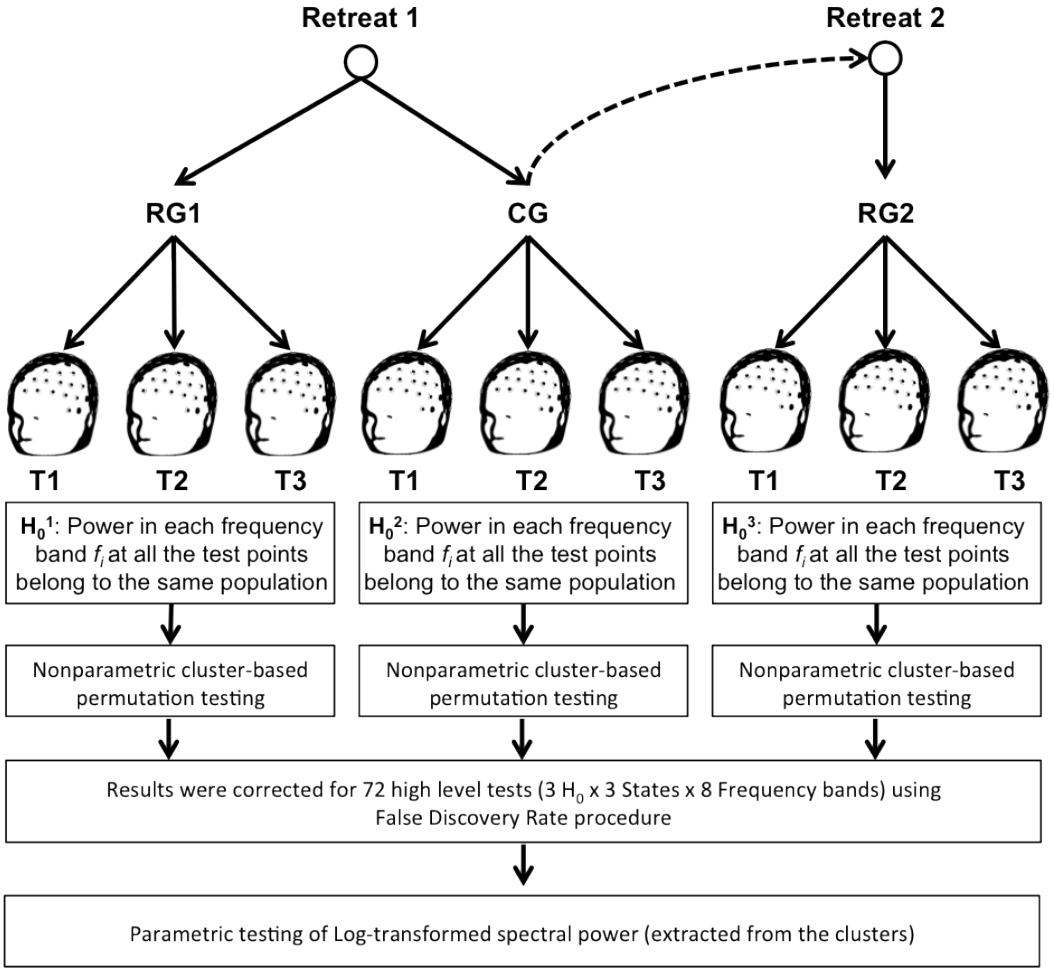

Figure 4.4: Experimental setup to measure longitudinal changes in spectral power. Three groups of participants were tested (RG1 and CG in Retreat1 and RG2 in Retreat2 (i.e. CG when they returned for their own retreat)). Each group was tested thrice during the three-month retreat period: beginning (T1), middle (T2), and end (T3). After estimating spectral power in each band, three null hypotheses were tested (H_0^1, H_0^2, and H_0^3) using the non-parametric cluster-based permutation analysis, followed by False Discovery Rate (FDR) correction (Benjamini and Hochberg, 1995) for 72 high level nonparametric tests. Later, log-transformed spectral power (extracted from the clusters found by nonparametric analysis) was tested using parametric approach to measure the interactions between group/retreat and test-points. Overall, this setup provides a hybrid statistical approach to do longitudinal analysis of spectral power.

First, in the alpha3 band (1.0×IAF-1.2×IAF Hz), changes in the spectral power, using cluster analysis, were observed only in RG2 at the right-anterior-frontal region (Figure 4.5). No effect was found for CG or RG1 in this band. Further, comparing CG and RG2, using the log-transformed spectral power extracted from the cluster location found in RG2, repeated-measures ANOVA with within-subjects factors revealed main effect of retreat ($F(1, 21) = 25.458, p < 0.001$) and an interaction between retreat and test-point ($F(2, 42) = 5.822, p < 0.01$). The interaction was further explored using post-hoc Student's t-test method (Bonferroni-corrected for six tests). Significant drop in alpha3-band power was found at the end of retreat (as compared to beginning of retreat) in RG2 ($p < 0.001$). No change was found in CG for the same cluster location. It is important to note that CG and RG2 are the same individuals, simply tested when they were controls vs. when they were subsequently (6 months later) engaged in their own retreat.

Another similar cluster was found in the full alpha band (0.6×IAF-1.2×IAF Hz), again only in RG2. However, this cluster just missed ($p_{\text{cluster}} = 0.0062$) the critical alpha level set by FDR ($p_{\text{cluster}}^{\text{critical}} <= 0.0046$). For completeness the cluster and its post-hoc results are shown in Figure 4.6.

Second, in the beta band (1.2×IAF-30 Hz), changes in the spectral power, using cluster analysis, were observed in both RG1 and RG2. However, as before, no such cluster was found in CG. In RG1, the cluster location was more posterior than RG2. But, in both retreats, clusters were found at bilateral-midline regions (Figure 4.7). Further, RG1 and CG were compared using the log-transformed spectral power extracted from the cluster location found in RG1. Repeated-measures ANOVA with between-subjects factors revealed main effects of group ($F(1, 42) = 4.693, p < 0.05$) and test-points ($F(2, 84) = 12.471, p < 0.001$) and an interaction between group and test-point ($F(2, 84) = 8.675, p < 0.001$). This interaction was further explored using post-hoc Student's t-test method (Bonferroni-corrected for six tests) and a significant drop in beta-band power was found at the middle ($p < 0.0000001$) and at the end ($p < 0.001$) of retreat (as compared to the beginning of

retreat) in RG1. Interestingly, an increase in beta-band power was found in CG at the end ($p = 0.0076$) of retreat (as compared to the middle of retreat). It is important to note that no cluster was found in CG itself (hence, tested on the channels found in RG1). Further, this small effect in CG was found in the opposite direction (increase in beta power) to that found in retreat groups. Thus, it is possible that this effect was found only due to multiple comparisons and is not a true effect.

CG and RG2 were also compared using the log-transformed beta-band power extracted from the cluster location found in RG2. Repeated-measures ANOVA with within-subjects factors revealed main effects of retreat ($F(1, 21) = 12.758, p < 0.01$) and test-points ($F(2, 42) = 5.384, p < 0.01$) and an interaction between group and test-point ($F(2, 42) = 11.965, p < 0.001$). The interaction was further explored using post-hoc Student's t-test method (Bonferroni-corrected for six tests) and a significant drop in beta-band power was found at the middle ($p < 0.0001$) and the end ($p < 0.0001$) test-points (as compared to the beginning of retreat) in RG2. No reduction or increase was found in beta-band power across test-points for CG.

Meditation During the six minutes of focused-attention meditation (on breath sensations), changes in spectral band power were observed only in the retreat groups. No cluster was found in the control group. The changes were again found in alpha3 and beta frequency bands.

First, in the alpha3 band (1.0×IAF-1.2×IAF Hz), cluster analysis of spectral power revealed significant changes in RG2 at frontal-midline channels (Figure 4.8). No cluster was found in RG1 or CG. Further, CG and RG2 were compared using log-transformed spectral power extracted from the cluster (found in RG2) and repeated-measures ANOVA with within-subjects factors revealed significant interaction between retreat and test-point factors ($F(2, 42) = 5.504, p < 0.01$). This interaction was further explored using post-hoc Student's t-test method (Bonferroni-corrected for six tests) and a significant drop in alpha3-band power was observed at the end ($p < 0.001$) of retreat (as compared to the beginning

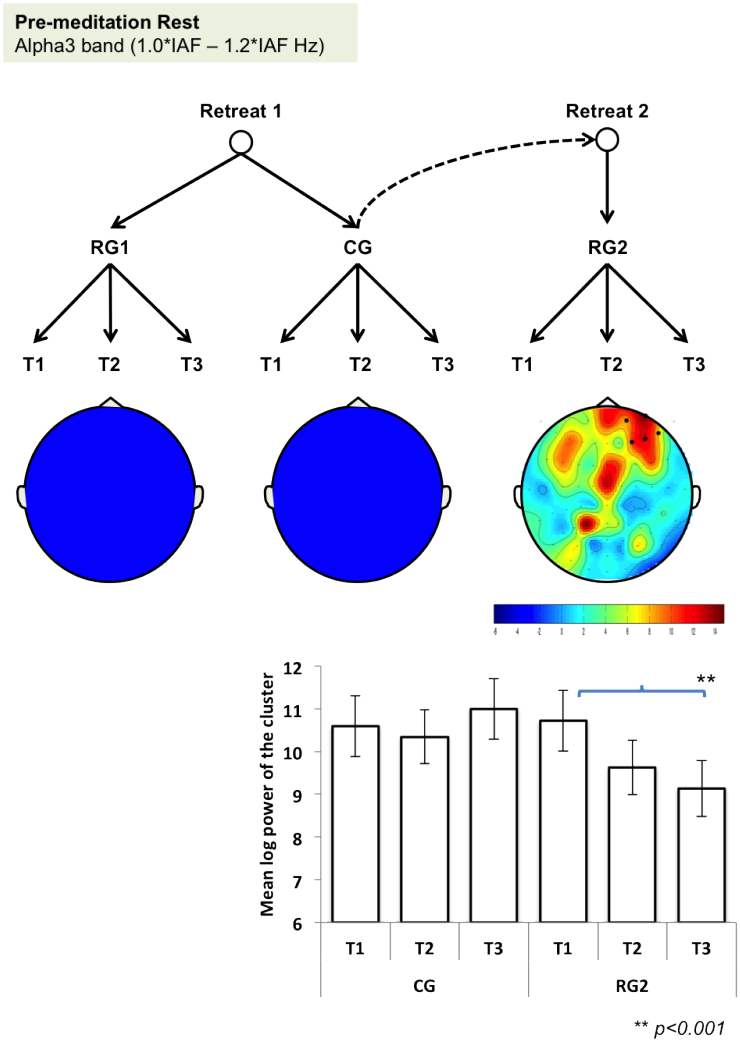

Figure 4.5: Reduction in alpha3-band power during pre-meditation rest (Color figure). No clusters were found for RG1 or CG. However, right-anterior-frontal cluster was found for RG2 ($p_{\text{cluster}} = 0.0046$). The topographic plot shows F-statistic for testing all three test-points. The critical alpha level set by FDR procedure is $p^{\text{critical}}_{\text{cluster}} <= 0.0046$. Further, retreat by test-point interaction was found using parametric analysis of this cluster (in RG2 and CG). Using Student's t-test method (Bonferroni-corrected for six tests), significant drop in alpha3 power was found at T3 (compared to T1) in RG2 ($p < 0.001$). No change was found in CG for the same cluster location. Overall, the result was in line with the second hypothesis about the trait effect to resting states.

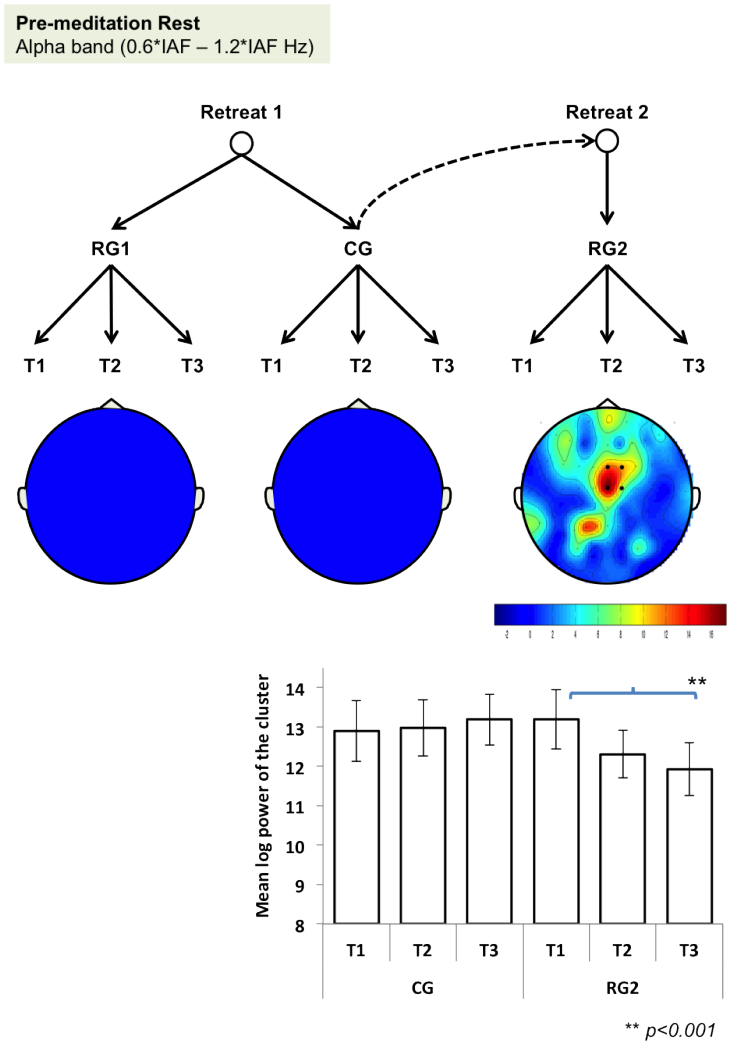

Figure 4.6: **Weak effect** Reduction in alpha-band power during pre-meditation rest (Color figure). This cluster just missed ($p_{\text{cluster}} = 0.0062$) the critical alpha level set by FDR ($p_{\text{cluster}}^{\text{critical}} <= 0.0046$). FDR procedure can be overly conservative at times, and hence for completeness the results are included here. Fronto-central-midline cluster was found only in RG2. The topographic plot shows F-statistic for testing all three test-points. Further, comparing CG and RG2, using the log-transformed spectral power extracted from the cluster location found in RG2, repeated-measures ANOVA with within-subjects factors revealed main effect of retreat ($F(1, 21) = 4.854, p < 0.05$) and an interaction between retreat and test-point ($F(2, 42) = 5.790, p < 0.01$). The interaction was further explored using post-hoc Student's t-test method (Bonferroni-corrected for six tests). Significant drop in alpha power was found at T3 (compared to T1) in RG2 ($p < 0.001$). No change was found in CG for the same cluster location. Again, the result was in line with the second hypothesis.

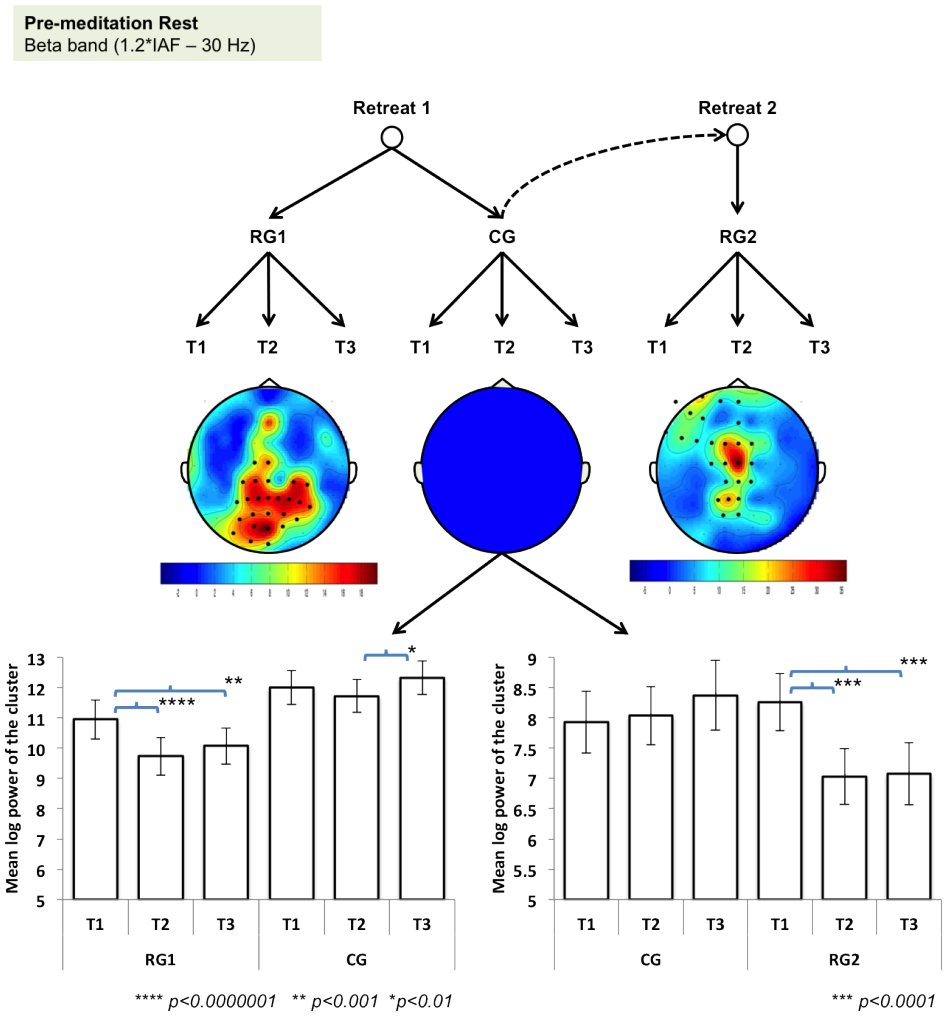

Figure 4.7: Reduction in beta-band power during pre-meditation rest (Color figure). No clusters were found for CG. However, bilateral-posterior-midline cluster was found for RG1 ($p_{\text{cluster}} = 0.000$) and midline-fronto-central-parietal cluster for RG2 ($p_{\text{cluster}} = 0.0001$). The topographic plot shows F-statistic for testing all three test-points. The critical alpha level set by FDR procedure is $p_{\text{cluster}}^{\text{critical}} <= 0.0046$. Further, group by test-point interaction, while comparing RG1 and CG, was found using parametric analysis of the cluster found in RG1. Using Student's t-test method (Bonferroni-corrected for six tests), significant drop in beta power was found at T2 ($p < 0.0000001$) and T3 ($p < 0.001$) (compared to T1) in RG1. Interestingly, a barely significant increase in beta power was found in CG at T3 (compared to T2). While comparing RG2 and CG, using parametric analysis, for the cluster found in RG2, a significant drop in beta power was found at T2 ($p < 0.0001$) and T3 ($p < 0.0001$) (compared to T1). No change in cluster power was found in CG. Overall, similar effects of beta-power reduction were found in both retreat groups and the results were in line with the second hypothesis.

of retreat). No change in alpha3-band power was observed in CG for this cluster.

Second, cluster analysis of the spectral power in beta band (1.2×IAF-30 Hz) revealed significant changes in both the retreat groups. No change was found for the control group. As in the case of pre-meditation rest, the location of cluster in RG1 was more posterior than in RG2. However, in both the retreats, clusters were found at bilateral-midline regions (Figure 4.9). Comparing RG1 and CG using parametric analysis of the log-transformed spectral power, extracted from the cluster found in RG1, revealed main effects of group ($F(1, 42) = 5.013, p < 0.05$) and test-point ($F(1.711^4, 84) = 8.008, p < 0.01$) and an interaction between group and test-point ($F(1.711, 84) = 5.342, p < 0.05$). The interaction was further explored using Student's t-test approach (with Bonferroni correction for six individual tests). A significant reduction ($p < 0.0000001$) in beta power was found at the middle test-point (as compared to the beginning) and a non-significant reduction ($p < 0.05$ compared to Bonferroni critical $p_{critical} = 0.0083$) was found at the end test-point (as compared to the beginning). No effect was found in the CG.

Similar parametric analysis between RG2 and CG, using the cluster found in RG2, was performed and a repeated-measures ANOVA with within-subjects factor revealed main effects of retreat ($F(1, 21) = 18.75, p < 0.001$) and test-point ($F(2, 42) = 7.534, p < 0.01$) and an interaction between retreat and test-point ($F(2, 42) = 11.817, p < 0.001$). The interaction revealed no effect in the CG, but did reveal a significant drop in beta power in RG2 at the middle ($p < 0.001$) and the end ($p < 0.00001$) of retreat (compared to the beginning of retreat).

Post-meditation rest Finally, the post-meditation rest was analyzed and a cluster was found in the beta band in RG2. No cluster was found for the CG or RG1. The cluster was located at posterior-bilateral midline region (Figure 4.10). This location was in line with the beta-band clusters found in other states. Parametric analysis between RG2 and CG

[4]Corrected using Greenhouse-Geisser method for violation of Sphericity assumption (Mauchly's Sphericity test $p < 0.05$)

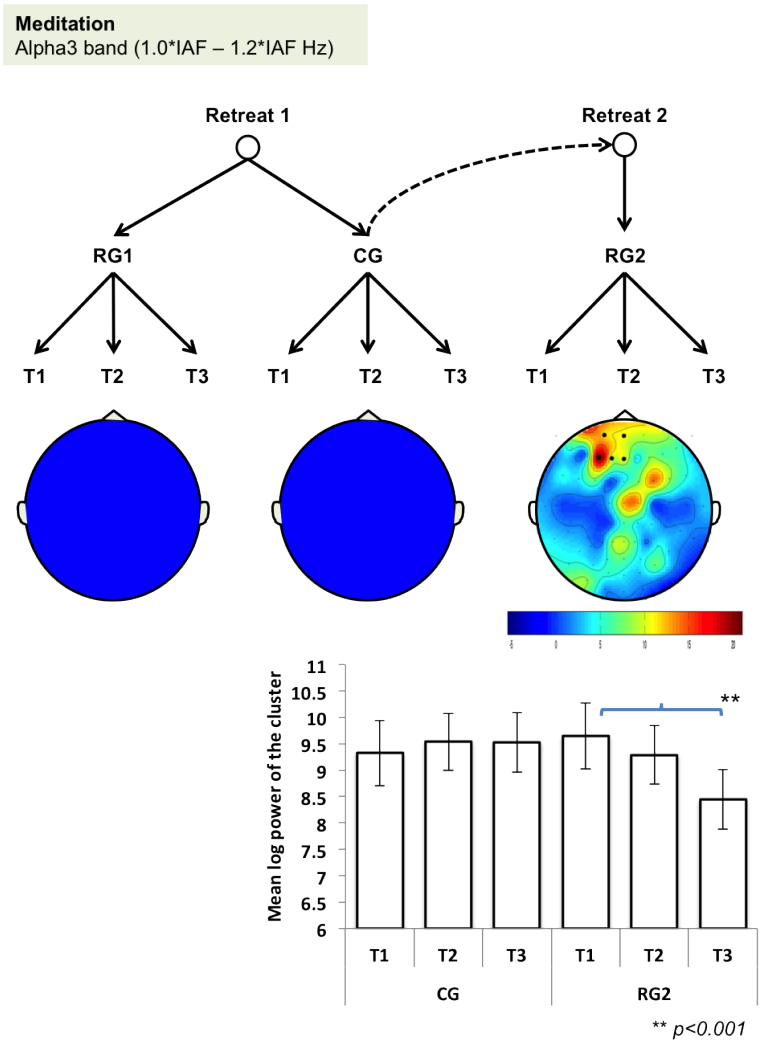

Figure 4.8: Reduction in alpha3-band power during focused-attention meditation (Color figure). No clusters were found for RG1 or CG. However, midline-anterior-frontal cluster was found for RG2 ($p_{\text{cluster}} = 0.0024$). The topographic plot shows F-statistic for testing all three test-points. The critical alpha level set by FDR procedure is $p_{\text{cluster}}^{\text{critical}} <= 0.0046$. Further, retreat by test-point interaction was found using parametric analysis of this cluster (in RG2 and CG). Using Student's t-test method (Bonferroni-corrected for six tests), significant drop in alpha3 power was found at T3 (compared to T1) in RG2 ($p < 0.001$). No change was found in CG for the same cluster location. Overall, the reduction was in line with the first hypothesis about increased cortical activity in the attention-related regions during meditation.

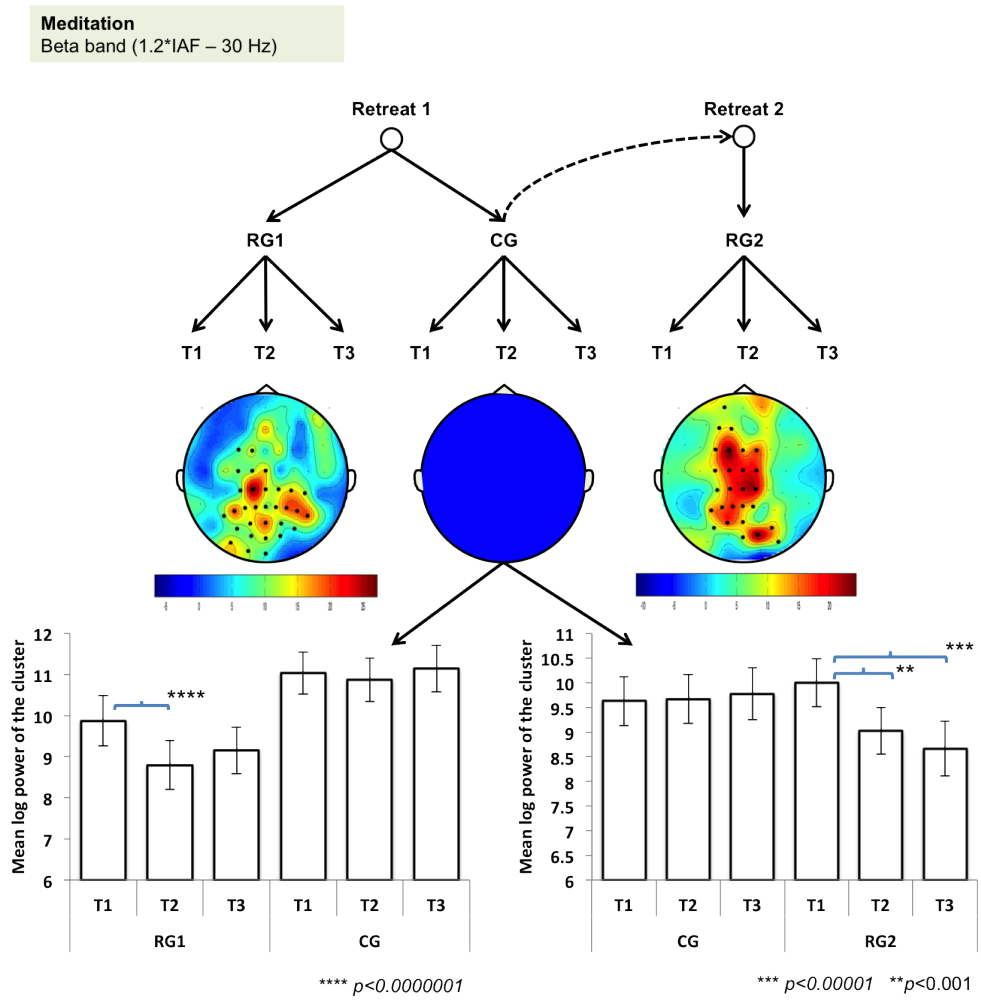

Figure 4.9: Reduction in beta-band power during focused-attention meditation (Color figure). No clusters were found for CG. However, bilateral-posterior-midline cluster was found for RG1 ($p_{\text{cluster}} = 0.000$) and midline-central-parietal cluster for RG2 ($p_{\text{cluster}} = 0.000$). The topographic plot shows F-statistic for testing all three test-points. The critical alpha level set by FDR procedure is $p_{\text{cluster}}^{\text{critical}} <= 0.0046$. Further, group by test-point interaction, while comparing RG1 and CG, was found using parametric analysis of the cluster found in RG1. Using Student's t-test method (Bonferroni-corrected for six tests), significant drop in beta power was found at T2 ($p < 0.0000001$) (compared to T1) in RG1. However, only a trend reduction ($p < 0.05$ compared to Bonferroni critical $p_{critical} <= 0.0083$) was found at T3 (compared to T1) in RG1. No change was found in CG for the same cluster location. While comparing RG2 and CG, using parametric analysis, for the cluster found in RG2, a significant drop in beta power was found at T2 ($p < 0.001$) and T3 ($p < 0.00001$) (compared to T1). No change in cluster power was found in CG. Overall, similar effects of beta-power reduction were found in both retreat groups, indicating increased cortical activity in the attention-related regions.

for this cluster revealed main effects of retreat ($F(1, 21) = 17.737, p < 0.001$), test-point ($F(2, 42) = 7.282, p < 0.01$), and an interaction between retreat and test-point ($F(2, 42) = 8.173, p < 0.01$). Further, post-hoc Student's t-test (with Bonferroni correction for six tests) revealed a significant drop in beta power in RG2 at the middle ($p < 0.0001$) and the end ($p < 0.001$) of retreat (as compared to the beginning). No change in beta-band power was found in the control group.

Summary Altogether, reduced spectral power in two frequency bands (alpha3 and beta) was found in both the retreat groups. The reduction was evident at the middle and the end point of the retreat, as compared to the beginning. No significant change was found between middle and end points of the retreat, indicating a step-wise drop in power. No cluster was found in the control group, and parametric analysis also revealed no change in power for the control group.

Reduction in alpha- and beta-band power has been related to increased cortical activity (Goldman et al., 2002; Laufs et al., 2003; Yuan et al., 2010; Ritter et al., 2009; Scheeringa et al., 2011). The results thereby indicate increased cortical activity in the retreat groups due to meditation training. Further, the clusters were located at the bilateral-midline-parietal locations for the beta band and the anterior-frontal for the alpha3 band. These areas have been previously implicated as attentional regions (Posner and Dehaene, 1994; Posner and Rothbart, 2007; Capotosto et al., 2009), hence substantiating the first hypothesis that meditation training provides increased cortical activity in the attention-related networks, even during resting states.

Regarding the second hypothesis, i.e. the trait effect of meditation training on resting states, the experiment found similar drop in alpha- and beta-band power during resting states as found during meditation state itself. Further, the effect was seen in both pre-meditation and post-meditation rest. This result indicates that the trait effect is not just limited to a small duration of time after meditation (i.e. during post-meditation rest), but also provides more generalized changes to the "default-mode" of the brain.

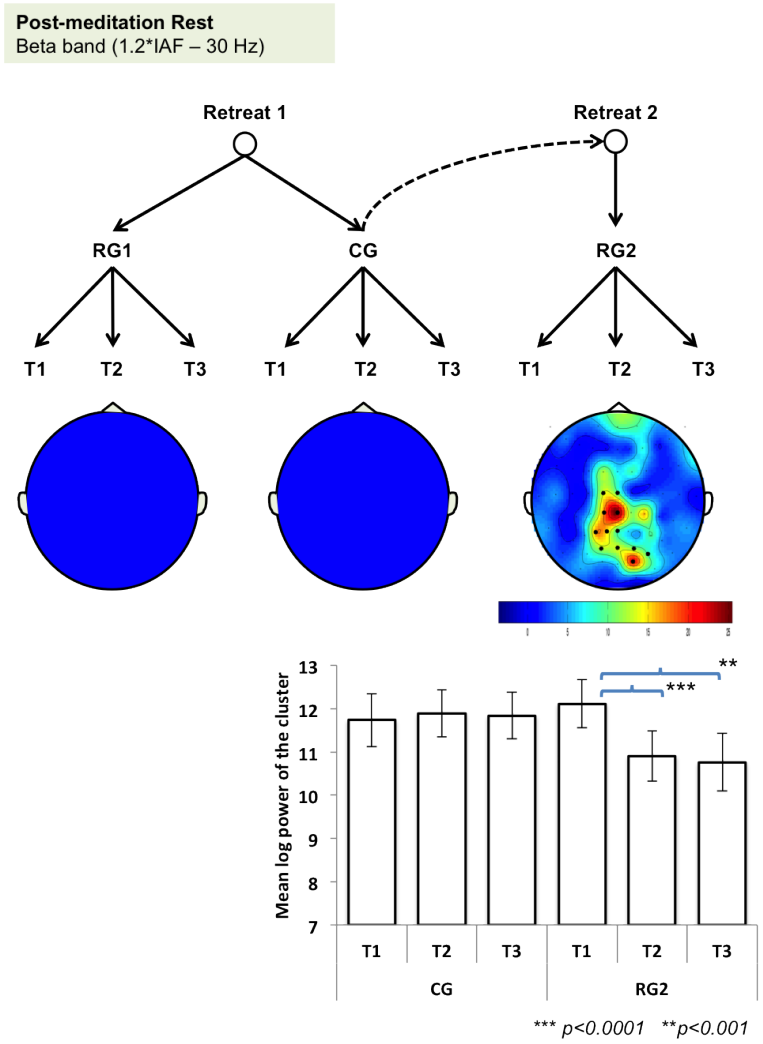

Figure 4.10: Reduction in beta-band power during post-meditation rest (Color figure). No clusters were found for RG1 or CG. However, posterior-midline cluster was found for RG2 ($p_{\text{cluster}} = 0.0002$). The topographic plot shows F-statistic for testing all three test-points. The critical alpha level set by FDR procedure is $p_{\text{cluster}}^{\text{critical}} <= 0.0046$. Further, retreat by test-point interaction was found using parametric analysis of this cluster (in RG2 and CG). Using Student's t-test method (Bonferroni-corrected for six tests), significant drop in beta power was found at T2 ($p < 0.0001$) and T3 ($p < 0.001$) (compared to T1) in RG2. No change was found in CG for the same cluster location. Overall, the reduction was in line the second hypothesis about the trait effects of meditation.

In sum, the observed changes in spectral power supported the hypotheses. Next, the changes found in cortical activity were correlated with other behavioral and psychological functions.

4.3.3 Experiment 3: Correlating longitudinal changes in cortical activity with other measures

In the third experiment, the observed changes in cortical activity patterns were correlated with behavioral and other measures also acquired during the retreat. There were two goals: (1) to ground the changes observed in cortical activation in behavior and other self-reported psychological functions; and (2) to disentangle the effects of meditation training from that of other factors.

The longitudinal changes in spectral power were compared with (a) self-reported measures, including lifetime hours spent in meditation, daily time spent in meditation during the retreat, and adaptive socio-emotional functioning (Sahdra et al., 2011); (b) performance in attention-related tasks, including sustained attention task (MacLean et al., 2010) and response inhibition task (Sahdra et al., 2011); and (c) difference in elevation between the participants' place of residence and the retreat location.

Self-reported measures In order to understand a complex brain phenomenon like meditation, it is necessary to complement the observer's perspective (i.e. scientific measurements) with first-person accounts of the actual lived experience (phenomenology; Varela and Shear, 1999). It is important to note that in the current work self-reported questionnaires were used for correlation, instead of actual accounts by the participants (e.g., structured interviews). Thus, the presented correlations are only first approximations of the unique individual experience.

During the retreat period, participants recorded the time spent in meditation practices each day. Additionally, the participants answered questionnaires about their adaptive functioning at the beginning and the end of retreats. If these observations correlate well

with the measured changes in cortical activity, the changes are likely due to the meditation practice and not other factors associated with the retreat. The hypothesis is that the participants with more hours of practice and with more enhanced mental states should have larger changes in the cortical activity with training.

It is important to note that some of these self-reported observations were quite easy to quantify, e.g. daily time spent in meditation. However, to quantify more complex parameters (from the questionnaires), theoretical models were constructed. One such model used second-order latent difference score approach to cover the following self-reported observations: avoidant attachment, attachment anxiety, depression, anxiety, neuroticism, difficulties in emotional regulation, mindfulness, ego resiliency, empathy, extroversion, agreeableness, conscientiousness, openness to experience, and psychological well-being (Sahdra et al., 2011). The longitudinal changes, due to meditation training, in these observations were attributed to a single latent factor named as adaptive socio-emotional functioning (AF; Sahdra et al., 2011).

Starting with longitudinal changes in the individual alpha-frequency values, significant correlations were found between reduction in IAF and daily time spent in meditation, for both the retreat groups (Figure 4.11). In RG1, the reduction in IAF values were related with daily time spent in the shamatha meditation ($r(20) = -0.442, p < 0.05$), while in RG2, the reduction in IAF values were related with daily time spent in the compassion meditation ($r(20) = -0.453, p < 0.05$). Thus, the more the participants meditated, the more the IAF values dropped. It is interesting that time spent in different meditation practices correlated with reduction in IAF in different retreats. However, still, the biological basis for this drop in IAF is unclear, perhaps computational modeling can shed more light on this.

Next, the observed changes in spectral power, across test-points, were correlated with the self-reported measures (Figure 4.12). In RG1, significant correlation ($r(20) = -0.445, p < 0.05$) between reduction in beta-band power during meditation and changes

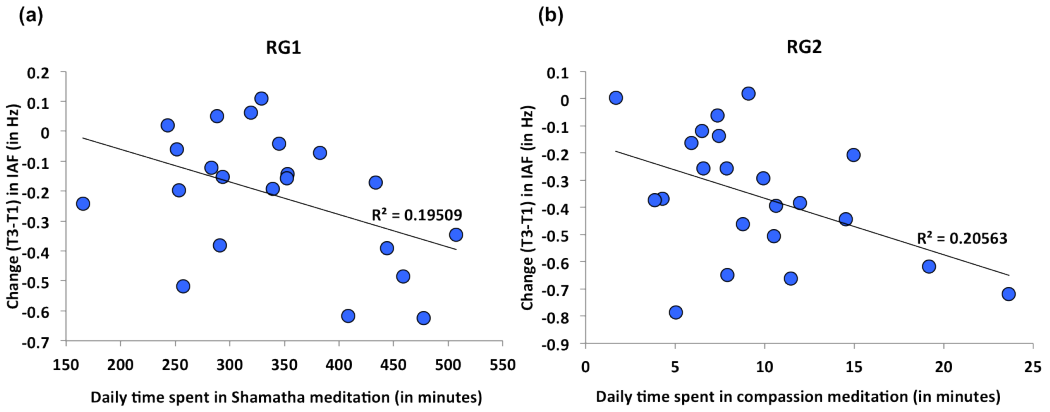

Figure 4.11: Correlation between reduction in individual alpha frequency (IAF) and self-reported measures (daily time spent in meditations). These relations suggest that the more the participants spent time in meditation, the more was the drop in IAF. Thereby providing some bases for the reduction observed in IAF (Figure 4.3).

in adaptive socio-emotional functioning were observed. This relation suggests that participants with more reduced beta-band power, during meditation, had better adaptive functioning at the end of retreat. No such correlation was found in RG2. However, in RG2, the reduction in beta-band power during meditation correlated with daily time spent in shamatha meditation ($r(20) = -0.584, p < 0.005$), suggesting that the more the participants meditated, the more beta-band power during meditation dropped.

Altogether, interesting correlations were found between the cortical activity changes and self-reported measures. These relations provide a basis for claiming that the cortical activity changes are associated with intensive meditation training. In the next set of correlations, the changes observed on the scalp were related to performance improvements in sustained attention and response inhibition tasks.

Performance in attention-related tasks In addition to participating in the meditation experiment, participants also took part in a number of attention related tasks (e.g. sustained attention (MacLean et al., 2010); response inhibition (Sahdra et al., 2011) etc.). Since

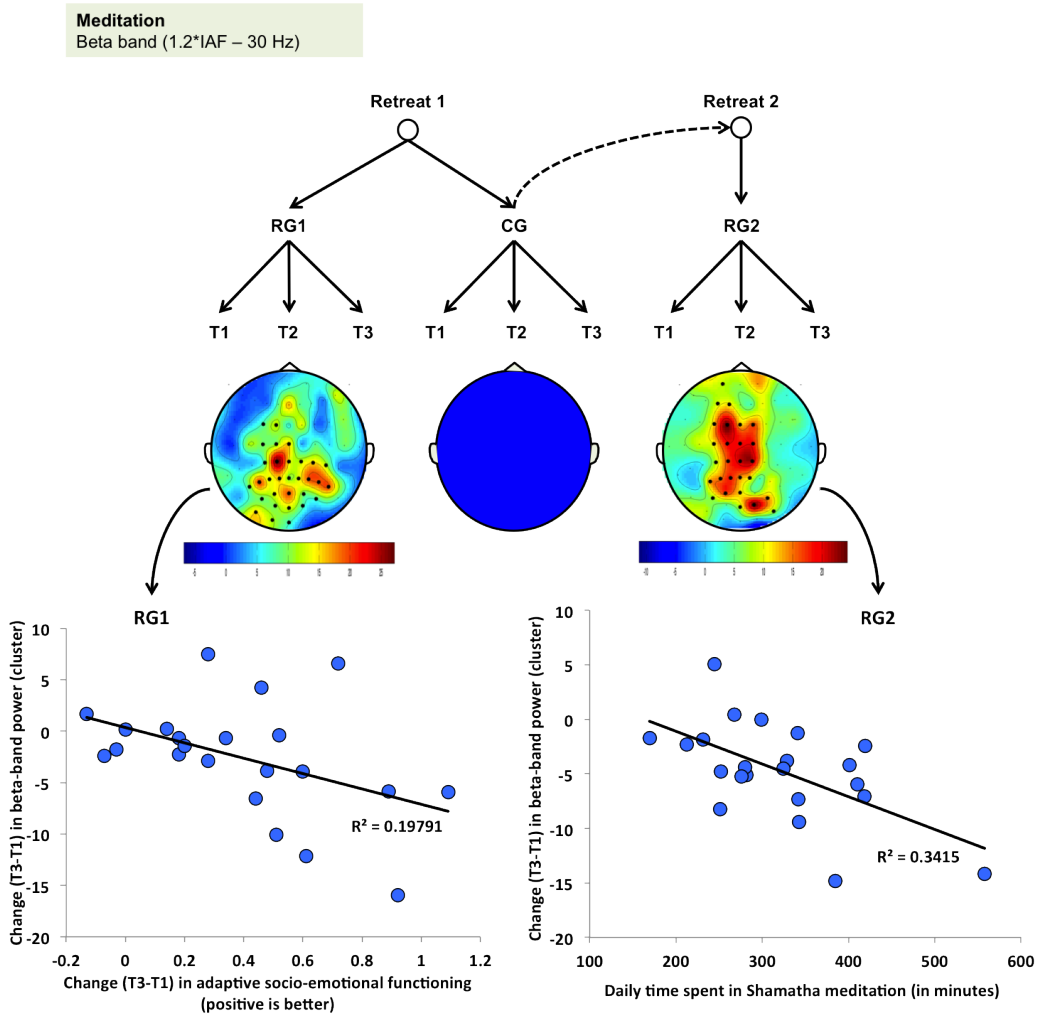

Figure 4.12: Correlation between reduction in beta-band power during meditation and the self-reported measures: daily time spent in meditations and change in adaptive socio-emotional functioning (Color figure). The relation found in RG1 suggests that higher reduction in beta-band power during meditation could result in higher adaptive functioning (or emotional well-being). In RG2, however, no such relation was found. Further, the drop in beta-band power in RG2 did correlate with daily time spent in shamatha meditation. Hence, the more participants meditated the more the beta-band power dropped during meditation. Overall, these relations grounded the change in cortical activity during meditation into self-reported psychological functions.

the primary meditation practice was that of sustaining attention on breath sensations, the hypothesis was that changes in cortical activity should correlate to performance in sustained attention tasks. Further, another study from the Shamatha project showed that meditation training enhances cognitive control (Sahdra et al., 2011). Thus, changes in cortical activity associated with meditation training should also correlate with participants' performance in the response inhibition task.

Previous work on the Shamatha project showed that the participants' improved sustained-attention (or vigilance), due to increased perceptual discrimination, after three-months of meditation training (MacLean et al., 2010). Performance was assessed on a 32-minute line discrimination task. The participants were required to press a button during rare-target trials (short lines, presented only in 10% of the stimuli). In the first retreat, parameter estimation using sequential testing (PEST) method was used at each test-point, to make the task highly demanding of sustained attention by setting the length of short lines at participants' visual discrimination threshold (75% accuracy). However, the perceptual threshold itself was improved in the retreat participants across test-points, thereby making the task harder for them as compared to the control group. Thus, the improvement in vigilance performance across test-points could not be evaluated. However, in the second retreat, PEST was only used at the first test-point, hence the improvements in vigilance dependent upon perceptual discrimination could be measured.

Changes in cortical activity observed during rest and meditation states were correlated with improvements in observed vigilance. A significant relation was found between reduction in alpha-band power, during pre-meditation rest, and change in vigilance decrement ($r(18) = -0.46, p < 0.05$) (Figure 4.13), thereby indicating that the participants with higher reduction in alpha-band power during resting state had better sustained attention performance during the task.

Second, correlations were performed between changes in cortical activity during rest and meditation and changes in participants' performance during response-inhibition

task (RIT). The task structure was similar to sustained attention task, but instead of responding to the rare target trials, the participants were asked to withhold their response to the target trials (Sahdra et al., 2011).

Unexpectedly, no significant correlation was found between reduction in spectral power, during rest and meditation and participants' improved performance in RIT.

Altogether, longitudinal change in cortical activity (although weak effect) was found to relate with performance improvements in sustained attention task, thereby substantiating the first hypothesis.

Difference in elevation The two retreats were conducted at the Shambhala Mountain Center in Red Feather Lakes, Colorado. The center is about 2370 meters above the sea level. For acclimatization, the participants in the control group arrived 3 days (range = 65-75 hr) before the beginning of testing.

Although every care was taken in collecting and preprocessing the scalp-recorded EEG data in order to avoid artifactual influence in the data, nonetheless sudden change in altitude is known to effect EEG (Guger et al., 2005). Thus, longitudinal changes in cortical activity, observed during rest and meditation, were correlated with difference in elevation between the participant's city of residence and the center. No significant correlations were found between the two, in any state or group.

Summary In sum, these three correlation experiments not only provided behavioral interpretation for the changes observed on the scalp, but also helped to rule out the influence of altitude.

4.4 Discussion

Summary of findings How does meditation affects oscillatory activity in the brain? - This question has been the driving force behind several EEG studies on meditation, for the

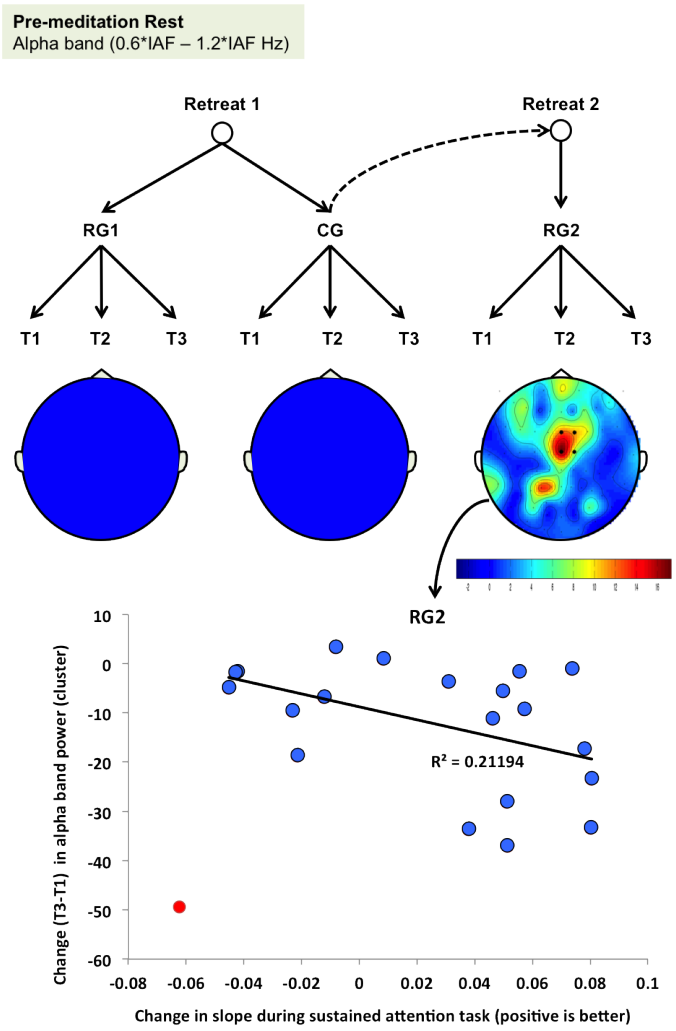

Figure 4.13: Correlation between reduction in alpha-band power (weak effect) during pre-meditation rest and performance in sustained attention task (Color figure). A significant correlation (after removing the outlier (> 1.5 s.d.) shown in red) was found between drop in alpha-band power for this cluster and improved vigilance during the sustained attention task. The relation suggests that the participants with higher drop in alpha power at fronto-central location, during rest, had less decrement in vigilance during the task, i.e. better sustained attention.

past 55 years or so (Cahn and Polich, 2006). Nonetheless, there is still a lack of consensus in answering this question (Cahn and Polich, 2006). Several factors, including inadequacy of control participants, individual differences, numerous meditation techniques, and lack of longitudinal studies, have lead to such a state of the field. The current study, however, aimed to control for several of these factors, while characterizing the longitudinal changes in cortical activity patterns during focused-attention meditation and rest. EEG data collected from two three-month retreats were analyzed. Reduction in alpha frequency was found in the retreat participants at the middle and the end point of retreat (as compared to the beginning). Further, the retreat participants also had reduced alpha- and beta-band power in the midline-frontal and bilateral-central-parietal areas, respectively, at the end of retreat. These longitudinal changes in cortical activity were then correlated with self-reported measures, performance in attention-related tasks, and altitude. Satisfactory correlations were found between self-reported progress in meditation practice, performance in sustained attention tasks, and changes in cortical activity. Hence, providing a behavioral interpretation for the observed cortical changes.

Individual alpha frequency In meditation research literature, several previous studies found a reduction in alpha frequency in experienced meditators (Cahn and Polich, 2006; Kasamatsu and Hirai, 1966; Wallace, 1970; Banquet, 1973; Zhang et al., 1988; Aftanas and Golocheikine, 2001; Aftanas and Golosheikin, 2003). In fact, this finding is among the very few consistent findings across meditation studies (Cahn and Polich, 2006). This reduction has been suggested to reflect one of the cumulative characteristic changes due to long-term meditation practice (Aftanas and Golosheikin, 2003). However, it is unclear as to what does this reduction mean in meditators.

Outside of meditation research literature, several studies have found the IAF (a.k.a. peak alpha frequency or PAF) to change with the task demands. For example, it has been shown to increase during a visuospatial, arithmetic, and auditory memory tasks as compared to control tasks (Osaka, 1984; Osaka et al., 1999). Further, Klimesch et al. (1990) suggested

that IAF can index the ability to memorize. Angelakis et al. (2004) showed that IAF can detect both trait and state differences in "cognitive preparedness" (which refer to the brain's capacity to perform high-level cognitive functions, and not simply alertness or arousal; Angelakis et al., 2004). Taking these studies into account would mean that the small (but statistically powerful) drop found in IAF indicates that retreat participants were at lesser cognitive capacity at end of retreat. However, this outcome is very unlikely, since the same retreat participants had enhanced perceptual discrimination, sustained attention, response inhibition, cognitive control, and even enhanced emotional well-being at the end of retreat (MacLean et al., 2010; Sahdra et al., 2011).

IAF is also shown to be highly stable intra-individual measure, which is also heritable (Posthuma et al., 2001). Further, a more recent study has suggested that IAF should be qualified as an individual's cortical activity signature, due to its high reproducibility (N*ä*pflin et al., 2007). Given these studies it becomes all the more important to understand the basis of reduction in IAF in meditators. Computational modeling can shed more light on the theoretical basis of this reduction, as will be discussed in the next chapter.

Alpha-band power Several early meditation studies found increased alpha-band power in meditators (Cahn and Polich, 2006; Aftanas and Golocheikine, 2001; Deepak et al., 1994; Wallace, 1970; Taneli and Krahne, 1987; Dunn et al., 1999). However, more recent work could not replicate these findings and rather reduction in alpha power was found in some (Baijal and Srinivasan, 2010; Cahn and Polich, 2006; Benson et al., 1990; Travis and Wallace, 1999; Jacobs and Lubar, 1989; Pagano et al., 1983). There could be several reasons for this variability, ranging from difference in assessed meditation techniques and lack of adequate controls, to individual differences. One important individual difference is that of alpha frequency. Experienced meditators are known to have reduced alpha frequency. Thus, if fixed frequency-band widths are used, the reduced IAF can cause changes in the theta-band to be wrongly attributed to the alpha-band.

In the current work, frequency-band widths were calculated individually for each

participant, based on their IAF values. A weak effect was found in the alpha-band power, during resting state at midline-frontal location, where a reduction in power was found at the end of retreat. Further, this reduction was related to the improvements in participants' performance in a vigilance task, thereby suggesting that intensive meditation practice of sustaining attention, primarily on breathing sensations, can induce changes in behavior even during rest. However, it is also important to understand the basis behind the reduction in alpha-band power. In previous research, alpha and beta rhythms have been shown to negatively correlate with the BOLD response in fMRI experiments (Goldman et al., 2002; Laufs et al., 2003; Yuan et al., 2010; Ritter et al., 2009; Scheeringa et al., 2011). Thus, it is reasonable to assume that the drop in alpha-band power during rest, at the frontal location, indicates increased frontal network engagement due to meditation. This increase could also be a sign of increased cognitive control (specifically the vigilance component) due to meditation retreat.

Spectral power in a sub-band of alpha rhythms, upper alpha-band (or alpha3), was also found to reduce in the anterior-frontal location after three months. This effect was evident during both rest and meditation states, but it was not replicated across the retreat groups and was only significant in the second retreat. Upper alpha power has been known to vary during development: it increases from early childhood to adulthood and then decreases during later part of life (Klimesch et al., 1990). It also decreases when the ability to respond to external stimuli decreases (e.g. transition from waking to sleeping stage; Tanaka et al., 1997). Desynchronization in the upper alpha band has been shown to be most sensitive (compared to other alpha sub-bands) to the encoding and processing of sensory-semantic information (Klimesch et al., 1997; Klimesch, 1999). It is hard to say exactly what the reduction in anterior-frontal upper-alpha power mean in the current study, due to lack of correlations with other variables. However, the reduction in upper alpha-band may reflect the inhibition of distracting external stimuli as a state effect during focused-attention on breathing sensations and as a trait effect during rest (in the absence of the task).

Beta-band power In the current study, participants practiced sustaining their attention on the breath sensations. This self-regulation of attention at such minute sensory events could in turn enhance cortical activity in the somatosensory regions. Previously, it has been argued that the anticipatory modulation of oscillatory activity in alpha- and beta-band can effect neural processing and behavior (van Ede et al., 2011). Since the alpha- and beta-band power are inversely correlated with cortical excitability (Goldman et al., 2002; Laufs et al., 2003; Yuan et al., 2010; Ritter et al., 2009; Scheeringa et al., 2011; Tamura et al., 2005; Sauseng et al., 2009), the reduction in power in these bands at posterior locations could indicate their functional role in sustaining attention to sensory events (van Ede et al., 2011). Thus, when the sensory input arrives at the time of high cortical activity in somatosensory regions, enhanced sensory processing is made possible. Similarly, distracting stimuli can be blocked with reduced cortical activity in sensory regions. Taking these studies into account, along with the fact that reduction in beta-band power was replicated across the retreat groups, and that these reductions correlated with daily time spent in meditation, it seems likely that the reduction in beta-band power facilitated enhanced sensory processing, thereby allowing continuous flow of sensory information associated with the breath sensations.

Previous studies on meditation have mixed results, on beta-band power, with some finding an increase (Benson et al., 1990; Dunn et al., 1999) and others a decrease in meditators (Ikemi, 1988; Jacobs et al., 1996; Travis et al., 2010). Future work in this area is required to disentangle the factors responsible for these variabilities. However, one plausible reason for this particular variability can be the difference in meditation techniques themselves. Thus, a technique where all sensory processing is inhibited could lead to increased beta-band power at posterior locations (thereby indicating reduced cortical excitability at those locations), whereas a technique where sustained focus is maintained on the sensory information will show reduced beta-band power at sensory regions (and hence more cortical activity).

Reduction in beta-band power has also been related to reduced complexity of EEG

dynamics during meditation (Aftanas and Golocheikine, 2002), thereby indicating that meditation involves "switching off" irrelevant networks to sustain focus on the object. Further, these nonlinear complexity estimates of EEG dynamics have been shown to increase with high emotional states (positive or negative, compared to neutral; Aftanas et al., 1998, 1994). Thus, given these studies on increased complexity with affective processing, the fact that less beta power indicates less complexity, and the correlation found (in current work) between reduced beta power and enhanced adaptive socio-emotional functioning at the end of retreat, all indicate that beta oscillations during meditation could play an important role in enhanced emotional balance (which is likely a prerequisite for increased adaptive functioning) in meditators.

Rest vs. Meditation states In the current work, longitudinal changes in cortical activity were analyzed in two resting states (one-minute before and after meditation) and in one meditation state (six minutes). However, the meditation state was not compared with the rest state, because of the difference in length of these states. By design, spectral analysis of meditation data would have higher SNR as compared to the short length resting state. However, in the future the plan is to study the temporal evolution of meditative states by dividing the six minutes of meditation data into smaller chunks and then comparing the pre- and post-meditation rest data with these chunks.

Nonetheless, just looking at the longitudinal changes, separately in rest and meditation, a similar pattern of changes was found in both states: Reduction in both alpha and beta power was found at the end of retreat. This similarity can be attributed to the trait effect of meditation, i.e. intensive meditation practice every day for three months altered the cortical activity such that the brain state during meditation generalized as the "default state" of the brain. This generalization infers that the participants at the end of meditation retreat were able to sustain their focus for longer durations even during rest. This inference is bolstered by the correlation found between reduction in alpha power during pre-meditation rest and improved participants' performance in the vigilance task.

4.5 Conclusion

Altogether, a comprehensive empirical study was conducted to find the cortical correlates of intensive meditation training. The spectral analysis on EEG data, collected during rest and meditation, provided crucial insights into how intensive meditation training alters the cortical activity during rest and meditation. Further, the ability to correlate these changes with other measures (like self-reported daily time spend in meditation) provided essential behavioral interpretations for these changes. Based on these analyses the next chapter theoretically explores how and why meditation training alters the cortical activity, the way it did.

Chapter 5

Computational Modeling

Measuring and interpreting longitudinal changes in cortical activity associated with intensive meditation training is a novel proposition in itself. However, it just answers "what" changed in the brain due to training and not "how" (mechanistic aspect) or "why" (teleological aspect) those changes appear. To begin to answer these questions, the dissertation employed computational modeling, which is presented in this chapter. First, an introduction to modeling and its application in neuroimaging is given. Second, the model architecture used in this dissertation and the extensions developed for it are presented. Third, four computational experiments are described, which were run to understand the mechanistic and teleological reasoning behind meditation. Fourth, correlations were performed to ground the modeling results into behavioral interpretations. Finally, the results and the broader implications of this work are discussed.

5.1 Introduction

Computational modeling was undertaken in order to formalize the mechanisms underlying meditation. This section provides an introduction to modeling, its previous applications in neuroimaging, and the approach used to model meditation.

5.1.1 What is computational modeling?

Computational modeling is a branch of mathematical modeling where extensive computational resources are employed to simulate, test, and refine theories about the behavior of a complex system. Usually, no intuitive closed-form analytical solutions are available for such complex systems. Hence, experimentation is done with the model parameters to decipher the underlying mechanisms responsible for apparent system behavior. Numerous computational models have been created to study a wide range of nonlinear complex systems, from weather forecasting (Done et al., 2004; Krishnamurti et al., 1999), financial markets (Campbell et al., 1997), and flight simulators (Zeigler et al., 2000), to brain behaviors (Itti and Koch, 2001; O'Reilly and Munakata, 2000; Saggar et al., 2007, 2010; Miikkulainen, 1993).

5.1.2 Why modeling?

The dissertation focuses on computational modeling of brain processes in general and in meditation in particular. The human brain is highly complex, and even a simple task involves several factors, e.g., attention, emotion, memory, learning, decision making, physical complexity of the brain itself, and the environment. Hence, it is currently impossible to create a single computational model to account for all aspects of the brain. In fact, it is impractical to model even a single factor completely. However, the goal of computational modeling is not necessarily to build absolutely correct theories. Some of the most successful models are based on approximate and relatively crude underlying assumptions. Rather, the goal is to enable progress in understanding a particular complex phenomenon (Shiffrin, 2010). The complex phenomena is simulated based on an initial formulation, of a theory, generating novel hypothesis from this simulation, collecting new data based on these predictions, and then refining the model (and the underlying theory itself). The process thereby implements the classic cycle of theory development, testing, and revision to advance the field (Figure 5.1; O'Reilly et al. (2010)).

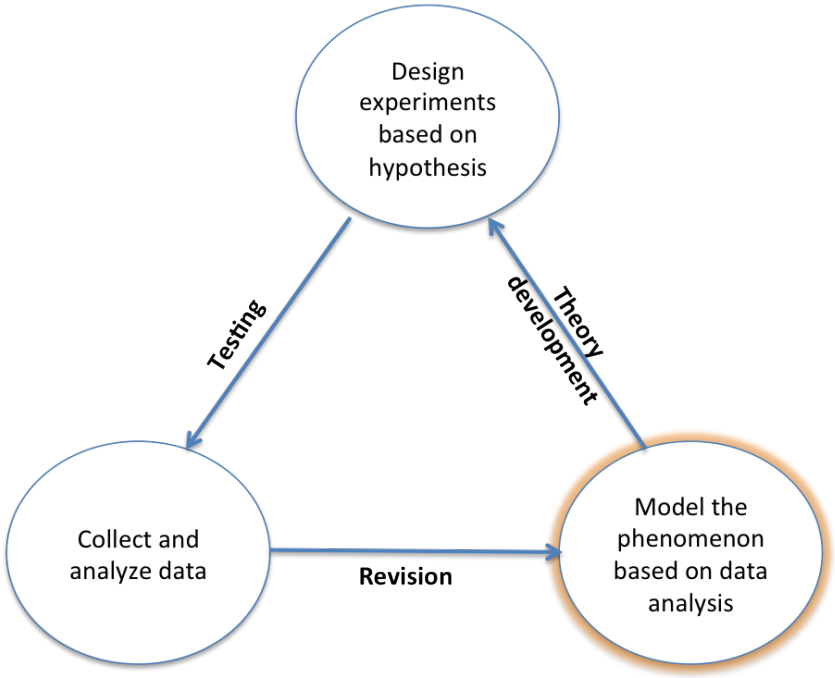

Figure 5.1: The cycle of theory development, testing, and revision. The modeling phase (highlighted) formalizes the analytical results and thereby provides concrete testable hypothesis to further understanding of a particular phenomenon.

5.1.3 Why model neuroimaging data?

With the recent advances in neuroimaging (fMRI, M/EEG, PET, DTI, etc.), an enormous amount of data is being collected to study human and animal cognition. These data are usually high-dimensional and voluminous, and require sophisticated statistical analyses (usually based on multivariate-regression) to extract meaningful information. However, it is becoming evident that it is not enough to just look at the areas where the changes in neural activity are found (even if those changes correlate with behavior), but it is more important to understand how the involved networks in the brain interact and evolve within the experimental context (Bullmore and Sporns, 2009; Shiffrin, 2010; Bassett and Bullmore, 2009). To this goal, models are now being developed to not just tie together neural activity and behavioral findings, but also advance our understanding of brain processes by providing

precise formulations and testable predictions about the underlying mechanisms (Anderson et al., 2008; Shiffrin, 2010).

5.1.4 Why model meditation?

Since the early 1960s, hundreds of studies have been performed to understand the effects of meditation (Cahn and Polich, 2006). Meditation has been shown to provide increased attentional stability (MacLean et al., 2010), enhanced cognitive control (Sahdra et al., 2011; Slagter et al., 2011), better regulation of attention and emotion (Lutz et al., 2008b), improved handling of brain resources (Slagter et al., 2007), better handling of physical pain (Grant et al., 2010), and even anatomical changes such as increased cortical thickness (Lazar et al., 2005). Due to such enhancements meditation research has generated a lot of interest in the cognitive neuroscience and health psychology community. However, to date, most of the research is done to find out the beneficial effects of meditation training. Very little is known about the neural processes underlying meditation. Exploration of such mechanisms can provide: (a) insights into cognitive system as a whole; and (b) better treatments of several neurodevelopmental disorders such as ADHD, autism, and schizophrenia.

The dissertation, thus, models the neuroimaging (EEG) data collected during two three-month long meditation retreats to advance our knowledge about meditation training. This is done by: (a) formulating the mechanisms underlying observed longitudinal changes in cortical-activity; and (b) providing testable hypotheses about the effects of meditation, for future research in this area.

5.1.5 Approach

Several approaches exist to model EEG (Rennie et al., 2002), ranging from purely phenomenological (Wright et al., 1990; Isaksson et al., 1981), to mean-field (Wilson and Cowan, 1972, 1973; Lopes da Silva et al., 1974; Freeman, 1972, 1987; Nunez, 1974a,b; Robinson et al., 2003), and detailed neural networks (Traub et al., 1997; Wilson and Bower,

1992; Lagerlund and Sharbrough, 1989; Lumer et al., 1997). Mean-field modeling is the best suited approach for this dissertation, since each EEG sensor (approximately 3-4 mm in diameter) covers thousands of neurons underneath (Pizzagalli, 2007). Hence, modeling a population of neurons for each sensor, while keeping the desired assumptions of anatomical and physiological constraints intact, is tractable. In contrast, modeling each sensor using a detailed neural network model would give rise to a combinatorial explosion during parameter fitting (73 EEG sensors times thousands of neurons for each sensor). Further, the purely phenomenological approach lacks the anatomical and physiological constraints required to understand the mechanisms underlying meditation. Please see Chapter 2 (Background) for a detailed comparison of these three approaches.

As a starting point for the model, the architecture of Robinson et al. (2001) was used. This model uses cortico-cortical, cortico-thalamic, and intra-thalamic loops to simulate EEG spectra at the scalp, which is appropriate in that sustained attention (the task under investigation during meditation) is believed to involve cortico-thalamic interactions. Further, the model was extended to measure (a) longitudinal changes in parameter values; and (b) connectivity changes in the reticular nucleus (TRN). The model architecture and extensions are provided in the next section, followed by novel computational experiments (Section 3), run to formalize the mechanisms underlying meditation. Section 4 presents the results from correlation analysis performed between the changes in model parameters, psychological function, and performance during attention-related tasks. Section 5 discusses current and future work, and is followed by concluding remarks.

Altogether, this dissertation presents the first computational model of meditation that grounds the empirical descriptions of meditation effects into a formal theory and makes testable predictions to advance the research in this area.

5.2 Methods

The current section describes the model architecture used and how it was extended to model the large EEG dataset. Further, it briefly introduces the data itself (see Chapter 2 for more details), followed by data fitting procedure.

5.2.1 Model Architecture

Broadly speaking, sustaining attention on an object (e.g., breath sensations), a task (e.g., balancing a pole), or even a phenomenon (e.g., movie watching) has been hypothesized to require cortico-thalamo-cortical interactions (LaBerge, 1997, 2005; Portas et al., 1998; McAlonan et al., 2008; Crick, 1984). The thalamus acts as a gateway to the cortex, filtering sensory information en route to cortex (bottom-up processing; McAlonan et al., 2008). The cortex also uses the reticular nucleus of thalamus (TRN) for attention modulation based on cortico-thalamic signals (top-down processing; Figure 5.2(a); McAlonan et al., 2008; Crick, 1984). Intra-thalamic circuits are also implicated in transferring sleep spindles to the cortex (Ferrarelli and Tononi, 2011). Thus, to model the core processes involved during sustained-attention meditation, the model architecture should include cortico-thalamic and thalamo-cortical interactions. Further, such a model should fit to high-density neuroimaging data (especially EEG), allowing dynamical analysis of the system, and generating concrete testable hypotheses about mechanisms underlying meditation.

Fortunately, such a model already exists: that of Robinson et al. (2001, 2002, 2003). The dissertation implements this model as it is and uses it as a starting point to understand core brain processes during meditation and rest. The model will then be extended, as described later in this section.

The Robinson et al. (2001) approach uses mean-field model of cortico-thalamic dynamics to simulate scalp-EEG. This approach is based on earlier work on continuum modeling for EEG (Freeman, 1975; Liley and Wright, 1994; Lopes da Silva et al., 1974; Nunez, 1974b; Rennie et al., 1999; Robinson et al., 1997, 1998; Wilson and Cowan, 1973).

The Robinson et al. (2001) model also includes primary neurophysiological principles and structures, ranging from transmission delays in axonal propagation, different neural populations (excitatory and inhibitory), connections dependent on range to subcortical and cortical networks.

The Robinson et al. (2001) model has been successfully used to mimic several features of the EEGs, including evoked potential (Kerr et al., 2008, 2011), seizure dynamics (Robinson et al., 2002; Breakspear et al., 2006), power spectra (Rennie et al., 2002; Robinson et al., 2001; Rowe et al., 2004a), coherence and correlations (Robinson, 2003), changes in arousal (Robinson et al., 2002), and even changes due to aging (Kerr et al., 2011, 2010b; van Albada et al., 2010). Further, model fitted to real data has been used to gain insights into subcortical and cortico-subcortical dynamics, by analyzing the changes in parameter values (a.k.a. inverse modeling; van Albada et al., 2010; Rowe et al., 2005a). Hence, the model provides an indispensable noninvasive method to generate hypothesis about the deep structures of the brain by providing average properties of large subcortical neural populations and their dynamics. Such an information about the populations cannot be retrieved even by the most invasive methods (van Albada et al., 2010).

A brief overview of this model is presented below, limited to modeling power spectra, divided into following parts: neurophysiology, cerebral connectivity, theoretical spectral and parameter sensitivity, and modeling the whole head. For more details see Rowe et al. (2004a).

Neurophysiology The neurophysiology of the model is presented in Figure 5.2(b), depicted using a cortical neuron. First, the action potentials from cortical excitatory, inhibitory, and subcortical neurons, represented as pulse-rate fields (ϕ_b; where, $b = e, i, s$ for cortical excitatory, inhibitory and subcortical connections), arrive at the dendritic tree. Second, due to this arrival the membrane potential (V_a) is perturbed. The magnitude of this perturbation is dependent upon the input and the rate constants of the dendrites. Third, the mean firing rate of this cortical neuron (Q_a) is set to follow nonlinear sigmoidal function.

Fourth, the action potential propagates away from the neuron, forming an average pulse density (ϕ_a). It is important to note that the magnitude of these densities reduce with distance and this effect was incorporated in the model as the damping rate, $\gamma_a = v_a/r_a$, where r_a is the characteristic range of type a axons and v_a is the velocity (Jirsa and Haken, 1996; Robinson et al., 1997; Rowe et al., 2004a).

By assuming that normal EEG activity is due to small perturbations about a steady state, the sigmoidal response of Q_a can be replaced by its steady-state slope ρ_a. This slope, when combined with the approximate number of input connections (N_{ab}) and an average synaptic strength (s_b), provides gain factor, $G_{ab} = \rho_a N_{ab} s_b$. These gains reflect the effect of input from various neural fields, ϕ_b, on the firing rate, Q_a, of excitatory and inhibitory neurons (Rowe et al., 2004a).

Cerebral connectivity The connectivity structure of the model is shown in detail in Figure 5.2(c). The pyramidal cells in the cortex have intracortical, cortico-cortical and subcortical connections. Each reciprocal connection can be represented as a gain, G_{ab}, where additional subscripts r and n refer to the TRN and the external source, respectively. Figure 5.2 provides detail about these gain factors.

To estimate the power spectrum, the interacting pathways can be written in Fourier domain (Rowe et al., 2004b) as,

$$\phi_s = T\phi_N + S\phi_e, \tag{5.1}$$

where

$$T = \frac{LG_{sn}e^{i\omega t_0/2}}{1 - LG_{sr}G_{rs}}, \tag{5.2}$$

$$S = \frac{(LG_{se} + LG_{sr}LG_{re})e^{i\omega t_0}}{1 - LG_{sr}LG_{rs}}. \tag{5.3}$$

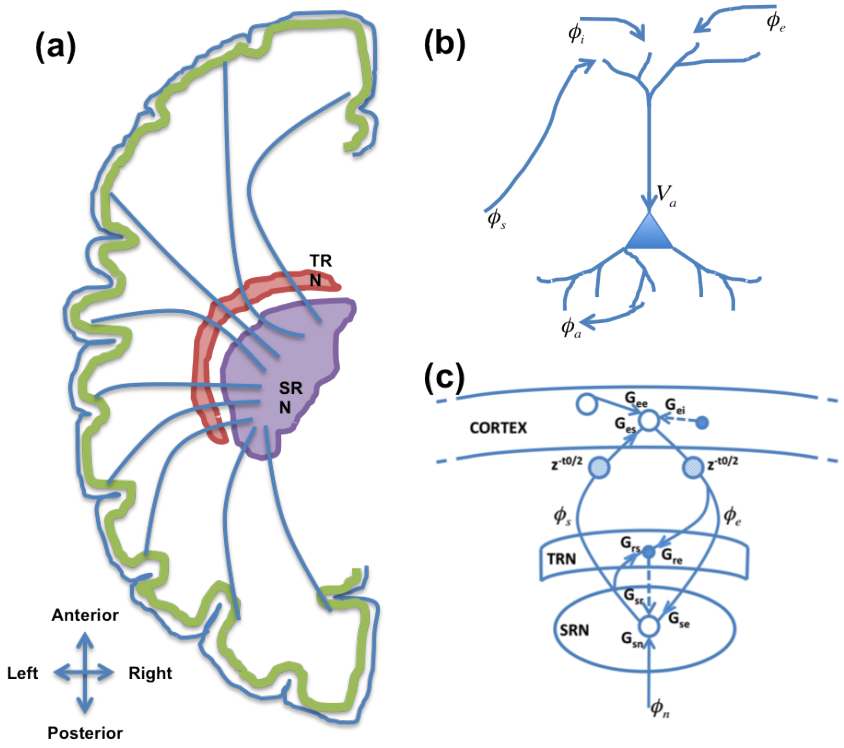

Figure 5.2: The cortico-cortical and the cortico-thalamo-cortical parameters of the Robinson et al. (2001) model. (a) Schematic of cortico-thalamic connections in the left hemisphere, via thalamic reticular nucleus (TRN). TRN acts as a shield for corticothalamic and thalamocortical signals, and is used by cortical areas for attention modulation (Crick, 1984; Zikopoulos and Barbas, 2007). (b) Basic neuronal physiology incorporated in the model, shown in a cortical neuron. Synaptic connections at the dendritic tree are shown emanating from pulse-rate fields ϕ_b, where, $b = e, i, s$ for cortical excitatory, inhibitory and subcortical connections. Somatic membrane potential is shown as V_a, where $a = e, i$, with resultant impulse firing rate Q_a and the spread of action potentials as field ϕ_a along the axons. (c) A schematic showing primary pathways between cortex, TRN, and thalamic secondary relay nuclei (SRN). The dashed line represents an inhibitory connection while the solid line represents an excitatory connection. The G_{ei} depicts the projections between local excitatory and inhibitory neurons in the cortex, while G_{ee} depicts similar projections between excitatory cortical neurons. These excitatory pyramidal neurons also project (through ϕ_e) to the thalamus, where signals may propagate (i) via TRN and then SRN with gain $G_{esre} = G_{es}G_{sr}G_{re}$, or (ii) directly via SRN with gain $G_{ese} = G_{es}G_{se}$. The SRN projects back (through ϕ_s) to the cortex, parametrized as the gain G_{es}. Within thalamus, the intrathalamic loop has the gain $G_{srs} = G_{sr}G_{rs}$. The cortical activation (through sensory input) occurs via ϕ_n and ϕ_s with the gain $G_{es}G_{sn}$. The diagram is adapted from Rowe et al. (2005a).

T represents the thalamic transfer function, S represents the corticothalamic transfer function, L represents the dendritic filtering, t_0 is the delay in the corticothalamic loop, and ϕ_N is the driving signal, approximated as white noise in space and time.

By linearizing the sigmoidal response, Q_a, and combining the Fourier domain forms of the remaining equations, spectral power density can be obtained (Robinson et al., 2001):

$$P_{\mathrm{EEG}}(\omega) = P_0 \left| \frac{L(\omega)T/G_{sn}}{1 - G_{ie}L(\omega)} \right|^2 \frac{(2\pi)^2}{l_x l_y} \sum_{m,n=-\infty}^{\infty} \frac{e^{-k_{m,n}^2/k_0^2}}{|k_{m,n}^2 r_e^2 + q^2(\omega) r_e^2|^2}, \tag{5.4}$$

where

$$q^2(\omega) r_e^2 = (1 - \frac{i\omega}{\gamma_e})^2 - \frac{G_{ee}L(\omega) + G_{es}L(\omega)S}{1 - G_{ei}L(\omega)}, \tag{5.5}$$

$$P_0 = \frac{\pi |\phi_n|^2}{r_e} G_{es} G_{sn}, \tag{5.6}$$

and the discrete wave numbers $k_{m,n}$ are defined by

$$k_{m,n}^2 r_e^2 = (2\pi m r_e / l_x)^2 + (2\pi n r_e / l_y)^2. \tag{5.7}$$

Here subscripts m, n denote mode numbers, related to boundary conditions. The value of these mode numbers can be restricted to $< f_{\max}/2$, where $f_{\max}$ is the maximum frequency one is interested in modeling (Robinson et al., 2001). The $e^{-k_{m,n}^2/k_0^2}$ factor is introduced to approximate the effect of volume conduction (Robinson et al., 2001).

The power due to EMG activity can also be accounted using a theoretical model, previously developed to determine the optimal bandwidth to measure pericranial EMG (Rowe et al., 2004b; Shwedyk et al., 1977; Van Boxtel et al., 1983; Van Boxtel, 2001). It is given by

$$P_{\mathrm{EMG}}(f) = \frac{A(f/f_c)^2}{[1 + (f/f_c)^2]^{1+\delta/2}}, \tag{5.8}$$

where f_c refers to low-frequency cut-off, δ the high frequency asymptotic power law index, and A the power normalization factor.

This theoretical spectrum can be fitted to the scalp EEG data; later in this section the fitting procedure is explained.

Theoretical power spectrum and sensitivity to parameters The model generated (or theoretical) power spectrum needs only ten or so parameters (Robinson et al., 2001), these parameters and their physiologically plausible range of values are listed in Table 5.1. The parameter set includes the gain for five loops: (a) excitatory cortico-thalamo-cortical loop ($G_{ese} = G_{es}G_{se}$); (b) inhibitory cortico-thalamo-cortical loop via TRN ($G_{esre} = G_{es}G_{sr}G_{re}$); (c) inhibitory intrathalamic loop ($G_{srs} = G_{sr}G_{rs}$); (d) excitatory cortico-cortical loop (G_{ee}); and (e) inhibitory cortico-cortical loop (G_{ei}). Additionally, the parameter set includes cortical damping rate (γ_e), decay rate of cell-body potential (α), cortico-thalamic axonal latency (t_0), normalization for power spectrum (p_0), and amplitude of the EMG component (A_{EMG}).

To analyze the sensitivity of each parameter on the spectrum, first, a theoretical spectrum was calculated using equations 1.4-1.8 and the nominal values for each of the ten parameters. As is evident from the figure (Figure 5.3), the theoretical spectrum is in accordance with the real EEG spectrum. Second, each parameter was varied (independently, keeping other parameters fixed to their nominal values) to see its effect on the power spectrum (Figure 5.3).

The sensitivity plots are useful in generating predictions about changes in the power spectrum, based on the changes in parameters. These predictions can also help infer changes in underlying physiology when the power spectrum changes in a particular way (Rowe et al., 2004a).

Modeling all the channels All the 73 channels in the EEG data were modeled independently using the Robinson et al. (2001) approach (as described above), making it possible to discover changes in parameters across the scalp. This methodology assumes spatial uniformity in model parameters, i.e., a change in a parameter value at a far away channel

Model	Parameter	Description	Limits	Initial Value
EEG model	γ_e	Cortical damping	[40, 400]	130 s^{-1}
	α	Dendritic decay rate	[10, 200]	75 s^{-1}
	β	Dendritic rise rate	-	3.8α*
	t_0	Conduction delay through thalamic nuclei and projections	[0.06, 0.13]	0.084s
	G_{ee}	Excitatory gain-pyramidal cells	[0, 50]	5.4
	G_{ei}	Local intracortical gain-stellate cells	[-35, -1]	-7
	G_{ese}	Corticothalamocortical gain via SRN	[0, 50]	5.6
	G_{esre}	Corticothalamocortical gain via TRN	[-30, 0]	-2.8
	G_{srs}	Intrathalamic gain	[-15,-0.5]	-0.6
	$k_0 r_e$	Volume conduction filter parameter	-	3.0*
	l_x, l_y	Linear dimension of cortex	-	0.5m*
	r_e	Characteristic pyramidal axon length	-	0.08m*
	P_0	Overall power normalization	-	Calculated
EMG model	A	Power normalization	[0, 99]	$0.5\mu V^2$/Hz
	f_{pk}	Spectra peak frequency	-	40Hz*
	δ	Asymptotic slope	-	2*

Table 5.1: Initial and fixed (indicated by *) values of the model parameters, as prescribed by Rowe et al. (2004a); these values were used as is for this work. The limits refer to the physiologically restricted ranges within which the solutions were explored. As per Rowe et al. (2004a), the limits, fixed values, and initial values are inline with independent sources and physiological measures (Robinson et al., 1997; Shwedyk et al., 1977; Van Boxtel, 2001; Rowe et al., 2004a).

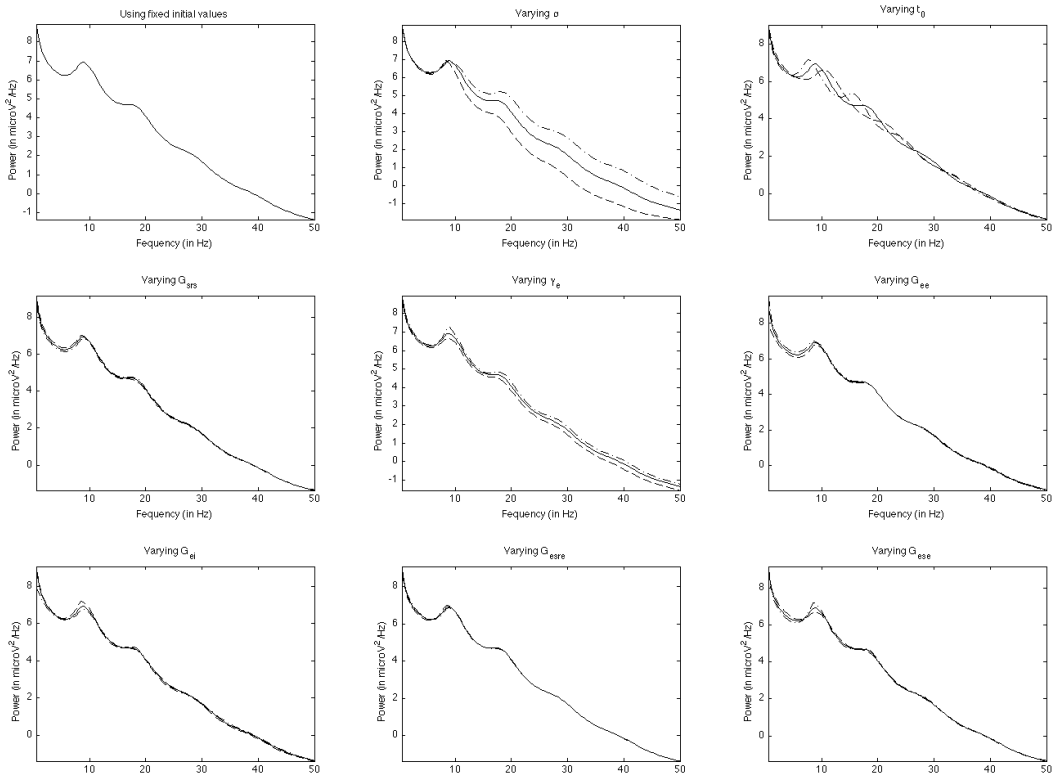

Figure 5.3: Independent effects of each parameter on the theoretical (simulated) power spectrum. Spectrum with solid line is estimated using fixed initial values. Spectrum with dashed (or dash-dotted) line is generated by decreasing (or increasing) the initial values by 20%. These sensitivity plots can be used to create and test hypothesis about the phenomenon under study.

will not affect the spectrum on the channel under observation (i.e., local independence is assumed). However, while modeling each channel, the values of parameters were chosen such that the modeled spectrum for each channel matched its real EEG spectrum. Such an approach, although just first approximation of real parameter values, has been previously used to successfully model various datasets and it is know as local effective value model (LEV; O'Connor and Robinson, 2004).

LEV models are favored, as compared to non-uniform coupled models, since they

are both analytically tractable and computationally light (O'Connor and Robinson, 2004). Further, it has been shown that for eyes-closed state, local independence assumption is maintained, except for two cases: (a) local activity at $<$ 2Hz frequency; and (b) local activity at alpha frequency. In these cases the local activity also depends on similar activity at distant sites. However, the effect at alpha frequency is much less than that at low-frequencies (O'Connor and Robinson, 2004). The model extensions, as described below, attempt to alleviate these issues.

5.2.2 Model Extensions

The model architecture was extended for two reasons: (1) to allow for measuring longitudinal changes in model parameters, and thereby gain insights into changes in cortical and subcortical interactions associated with meditation; and (2) to understand the role of TRN in regulating attention during meditation.

Longitudinal analysis The dissertation aims at modeling longitudinal changes in EEG data associated with meditation training. To fulfill this goal, the Robinson et al. (2001) approach was extended to find changes in parameter values across time (three test-points during the two three-month retreats) and space (73 channels). Analyzing temporal change will help understand the evolution of brain dynamics with meditation training. Further, analyzing changes in space would not only help in recognizing regional differences, but would also strengthen the LEV modeling approach (by taking information about the neighbors into account).

It is important to note that finding spatiotemporal changes in model parameters is a statistically difficult task, due to the multiple comparisons problem (MCP). For example, to assess changes in any one parameter for all 73 channels and at all three test-points (beginning, middle, and end of the retreat) would require $73 \times 3 = 219$ multiple comparisons. Now, for a predefined critical alpha level (e.g., $p = 0.05$), one needs to calculate a corrected critical alpha level to account for 219 multiple comparisons, to control for the

family-wise error rate (FWER). A simple method to correct for MCP, without taking into account any spatial information, would be to use Bonferroni correction (Bonferroni, 1935). But Bonferroni, being an overly conservative approach, would bring down the critical alpha value to $p = 0.05/219 = 0.00023$, thereby loosing sensitivity. Thus, to avoid being overly conservative and at the same time include spatial information, nonparametric cluster-based permutation testing (Maris and Oostenveld, 2007) was used to find out the spatio-temporal changes in model parameters. In contrast to parametric testing, nonparametric testing can solve the MCP in a straightforward way. Nonparametric testing is powerful for two reasons: (a) their validation does not dependent on the distribution of the data; and (b) any test statistic can be used to base the statistical inference (t- or F-statistic or any other). In particular, a cluster-based (to avoid spatial MCP) F-statistic (to avoid temporal MCP) can be used to keep the family-wise error rate low. This approach has been used previously for analyzing changes in power spectra (Maris and Oostenveld, 2007) and coherence (Maris et al., 2007) in MEG and EEG data. The algorithms for finding changes in model parameters are presented in Algorithm 4 and 5, based on previous work by Maris et al. (2007). Fieldtrip (Oostenveld et al., 2011), the open-source toolbox for Matlab®(MATLAB, 2010), was used to do these statistical tests.

Connectivity in TRN The current model accounts for the interactions between cortex, reticular nucleus (TRN), and specific relay nucleus (SRN) of the thalamus. However, it does not account for the within-TRN interactions.

The TRN has been known to play a crucial role in modulating the thalamic information to the cerebral cortex and vice versa (Guillery and Harting, 2003; Jones, 1975; Crick, 1984; Steriade et al., 1986; Sherman and Guillery, 2006; Zikopoulos and Barbas, 2007). This modulation is believed to be due to TRN's unique influential sieve-like positioning (Crick, 1984; Guillery et al., 1998; Sherman and Guillery, 2006) and extensive lateral connectivity (Scheibel and Scheibel, 1966). These properties are in marked contrast with the other thalamic nuclei, where the neurons rarely have lateral connections (Crick, 1984). An-

Algorithm 4 Group-level nonparametric statistical test for each model parameter p_i

Null Hypothesis(H_0): p_i does not differ across the three test-points

1. Collect p_i for all the 73-channels and all the subjects, during the three test-points in a single super-set.
2. Randomly partition the super-set to three equal sets.
3. Calculate the cluster-based test-statistic (using Algorithm 5).
4. Repeat Steps 2 and 3 a large number of times (e.g., 10,000) and construct a histogram of the test statistics.
5. Using the actually observed test-statistic and the histogram from Step 4, estimate the proportion of random partitions that resulted in larger test-statistic that the observed. This proportion is the p-value.
6. If the p-value is less that the critical alpha-level, then conclude that the null hypothesis H_0 is rejected and that the parameter p_i is different across test points.

Algorithm 5 Cluster-based test statistic

1. For every channel, compare the parameter value p_i across the three test-points, using F-statistic.
2. Select all channels, with F-statistic value larger than some threshold.
3. Cluster the selected channels in connected sets on the basis of spatial adjacency.
4. Calculate the cluster-level F-statistic, by taking a sum over all F-values within a cluster.
5. Output the largest of the cluster-level statistic.

other important distinction between TRN and other thalamic nuclei is that almost all the neurons in TRN are GABAergic (GABA = γ-aminobutryic acid), and hence inhibitory in nature, as opposed to the neurons in other nuclei that are almost always excitatory in nature (Houser et al., 1980; Oertel et al., 1983; Ohara et al., 1983; Crick, 1984). The structural topography of TRN has also been widely studied. Both the afferent and efferent connections are believed to be topographically organized according to the relevant cortical areas

and thalamic nuclei. (Scheibel and Scheibel, 1966; Montero and Scott, 1981; Jones, 1975; Minderhoud, 1971; Crabtree and Killackey, 1989; Lozsadi, 1995; Guillery et al., 1998; Lam and Sherman, 2011).

Due to such unique properties TRN acts like a nexus, providing ample opportunities for several functionally and structurally related cortical and thalamic areas to interact (Guillery et al., 1998). This hub of connections is thought to be responsible for attention regulation and other related cognitive control faculties (Crick, 1984; Sherman, 1996; Sherman and Guillery, 2002). The sustaining of attention during meditation is also hypothesized to involve TRN (Newberg and Iversen, 2003; Austin, 1999). Hence, it is crucial to model the intra-TRN dynamics to understand how regulation of attention is manifested using the TRN and how this regulation evolves with intensive meditation training. Such an understanding can also provide testable hypotheses for treating neurodevelopmental disorders, which occur due to lack of within-TRN connectivity (e.g., schizophrenia, Pinault, 2011; Ferrarelli and Tononi, 2011).

One approach for modeling lateral connectivity in TRN, using the Robinson et al. (2001) model, is to add additional parameters in the TRN layer and fit the data to these additional parameters. The challenge, however, is that modeling coupled connectivity between 73 TRN cells (due to 73 channel EEG) would be computationally and analytically intractable. Thus, a novel procedure was used to model the lateral connectivity, shown in Figure 5.4.

First, all the EEG channels were fit independently using the LEV approach. Second, to determine the lateral connectivity in TRN, white noise was injected into the modeled cortical cells. Third, activity in the TRN cells, due to injected noise in the cortical cells, was recorded using a formula derived using linear algebra on the model equations in time domain:

$$\phi_r(t) = \frac{\phi_e(t - t_0/2)[G_{esre} + G_{ese}G_{srs}] + \phi_n(t)[G_{es}G_{sn}G_{srs}]}{(G_{es}G_{sr})(1 - G_{srs})}, \tag{5.9}$$

where $G_{sn} = 1$, $G_{es} = \sqrt{G_{ese}}$, and $G_{sr} = -\sqrt{|G_{srs}|}$. Fourth, functional connectivity analysis was performed on the signal extracted from TRN cells (Figure 5.5). It is important to note that the injected noise will not induce any connectivity structure into the TRN cells and hence the extracted structure should depict the true connectivity. Fifth, longitudinal changes were assessed in the connectivity structure of TRN cells, due to meditation training, to understand the temporal and structural evolution of such changes.

Altogether, two extensions were applied to the model architecture. These extensions should allow for better understanding of the mechanisms underlying meditation. Section 5.3 uses this extended model to run four computational experiments.

5.2.3 Data acquisition and preparation

Details of the data are provided in Chapter 2. To recap, a high-density EEG cap was used in the project, with 88 equidistant scalp channels (later converted to normalized 10-10 system of 81-channels (Chatrian, 1985) for analysis). However, eight channels were rejected (out of the standard 81-channel system) due to the fact that the original 88-channel cap did not cover the scalp locations of these eight channels. Hence, 73-channels were used in the analysis. The 3-D locations of the electrodes on each participant were determined with a magnetic digitizer. The data was collected using the Biosemi Active Two system (BIOSEMI, 2006), at a sampling rate of 2048 Hz.

As was described in detail in Chapter 3, data preprocessing was done using second-order blind source separation (Belouchrani et al., 1997) and semi-automatic artifact removal tool. Components related to muscular activity, ocular activity, and interference from power lines were removed, without losing the neural components.

As described in Chapter 4, after preprocessing, data was transformed using scalp current density estimation (Kayser and Tenke, 2006; Kayser, 2009), to reduce the effects of volume conduction (Pizzagalli, 2007). Power spectra was then calculated using multi-tapered power spectral density estimation method (Mitra and Pesaran, 1999; Oostenveld

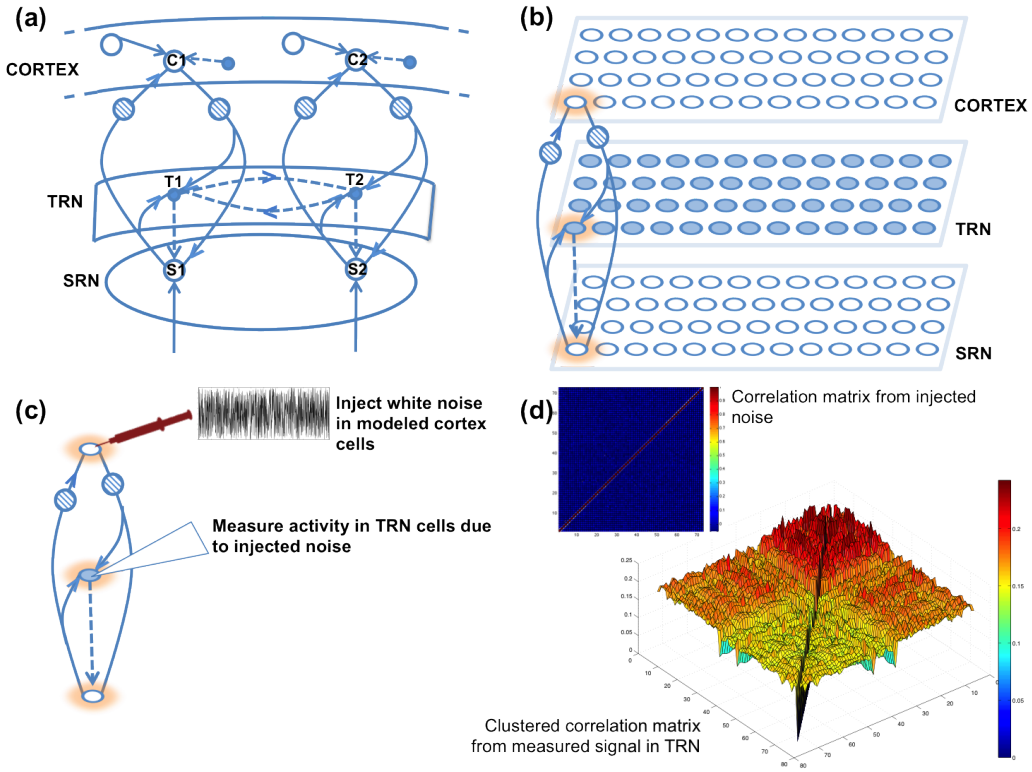

Figure 5.4: Measuring interactions in the modeled TRN layer. (a) Two units of the model and their interactions (dashed lines) in the TRN layer are shown. Ideally, gains for such interactions should be fitted along with all the other parameters of the model. However, given 73 such units in total, this approach will lead to a combinatorial explosion of the fitting procedure. (b) The three layers of the model. Each column is modeled independently using the LEV approach. (c) The procedure formalizing within-TRN connectivity. After fitting the model to real EEG data, white noise was injected in the cortical cells and the resulting activity in the TRN cells was measured. Further, connectivity analysis in the TRN layer was performed to understand the role of connectivity in TRN during meditation training. (d) Correlation matrix of injected white noise and of resulting activity in the TRN cells are shown. The diagonal elements in the TRN layer are set to zero for clarity. The structure found in the correlation matrix of TRN cells activity suggests that even though these cells were modeled independently, connectivity information between them can still be discovered.

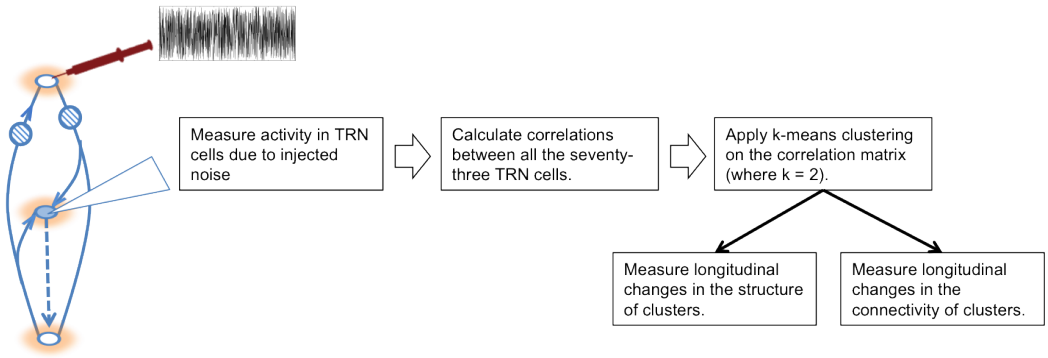

Figure 5.5: Connectivity analysis in the TRN layer. The resulting activity in TRN cells, due to injected white noise in the cortical cells, is measured using equation 5.9. Correlations between all the 73 TRN cells are estimated. For robust estimation several trials (n=100) of injecting noise and measuring correlation matrix was performed for each cell. The correlation matrix was then averaged over all trials and k-means clustering was performed on the matrix. The value of k was chosen based on the dendrogram generated by hierarchical clustering. Longitudinal changes in the structure and the connectivity of the clusters were evaluated. Altogether, using this procedure, it was possible to assess connectivity in TRN cells in a simple but elegant fashion.

et al., 2011).

Overall, this rich spatio-temporal dataset provides a unique opportunity to understand the mechanisms underlying meditation using computational modeling.

5.2.4 Participants

As discussed in detail in Chapter 2, thirty participants in the retreat group (RG1), and another thirty in wait-list control group (CG) were matched on age, sex, handedness, psychological measures, attention performance, and previous meditation experience. Retreat participants stayed at a remote mountain retreat center (Shambhala Mountain Center, CO) during the three months of training. Control group participants were flown to the retreat center for testing during Retreat1, and later comprised as participants for Retreat2 (RG2). Thus, data from the control group in Retreat1 acted a control for the retreat group in Re-

treat1, and as a control for themselves in Retreat2. Due to technical difficulties, data was analyzed only for twenty-two subjects in each group (RG1, CG, and RG2).

5.2.5 Task

Chapter 2 also provides detailed instructions for the task. The participants were assessed at several psychological tasks, at the three test-points (beginning, middle, and end) during the retreats. The model, however, is developed for the task where participants practiced eyes-closed focused-attention meditation (12 minutes) and rest (one minute before and after meditation). Due to technical difficulties, only the first six minutes of EEG data was recorded during meditation. Hence, the model was based on three eyes-closed states: one minute of pre-meditation rest, six minutes of focused-attention meditation, and one minute of post-meditation rest.

5.2.6 Meditation Training

The participants in this project practiced meditation under the guidance of Dr. Alan Wallace. Each participant practiced meditation for 6 hours each day, on average. Training consisted of sustained attention to breath sensations (primarily), mental events, or awareness, on average six hrs/day combined, and generating beneficial aspirations, on average one hr/day (Wallace, 2006). Detailed training structure is provided in Chapter 2.

5.2.7 Data Fitting

The sum of EEG and EMG spectrum was fit to that of the experimental spectrum $P_{\rm exp}(f)$ at each site on the head. The estimated power spectrum is given by

$$P_{\rm est}(f) = P_{\rm EEG}(f) + P_{\rm EMG}(f). \tag{5.10}$$

No smoothing was done on the experimental spectrum. The χ^2 error between $P_{\rm est}(f)$ and $P_{\rm exp}(f)$ was reduced using the trust-region-reflective constrained optimiza-

tion algorithm (Coleman and Li, 1993), implemented in MATLAB (MATLAB, 2010), in which χ^2 is calculated for each site as

$$\chi^2 = \sum_{i=1}^{N} [log(P_{\exp}(f_i)) - log(P_{\text{est}}(f_i))]^2. \tag{5.11}$$

The range for parameter values was physiologically bounded using the limits presented in Table 5.1).

5.3 Computational Experiments

The extended model was used to run four computational experiments to formally understand the mechanisms underlying meditation training. First, to test the ability of the model to account for real high-density EEG data, a data fitting experiment was performed. After fitting the model to the data collected during rest and meditation, a second experiment was run to understand *how* the model parameters changed during the three months of meditation training. Such insights would provide information about the evolution of cortical, cortico-thalamic, and intrathalamic dynamics. The third experiment was run to find the teleological reasoning behind the changes observed in model parameters, thus theoretically revealing *why* such changes were preferred by the brain (and what purpose those changes served). The fourth experiment was designed to understand how lateral connectivity in the modeled TRN changes with meditation training. Such an understanding can provide insight into how the TRN helps regulate attention in general (and during meditation in particular).

5.3.1 Experiment 1: Data Fitting

The extended model was used to fit the power spectra estimated from all the channels independently, during rest and meditation states, for each group (RG1, CG, and RG2), and at each test-point (before, middle, and end of retreat). The model successfully fitted all the channels over the scalp, as shown graphically in Figures 5.6, 5.7, and 5.8, while keeping all

the parameters in the physiologically plausible range (Tables 5.2 and 5.3).

Further, the statistics to measure the goodness-of-fit were calculated using the R-square method (MATLAB, 2010). R-square is used to find out how much variance in the data can be explained by the model and is defined as follows,

$$\mathrm{R}_{\mathrm{square}} = 1 - \frac{\sum_{i=1}^{n}(y_i - \hat{y}_i)^2}{\sum_{i=1}^{n}(y_i - \overline{y})^2}, \tag{5.12}$$

where y_i is the original data, $\hat{y}_i$ is the modeled data, and n represents the number of data points. The value of R-square can vary between 0 and 1, with a value closer to 1 indicating that a large proportion of variance in the data is accounted for by the model. Thus, a value of 0.9234 means that the model accounts for 92.34% variance in the data about the mean. Table 5.4 shows average R-square values for each group, state, and test-point. The model consistently accounted for more than 97% variance in the data in each group, state, and test-point.

To make sure that the fitting procedure did not differentiate between groups or test-points, a non-parametric false-discovery-rate (FDR) based approach was used to find differences in sum-squared errors for each channel across the three test-points within each group. Dependent sample F-statistic was used (with an alpha level of $p < 0.05$) to test difference across test-points. The results were post-hoc corrected for doing three such tests for each group (RG1, CG, and RG2). This approach is similar to the one used in longitudinal analysis of model parameters, except in this case an FDR-based test-statistic was used instead of the cluster-based test-statistic used in longitudinal analysis. The reason was that the accuracy of fitting each channel was to be tested independent of its neighbors (as opposed to the cluster-based approach). No channel was found to be fit differently across test-points in each group, thereby concluding that the model is not biased for (or against) any test-point or group.

Altogether, this experiment turned out to be successful. This result is important computationally, since it is the building block for all the other experiments. After fitting the

			α	t_0	G_{srs}	γ_e	G_{ee}	G_{ei}	G_{esre}	G_{ese}	p_0	A
RG1	T1	R1	114.35	0.0867	-0.9679	265.52	23.48	-29.60	-5.57	16.53	0.2204	7.97
		M	113.71	0.0889	-0.8977	282.67	24.51	-29.93	-4.99	15.12	0.1652	7.82
		R2	116.03	0.0881	-0.8723	278.75	24.73	-30.32	-5.15	15.14	0.1602	8.21
	T2	R1	116.68	0.0851	-0.9039	262.04	24.38	-29.81	-4.84	15.04	0.1895	7.88
		M	116.88	0.0865	-0.8027	287.09	24.65	-30.34	-3.73	14.48	0.1468	6.81
		R2	117.71	0.0860	-0.7774	289.14	25.17	-30.78	-4.30	14.42	0.1458	7.44
	T3	R1	115.44	0.0851	-0.9411	252.68	23.25	-29.18	-5.41	16.04	0.1890	7.44
		M	113.81	0.0860	-0.8471	287.88	24.04	-30.10	-3.94	15.54	0.1694	7.15
		R2	115.31	0.0872	-0.8368	281.21	24.46	-30.01	-4.78	14.62	0.1518	7.71
CG	T1	R1	110.47	0.0867	-0.9760	266.94	23.02	-29.86	-4.60	18.97	0.3391	8.43
		M	112.00	0.0863	-0.9474	275.61	24.03	-29.89	-3.86	16.31	0.2702	8.09
		R2	111.78	0.0877	-0.9183	267.90	23.21	-29.36	-4.85	16.93	0.3225	10.58
	T2	R1	112.21	0.0844	-0.9428	263.04	23.24	-29.86	-3.62	17.33	0.2763	7.93
		M	113.20	0.0850	-0.9288	281.82	25.02	-30.75	-3.64	15.04	0.2117	7.92
		R2	112.11	0.0847	-0.9000	262.68	24.03	-29.97	-4.25	16.31	0.2653	8.75
	T3	R1	111.61	0.0849	-0.9559	254.00	23.17	-29.86	-4.80	18.88	0.2811	7.81
		M	111.19	0.0850	-0.9295	273.61	23.92	-29.87	-3.81	16.38	0.2508	7.60
		R2	111.90	0.0847	-0.9256	262.02	23.74	-29.28	-5.09	17.02	0.2541	9.07
RG2	T1	R1	110.31	0.0882	-0.9647	284.63	23.89	-30.00	-4.57	16.17	0.2699	9.53
		M	111.58	0.0913	-0.8419	296.06	25.51	-30.68	-4.95	15.50	0.2244	9.37
		R2	110.65	0.0911	-0.9013	286.76	24.35	-30.21	-4.72	16.11	0.2466	9.35
	T2	R1	112.84	0.0862	-0.9490	272.19	23.79	-29.94	-4.27	16.34	0.2779	8.98
		M	112.40	0.0897	-0.8046	293.95	26.09	-31.16	-4.35	15.02	0.2051	8.88
		R2	110.20	0.0890	-0.8554	281.21	24.79	-30.53	-4.16	16.32	0.2374	8.04
	T3	R1	113.38	0.0860	-0.9373	270.83	23.75	-29.50	-4.90	17.39	0.2876	10.14
		M	114.57	0.0896	-0.8030	287.75	25.83	-30.26	-4.72	14.83	0.1937	8.92
		R2	111.19	0.0898	-0.8280	287.86	24.89	-30.45	-4.13	16.10	0.2312	8.86

Table 5.2: Average values of fitted model parameters. The values are averaged over all channels and participants for each state (rest-before-meditation (R1), meditation (M), and rest-after-meditation (R2)), test-point (beginning (T1), middle (T2), and end (T3) of retreat), and group (RG1, CG, and RG2), after fitting to the real EEG spectrum. The final parameter values were within physiologically plausible range (refer to Table 5.1).

			α	t_0	G_{srs}	γ_e	G_{ee}	G_{ei}	G_{esre}	G_{ese}	p_0	A
RG1	T1	R1	15.67	0.0065	0.4248	60.21	3.92	3.63	3.03	4.30	0.1673	4.44
		M	13.53	0.0047	0.4006	57.31	3.09	2.07	2.53	4.14	0.1384	4.09
		R2	13.97	0.0064	0.3485	52.56	3.36	1.97	2.87	5.03	0.1157	4.25
	T2	R1	12.74	0.0060	0.3490	60.30	4.65	3.75	4.12	4.79	0.1667	4.79
		M	13.90	0.0056	0.2812	49.51	3.17	2.40	2.72	4.92	0.1245	3.69
		R2	14.10	0.0057	0.2735	49.74	3.32	2.18	3.15	5.11	0.1177	4.34
	T3	R1	14.63	0.0058	0.3812	50.06	3.90	3.56	3.44	4.58	0.1458	4.39
		M	13.03	0.0060	0.3318	52.82	4.04	2.32	3.01	4.92	0.1552	4.37
		R2	13.73	0.0059	0.3461	52.95	2.99	2.88	2.64	4.69	0.1173	4.31
CG	T1	R1	11.17	0.0066	0.4196	54.15	3.14	1.98	2.77	5.34	0.2685	3.19
		M	11.21	0.0066	0.4187	55.60	2.77	2.05	2.01	4.62	0.1910	2.91
		R2	10.28	0.0056	0.3938	51.77	2.54	2.44	2.15	4.73	0.2527	6.70
	T2	R1	11.19	0.0065	0.4188	57.88	3.61	2.53	2.62	6.67	0.2083	3.02
		M	11.27	0.0072	0.4193	62.91	3.25	2.55	2.50	6.22	0.1578	2.89
		R2	8.19	0.0061	0.3855	59.11	2.37	1.92	2.55	5.76	0.2147	4.38
	T3	R1	10.51	0.0074	0.4391	56.11	3.57	1.74	2.82	5.08	0.2365	3.88
		M	11.12	0.0064	0.4239	60.13	3.61	1.99	2.22	6.31	0.1849	2.64
		R2	9.54	0.0070	0.4303	70.23	3.00	2.63	3.26	6.00	0.1870	4.52
RG2	T1	R1	11.30	0.0055	0.4748	63.73	2.80	2.52	2.26	3.94	0.1716	4.96
		M	10.90	0.0059	0.3918	65.96	3.16	2.12	2.84	5.14	0.1696	4.13
		R2	8.53	0.0065	0.4177	63.27	3.79	2.73	2.37	4.38	0.2359	4.38
	T2	R1	12.76	0.0064	0.4568	64.62	2.67	2.84	3.00	5.91	0.2307	4.50
		M	9.44	0.0070	0.3619	66.38	3.54	2.90	2.71	5.39	0.1566	3.71
		R2	6.78	0.0071	0.3659	65.17	3.86	3.27	2.31	5.54	0.2356	3.76
	T3	R1	13.21	0.0064	0.4372	62.02	2.45	2.73	2.81	5.43	0.2530	5.54
		M	9.94	0.0077	0.3691	64.37	3.63	2.89	2.63	4.18	0.1687	3.81
		R2	6.87	0.0069	0.3661	60.29	3.28	2.87	2.00	4.93	0.2064	5.10

Table 5.3: Standard deviation of parameter values, averaged over all channels and participants for each state.

data, the next step is to see changes in model parameters with meditation training. These changes will provide crucial insights from the model that may reflect changes in attention-related brain mechanisms due to meditation training. The next computational experiment will explore them.

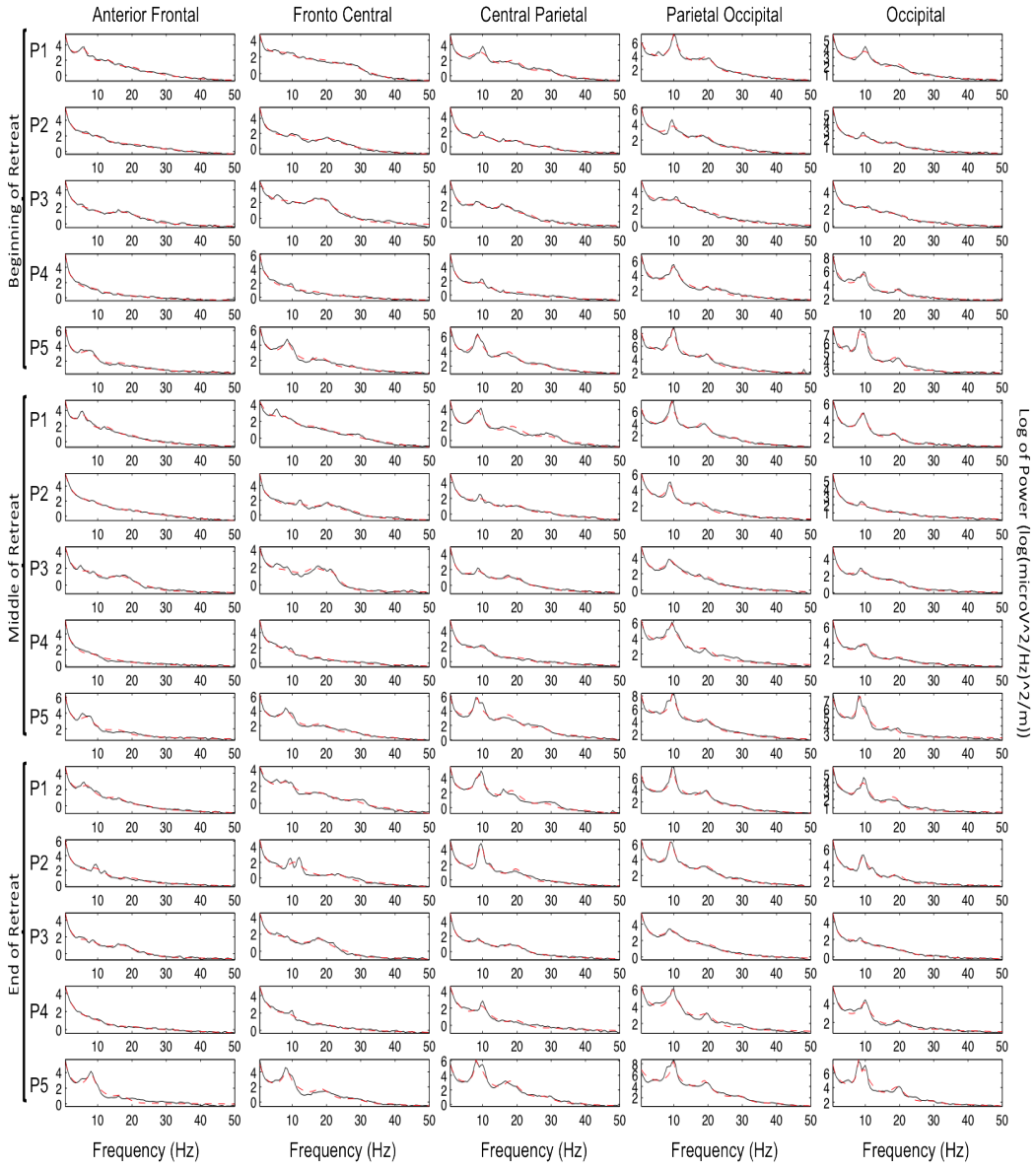

Figure 5.6: Model fitting results for the meditation state for RG1 (Color figure). Real EEG spectrum is shown in solid black line and modeled EEG spectrum in dashed red line. Each cluster of five rows displays results from the first five participants (P1, P2, ..., P5; out of twenty-two, due to space limitations) is shown at a different test-point (beginning, middle, and end of retreat). Each column shows a different mid-line channel across the scalp (out of seventy-three channels, due to space limitations). The model successfully fitted the channels across the scalp, the participants, and the test-points. Only meditation state is shown, due to space limitations, but similar results were obtained for both the resting states as well.

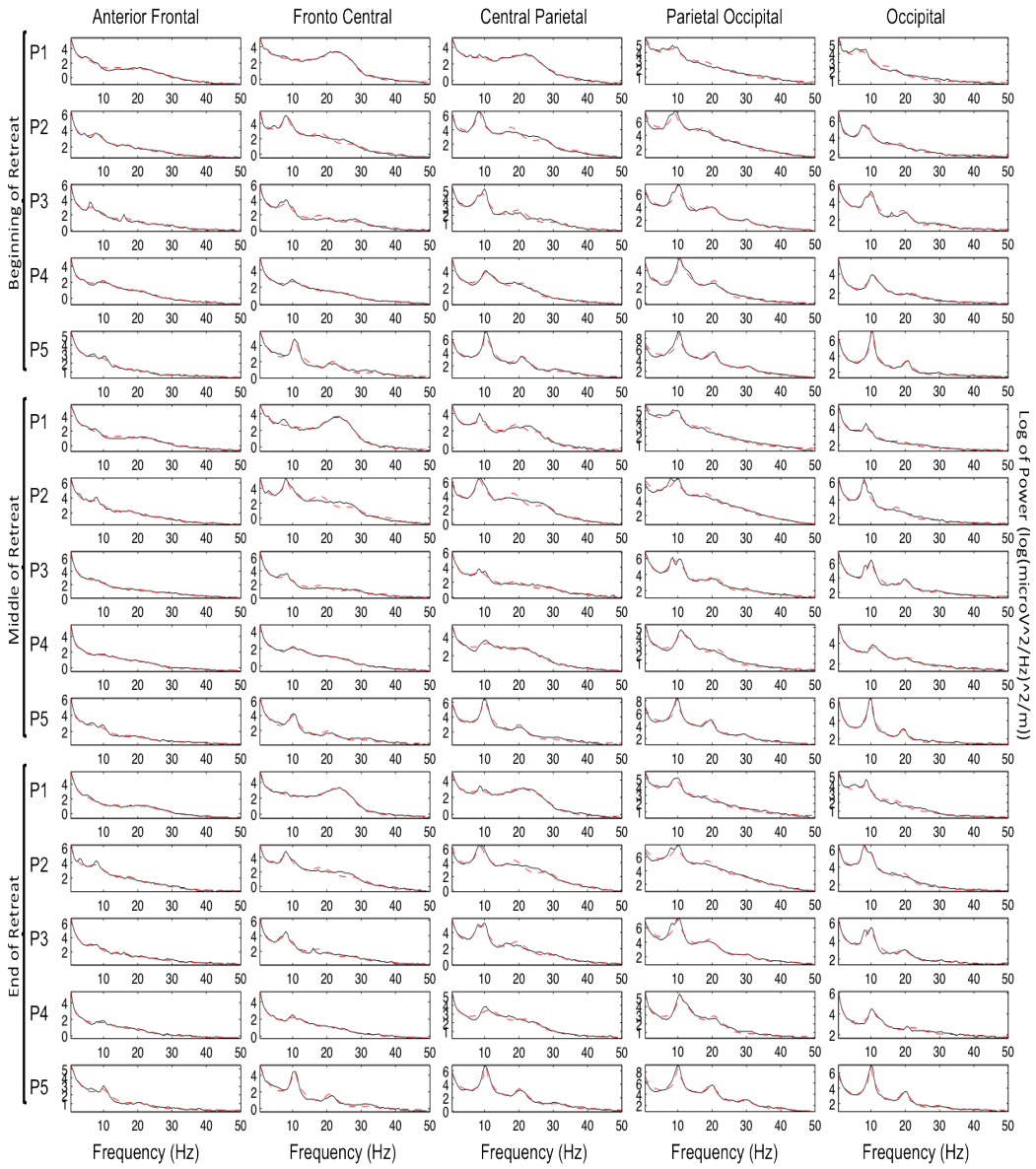

Figure 5.7: Model fitting results for the meditation state for CG (Color figure). The model successfully fitted the channels across the scalp, the participants, and the test-points.

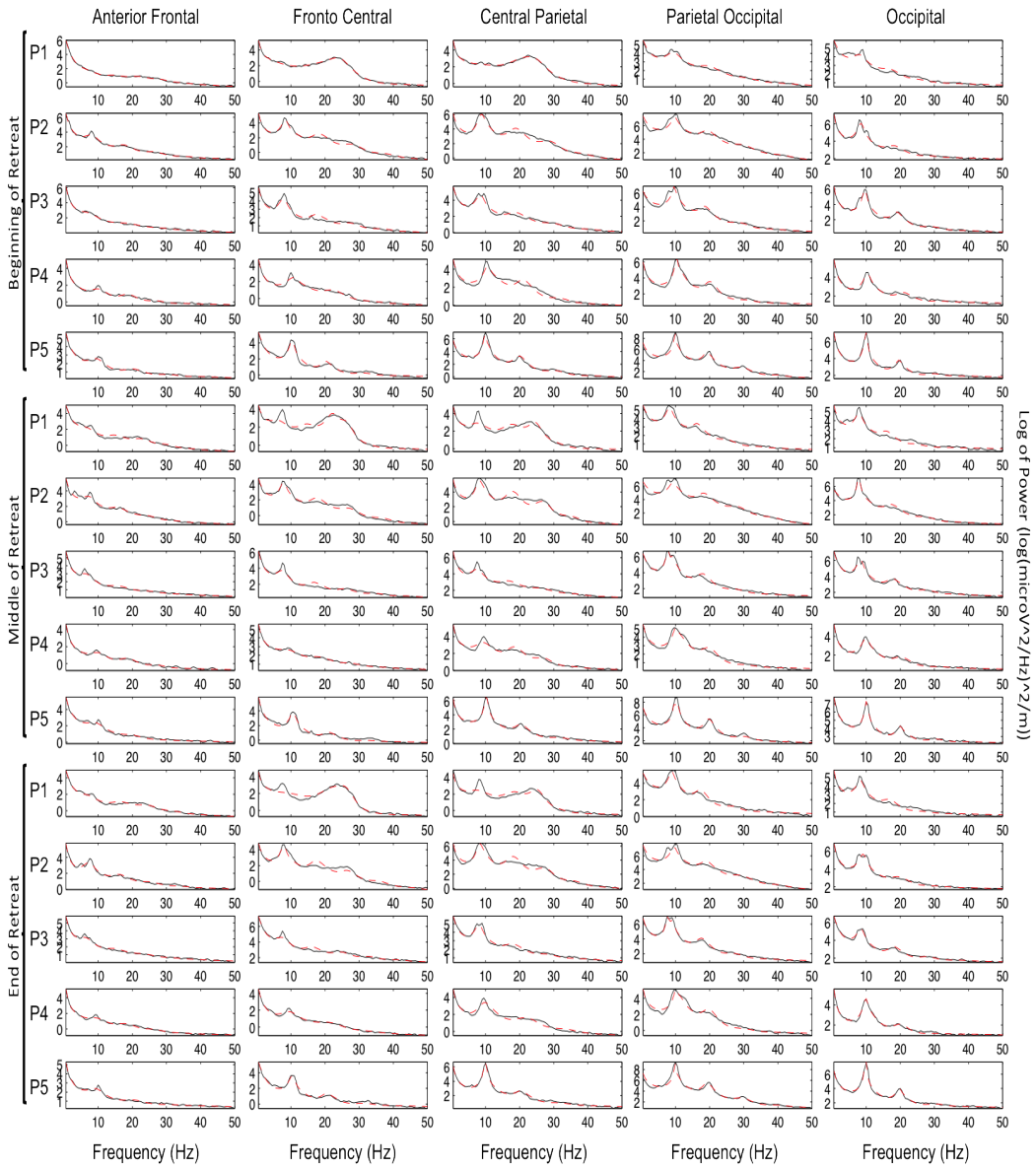

Figure 5.8: Model fitting results for the meditation state for RG2 (Color figure). The model successfully fitted the channels across the scalp, the participants, and the test-points.

		RG1		CG		RG2	
		$\mu_{\mathrm{R_{square}}}$	$\sigma_{\mathrm{R_{square}}}$	$\mu_{\mathrm{R_{square}}}$	$\sigma_{\mathrm{R_{square}}}$	$\mu_{\mathrm{R_{square}}}$	$\sigma_{\mathrm{R_{square}}}$
R1	T1	0.9745	0.0066	0.9734	0.0077	0.9732	0.0074
	T2	0.9734	0.0077	0.9757	0.0056	0.9752	0.0066
	T3	0.9739	0.0067	0.9717	0.0138	0.9734	0.0067
M	T1	0.9846	0.0055	0.9837	0.0053	0.9834	0.0063
	T2	0.9829	0.0076	0.9850	0.0057	0.9841	0.0057
	T3	0.9836	0.0061	0.9845	0.0063	0.9830	0.0069
R2	T1	0.9748	0.0053	0.9737	0.0066	0.9737	0.0061
	T2	0.9732	0.0079	0.9756	0.0060	0.9746	0.0079
	T3	0.9741	0.0069	0.9750	0.0065	0.9750	0.0070

Table 5.4: Goodness-of-fit results, based on R-square values. The results are averaged over all channels and participants for each state, test-point, and group, after fitting to the real EEG spectrum. Overall, the model accounted for more than 97% variance in all the cases. More importantly, low standard deviation $\sigma_{\mathrm{R_{square}}}$ indicates that the model fits the data consistently across the scalp and the participants. It is important to note that the meditation state was fitted slightly more accurately than the resting state, probably because it had a high signal-to-noise ratio (SNR; since it was estimated from six minutes of data, as opposed to the one minute available for resting states).

5.3.2 Experiment 2: Inverse Modeling

Inverse modeling refers to a method in which the fitted model parameters are analyzed to gain insight about how the observed changes in the data are emerged. Changes found in the model parameters can be used to construct formal theories about the underlying mechanisms and even guide future experiments. Further, in the current modeling approach, inverse modeling cannot only provide useful information about the longitudinal changes in cortico-cortical dynamics, but also cortico-thalamic and intra-thalamic dynamics due to meditation training. Thus, allowing for generating hypothesis at the level of neural populations, which is hard to obtain even with the most sophisticated invasive approaches.

After the extended model was fit to the real EEG spectrum in the previous experiment, parameters were analyzed using the longitudinal analysis extension to the model. Figure 5.9 shows the experimental design and Figure 5.10 shows the model parameters an-

alyzed. Based on the meditation type (focused-attention) and the results from spectral analysis (Chapter 4), the role of cortico-thalamic and intra-thalamic dynamics was suspected.

Overall, changes in three (out of ten) parameters were found using the longitudinal analysis. These parameters were intrathalamic gain (G_{srs}), cortico-thalamic delay (t_0), and normalization factor (p_0). The changes in intrathalamic gain and corticothalamic delay were evident in both retreat groups, however, no such change was found in the control group. Further, the normalization factor was the only parameter that changed in CG (Figure 5.11). It was found to drop from the beginning to the middle test-point in left lateral parietal region, but no difference was found between the beginning or the middle and the end test-point. A similar drop was also found in RG1 at the right anterior frontal region: the normalization factor dropped at the middle of retreat, but no difference was found at the end of retreat (compared to the beginning; Figure 5.12). The normalization parameter is responsible for the scaling of the theoretical spectrum, according to Experiment 1, and is related to parameters G_{es}, G_{sn}, ϕ_n, and r_e (equation 5.6). In the current work, parameter r_e was kept constant (Table 5.1) and parameters G_{sn} and ϕ_n represented white noise in space and time. Further, no longitudinal change in parameters G_{ese} or G_{esre}, and hence G_{es}, were found. Considering all these facts, it seems that the changes observed in p_0 at the middle test-point are not related to physiological changes. Correlation analysis (section 5.5) between changes in p_0 and other measures, if found, will shed more light on why normalization factor dropped.

The intrathalamic gain parameter represents the interaction between reticular (TRN) and relay (SRN) nuclei of thalamus. Reduced intrathalamic gain was found in right lateral parietal areas, during rest and meditation, in RG1 and RG2 after the retreat. Figures 5.13 and 5.14 show the location of clusters and the results from posthoc Wilcoxon tests for each state (see the caption for statistics). These revealed a step-wise drop in G_{srs} during both retreats, i.e., significant drop from beginning (T1) to middle (T2) and from the beginning to the end (T3) of the retreat, but no change from the middle to the end of the retreat.

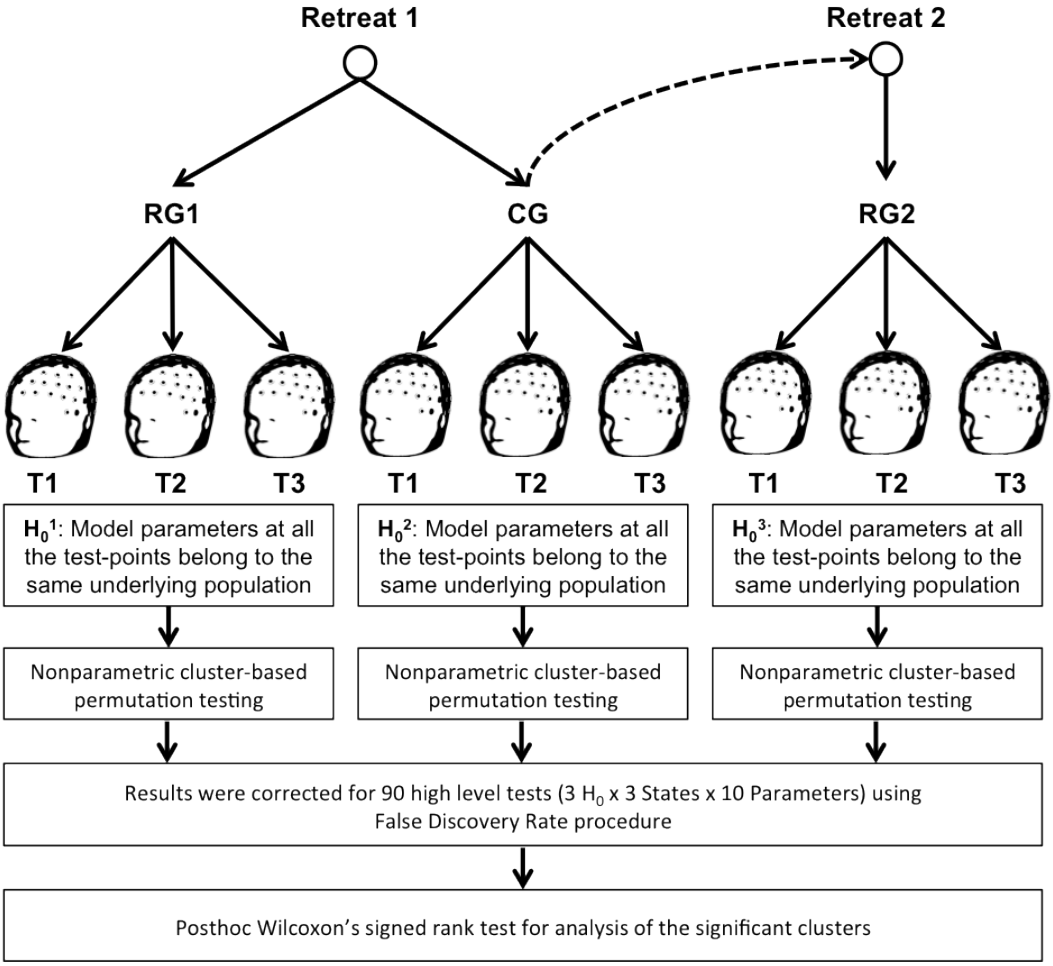

Figure 5.9: Experimental design for inverse modeling. Three groups of participants were tested (RG1 and CG in Retreat1 and CG later underwent its own retreat (Retreat2) and became RG2). Each group was tested thrice during the three-month retreat period: beginning (T1), middle (T2), and end (T3). After fitting the model for each test-point, three null hypotheses were tested (H_0^1, H_0^2, and H_0^3) using the nonparametric cluster-based permutation analysis, followed by False Discovery Rate (FDR) correction for 90 nonparametric tests. Later the parameter values from the significant clusters were fed into Wilcoxon's test (with Bonferroni correction) to determine the direction of effects, i.e., how parameter values change from T1 to T2 to T3. Overall, this experiment provides a statistical approach to longitudinal analysis of model parameters.

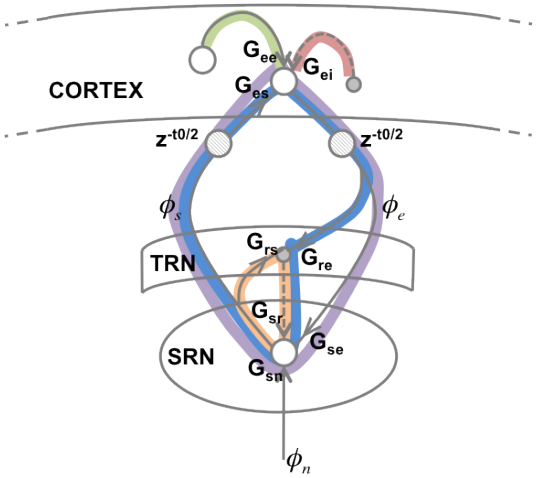

Figure 5.10: Model parameters analyzed during inverse modeling (Color figure). Five model parameters (or loops) are shown in the figure: cortico-cortical excitatory (G_{ee}; in green), cortico-cortical inhibitory (G_{ei}; in red), cortico-thalamo-cortical via TRN (G_{esre}; in blue), cortico-thalamo-cortical without TRN (G_{ese}; in purple), and intrathalamic loop (G_{srs}; in orange). Apart from these loops, five other parameters (not shown in the figure) were also analyzed: cortical damping rate (γ_e), dendritic decay rate (α), conduction delay in the signal from cortex to thalamus and back (t_0), normalization parameter for the spectrum (p_0), and normalization parameter for the EMG model (A). The oscillatory activity produced by the model is due to the temporal dynamics in the five loops.

Simply put, increase in G_{srs} will lead to increased inhibition of SRN using TRN, and decrease in G_{srs} will lead to reduced inhibition of SRN (Steriade and Amzica, 1998; Timofeev et al., 1996). The latter is characteristic of increased arousal states, where SRN cells become more depolarized and TRN cells become more hyperpolarized (Steriade, 2000). Thus, the reduction in magnitude of intrathalamic gain after three months of intensive meditation training in consistent with increased arousal or alert state during rest and meditation.

The corticothalamic delay (t_0) parameter represents axonal and other propagation delays in transmitting signal from cortex to thalamus and back to cortex (Robinson et al., 2001). Increased corticothalamic delay was found in midline and right-lateral parietal areas,

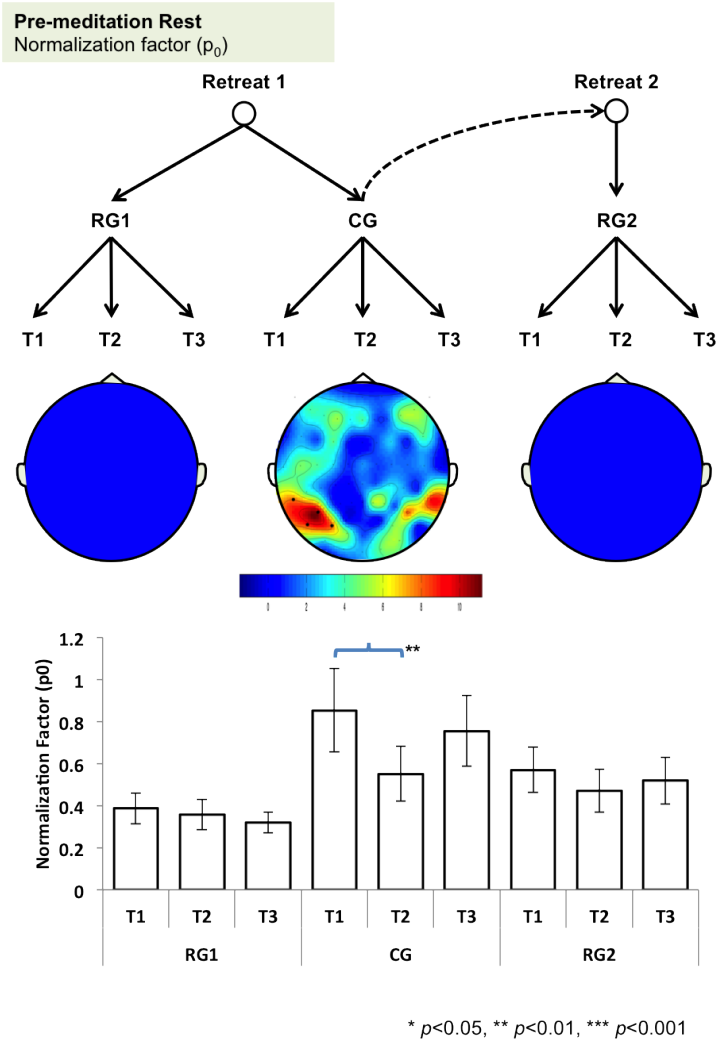

Figure 5.11: Changes in normalization factor (p_0) during pre-meditation rest (Color figure). A cluster in the left lateral parietal location was found for CG ($p_{\text{cluster}} = 0.0018$), no clusters were found for either retreat groups. The location of cluster is separate from all the other effects found in RGs, such as intrathalamic gain and corticothalamic delay. Post-hoc Wilcoxon test revealed a reduction in normalization factor at the middle of retreat (as compared to the beginning; $p_w = 0.005$). No difference was found between the beginning and the end of retreat. Further, p_0 values extracted from RG1 and RG2 for the same cluster as in CG showed no change. It is important to note that no effect was found in the parameters from which p_0 is calculated (equation 5.6), thus it is not clear why this change was seen in CG alone. This effect does not seem to be due to physiological reasons.

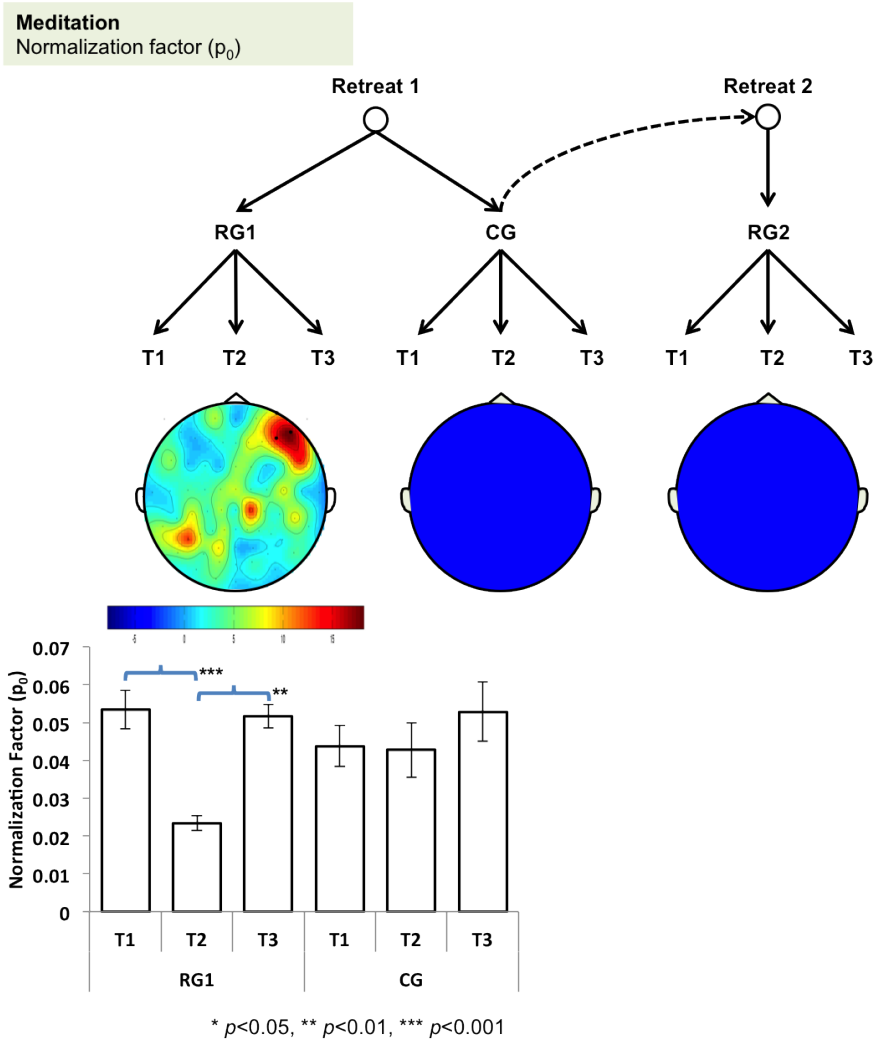

Figure 5.12: Changes in normalization factor (p_0) during meditation (Color figure). Cluster was found in the right anterior-frontal location in RG1 ($p_{\text{cluster}} = 0.0018$), no clusters were found in either CG or RG2. The location of this cluster separate from all the other effects. Post-hoc Wilcoxon test revealed a reduction in normalization factor at the middle of retreat ($p_w = 0.000$), as compared to the beginning, and at the end of retreat ($p_w = 0.003$), as compared to the middle, but, no difference was found between the beginning and the end of retreat, indicating a weak effect. Further, p_0 values extracted from CG for the same cluster as in RG1 showed no change. It is important to note that no effect was found in the parameters from which p_0 is calculated (equation 5.6), thus, it is not clear why this change was seen in RG1 during meditation. As with the effect found in CG (Figure 5.11), this effect also does not seem to be due to physiological reasons.

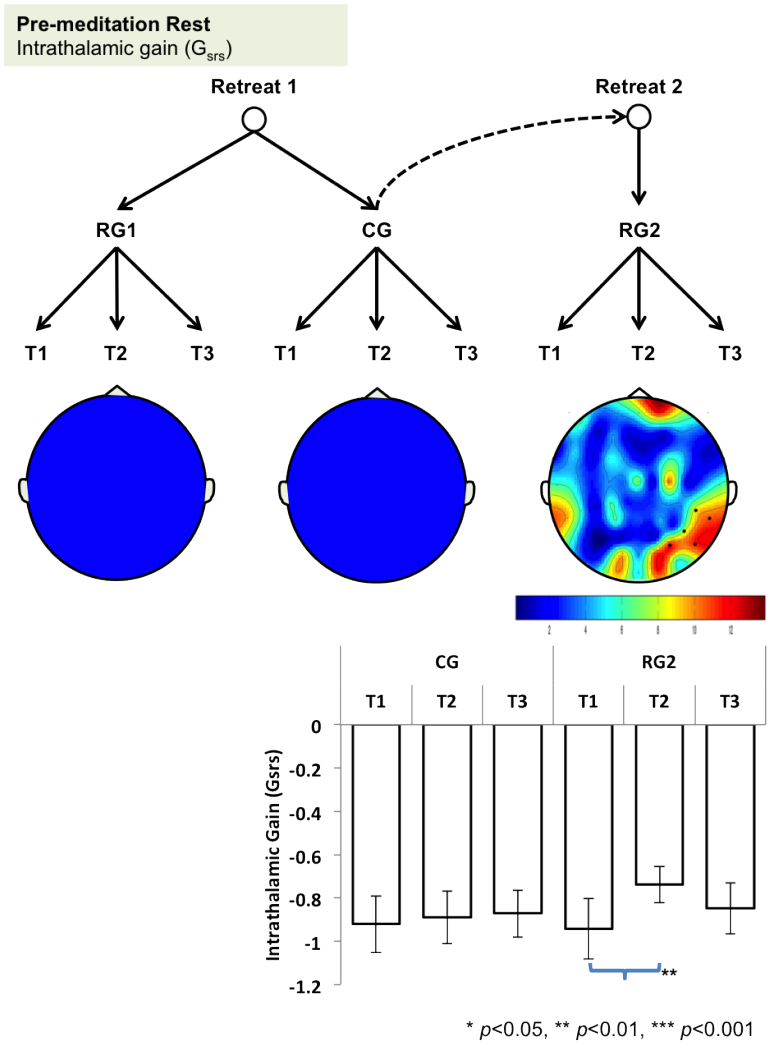

Figure 5.13: Reduction in intrathalamic gain (G_{srs}) during pre-meditation rest (Color figure). No cluster was found in RG1 or CG. However, right lateral parietal cluster was found in RG2 ($p_{\text{cluster}} = 0.0022 \leq p_{\text{FDR}}^{\text{critical}} = 0.0022$). Post-hoc Wilcoxon test for the cluster revealed a significant reduction in intrathalamic gain at T2 when compared with T1 ($p_w = 0.001$, which cleared Bonferroni critical alpha level for six tests $p_{\text{Bonferroni}}^{\text{critical}} = 0.0083$). However, the reduction was lost at T3 (compared to T1) and only a trend of reduction was found at the end of retreat ($p_w = 0.072$). Overall, a relatively weak effect was found for intrathalamic gain at pre-meditation rest.

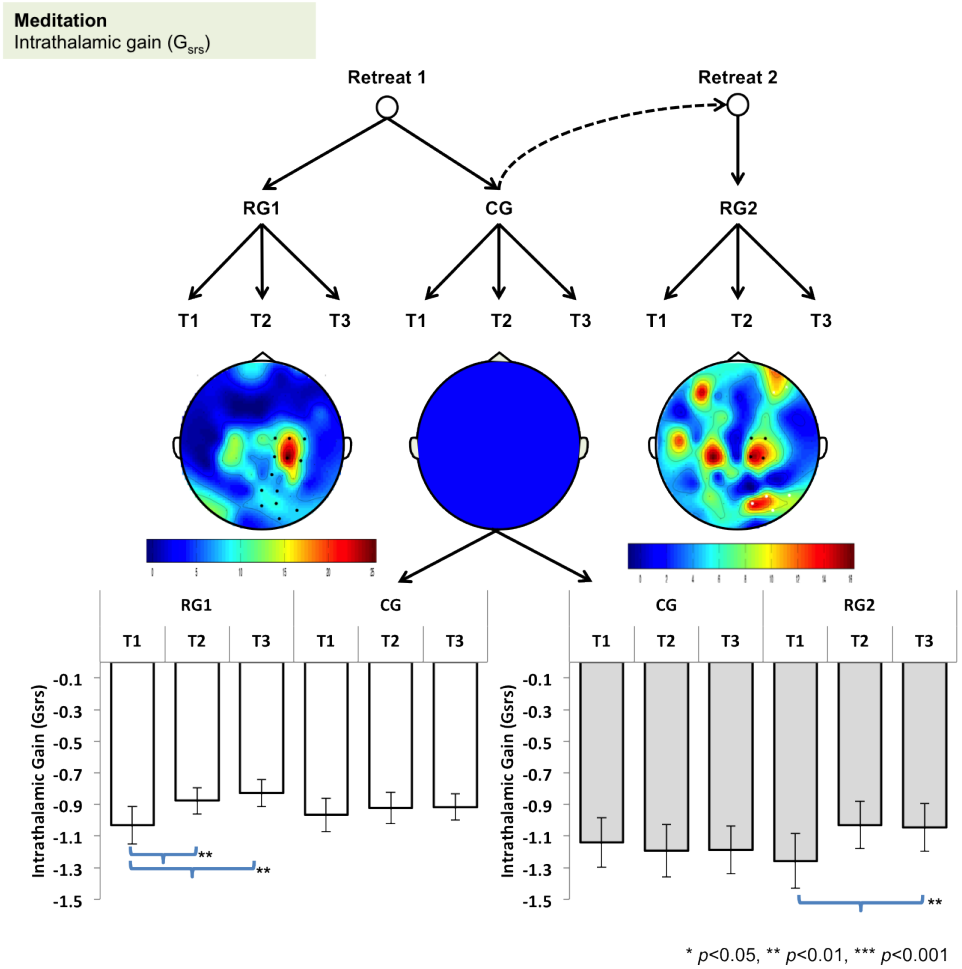

Figure 5.14: Reduction in intrathalamic gain (G_{srs}) during meditation (Color figure). Using nonparametric cluster-based permutation approach, significant clusters were found in RG1 and RG2, whereas no clusters were found in CG. In RG1, a large right lateral parietal-occipital cluster was found ($p_{\text{cluster}} = 0.001 \leq p_{\text{FDR}}^{\text{critical}} = 0.0022$). Post-hoc Wilcoxon test for the cluster revealed a significant reduction in intrathalamic gain at T2 ($p_w = 0.000$) and T3 ($p_w = 0.007$) when compared to T1 (both less than $p_{\text{Bonferroni}}^{\text{critical}} = 0.0083$). In RG2, a right-parietal cluster was found ($p_{\text{cluster}} = 0.0066$). It just missed the $p_{\text{FDR}}^{\text{critical}} = 0.0022$ and hence it is a weak effect, indicated by gray-colored bar plots underneath. FDR-based cutoff can be overly conservative (especially when testing for 90 tests), thus results from this cluster are still included. Post-hoc Wilcoxon tests for the cluster in RG2 revealed reduction in G_{srs} at T3 (as compared to T1; $p_w = 0.001$, which cleared Bonferroni critical alpha level for six tests $p_{\text{Bonferroni}}^{\text{critical}} = 0.0083$). Overall, the reduction in intrathalamic gain during meditation was replicated across the retreats in similar spatial locations and no effect was found for the CG.

during meditation and rest, after the retreat. No effect was found in the control group. Figures 5.15, 5.16, and 5.17 show the location of the clusters and the results from posthoc Wilcoxon tests for each state, respectively. Parallel to the intrathalamic gain, a step-wise change (although increase) in delay values was found in both retreat groups.

The temporal dynamics of cortico-thalamo-cortical loop are considered as one of the generators for alpha frequency on the scalp (Pizzagalli, 2007; Fisch and Spehlmann, 1999; Larson et al., 1998). The main impact of increasing cortico-thalamic and thalamo-cortical delay parameter is to reduce the alpha and beta frequency (Robinson et al., 2001). Sensitivity analysis of model parameters confirms this theory (Figure 5.3). Further, various previous studies on meditation research showed that long-term meditators have reduced alpha frequency even during baseline rest (Cahn and Polich, 2006). Similar results were also found with the current dataset with just three months of meditation (see Chapter 4). However, the biological basis for this finding in meditators is still unknown. The model, however, proposes that the increased corticothalamic delay can account for the reduced alpha frequency found in meditators. Correlation analysis (section 5.5) will further test this claim.

Altogether, the inverse modeling experiment provided crucial insights into what might be happening inside the brain during focused-attention meditation training, thereby creating a putative mechanistic account for the cortical changes seen after the retreat. However, another important aspect about these changes is that of the teleological reasoning behind them, i.e., why such changes were preferred by the brain (and what purpose did those changes serve). The next computational experiment attempts to develop such reasoning.

5.3.3 Experiment 3: Stability Analysis

The previous experiment showed how the cortico-cortical, cortico-thalamo-cortical, and intrathalamic dynamics change due to intensive meditation training. This result is novel and important by itself, but it provides only a mechanical explanation. To provide a teleological

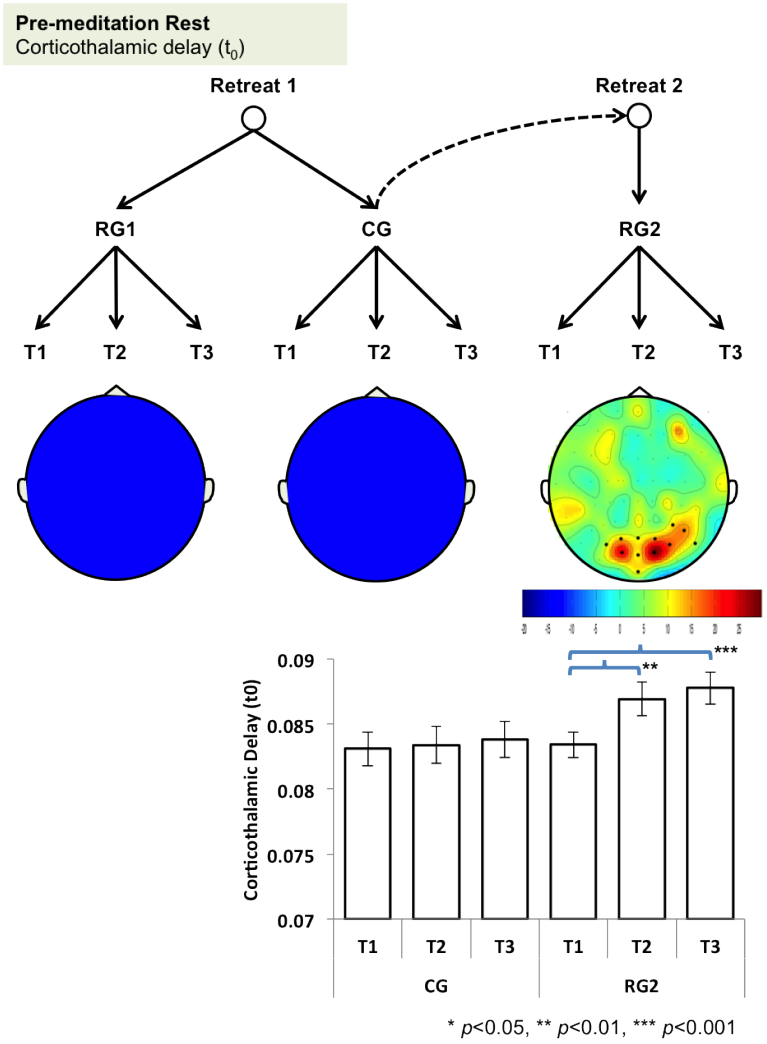

Figure 5.15: Increase in corticothalamic delay (t_0) during pre-meditation rest (Color figure). No cluster was found in RG1 and CG. However, in RG2 a bilateral parietal-occipital cluster was found ($p_{\text{cluster}} = 0.0002 \ll p_{\text{FDR}}^{\text{critical}} = 0.0022$). Post-hoc Wilcoxon tests revealed a significant increase in corticothalamic delay at T2 ($p_w = 0.001$) and T3 ($p_w = 0.000$) (as compared to T1), but no difference between T2 and T3. The pattern in corticothalamic delay is thus similar, but in opposite direction, to the reduction found in the intrathalamic gain.

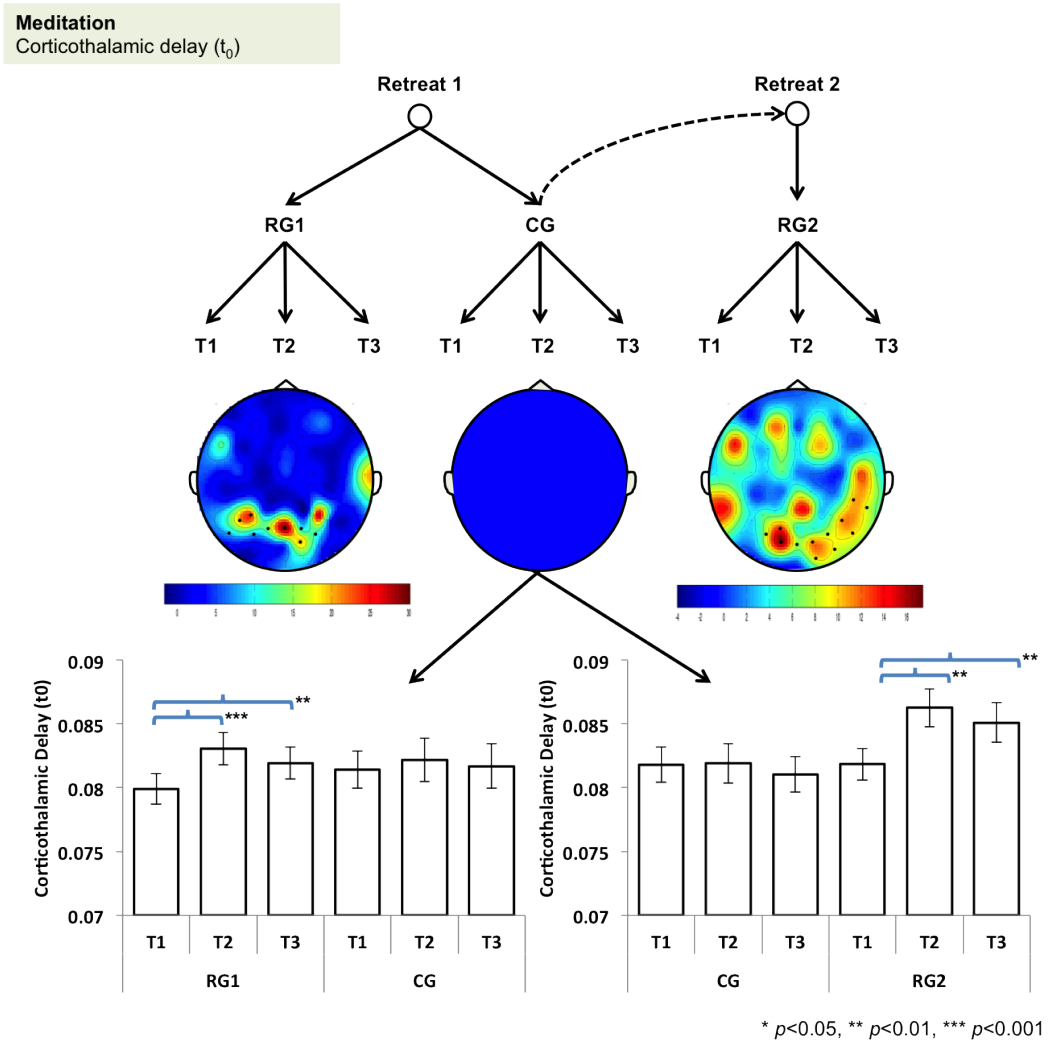

Figure 5.16: Increase in corticothalamic delay (t_0) during meditation (Color figure). No clusters were found in the CG. However, parietal-occipital clusters were found in both retreat groups. In RG1, a bilateral parietal-occipital cluster was found ($p_{\text{cluster}} = 0.0001 \ll p_{\text{FDR}}^{\text{critical}} = 0.0022$). Post-hoc Wilcoxon test for the cluster revealed a significant increase in the corticothalamic delay at T2 ($p_w = 0.000$) and T3 ($p_w = 0.007$) when compared to T1. In RG2, a right parietal-occipital cluster was found ($p_{\text{cluster}} = 0.0008 \ll p_{\text{FDR}}^{\text{critical}} = 0.0023$). Post-hoc Wilcoxon tests were performed to find the direction of change. Increased delay value was found at T2 ($p_w = 0.001$) and T3 ($p_w = 0.001$), when compared with T1, but no change was found between T2 and T3. Overall, increased cortico-thalamic delay was found parietal-occipital regions, in both retreat groups, at the middle and the end test-points of the retreat.

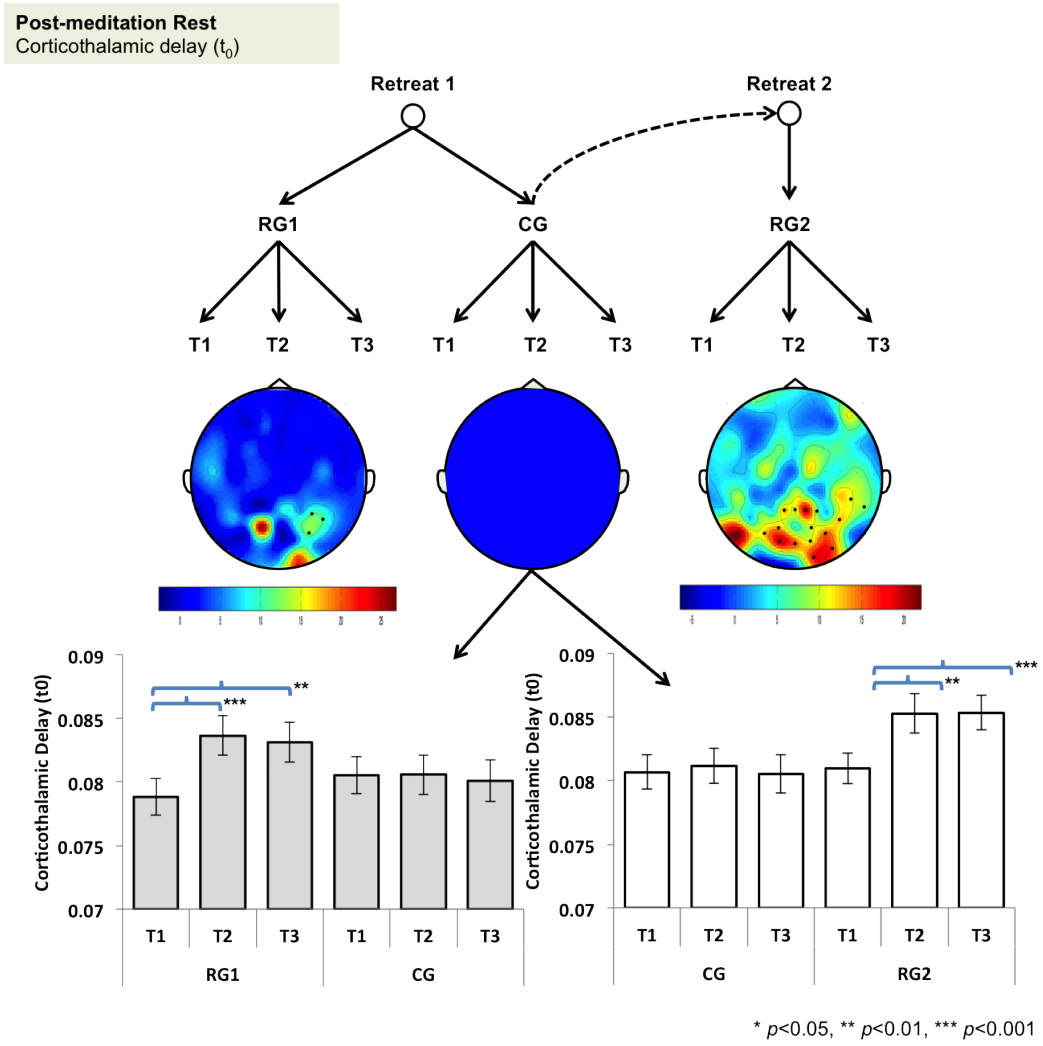

Figure 5.17: Increase in corticothalamic delay (t_0) during post-meditation rest (Color figure). No cluster was found in CG, but, parietal-occipital clusters were found in both retreat groups. In RG1, a small right parietal cluster was found ($p_{\text{cluster}} = 0.008$). It just missed the $p_{\text{FDR}}^{\text{critical}} = 0.0022$ and hence it is a weak effect, indicated by gray-colored bar plots underneath. Post-hoc Wilcoxon test for the cluster revealed a significant increase in the corticothalamic delay at T2 ($p_w = 0.000$) and T3 ($p_w = 0.001$) when compared to T1. In RG2, relatively large right parietal-occipital cluster was found ($p_{\text{cluster}} = 0.0002 \ll p_{\text{FDR}}^{\text{critical}} = 0.0023$). Increased delay value was found using post-hoc Wilcoxon tests at T2 ($p_w = 0.001$) and T3 ($p_w = 0.000$), when compared with T1, but no change was found between T2 and T3. The overall results here are similar to those found during meditation, indicating trait effect of meditation training at post-meditation rest.

explanation as well, i.e., why the model parameters changed the way they did and what purpose those changes serve, stability analysis was done on the model equations. The hypothesis for this experiment was that the changes found in Experiment 2 induce more stability in the brain. Thus, three months of intensive meditation practice should transform the brain such that it becomes less chaotic and more stable.

Previously, Robinson et al. (2002), showed that the stability boundaries in parameter space occur approximately where

$$(1 - i\omega/\gamma_e)^2 - x - \frac{y(1 - G_{srs})}{1 - G_{srs}L^2} e^{i\omega t_0} = 0 \tag{5.13}$$

is satisfied. Here,

$$x = G_{ee}/(1 - G_{ei}) \tag{5.14}$$

and

$$y = \frac{G_{ese} + G_{esre}}{(1 - G_{srs})(1 - G_{ei})}. \tag{5.15}$$

The parameter x represents cortical and y represents corticothalamic activity. Another parameter z was chosen to represent the intrathalamic activity,

$$z = -G_{srs}\alpha\beta/(\alpha + \beta)^2. \tag{5.16}$$

Thus, the whole parametric space can be reduced to a three-dimensional space $< xyz >$. The stability zone in the $< xyz >$ space, defined by equation 5.13, is shown in Figure 5.18. The stable zone for the brain is under the multicolored tent. Above the tent lies different instabilities as shown with the different different colors. Different brain states can be mapped to this $< xyz >$ space and changes in the coordinates of those states result in increased stability (or instability) in the brain (Robinson et al., 2002).

The experimental design for this experiment was similar to the previous one, except instead of model parameters, longitudinal changes in the three coordinates were assessed.

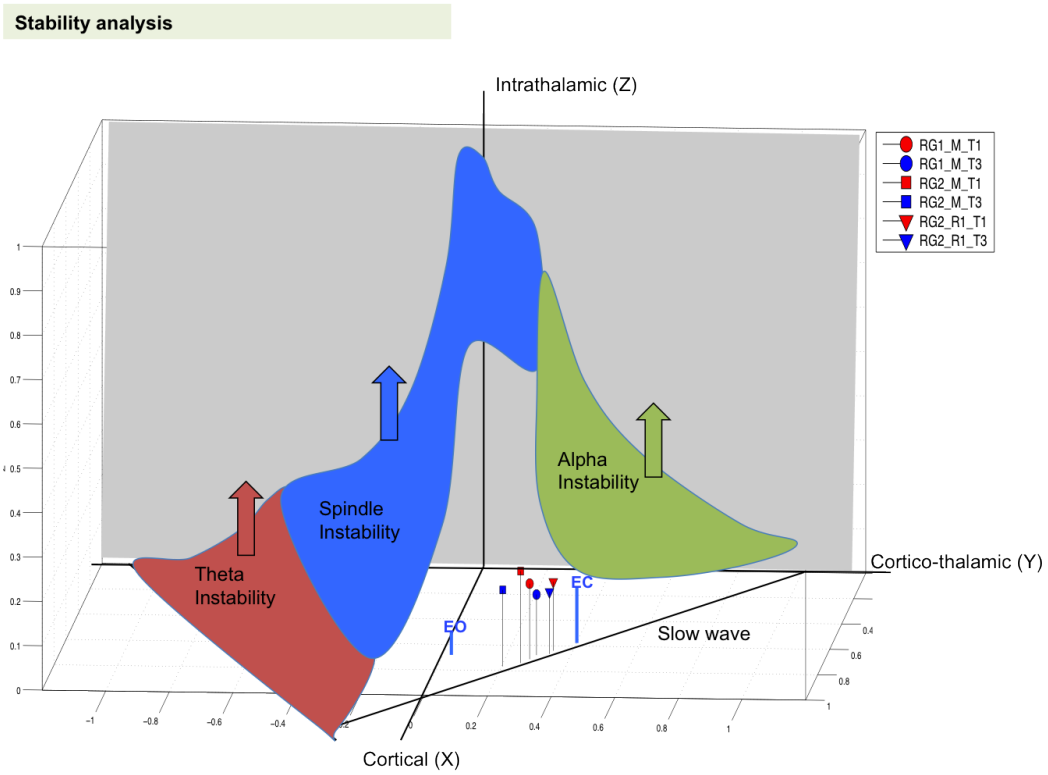

Figure 5.18: Stability of different brain states, and the states of participants before and after meditation training (Color figure). Brain states are reported by points in the 3-D volume. The colored surfaces represent the boundary between stable (below) and unstable (above) states. Four such boundaries are shown (cartoon adapted from a real data plot in Robinson et al., 2002). First, above the red surface, is the theta instability defined area, for small z. Second, above the blue surface, is the spindle instability which peaks at $z = 1$. Third, above the green surface, is the alpha instability. Fourth, the invisible (to clearly show the inside) front of the tent towards the reader, is the slow-wave instability, defined by the plane $x + y = 1$. Overall, this colored tent surface marks the onsets of generalized seizures (Robinson et al., 2002). Approximate locations for eyes-closed rest (EC) and eyes-open rest (EO) are shown as labeled points. These locations were determined previously by Robinson et al. (2002). Locations of group mean are also shown for the retreat groups, using the legend on right. These values were extracted from the cluster found in longitudinal analysis of z stability parameter. Significant reduction in z values show that the participants were further away from the unstable tent surface and hence in a more stable zone, after the retreat.

Significant clusters were found in both retreat groups, during rest and meditation states, for the intrathalamic stability parameter z. It is important to note that the cluster locations found for z were identical to the ones found for G_{srs} (in Experiment 2). No cluster was found for the CG. In RG1, a significant cluster was found at the right lateral parietal-occipital location, during meditation (Figure 5.19). Post-hoc Wilcoxon test revealed a reduction in z at the middle and the end of retreat as compared to the beginning. Similar, but weak, effect was also found in RG2 during meditation (Figure 5.19). Another right parietal cluster was found in RG2 during pre-meditation rest. Post-hoc tests revealed a significant reduction in z at the middle and a trend reduction at the end of retreat (as compared to the beginning), but no difference between the middle and the end of retreat (Figure 5.20).

Why is the change only in z-dimension, and why is it a reduction? The only model parameter that changed longitudinally, and was also used in stability analysis, was G_{srs}. Both y and z are estimated using G_{srs} and the change in z is obviously due the reduction found in G_{srs}: Even the exact same cluster locations were found for both G_{srs} and z. Apparently y did not change in the same way because changes in its numerator and denominator canceled each other. That is, the increase due to reduction of G_{srs} in the denominator was diminished, due to decrease in G_{esre} [1].

What does the reduction in z-dimension mean? Most likely more stability. Figure 5.18 shows the location of average brain states of the participants in $< xyz >$ space before and after the retreat. For reference, the figure also shows approximate locations for eyes-closed and eyes-open resting brain states, estimated in a separate study and a different group of people (Robinson et al., 2002). Although the participants were already in the stable zone, the decrease found in z-dimension after three months of intensive meditation, suggests that participants were even further away from the instability boundaries (or the tent surface). Hence, they were in a significantly more stable state after meditation training than before it.

Altogether, this experiment suggests that the teleological purpose of reduced in-

[1] Since, $G_{esre} = G_{es}G_{sr}G_{re}$ and reduction in G_{srs} implies reduction in G_{sr} and hence reduction in G_{esre} too.

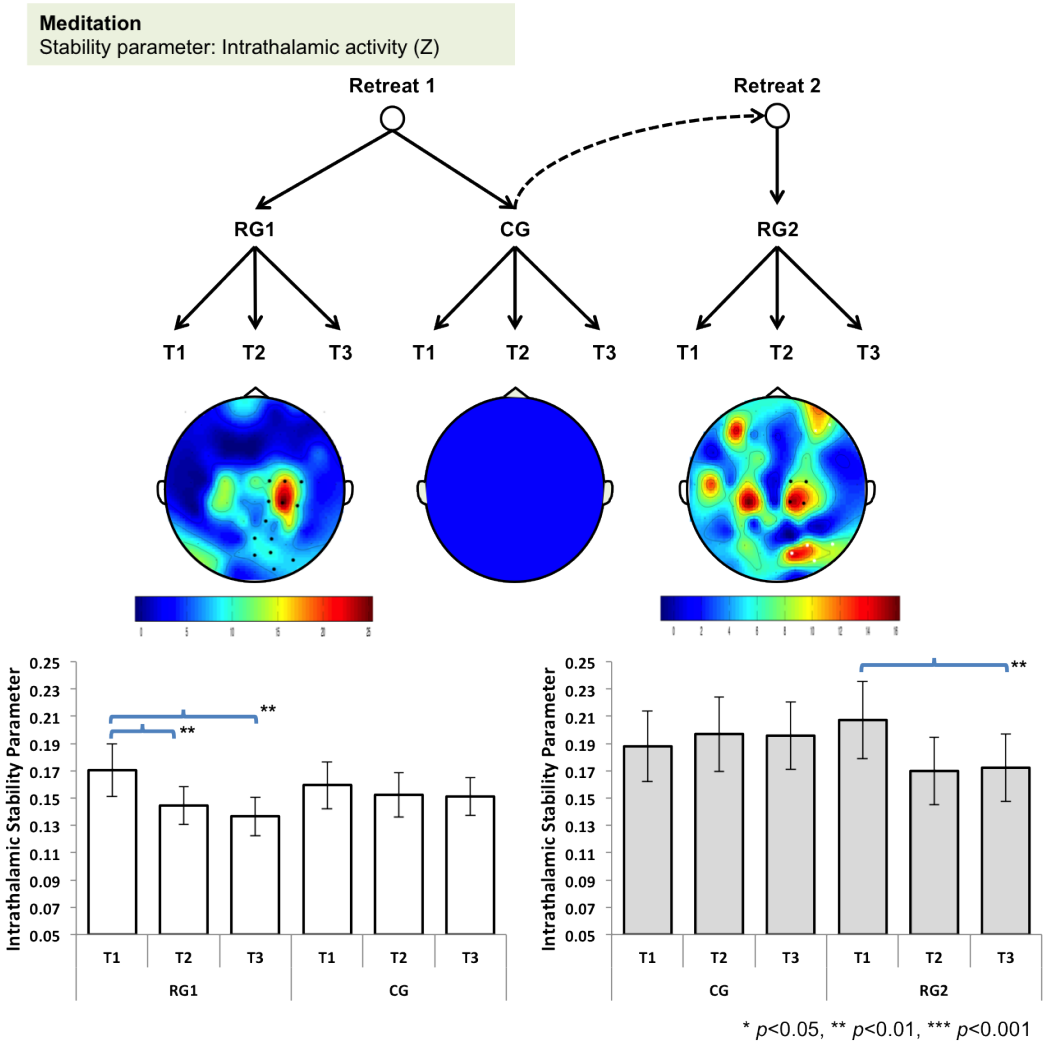

Figure 5.19: Stability analysis during meditation (Color figure). No clusters were found in CG, however, right lateral parietal clusters were found in both RG1 ($p_{\text{cluster}} = 0.0012 \leq p_{\text{FDR}}^{\text{critical}} = 0.002$) and RG2 ($p_{\text{cluster}} = 0.0074 > p_{\text{FDR}}^{\text{critical}} = 0.002$). The cluster in RG2 just missed the FDR critical alpha level and hence is a weak effect, but is included here for completeness. Post-hoc Wilcoxon test, for the cluster in RG1, revealed a significant decrease in the z at T2 ($p_w = 0.0015$) and T3 ($p_w = 0.0005$) when compared to T1, however no change in z values extracted from CG for the same cluster. Post-hoc Wilcoxon test, for the cluster in RG2, revealed a significant decrease in the z at T3 ($p_w = 0.0007$), when compared to T1, but again, no change in z values extracted from CG for the same cluster. Overall, a strong effect was found for reduction in value of inthrathalamic stability parameter. This reduction implies participants were more stable after meditation training.

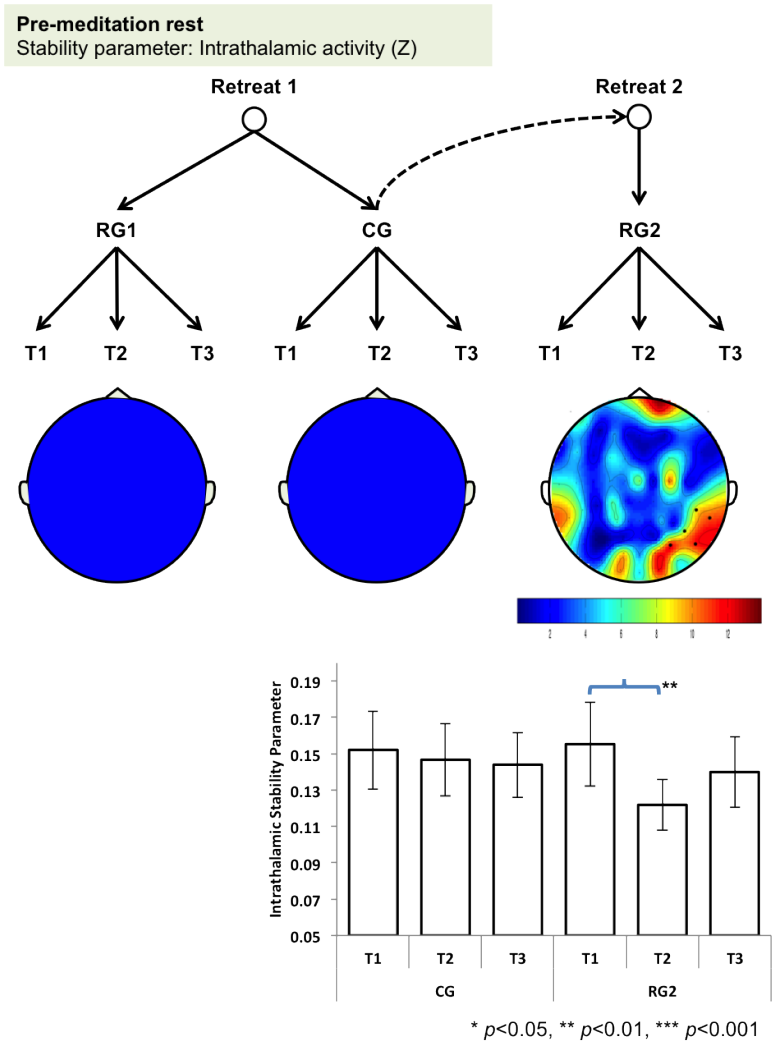

Figure 5.20: Stability analysis during pre-meditation rest (Color figure). No clusters were found in RG1 and CG. However, a right lateral parietal cluster was found in the RG2 ($p_{\text{cluster}} = 0.002 \leq p_{\text{FDR}}^{\text{critical}} = 0.002$). Post-hoc Wilcoxon test for the cluster revealed a significant decrease in the z parameter at T2 ($p_w = 0.0009$) and a trend decrease at T3 ($p_w = 0.07$) when compared to T1, but no change in z values extracted from CG for the same cluster. Overall, a weak effect was found for reduction in value of inthrathalamic stability parameter. This reduction implies that participants were more stable after meditation training.

trathalamic gain after intensive meditation training is to provide more stability to the brain dynamics. This finding has great consequences for patient populations suffering from instability, such as epilepsy. Focused-attention meditation might provide a therapeutic approach to treat such disorders.

5.3.4 Experiment 4: Connectivity in TRN

The unique influential positioning of the TRN and its extensive lateral, mostly inhibitory, connectivity suggests that it acts as a nexus between several functionally and structurally related cortical and thalamic areas (Scheibel and Scheibel, 1966; Guillery and Harting, 2003; Jones, 1975; Crick, 1984; Steriade et al., 1986; Sherman and Guillery, 2006; Zikopoulos and Barbas, 2007). This nexus has been suggested to be responsible for attention regulation and cognitive control functions (Crick, 1984; Sherman, 1996; Sherman and Guillery, 2002; Zikopoulos and Barbas, 2007), even during meditation (Austin, 1999; Newberg and Iversen, 2003). Thus, it is important to model and understand the intra-TRN dynamics in order to understand how attention is regulated during intensive meditation retreat.

Methodological details about this experiment are provided in section 5.2.2. Briefly, after fitting the model with real EEG data, white noise was injected in the cortical cells of the model. The resulting activity was measured in the TRN cells and connectivity analysis was performed to gauge the lateral connectivity in the TRN layer. Further, longitudinal analysis was performed on the structural changes in TRN (i.e., the location of the clusters) and connectivity changes within and between clusters.

Using a cluster dendrogram, the value for maximum number of clusters was chosen to be two. The clusters were then visualized using topographical maps, as shown in Figure 5.21(b). Overall, clear anterior-posterior division was found at each test-point (for all groups and states) in the TRN layer. This discovery is in line with the idea of afferent cortical connections to the TRN layer are topologically structured (Zikopoulos and Barbas, 2007): The clear functional division in the modeled layer, rather than some messy arrange-

ment, thus provides computational support to such experimental results.

To measure the longitudinal changes in this division, nonparametric cluster-based permutation testing was performed on these topographical maps. However, no significant change was found across test-points in the retreat for any group or state.

To gauge changes in connectivity in the TRN layer, correlations were estimated within and between clusters. No difference was found in these correlations for pre-meditation rest and meditation states in any group. However, for post-meditation rest, significant increase in within-cluster correlation, for the posterior cluster, was found in both retreat groups. No significant effect was found for the control group (Figure 5.21(a)). This increase could indicate a temporary "after-effect" of meditation, resulting in more synchronized activity in TRN at the end of retreat (as compared to the beginning). Thus, even a small lateral (inhibitory) or cortical (excitatory) input to the posterior TRN can have a spatially large, and perhaps, a strong impact. More work is required to understand the exact reasons behind such a change in the posterior region of TRN. Correlation analysis and discussion, in the next two sections, will shed some light on this issue.

5.4 Correlation Analysis

Correlation analysis between the observed changes in model parameters and the other measures, also acquired during the retreat, was performed in order to (a) provide behavioral interpretations for the changes observed in model parameters; and (b) disentangle the effects of meditation training from those of other factors of the retreat.

The longitudinal changes in the model parameters were compared with, (a) self-reported measures, including lifetime hours spent in meditation, daily time spent in meditation during the retreat, and adaptive socio-emotional functioning (Sahdra et al., 2011); (b) performance in attention-related tasks, including sustained attention task (MacLean et al., 2010) and response inhibition task (Sahdra et al., 2011); (c) longitudinal changes found in cortical activity patterns (Chapter 4); and (d) difference in elevation between the place of

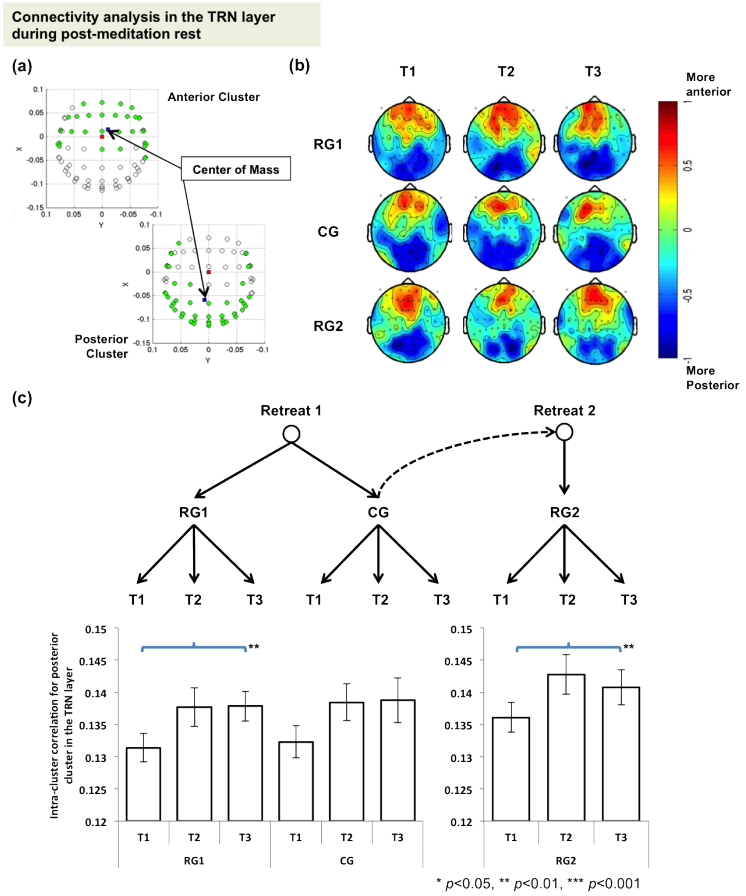

Figure 5.21: Connectivity analysis of the TRN layer during post-meditation rest (Color figure). (a) Sample posterior and anterior clusters, found after k-means clustering on the correlation matrix of TRN cells. (b) Topographical maps for each test-point (and group) are shown during the post-meditation rest state. Across test-points, no topographical changes were found in any group or state. These group maps were created by tagging each channel with -1 (when it was in posterior cluster) or +1 (for anterior cluster) region. The regional location was determined using center of mass of the channels in it, thus negative x indicates posterior and positive x indicated anterior (as shown in (a)). (c) Significant increase was found in within-cluster correlation for the posterior cluster in both RG1 and RG2, whereas no change was found for CG. To reduce the number of tests in this experiment, only T3 was compared to T1. Wilcoxon's test was used to compare T3 with T1 in each state and group for each retreat. Error-rate due to multiple comparisons was checked using FDR-based correction (for 18 tests in R1 and 9 tests in R2). Overall, clear separation between anterior and poster regions of the TRN was found and increased correlation within posterior region of TRN indicates more synchronized activity in that region, after retreat. The meaning of such connectivity changes is discussed in section 5.4 and 5.5.

residence (of participants) and the retreat center. Each one of these correlations will be discussed in turn below.

Self-reported measures As described in the previous chapter, to understand a complex cognitive phenomenon, such as meditation, the first person perspective must be taken into account (Varela and Shear, 1999). Such phenomenological accounts will not only help in providing meaningful explanation for the changes observed in model parameters, but also help develop the theory of meditation itself. It is important to note, however, that in the current work self-reported questionnaires were used for correlation, instead of actual accounts by the participants. Thus, the presented correlations are only the first approximations of the unique individual experience.

Some of the self-reported measures were easy to quantify, such as, daily time spent in meditation. To quantify more complex measures theoretical models were constructed. One such model used second-order latent difference score approach, to cover avoidant attachment, attachment anxiety, depression, anxiety, neuroticism, difficulties in emotional regulation, mindfulness, ego resiliency, empathy, extroversion, agreeableness, conscientiousness, openness to experience, and psychological well-being (Sahdra et al., 2011). Longitudinal changes in these parameters, due to meditation training, were attributed to a single latent factor named adaptive socio-emotional functioning (Sahdra et al., 2011).

Starting with Experiment 2, significant correlations were found between longitudinal increase in corticothalamic delay (during pre- and post-meditation resting states) and lifetime hours of meditation (Figure 5.22): more experienced meditators had higher increase in corticothalamic delay at the end of retreat.

Longitudinal changes found Experiment 3 (stability analysis) and Experiment 4 (connectivity analysis) did not correlate with any self-reported measures. One explanation for the former one could be that since the participants were already neurologically typical (or stable) the increase in brain stability was not large enough to be evident in behavior.

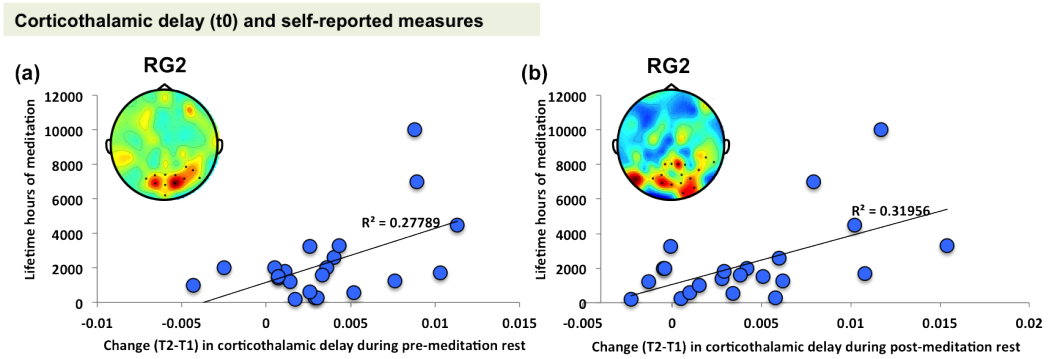

Figure 5.22: Correlations between corticothalamic delay and self-reported measures (Color figure). Strong correlations were found between t_0 and lifetime hours of meditation, indicating that more experienced meditators had higher increase in t_0. In total, three such correlations were found and the most representative ones are shown here. These correlations were: (a) change (T2-T1) in t_0 during pre-meditation rest, and lifetime hours of meditation ($r(20) = 0.527, p < 0.05$); and (b) change (T2-T1) in t_0 during post-meditation rest, and lifetime hours of meditation ($r(20) = 0.565, p < 0.01$);

Performance in attention-related tasks In addition to participating in the meditation experiment, the participants also took part in a number of attention related tasks, such as, sustained attention (MacLean et al., 2010) and response inhibition (Sahdra et al., 2011). Since the primary meditation practice was that of sustaining attention on breath sensations the hypothesis was that change in model parameters could correlate to performance in sustained attention tasks. Considering widespread theories about TRN and its role in attention regulation, the main focus for this correlation was the TRN experiment.

Details about the data from sustained attention and response inhibition tasks are provided in Chapter 4. Quite unexpectedly, no significant correlation was found between any model parameters in any computational experiment and the participants' performance in these attention-related tasks. Since attention regulation and cognitive control has been associated with the frontal areas of the brain, it is possible that the lack of relation between changes in TRN layer and performance in attention-related tasks can be attributed to the

fact that the changes in TRN were only significant in the posterior regions.

Longitudinal changes in cortical activity patterns In Chapter 4, spectral analysis was performed on the EEG data to explore the longitudinal changes in cortical activity, and interesting changes were indeed found. Among them was reduction in individual alpha frequency after three months, which has been consistently shown in experienced meditators (Cahn and Polich, 2006). However, no biological basis is known for this change. The sensitivity maps of model parameters (Figure 5.3) indicate that increased corticothalamic delay is a possible explanation. To corroborate this hypothesis, correlations were measured between reductions in the alpha frequency and the increment in corticothalamic delay. As expected, the correlations were indeed very large during all the three states (Figure 5.23). This result predicts that, perhaps, increased corticothalamic delay (and hence reduced alpha frequency) could be the signature of experienced meditators. It is also important to provide a teleological reason for such an increase, as will be done in Chapter 6.

Another consistent cortical activity change found in both retreat participants was the reduction in beta-band power at posterior sites of the brain. This reduction was attributed to increased cortical activity in the parietal lobes, i.e. enhanced processing of breath sensations during meditation (Chapter 4). However, the exact mechanism for such a enhancement and the role of sensory information filtering (i.e., through thalamus) was unclear. One hypothesis is that reduced intrathalamic gain leads to increased cortical activity. This hypothesis quite plausible, considering that reduced inhibition of thalamic nuclei by TRN can selectively increase the flow of incoming stream of sensory information to the cortex. To test this theory, correlations were measured between reduction in intrathalamic gain and in spectral power in the beta-band. Strong correlations were indeed found in both retreat groups (Figure 5.24). This relation corroborates the theory that higher the reduction in intrathalamic gain, higher the drop in beta-band power. In other words, increased inhibition of TRN lead to increased cortical activity in the parietal region. However, more questions arise before this hypothesis can be accepted. For example, TRN and cortical areas are connected in a

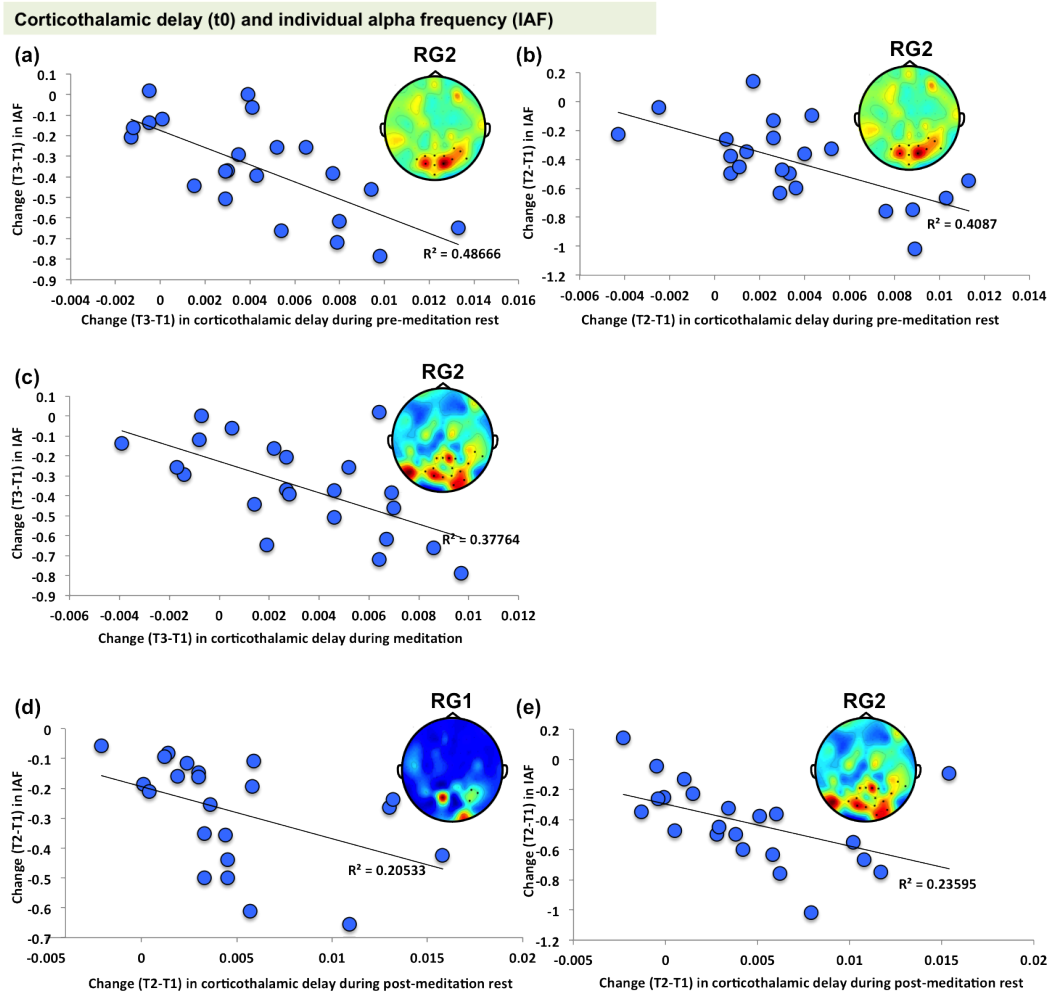

Figure 5.23: Correlations between corticothalamic delay and individual alpha frequency (IAF) (Color figure). Very strong correlations were found between changes in t_0 and in reduction in IAF, indicating that participants with larger drop in IAF also had larger increase in t_0. These relations and parameter sensitivity plots (Figure 5.3) suggest that t_0 is indeed responsible for reduction in IAF in meditators. In total seven similar correlations were found and the most representative ones are shown here. These correlations were: (a-b) between change in t_0 during pre-meditation rest, and change in IAF (for (a), $r(20) = -0.698, p < 0.0001$, and for (b), $r(20) = -0.639, p < 0.01$); (c) between change (T3-T1) in t_0 during meditation, and in IAF ($r(20) = -0.615, p < 0.01$); and (d-e) between change in t_0 during post-meditation rest, and in IAF (for (d), $r(20) = -0.453, p < 0.05$, and for (e), $r(20) = -0.486, p < 0.05$).

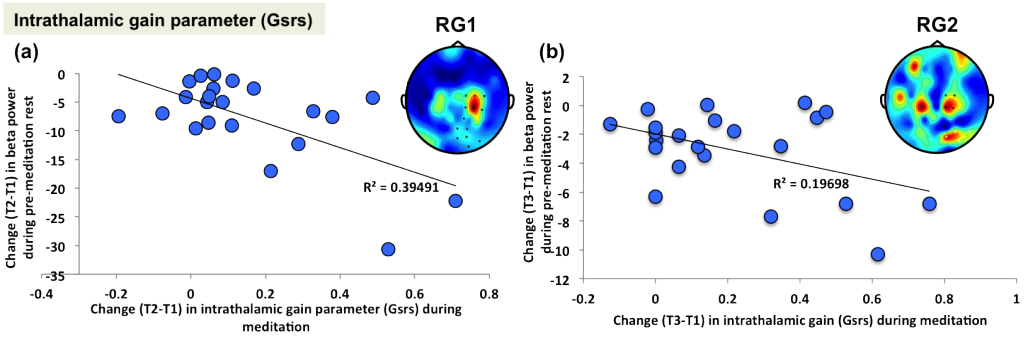

Figure 5.24: Correlations between the change in the intrathalamic gain parameter and reduction in beta band-power (Color figure). Reduction in G_{srs} was found to correlate with reductions in beta power, indicating the higher the drop in G_{srs} corresponds to higher reduction in beta-band power (for (a), $r(20) = -0.628, p < 0.01$, and for (b), $r(20) = -0.444, p < 0.05$).

feedback loop, where an increased activity in cortical areas will induce high activity in the TRN and hence reduce TRN's inhibition. This reduction will in turn block underlying thalamic nuclei and hence sensory information reaching cortical areas. Thus, the first question is how is TRN's activity inhibited in a sustained fashion, while keeping the cortical areas active? The second question is what inhibits the activity in TRN in the first place? Third question is what is role of other parameters (e.g., corticothalamic delay, increase in which also correlates with drop in beta band-power; Figure 5.26)? To answer these questions, Chapter 6 proposes a plausible mechanism by taking into account changes in all model parameters related to meditation training.

A parameter related to the intrathalamic gain was the intrathalamic stability z. Due to reduced intrathalamic gain at the end of retreat, reduced values for z were also found in the exact same locations. Thus, it was expected that reduction in z was also correlated with reduction in beta power. This relation was indeed found (Figure 5.25) indicating that reduction in beta power lead to increased stability of the brain, thereby suggesting stability as the teleological cause for such reduction.

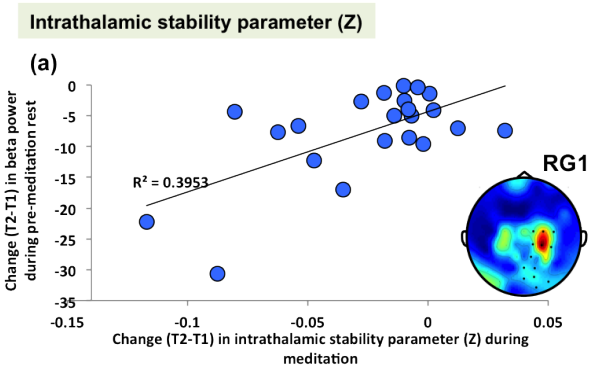

Figure 5.25: Correlations between the change in stability parameter z and reduction in beta band-power (Color figure). Significant correlation was found between change in intrathalamic stability parameter during meditation and reduction in beta-band power during pre-meditation rest ($r(20) = 0.629, p < 0.01$). Although this effect was only significant in RG1, it suggests that more stability was attained by participants with higher drops in beta power.

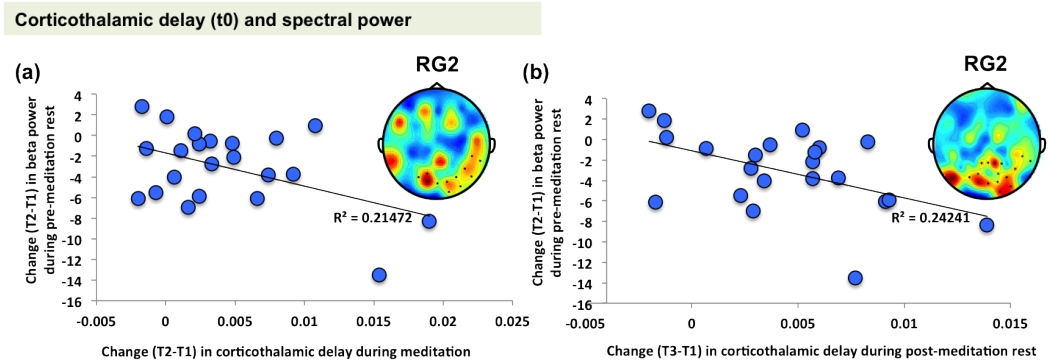

Figure 5.26: Correlations between corticothalamic delay and spectral power (Color figure). Strong correlations were found between changes in t_0 and in reduction in beta power, indicating that participants with larger drop in beta power also had larger increase in t_0. In total, three such correlations were found and the most representative ones are shown here. These correlations were: (a) between change (T2-T1) in t_0 during meditation, and in beta power, during pre-meditation rest ($r(20) = -0.463, p < 0.05$); and (b) between change (T3-T1) in t_0 during post-meditation rest, and change (T2-T1) in beta power, during pre-meditation rest ($r(20) = -0.492, p < 0.05$).

Fourth, during spectral analysis, reduction in alpha power was also found at pre-meditation rest in the second retreat. This reduction was related to increased vigilance in a sustained-attention task, i.e., participants with higher reduction in alpha-band power were able to sustain their attention longer (Chapter 4). Based on the location of the cluster (midline-frontal) and the nature of alpha-rhythms (inversely related to cortical activity), it was proposed that the increased cortical activity in the frontal areas enabled better sustaining of attention. To find out the underlying mechanism, changes in connectivity values within posterior cluster of TRN layer were correlated with reduced alpha power. Strong correlation was found (Figure 5.27), suggesting that increased intra-cluster correlation in posterior region of modeled TRN was responsible. Ideally, a correlation between connectivity changes in frontal regions of TRN and reductions in frontal alpha power should have been found. However, the change in connectivity in frontal regions of TRN, although in the same direction as posterior, was not significant. Thus, it seems that the found correlation is secondary, although still quite strong. The lack of connectivity changes in the frontal regions of TRN might also be responsible for the lack of correlations with participants' performance in attention-related tasks (as described in previous subsection).

Difference in elevation The two retreats were conducted at the Shambhala Mountain Center in Red Feather Lakes, Colorado. The center is about 2370 meters above the sea level. The participants in the control group arrived 3 days (range = 65-75 hr) before the beginning of testing, for acclimatization.

Although every care was taken to collect and preprocess the scalp recorded EEG data, nonetheless high altitudes are known to effect EEG data (Guger et al., 2005). Thus, longitudinal changes in model parameters, observed during rest and meditation, were correlated with difference in elevation between the participant's city of residence and the center. No significant correlations were found between the two in any state or group. Thus, providing more confidence that the changes found in model parameters are indeed due to meditation training.

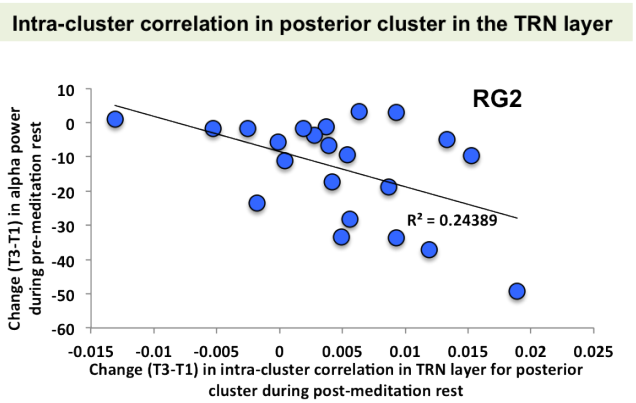

Figure 5.27: Correlations between changes in connectivity in the TRN layer and reduction in alpha band-power. Reduction in frontal alpha power correlated with increased posterior connectivity in TRN ($r(20) = -0.494, p < 0.05$). Such strong correlation indicates that more posterior connectivity was related with higher drops in frontal alpha power. The reduction in alpha power correlated with improved performance in sustained attention task (Chapter 4). Although no direct correlation was found between connectivity in TRN and participants' performance, based on this secondary correlation the role of TRN in attention regulation can be suspected.

Summary In sum, four correlation experiments fulfilled their purpose: they not only provided meaning for the changes observed in computational experiments, but also helped corroborate theories proposed in previous chapters.

5.5 Discussion

Computational modeling was employed to provide a theoretical grounding for the mechanisms underlying focused-attention meditation. A mean-field model, originally created by Robinson et al. (2001), was extended to assess longitudinal changes in model parameters and to explore the role of TRN in attention regulation during meditation. After successful data fitting, model parameters were analyzed to gain insights into the cortico-cortical, cortico-thalamic, intra-thalamic dynamics and their evolution with intensive meditation

training. Two model parameters: intrathalamic gain and corticothalamic delay were found to change with meditation training, thereby providing a mechanistic view of what might be happening inside the brain. Further, stability analysis revealed that the drop in intrathalamic gain increased the overall stability of the system. This finding provides a teleological purpose for the changes observed in model parameters. Fourth, connectivity analysis in the TRN layer discovered an anterior-posterior functional division and a change in connectivity within the posterior division due to training. To provide behavioral interpretations to these changes, they were correlated with self-reported measures, performance in attention-related tasks, longitudinal changes in cortical activity, and difference in elevation. In this section, advanced issues related to the model architecture, the model fitting procedures, the computational experiments, and the task itself are discussed.

Model architecture As a starting point, the model developed by Robinson et al. (2001) was used. This model has been successfully employed to understand various complex brain phenomena, ranging from seizures and tumors (Robinson et al., 2002; Kim et al., 2009; Breakspear et al., 2006; Roberts and Robinson, 2008; O'Connor and Robinson, 2005), to depression (Kerr et al., 2010a), to age-trends in EEG (van Albada et al., 2010; Kerr et al., 2010b, 2011), and attention-related disorders (Rowe et al., 2005a,b, 2004b).

Even though sophisticated, this model is obviously still a simplified version of what might be happening inside the brain. One might ask why only cortico-cortical, cortico-thalamic, and intrathalamic interactions are included, while other subcortical areas are also hypothesized to be involved in meditation training (Newberg and Iversen, 2003).

To answer this question one must first understand how the scalp-recorded EEGs are generated. A significant body of research focuses on three main physiological bases (Pizzagalli, 2007). The first is the summation of excitatory and inhibitory post-synaptic potentials in the pyramidal cells of the cortex (Pizzagalli, 2007; Speckmann and Altrup, 1993). The idea is that synchronized activity of these cells, which are perpendicular to the cortical surface and parallel to each other, can sum up to a high enough electric field that

can reach the scalp (Nunez and Srinivasan, 2006; Pizzagalli, 2007; Baillet et al., 2001).

The second major contributor to scalp-recorded EEG is subcortical areas, especially the thalamus (Steriade et al., 1993). In animals, reliable signals were measured on the scalp induced by thalamic oscillations (Steriade et al., 1993). Further, in human neurophysiology, cortico-cortical and cortico-thalamic interactions are known to contribute oscillations in delta, alpha, and beta band (Pizzagalli, 2007; Fisch and Spehlmann, 1999; Larson et al., 1998). However, limbic regions were implicated for the generation of oscillations in theta band (Pizzagalli, 2007; Vinogradova, 1995; Bland et al., 1999).

Third, recent evidence indicates that local and large-scale synchronization also plays a role in the generation of EEG (Pizzagalli, 2007; Buzsaki and Draguhn, 2004). High-frequency oscillations (e.g., gamma) are generated due to local-scale synchrony with smaller populations, while low-frequency oscillations (e.g., theta) are generated using long-range synchrony between larger neural populations (Buzsaki and Draguhn, 2004).

The architecture of the model is based on the mean-field approach, and it assumes that the scalp-recorded EEG signal is generated primarily by the pyramidal cells of the cortex. Further, it uses the cortico-thalamic and other loops to simulate the oscillatory activity in EEG. Given that only alpha- and beta-band power changes were observed in the spectral analysis of meditation data, this model is appropriate. In the future, however, it can certainly be extended to include limbic areas as well, so that other meditation types, like compassion meditation, can also be formally analyzed.

Modeling the whole head All the 73 channels of EEG were modeled independently, using the local effective value (LEV) approach. LEV is analytically tractable and computationally light (O'Connor and Robinson, 2004). For eyes-closed state, the local independence assumption has been shown valid for all but two cases (O'Connor and Robinson, 2004). At $<$ 2Hz and at alpha frequency, local activity is dependent on similar activity at distant sites (O'Connor and Robinson, 2004).

In the current work, steps were taken to avoid these two violations, and at the same

time, model all channels. First, the lowest frequency band was defined to be $2 - 4$Hz, thus the first violation was avoided by not analyzing lower frequencies. Two measures were taken to avoid the second violation. First, scalp current density (SCD) was estimated during the preprocessing of EEG data. SCD transformed data was used to calculate power spectra density, which was then used to fit the model. SCD not only helps create reference-free EEG data, but also reduces the effects of volume conduction (Pizzagalli, 2007). Thus, the effect of distant activity on the local sensor is greatly reduced. Second, the model was extended to include longitudinal analysis. This analysis uses nonparametric cluster-based permutation approach to find longitudinal changes in model parameters. This cluster-based approach is similar to the cluster-corrected algorithms in fMRI data analysis, where neighborhood information is taken into account when considering the activity at local locations. For example, consider a channel that has high t-test value (when comparing two conditions) but has no neighboring channels with higher t-values. Such a channel will be considered noisy (or by chance only) and will be rejected. Thus, only channels with similar neighboring activations will be taken into account in the analysis. This approach, although insensitive to extremely local changes, works well for EEG data (Maris and Oostenveld, 2007). This approach also benefits the LEV modeling, by including information about neighboring sites and by reducing the chances of violation of local independence. Thus, together, SCD and nonparametric cluster-based approach should reduce the chances for local independence violation at alpha frequency due to distant sites. In future, more rigorous empirical testing can be employed to quantify the improvement.

Fitting experiment During data fitting, on average more than 97% variance was explained by the model, across sites, test-points, and groups. Fitting was done using trust-region-reflective-constrained optimization algorithm (Coleman and Li, 1993). The parameter values were limited by previously set physiologically plausible range (Table 5.1). Further, all the test-points and groups were fitted in the same way and no difference was found in accuracy across test-points or groups.

Although the model-fitting was successful, it is possible to improve accuracy even further with a more sophisticated fitting algorithms. For example, Kerr et al. (2011) showed that multiple random initializations for data fitting can be done, using thousands of Monte Carlo simulations. This way, the initial bias was reduced. Further, an unconstrained optimization algorithm can also be used, however, in the end only those solutions that are in the physiologically plausible range of parameter values should be kept (Robinson et al., 2004). In current work, most of the effort went into cleaning and preprocessing of EEG data, so that every analysis would have a higher SNR. Perhaps that is the reason why even basic optimization lead to good results. In the future, more sophisticated optimization approaches can be tested to gauge if they are worth the time and effort.

Inverse modeling Using inverse modeling and nonparametric cluster-based statistics, the intrathalamic gain for the TRN-SRN-TRN loop was found to decrease over the right parietal region, during rest and meditation, in both retreat groups. Reduced inhibition by the TRN has been linked with increase in arousal or alertness (Steriade et al., 1993), thereby indicating that the participants were more alert even during baseline rest. Interestingly, Rowe et al. (2005a) showed that the same intrathalamic gain parameter can be reduced in attention-deficit hyperactivity disorder (ADHD) patients, through proper medication. Hence, the model predicts that customized focused-attention meditation might provide the same effect without any chemical interaction.

In another study using SPECT, Newberg et al. (2001) found increased thalamic activity in the right hemisphere in experienced meditators at baseline rest. This finding is in agreement with the results from the second computational experiment: Reduction in TRN inhibition naturally increases the activity of the thalamus. Further, the location of this effect is the same as the region where increased thalamic activity was found using SPECT (Newberg et al., 2001). It is important to note that while Newberg et al. (2001) used a neuroimaging technique that has better spatial resolution than EEG, the modeling results using EEG data alone hypothesized even finer resolution of this subcortical interaction. This

result bolsters the argument that the fusion of computational modeling and neuroimaging techniques is essential to uncover the mechanisms underlying complex brain phenomena.

Another parameter, corticothalamic delay, was found to change with meditation training. Increased delay was found in the parietal-occipital regions after training, and strongly correlated with reduction in IAF in both retreat groups. Further, using parameter-sensitivity analysis, it was found that increasing corticothalamic delay, keeping all the other model parameters constant, shifts the alpha frequency to lower values. Given these two pieces of evidence, the model predicts that increased corticothalamic delay is the biological basis for reduction in alpha frequency. However, what purpose such increased delay would serve is unclear. The next chapter provides one plausible account for the same.

Stability analysis Experiment 3 was run to understand what purpose the longitudinal changes in model parameters serve, especially in terms of stability of brain activations. Although the participants in this study were healthy normal individuals, even more stability in the brain was found at the end of three months retreat. This finding implies that focused-attention meditation can be applied to treat patients with unstable brain states (e.g., epileptic patients). In fact, a group of researchers at UCLA are working towards reducing the frequency and intensity of epileptic seizures in this manner (Project: Mindful Attention Training for Epilepsy; Engel et al., 2006). This finding might also help end the debate as to whether meditation is epileptogenic (Jaseja, 2005, 2006) or antiepileptic influence (Orme-Johnson, 2006; Fehr, 2006).

Connectivity analysis in TRN Due to its strategic location and intensive lateral inhibition, TRN has been previously implicated in attention regulation and cognitive control (Zikopoulos and Barbas, 2007; Crick, 1984; Sherman, 1996; Sherman and Guillery, 2002; Austin, 1999; Newberg and Iversen, 2003). TRN is also known to play an important role in building up reciprocal connections between the thalamus and the cortex (Mitrofanis and Guillery, 1993; Ulfig et al., 1998; Pinault, 2011). Due to its pivotal role, connectivity anal-

ysis was performed in the modeled TRN layer to explore the longitudinal changes, if any, associated with meditation training. Two interesting results came out. First, an anterior-posterior functional division that did not change with training was found in TRN. Second, increased connectivity within (significant only in posterior division) and among (although trend) these divisions was found at the end of the meditation retreat (in both RG1 and RG2). These findings suggest that meditation training, at least partly, influence the connectivity structure of the TRN layer by increasing lateral connectivity. This result can have implications in treatment of neurodevelopmental disorders (especially schizophrenia), which are manifested due to lack (or reduction) of this lateral connectivity in TRN (Pinault, 2011; Ferrarelli and Tononi, 2011). Thus, the modeling results predict that focused-attention training can potentially help patients with mental disorders related to connectivity in TRN.

Trait effect of meditation training In the current work, longitudinal changes in the model parameters were analyzed in two rest states (one minute before and after meditation) and one meditation state (of six minutes). However, the meditation state was not compared with the rest state, because of the difference in length of these states. By design, the power spectral density of meditation data would have higher SNR as compared to the short resting state. In the future, the plan is to study the temporal evolution of the meditative state by dividing the six minutes of meditation data into smaller chunks and then modeling and comparing each of those chunks with the resting data.

Nonetheless, by just looking at the longitudinal changes separately in rest and meditation, similar pattern of changes in model parameters was found in both the states. This similarity can be attributed to the trait effect of meditation training, i.e., intensive meditation practice every day for three months altered the cortical activity such that the rest state (or "default state") started to resemble the meditation brain state.

5.6 Conclusion

A comprehensive theoretical model, based on the EEG data, was developed to understand the mechanisms underlying meditation training. Both mechanistic and teleological explanations were theoretically discovered for the longitudinal changes in cortical activity. Further, by correlating changes in model parameters with other measures (including cortical activity changes), biological basis was provided to some of the most consistent findings of meditation research. Interesting future predictions were also generated using the model, including suggestion that focused-attention training can help treat several neurodevelopmental disorders. Future work is particularly compelling in this area. The next chapter presents a biologically plausible theory of focused-attention meditation, by taking all the changes (both in cortical activity and model parameters) into account.

Chapter 6

Discussion and Future Work

In this chapter, first, the empirical and theoretical results are combined into a global theory of what goes on in the brain during focused-attention meditation. Second, this theory is linked to the long-held views about what meditation does to the brain. Third, the chapter explored how a secluded retreat setting could have affected the participants and which factors to keep in mind while assimilating the results. Fourth, future implications of this research are explored in the areas of cognitive science, medicine, and engineering.

6.1 An interdisciplinary account of meditation

Given the comprehensive empirical and theoretical analysis of cortical activity during the intensive meditation training, let us see if a common theory can be built. Regarding spectral analysis three main results were found at the end of retreat, only in retreat participants: (a) reduced individual alpha frequency; (b) reduced frontal midline alpha band-power; and (c) reduced parietal-occipital beta-band power. In the computational experiments four main results were also found in the retreat participants, at the end of retreat, (a) increased cortico-thalamic delay at the parietal locations; (b) reduced intrathalamic gain at the parietal locations; (c) increased stability due to reduced intrathalamic gain; and (d) anterior-posterior

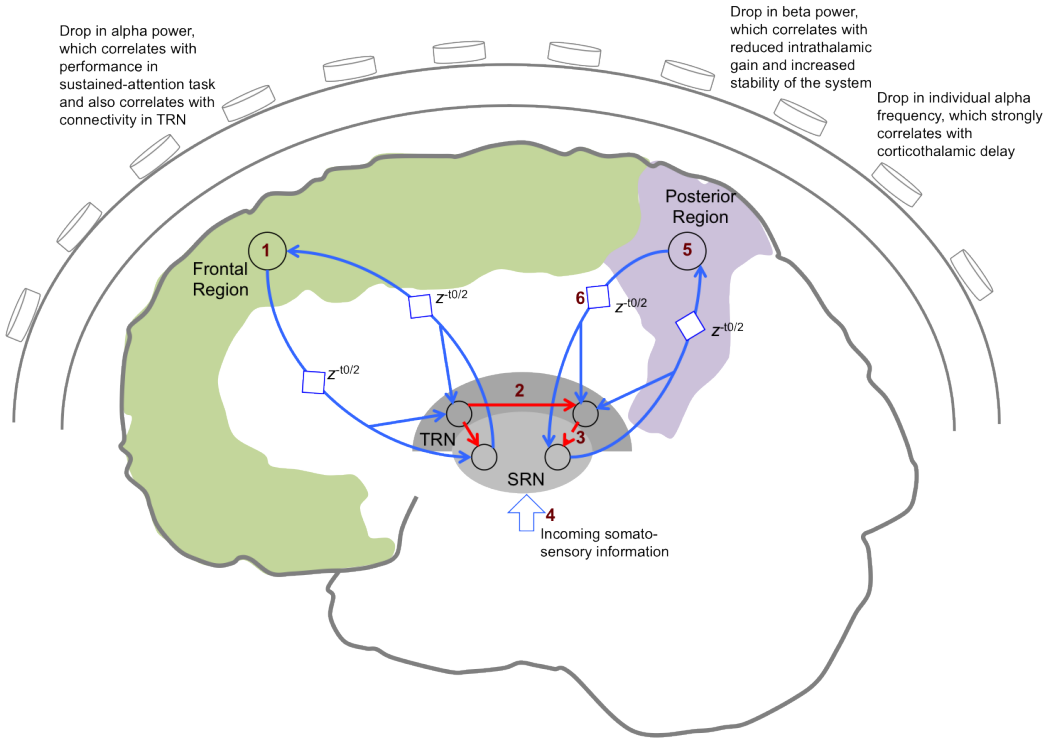

Figure 6.1: Theory of focused-attention meditation (Color figure). As a participant begins, he or she will focus attention on sensations of breath, activating frontal areas. These areas use the reticular nucleus of the thalamus (TRN) to regulate the focus, by inhibiting posterior regions of TRN so that incoming sensory information can flow straight to the posterior cortex. To avoid re-activating the posterior TRN region through reciprocal connections the cortex introduces a delay in the signal transmission. Thus, to let the participant be in the state of *śamatha* (i.e. focusing continuously on breath sensations) the incoming flow of sensory information is not disturbed and the cortical activation in the posterior cortex is maintained.

division in TRN and increased connectivity in the posterior cells of the TRN layer. Based on these findings, following formalization is proposed (also shown in Figure 6.1).

1. At the end of the retreat, as a participant starts meditating, by willfully focusing and sustaining his/her attention on breath sensations, the frontal areas are activated. This initial step is supported by the following three pieces of evidence. First, the volitional

acts of sustaining attention are known to be initiated by the activation in the prefrontal cortex and cingulate gyrus (Newberg and Iversen, 2003; Ingvar, 1994; Frith et al., 1991; Pardo et al., 1991; Posner, 1989; Vogt et al., 1992). Second, in previous studies, these areas were found to be active during meditation (Lazar et al., 2000; Newberg and Iversen, 2003; Brefczynski-Lewis et al., 2007; Newberg et al., 2001). Third, the reduction in alpha power, found during spectral analysis, indicates increased cortical activation in frontal areas. Additionally, this reduced alpha power correlated with increased performance in the vigilance task. Future research using causality analysis (Ding et al., 2006; Pearl, 2000) might be able to provide even more evidence for this initiation of brain activity in frontal cortices, at the start of meditation.

2. The activation in the frontal regions of the brain should in turn activate the thalamic nuclei, including both reticular and sensory-relay nuclei. This flow of activation from frontal regions to thalamus is due to the dense reciprocal connectivity between frontal and thalamic nuclei (Cornwall and Phillipson, 1988; Crick, 1984; Portas et al., 1998). However, the reticular nucleus (TRN) also has dense lateral inhibitory connections (Guillery and Harting, 2003; Jones, 1975; Crick, 1984; Steriade et al., 1986; Sherman and Guillery, 2006; Zikopoulos and Barbas, 2007). These connections will inhibit other TRN cells, especially in the posterior regions of TRN. This proposal of division of anterior-posterior regions of TRN is based on the results from connectivity analysis in Chapter 5.

3. Apart from inhibiting other cells in the TRN laterally, the TRN cells also inhibit the underlying sensory-relay nuclei of thalamus. Hence, they modulate the incoming stream of sensory input to the cortex and act as a gateway of sensory information (Crick, 1984; Guillery et al., 1998; Sherman and Guillery, 2006; Scheibel and Scheibel, 1966). The inhibition of posterior TRN cells will in effect reduce the inhibition of underlying sensory relay nucleus (SRN) of thalamus. This step is consistent with the computational modeling results, where reduction in intrathalamic gain (and

hence reduced inhibition of SRN) was found at the end of meditation training in the posterior regions of TRN.

4. Since the participants are trying to focus on breath sensations, reduced inhibition of SRN cells will in turn allow for an increased flow of incoming sensory information to the cortex. Hence, the sensory information is not gated at the thalamic level and reaches the parietal cortex (i.e. somatosensory areas) of the brain.

5. Previous work showed that in order to attend to the upcoming sensory stimuli, the cortical regions must also be active (van Ede et al., 2011). Further, due to reciprocal connections between thalamus and cortical areas, posterior cortical regions will have increased activation. This activation and the continuous flow of sensory information from the thalamus will allow the participants to constantly attend to the breath sensations (and hence be focused at the object). The drop in beta-band power (and hence increased cortical activity) at the end of retreat over the parietal regions supports this claim.

   However, there is an issue: such an increased activation of the parietal cortex would in turn, due to reciprocal connections, activate the parietal TRN cells and this activation would make the TRN cells inhibit the incoming sensory information (by inhibiting the SRN cells) and hence reduce the ongoing flow of information to cortex. Yet no sensory input will distract the participant to lose the focus.

6. As a solution, a significant delay in the corticothalamic loop is introduced. One plausible mechanism for such delay in signal transmission could be due to the repeated firing of cortical cells in the parietal region. This increase in delay will cause a phase shift in the usual transmission of signal from the cortex to the thalamus. Such phase-shifted cortical signals to the TRN cells selectively suppress and weaken their activity (similar out-of-phase inputs are also shown to be responsible for weakening of previously strengthened inputs in hippocampal cells; Huerta and Lisman, 1995; Csicsvari

et al., 2003). Thus, the system makes sure that the incoming stream of sensory stimuli is not disturbed by TRN cells and the focus on breath sensations is maintained.

The modeling experiments confirm this proposal: Increased corticothalamic delay was found in the retreat participants in the parietal regions of the brain. Further, modeling experiments also suggested that the increase in corticothalamic delay is the biological basis for the consistent finding of reduced alpha frequency in experienced meditators (Cahn and Polich, 2006). The current theory, however, provides a novel (and perhaps the only) teleological reasoning behind increased corticothalamic delay (and hence, reduction in alpha frequency) in meditators.

Altogether, a plausible theory follows from the analysis and modeling, which not only accounts for all the empirical and theoretical results but also uncovers biologically plausible mechanisms underlying focused-attention meditation. The theory also provides concrete and testable hypotheses, which can be tested and refined in future (as outlined in section 6.4).

6.2 Linking theory to folklore

Earliest accounts of meditation can be found in the Hindu texts of Vedic traditions (2000-3000 B.C.). The concept of meditation grew rapidly in the east after the advent of Buddhism (500-600 B.C.). The term meditation is derived from its Sanskrit counterpart $bhavana$, which literally means cultivation. In Tibetan Buddhism the term implies the idea of cultivation of familiarity (Jinpa, 2006). Several cultures and religions assimilated this concept in their own way, giving rise to numerous styles of meditation techniques. Nonetheless, in almost all the traditions it is believed that meditation provides emotional and mental equanimity and that this equanimity is the stepping stone towards attaining enlightenment (Singh, 1999; Wallace, 2006). Further, given that many people find modern life stressful, the belief that meditation can provide the tranquility of the mind actually attracts many

contemporary people to it. It is therefore pertinent to evaluate whether the scientific theory developed in this dissertation can be linked to these traditional beliefs about the nature and effects of meditation.

Living in the moment One of the most common beliefs about the effects of meditation is that it teaches one to always live in the present moment, be it meditation or just cleaning dishes. This moment-to-moment awareness is supposed to employ the mind, so that it stops worrying about the past (remorse for the previous actions) and the future (fear of the unknown). The idea is that by focusing one's attention fully at the task at hand such an unnecessary drainage of energy can be stopped. A recent study found that people spend more than half of their time thinking about something other than what they were actually doing (Killingsworth and Gilbert, 2010). The authors also noted that it is indeed a unique ability to focus on something else, e.g., to reflect on the past or to plan for the future, while working on jobs that are not very demanding. But at the same time, this cognitive ability was shown to come at an additional cost of decreased happiness (Killingsworth and Gilbert, 2010). In meditation traditions, emotional tranquility is the exact reason given for living in the moment (Kabat-Zinn, 1994). But what mechanisms underlying meditation could be responsible for this change and how does one achieve this awareness through meditation?

Link to theory Consider the following thought experiment with a traditional story. If a child is left alone in a dark room without any toys or other attractions, very soon he will grow restless and will start banging the door. Now, in traditional language, replace the child with the mind and the dark room with one's inner space (eyes-closed state). If there is no object to which to pay attention the mind will grow restless and starts bombarding thoughts of the past and future, which in turn will cause the turmoil and loss of inner peace. The theory states that during focused-attention meditation the participants were allowed continuous flow of incoming sensory information (breath sensations at the nostrils), so that they could constantly attend to it and stay focused at the task at hand (meditation).

This constant awareness of each breath sensation provided participants a taste of living in the moment. Both empirical and theoretical experiments suggested that the changes observed during meditation persisted in the resting state. Perhaps the intensive practice of focusing attention on breath sensations led to the generalization of the meditative state into a new "default process" of the brain.

The theory also claims that after three-months of intensive meditation retreat the participants were able to hold this state of focused-attention for longer durations, which should provide better emotional balance (Wallace, 2006). This claim is supported by correlations found between (1) daily time spent in meditation and change in cortical activity, i.e. the more the participant meditates the more reduced beta power (and hence increased cortical activity); and (2) change in cortical activity and improvements in adaptive self-reported socio-emotional functioning, i.e. the more the drop in beta power the more enhanced emotional well being.

From chaos to stability Another common belief about meditation is that it can help reduce mental turmoil and can lead to more stable and calming states of the mind. In Buddhist traditions stability of the mind is considered a crucial requirement for attaining higher stages of spirituality. Wallace (2006) compares meditation practice with looking at the stars using a telescope. If the tripod at which the telescope is based is not stable, the user cannot focus and see clearly. Similarly, if the mind is full of anxiety and restlessness it will not allow the participant to focus. Buddhist teachers prescribe regular meditation practice and relaxation for attaining stability. However, it is unclear how meditation practice provides it and using which mechanisms.

Link to theory The brain is commonly considered as a highly complex self-organizing nonlinear dynamical system (Buzsaki, 2006). As with any dynamical system there are stable and unstable states. Although the retreat participants were already healthy, stability analysis of the computational model showed that reduced intrathalamic gain pro-

vided even more stability to the brain, by retracting from the unstable (hyperactive) boundaries. Thus, apparently, the more the incoming sensory information, the more stable was the system. It is interesting to note that the effect of reduced intrathalamic gain found in retreat participants was also achieved in patients suffering from attention-deficiency-hyperactivity-disorder (ADHD) using medication (Rowe et al., 2005a). Further, in previous work, meditation practice was shown to reduce the nonlinear complexity of the brain (Aftanas and Golocheikine, 2002). Thus it seems that intensive meditation practice led to more simple and stable brain states. In future, it would be interesting to correlate such changes in brain state and self-reported experiences of stability and calmness.

Loss of sense of self Another claim about the effects of meditation on the brain is that it allows for alterations to the sense of self (Newberg and Iversen, 2003). In the Zen Buddhism tradition, such a loss of sense of "self" is associated with the loss of "ego" and hence with the sense of unity with the outer world (Austin, 1999). Further, the traditional claim is that experienced meditators lose the subjectivity (or bias) and attain "objective reality", i.e., interpreting reality in an unbiased fashion (Austin, 1999). In Tibetan Buddhism similar objectivity is attained using non-referential meditation practice (Lutz et al., 2006).

Link to theory: Previous neuroimaging studies have bolstered this claim by showing reduced activity in the posterior superior parietal lobule during meditation (PSPL; Newberg et al., 2001). The PSPL is believed to be involved in creating a 3D representation of the body in space (Steinmetz et al., 1987; Newberg and Iversen, 2003). Thus, the deafferentation of PSPL, and hence its reduced activity, is linked to the loss of sense of "self" during meditation[1]. This claim, however, is in contrast with the findings and the theory presented in this work, where increased activity in the parietal regions was found during meditation and rest after intensive meditation training. This contrast makes sense because

[1]It is important to note that the so-called sense of "self" is malleable and can be modified using virtual reality paradigms (Lenggenhager et al., 2007).

of the difference in the meditation techniques assessed. Newberg et al. (2001) had participants that focused on an internally visualized image and tried to lose the sense of space and time by absorbing their attention into this image. Due to this internalized attention, external sensory information was reduced and hence less sensory information was sent to the parietal regions. However, in the current work, participants focused on their breath sensations at an external point (nostrils). Thus, the goal was opposite to that in visualized imagery meditation: Rather than blocking out sensory information, increased sensory information was desired. In sum, such contrasts beg for the need of systematic evaluations of different kinds of meditation, before all the claims about meditation can be founded in neuroscience.

Altogether, this exercise suggests that it is indeed possible, to some extent, to ground the folklore about meditation into tangible scientific results. Based on these links it would be appropriate to suggest that in simple terms meditation is a mental exercise, which allows the mind to stay more alert and stable. It is perhaps analogous to the musicians practicing scales, which then form a good foundation to playing real musical pieces.

Next, several factors associated with an isolated retreat setting and their potential contributions to the results are discussed.

6.3 Effect of retreat setting

In previous work on meditation, it has been difficult to draw conclusions because it is hard to rule out alternative explanations, due to multiplicity of meditation techniques assessed, individual differences among the practitioners, unsophisticated measures, lack of longitudinal studies, etc. This dissertation controlled for several of these factors by using a longitudinal design and a randomized matched control group of participants. Additionally, state of the art measures and techniques were used at each step of the analysis. Thus, the observed results are likely due to intensive meditation practice. However, certain factors related to the retreat setting may have contributed to the results and need to be understood.

The main such factor is the environmental setting of the retreat at an altitude of approximately 2400 meters above the sea level. Sudden change in altitude is known to affect EEG recording and analysis (Fast cable car ascent to 2700 meters; Guger et al., 2005). The data from the retreat and control participants were collected only after they had acclimatized[2] to the environment. More importantly, lack of correlation between change in altitude (difference in altitude at the participant's residence and the retreat center) and any effect found in the current study shows that the effects of meditation are not likely affected by altitude. Further, several of the results strongly correlated with the hours spent daily in meditations, thereby suggesting main contribution of the practice itself.

Other important factors of the retreat setting include the role of the meditation teacher and the personal motivation of the retreat participants (as opposed to that of controls). One interesting experimental design to test both of these factors, simultaneously, is to have the same meditation teacher provide meditation training to the retreat participants and a controlled relaxation training to the control group (MacLean et al., 2010). In the current work, such a design was not available, but could be explored in the future.

A third factor is social-connectedness. The participants spent most of their time alone in meditations, but they also practiced meditation as a group (twice a day) in addition to occasional conversations with their peers. As pointed out by Sahdra et al. (2011), it is unlikely that just social-connectedness can contribute to enhancements in both cognitive control and psychological well-being. However, in future the contribution of this factor should also be taken into account.

In sum, although great care was taken to control possible complicating factors, certain aspects of the study still need refinement in future. Nonetheless, the current work will hopefully provide a solid starting point for future research in understanding cognitive control and meditation, as will be discussed next.

[2]The participants in the control group reached 3 days (range = 65-75 hr) before the beginning of testing.

6.4 Future Work

Using a tight interaction between data analysis and computational modeling this dissertation developed a concrete theory of meditation training. In the future, the work can be expanded further into several directions, to understand the mechanisms underlying cognitive control in general and meditation in particular. The most compelling directions are:

Broader understanding of meditation The scope of the research can be expanded from focused-attention meditation to emotion-regulation meditation (a.k.a. compassion meditation). Such an extension requires incorporating limbic areas into the computational model. The EEG data required for this extension is already part of the Shamatha project, where EEG was recorded during compassion meditation and emotion-related tasks (e.g. measuring participants' emotional response to a movie using facial expressions encoding). Analyzing both attention and emotion regulation will help in creating a general theory of cognitive control during meditation.

Medical Applications The theory of attention-regulation during meditation can be used to develop better treatments for patients suffering from neurodevelopmental disorders. The computational model suggests that meditation training has an effect *similar* to that of medication on ADHD patients (Rowe et al., 2005a). Further, the model suggests that meditation makes brain activity more stable (and less prone to seizures), suggesting that it can also help epileptic patients. Researchers in UCLA are already working on understanding how effective attention training is in reducing the frequency and intensity of epileptic seizures (Mindful Attention Training or MAT project for epilepsy; Engel et al., 2006). In the future customized meditation trainings based on formal theories, like the one proposed in this dissertation, can be more effective. For example, just like focused-attention meditation, other meditation techniques can be modeled and analyzed to assess their effects on brain stability; and custom meditation techniques can then be prescribed to the patients based on their

brain's instability (e.g., theta vs. spindle). Similarly, video games and other virtual reality systems based on computational modeling can also be developed to help children and adult patients improve their sustained attention, response inhibition, and overall cognitive control. Such approaches may in turn provide a better understanding of neurodevelopmental disorders and the root causes behind them.

Engineering Applications The current theories of cognitive control (of attention or emotions; Cooper, 2011) have rarely been put to test in real world applications. However, they could be useful in domains like neural engineering, robotics, and human-computer interaction systems. Such applications would initiate knowledge sharing between neural/psychological labs and hands-on engineering, e.g. by applying cognitive control theory to improve regulation of neural-prosthetics and human-computer interaction systems, and by simulating real world tasks, like driving a car, in the lab experiments to better understand cognitive control.

Towards a unified theory of cognitive control Starting from the theory of attention- and emotion-regulation, other important cognitive control components, such as response priming and memory monitoring/update, can also be modeled to create a comprehensive theory of cognitive control. Such a model would provide a unique window into the cognitive system as a whole and would make it possible to understand the interactions between the individual control components. It is important to note that only computational modeling can provide such a platform, since it is quite difficult to design experiments which can study all (or several) of them at once.

6.5 Conclusion

This chapter provided a concrete theory of focused-attention meditation. This theory not only accounts for the results seen in the empirical and theoretical experiments, but also helps

uncover teleological explanations for the observed changes in the cortical activity. Further, the chapter also provided scientific basis to several ancient views about meditation does to the brain and behavior, by linking those views with solid scientific findings. Additionally, crucial factors of the retreat setting were discussed and experiments to evaluate them are presented. Lastly, the work in this dissertation may make is possible to use mechanisms underlying meditation for not only understanding cognitive control but also enhance (or retrieve) it.

Chapter 7

Conclusion

This dissertation aims at understanding the mechanisms underlying focused-attention meditation. The results from spectral analysis and computational modeling helped in developing a concrete and testable theory regarding such mechanisms. This chapter concludes this work by reviewing the main contributions (Figure 7.1) and by estimating the impact of this area of research.

7.1 Contributions

The dissertation was presented in four steps: preprocessing, spectral analysis, computational modeling, and correlation analysis. Starting with the preprocessing phase, advanced blind source separation method (SOBI) was implemented as it is (Belouchrani et al., 1997) to separate sources of activity in the EEG data. However, given the huge dataset, manual identification and separation of sources was not feasible or advised (due to subjective bias). Thus, a semi-automated tool (SMART) was developed to identify and remove artifactual sources of contamination. SMART extracts several spatio-temporal features from the sources and uses rule-based classification to identify them. Further, it creates an interactive web page for quick and efficient quality check, where the user can overrule SMART's

decision for classification of any source. This novel and successful integration of SOBI and SMART is currently being applied to several other datasets (in both healthy and patient population) at UC Davis (Saron et al., 2008).

Next, the reconstructed and clean EEG data was transformed using scalp current density estimation. This advanced preprocessing step was implemented as it is, using the CSDToolbox (Kayser, 2009; Kayser and Tenke, 2006). Scalp current density estimation resolves the problem of choosing an optimal reference point for measuring voltage in EEG datasets, by calculating reference-free estimation. Further, it also controls for the volume conduction issue in EEG (Nunez et al., 1997).

In the second step, spectral analysis, preprocessed EEG data was analyzed to determine how brain oscillations change due to meditation training. Spectral power in several frequency bands (i.e. range of frequencies that can be mapped to functional roles) was estimated and changes in power analyzed. Considering the wide age-range of participants in the Shamatha project and the fact that power spectrum is known to change with age (Klimesch et al., 1997), individual alpha frequency was used to determine frequency bands for each participant at each test point. This determination is crucial: If instead fixed band widths were used for all the participants, then changes in power in one frequency band could be wrongly attributed to the other. Such misattribution in turn would lead to wrong conclusions about how meditation affects the brain.

Next, in order to assess longitudinal changes in cortical activity, a novel statistical approach using advanced nonparameteric cluster-based permutation testing was developed. Nonparametric approach was chosen over parametric methods, since it does not require any assumptions about the underlying data distribution. Further, cluster-based approach was used to determine changes in spectral power across neighboring EEG sensors. This approach avoids region of interest analysis, which requires a priori assumptions, and also avoids division of high-density EEG sensor grid into a small number of sparse regions. Lastly, since nonparametric analysis can only handle one independent variable at a time,

spectral power from clusters found during nonparametric analysis was log-transformed and fed into parametric ANOVA (to determine interaction between group/retreat and test-points). Thus, using this hybrid approach of nonparametric and parametric analysis best of both worlds was achieved.

After determining what has changed, the dissertation aimed at understanding how and why those changes appear due to meditation training. Thus, in the third step, computational modeling was employed to build a formal theory. The model architecture (Robinson et al., 2001) was implemented as it is and was later extended to include (1) longitudinal analysis of model parameters; and (2) connectivity analysis in the TRN layer. Four computational experiments were run: First, the EEG power spectrum from all the seventy-three channels and all the three test-points was fitted independently. Second, the novel longitudinal analysis extension was used to gain insights into the changes observed in model parameters due to training. Third, a stability analysis was performed on model equations to understand why the brain preferred such changes. Fourth, novel connectivity analysis was performed in the modeled TRN layer to measure changes in connectivity and the role of TRN in attention regulation. Thus, overall, a set of comprehensive computational experiments was run, so that a concrete and testable model could be constructed.

In the fourth and final step, correlation analysis was performed to ground the changes in cortical activity and model parameters into changes in behavioral and self-reported psychological functions. Such grounding is necessary to make sure that the results are indeed relevant. This step not only helps understand the basis for the observed changes, but also provides hypotheses for future research.

After completing all four steps, a comprehensive theory of focused-attention meditation was constructed. Further, this scientific theory was linked to the "folk-wisdom" about meditation and its effects on the brain. Thus, the results from this dissertation were successfully, although speculatively, grounded in the age-old beliefs about meditation. Next section concludes this chapter by estimating the overall impact of this work.

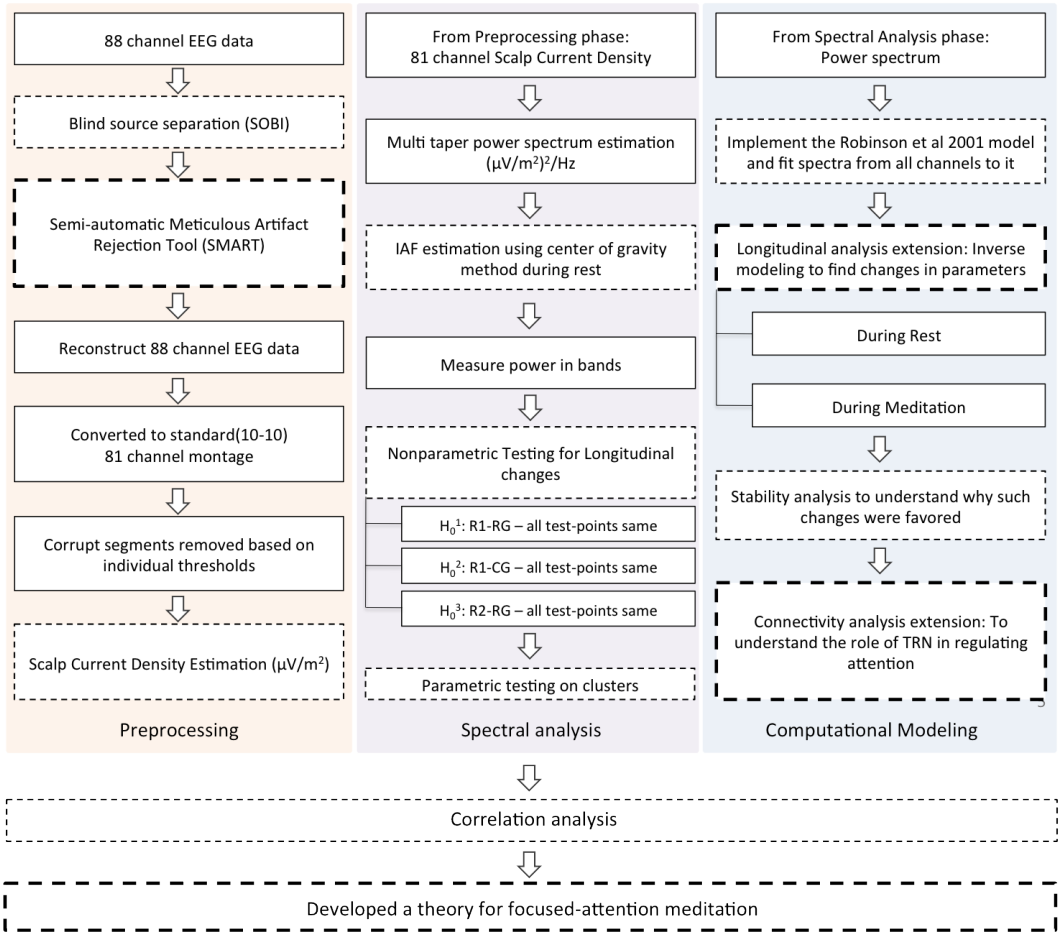

Figure 7.1: Contributions of the four steps in the dissertation. The new analyses developed during the course of dissertation are identified in bold dashed outline. Advanced signal processing steps and/or their novel application, required for the analysis are shown in regular dashed outline. Overall a large interdisciplinary framework was developed as a first step towards understanding meditation in neurobiological terms.

7.2 Conclusion

The dissertation was aimed at constructing a concrete and testable theory of mechanisms underlying meditation. This theory is supported by evidence from computational experiments, spectral analysis, behavioral performance, and self-reported measures of psycholog-

ical functions. Further, since the theory is formalized in a computational model, one cannot only test its predictions but can also refine it using more advanced analyses (e.g. causality analysis).

Before this dissertation, no such concrete and testable theory of meditation existed, previous work had been limited to verbal formulations. Although the dissertation is just a beginning it should set an example that similar interdisciplinary approaches are useful in understanding complex cognitive phenomena, like meditation.

Bibliography

Aftanas, L. and Golocheikine, S. (2001). Human anterior and frontal midline theta and lower alpha reflect emotionally positive state and internalized attention: high-resolution eeg investigation of meditation. *Neuroscience Letters*, 310(1):57–60.

Aftanas, L. and Golocheikine, S. (2002). Non-linear dynamic complexity of the human eeg during meditation. *Neuroscience Letters*, 330(2):143–146.

Aftanas, L. and Golosheikin, S. (2003). Changes in cortical activity in altered states of consciousness: The study of meditation by high-resolution eeg. *Human Physiology*, 29(2):143–151.

Aftanas, L., Koshkarov, V., Mordvintsev, Y., and Pokrovskaja, V. (1994). Dimensional analysis of human eeg during experimental affective experience. *International journal of psychophysiology*, 18(1):67–70.

Aftanas, L., Lotova, N., Koshkarov, V., Makhnev, V., Mordvintsev, Y., and Popov, S. (1998). Non-linear dynamic complexity of the human eeg during evoked emotions. *International journal of psychophysiology*, 28(1):63–76.

Altmann, C., Wilczek, E., and Kaiser, J. (2009). Processing of auditory location changes after horizontal head rotation. *The Journal of Neuroscience*, 29(41):13074.

Anand, B., Chhina, G., and Singh, B. (1961). Studies on shri ramanand yogi during his stay in an air-tight box. *Indian J Med Res*.

Anderson, J., Carter, C., Fincham, J., Qin, Y., Ravizza, S., and Rosenberg-Lee, M. (2008). Using fmri to test models of complex cognition. *Cognitive science*, 32(8):1323–1348.

Andresen, J. (2000). Meditation meets behavioural medicine. the story of experimental research on meditation. *Journal of Consciousness Studies, 7*, 11(12):17–74.

Angelakis, E., Lubar, J., Stathopoulou, S., and Kounios, J. (2004). Peak alpha frequency: an electroencephalographic measure of cognitive preparedness. *Clinical Neurophysiology*, 115(4):887–897.

Asada, H., Fukuda, Y., Tsunoda, S., Yamaguchi, M., and Tonoike, M. (1999). Frontal midline theta rhythms reflect alternative activation of prefrontal cortex and anterior cingulate cortex in humans. *Neuroscience Letters*, 274(1):29–32.

Austin, J. (1999). *Zen and the brain: Toward an understanding of meditation and consciousness*. The MIT press.

Baijal, S. and Srinivasan, N. (2010). Theta activity and meditative states: spectral changes during concentrative meditation. *Cognitive Processing*, 11(1):31–38.

Baillet, S., Mosher, J., and Leahy, R. (2001). Electromagnetic brain mapping. *IEEE Signal processing magazine*, 18(6):14–30.

Balconi, M. and Lucchiari, C. (2008). Consciousness and arousal effects on emotional face processing as revealed by brain oscillations. a gamma band analysis. *International Journal of Psychophysiology*, 67(1):41–46.

Banquet, J. (1973). Spectral analysis of the eeg in meditation. *Electroencephalography and Clinical Neurophysiology*, 35(2):143–151.

Bassett, D. and Bullmore, E. (2009). Human brain networks in health and disease. *Current opinion in neurology*, 22(4):340.

Belouchrani, A., Abed-Meraim, K., Cardoso, J., and Moulines, E. (1993). Second-order blind separation of temporally correlated sources. In *Proc. Int. Conf. Digital Signal Processing*, pages 346–351.

Belouchrani, A., Abed-Meraim, K., Cardoso, J., and Moulines, E. (1997). A blind source separation technique using second-order statistics. *IEEE Transactions on signal processing*, 45(2):434–444.

Belouchrani, A. and Amin, M. (1998). Blind source separation based on time-frequency signalrepresentations. *IEEE Transactions on Signal Processing*, 46(11):2888–2897.

Benjamini, Y. and Hochberg, Y. (1995). Controlling the false discovery rate: a practical and powerful approach to multiple testing. *Journal of the Royal Statistical Society. Series B (Methodological)*, 57(1):289–300.

Benson, H., Malhotra, M., Goldman, R., Jacobs, G., and Hopkins, P. (1990). Three case reports of the metabolic and electroencephalographic changes during advanced buddhist meditation techniques. *Behavioral Medicine*, 16(2):90–95.

Bichot, N., Rossi, A., and Desimone, R. (2005). Parallel and serial neural mechanisms for visual search in macaque area v4. *Science*, 308(5721):529.

BIOSEMI (2006). http://www.biosemi.com. *Netherlands, Amsterdam*.

Biswas, A. and Guha, A. (2010). Time series analysis of hybrid neurophysiological data and application of mutual information. *Journal of computational neuroscience*, 29(1):35–47.

Bland, B., Oddie, S., and Colom, L. (1999). Mechanisms of neural synchrony in the septo-hippocampal pathways underlying hippocampal theta generation. *The Journal of neuroscience*, 19(8):3223.

Bonferroni, C. (1935). *Il calcolo delle assicurazioni su gruppi di teste*. Tipografia del Senato.

Breakspear, M., Roberts, J., Terry, J., Rodrigues, S., Mahant, N., and Robinson, P. (2006). A unifying explanation of primary generalized seizures through nonlinear brain modeling and bifurcation analysis. *Cerebral Cortex*, 16(9):1296.

Brefczynski-Lewis, J., Lutz, A., Schaefer, H., Levinson, D., and Davidson, R. (2007). Neural correlates of attentional expertise in long-term meditation practitioners. *Proceedings of the National Academy of Sciences*, 104(27):11483.

Brovelli, A., Ding, M., Ledberg, A., Chen, Y., Nakamura, R., and Bressler, S. (2004). Beta oscillations in a large-scale sensorimotor cortical network: directional influences revealed by granger causality. *Proceedings of the National Academy of Sciences of the United States of America*, 101(26):9849.

Bullmore, E. and Sporns, O. (2009). Complex brain networks: graph theoretical analysis of structural and functional systems. *Nat Rev Neurosci*, 10(3):186–198.

Buzsaki, G. (2006). *Rhythms of the Brain*. Oxford University Press, USA.

Buzsaki, G. and Draguhn, A. (2004). Neuronal oscillations in cortical networks. *Science*, 304(5679):1926.

Cahn, B., Delorme, A., and Polich, J. (2010). Occipital gamma activation during vipassana meditation. *Cognitive processing*, 11(1):39–56.

Cahn, B. and Polich, J. (2006). Meditation states and traits: Eeg, erp, and neuroimaging studies. *Psychological Bulletin*, 132(2):32.

Campbell, J., Lo, A., and MacKinlay, A. (1997). *The econometrics of financial markets*, volume 1. Princeton University Press Princeton, NJ.

Capilla, A., Pazo-Alvarez, P., Darriba, A., Campo, P., and Gross, J. (2011). Steady-state visual evoked potentials can be explained by temporal superposition of transient event-related responses. *PloS one*, 6(1):e14543.

Capotosto, P., Babiloni, C., Romani, G., and Corbetta, M. (2009). Frontoparietal cortex controls spatial attention through modulation of anticipatory alpha rhythms. *The Journal of Neuroscience*, 29(18):5863.

Chambers, R., Gullone, E., and Allen, N. (2009). Mindful emotion regulation: An integrative review. *Clinical Psychology Review*, 29(6):560–572.

Chatrian, G. (1985). Ten percent electrode system for topographic studies of spontaneous and evoked eeg activity. *Am J Electroencephalogr Technol*, 25:83–92.

Chklovskii, D., Mel, B., and Svoboda, K. (2004). Cortical rewiring and information storage. *Nature*, 431(7010):782–788.

Coan, J. and Allen, J. (2004). Frontal EEG asymmetry as a moderator and mediator of emotion. *Biological Psychology*, 67(1-2):7–50.

Coleman, T. and Li, Y. (1993). An interior trust region approach for nonlinear minimization subject to bounds. *SIAM Journal on Optimization*.

Cooper, N., Croft, R., Dominey, S., Burgess, A., and Gruzelier, J. (2003). Paradox lost? exploring the role of alpha oscillations during externally vs. internally directed attention and the implications for idling and inhibition hypotheses. *International Journal of Psychophysiology*, 47(1):65–74.

Cooper, R. (2010). Cognitive Control: Componential or Emergent? *Topics in Cognitive Science*.

Cooper, R. (2011). Complementary perspectives on cognitive control. *Topics in Cognitive Science*, 3(2):208–211.

Cornwall, J. and Phillipson, O. (1988). Mediodorsal and reticular thalamic nuclei receive collateral axons from prefrontal cortex and laterodorsal tegmental nucleus in the rat. *Neuroscience letters*, 88(2):121–126.

Crabtree, J. and Killackey, H. (1989). The topographic organization and axis of projection within the visual sector of the rabbit's thalamic reticular nucleus. *European Journal of Neuroscience*, 1(1):94–109.

Crick, F. (1984). Function of the thalamic reticular complex: the searchlight hypothesis. *Proceedings of the National Academy of Sciences of the United States of America*, 81(14):4586.

Crick, F. and Koch, C. (2003). A framework for consciousness. *nature neuroscience*, 6:119–126.

Csibra, G., Davis, G., Spratling, M., and Johnson, M. (2000). Gamma oscillations and object processing in the infant brain. *Science*, 290(5496):1582.

Csicsvari, J., Jamieson, B., Wise, K., and Buzsáki, G. (2003). Mechanisms of gamma oscillations in the hippocampus of the behaving rat. *Neuron*, 37(2):311–322.

Cui, X., Bray, S., Bryant, D., Glover, G., and Reiss, A. (2010). A quantitative comparison of nirs and fmri across multiple cognitive tasks. *NeuroImage*.

Das, N. and Gastaut, H. (1955). Variations de l'activite electrique du cerveau, du coeur et des muscles squelettiques au cours de la meditation et de l'extase yogique. *Electroencephalogr Clin Neurophysiol*, 6:211–9.

Davidson, R. and Goleman, D. (1977). The role of attention in meditation and hypnosis: A psychobiological perspective on transformations of consciousness. *International Journal of Clinical and Experimental Hypnosis*, 25(4):291–308.

Davidson, R., Jackson, D., and Larson, C. (2000). Human electroencephalography. *Handbook of psychophysiology*, 2:27–52.

Davidson, R. and Lutz, A. (2008). Buddha's brain: Neuroplasticity and meditation. *IEEE Signal Processing Magazine*, 25(1):176.

Davis, S. (2003). *Handbook of research methods in experimental psychology*. Blackwell Pub.

Deepak, K., Manchanda, S., and Maheshwari, M. (1994). Meditation improves clinicoelectroencephalographic measures in drug-resistant epileptics. *Applied Psychophysiology and Biofeedback*, 19(1):25–40.

Dichter, G. and Belger, A. (2007). Social stimuli interfere with cognitive control in autism. *Neuroimage*, 35(3):1219–1230.

Dien, J. (1998). Issues in the Application of the Average Reference Review, Critiques, and Recommendations. *Behavior Research Methods Instruments and Computers*, 30:34–43.

Ding, M., Chen, Y., and Bressler, S. (2006). *Granger causality: Basic theory and application to neuroscience*. Wiley Online Library.

Done, J., Davis, C., and Weisman, M. (2004). The next generation of NWP: Explicit forecasts of convection using the Weather Research and Forecasting (WRF) model. *Atmospheric Science Letters*, 5(6):110–117.

Dumermuth, G. and Molinari, L. (1987). Spectral analysis of the EEG. *Neuropsychobiology*, 17(1-2):85–99.

Dunn, B., Hartigan, J., and Mikulas, W. (1999). Concentration and mindfulness meditations: unique forms of consciousness? *Applied psychophysiology and biofeedback*, 24(3):147–165.

Engel, A., Fries, P., König, P., Brecht, M., and Singer, W. (1999). Temporal binding, binocular rivalry, and consciousness* 1. *Consciousness and Cognition*, 8(2):128–151.

Engel, A. and Singer, W. (2001). Temporal binding and the neural correlates of sensory awareness. *Trends in cognitive Sciences*, 5(1):16–25.

Engel, J. P., Baumgartner, C., and Wallace, B. (2005-2006). Mindful attention training (mat) for epilepsy. Unpublished work; From wikipedia page of Alan Wallace.

Farb, N., Segal, Z., Mayberg, H., Bean, J., McKeon, D., Fatima, Z., and Anderson, A. (2007). Attending to the present: mindfulness meditation reveals distinct neural modes of self-reference. *Social Cognitive and Affective Neuroscience*, 2(4):313.

Fehr, T. (2006). Transcendental meditation may prevent partial epilepsy. *European Journal of Cardiovascular Nursing*, 67(6):1462–1463.

Fernandez-Bouzas, A., Harmony, T., Bosch, J., Aubert, E., Fernandez, T., Valdes, P., Silva, J., Marosi, E., Martinez-Lopez, M., and Casian, G. (1999). Sources of abnormal eeg activity in the presence of brain lesions. *Clinical EEG electroencephalography*, 30(2):46–52.

Ferrarelli, F. and Tononi, G. (2011). The thalamic reticular nucleus and schizophrenia. *Schizophrenia bulletin*, 37(2):306.

Fisch, B. and Spehlmann, R. (1999). *Fisch and Spehlmann's EEG primer: basic principles of digital and analog EEG*. Elsevier Science Health Science div.

Freeman, W. (1972). Linear analysis of the dynamics of neural masses. *Annual Review of Biophysics and Bioengineering*, 1(1):225–256.

Freeman, W. (1975). *Mass action in the nervous system*. Academic Press New York.

Freeman, W. (1987). Simulation of chaotic EEG patterns with a dynamic model of the olfactory system. *Biological Cybernetics*, 56(2):139–150.

Freeman, W., Holmes, M., Burke, B., and Vanhatalo, S. (2003). Spatial spectra of scalp eeg and emg from awake humans. *Clinical Neurophysiology*, 114(6):1053–1068.

Fries, P., Reynolds, J., Rorie, A., and Desimone, R. (2001). Modulation of oscillatory neuronal synchronization by selective visual attention. *Science*, 291(5508):1560.

Frith, C., Friston, K., Liddle, P., and Frackowiak, R. (1991). Willed action and the prefrontal cortex in man: a study with pet. *Proceedings: Biological Sciences*, 244(1311):241–246.

Gasser, T. and Molinari, L. (1996). The analysis of the EEG. *Statistical Methods in Medical Research*, 5(1):67.

Gilmore, P. and Brenner, R. (1981). Correlation of eeg, computerized tomography, and clinical findings. study of 100 patients with focal delta activity. *Archives of neurology*, 38(6):371.

Goldman, R., Stern, J., Engel Jr, J., and Cohen, M. (2002). Simultaneous eeg and fmri of the alpha rhythm. *Neuroreport*, 13(18):2487.

Grant, J., Courtemanche, J., and Rainville, P. (2010). A non-elaborative mental stance and decoupling of executive and pain-related cortices predicts low pain sensitivity in zen meditators. *PAIN*®.

Grützner, C., Uhlhaas, P., Genc, E., Kohler, A., Singer, W., and Wibral, M. (2010). Neuroelectromagnetic correlates of perceptual closure processes. *The Journal of Neuroscience*, 30(24):8342.

Gruber, T., Trujillo-Barreto, N., Giabbiconi, C., Valdes-Sosa, P., and Muller, M. (2006). Brain electrical tomography (bet) analysis of induced gamma band responses during a simple object recognition task. *Neuroimage*, 29(3):888–900.

Gruber, T., Tsivilis, D., Montaldi, D., and Müller, M. (2004). Induced gamma band responses: an early marker of memory encoding and retrieval. *Neuroreport*, 15(11):1837.

Guger, C., Domej, W., Lindner, G., Pfurtscheller, K., Pfurtscheller, G., and Edlinger, G. (2005). Effects of a fast cable car ascent to an altitude of 2700 meters on eeg and ecg. *Neuroscience letters*, 377(1):53–58.

Guillery, R., Feig, S., and Lozsadi, D. (1998). Paying attention to the thalamic reticular nucleus. *Trends in Neurosciences*, 21(1):28–32.

Guillery, R. and Harting, J. (2003). Structure and connections of the thalamic reticular nucleus: advancing views over half a century. *The Journal of Comparative Neurology*, 463(4):360–371.

Handy, T. (2005). *Event-related potentials*. MIT Press.

Handy, T. (2009). *Brain signal analysis advances in neuroelectric and neuromagnetic methods*. MIT Press.

Hebert, R. and Lehmann, D. (1977). Theta bursts: an eeg pattern in normal subjects practising the transcendental meditation technique. *Electroencephalography and Clinical Neurophysiology*, 42(3):397–405.

Herzog, H., Lele, V., Kuwert, T., Langen, K., Kops, E., and Feinendegen, L. (1990). Changed pattern of regional glucose metabolism during yoga meditative relaxation. *Neuropsychobiology*, 23(4):182–187.

Hodgkin, A. and Huxley, A. (1952). The components of membrane conductance in the giant axon of Loligo. *The Journal of physiology*, 116(4):473.

Houser, C., Vaughn, J., Barber, R., and Roberts, E. (1980). Gaba neurons are the major cell type of the nucleus reticularis thalami. *Brain Research*, 200(2):341–354.

Huerta, P. and Lisman, J. (1995). Bidirectional synaptic plasticity induced by a single burst during cholinergic theta oscillation in ca1 in vitro. *Neuron*, 15(5):1053–1063.

Hyvärinen, A., Karhunen, J., and Oja, E. (2001). *Independent component analysis*, volume 26. Wiley-interscience.

Ikemi, A. (1988). Psychophysiological effects of self-regulation method: Eeg frequency analysis and contingent negative variations. *Psychotherapy and psychosomatics*.

Ingvar, D. (1994). The will of the brain: cerebral correlates of willful acts. *Journal of theoretical biology*, 171(1):7–12.

Isaksson, A., Wennberg, A., and Zetterberg, L. (1981). Computer analysis of eeg signals with parametric models. *Proceedings of the IEEE*, 69(4):451–461.

Itti, L. and Koch, C. (2001). Computational modelling of visual attention. *Nature reviews neuroscience*, 2(3):194–203.

Jacobs, G., Benson, H., and Friedman, R. (1996). Topographic eeg mapping of the relaxation response. *Applied Psychophysiology and Biofeedback*, 21(2):121–129.

Jacobs, G. and Lubar, J. (1989). Spectral analysis of the central nervous system effects of the relaxation response elicited by autogenic training. *Behavioral Medicine*, 15(3):125–132.

Jacobs, T., Epel, E., Lin, J., Blackburn, E., Wolkowitz, O., Bridwell, D., Zanesco, A., Aichele, S., Sahdra, B., MacLean, K., et al. (2010). Intensive meditation training, immune cell telomerase activity, and psychological mediators. *Psychoneuroendocrinology*.

Jaseja, H. (2005). Meditation may predispose to epilepsy: an insight into the alteration in brain environment induced by meditation. *Medical hypotheses*, 64(3):464–467.

Jaseja, H. (2006). Meditation potentially capable of increasing susceptibility to epilepsy-a follow-up hypothesis. *Medical hypotheses*, 66(5):925–928.

Jensen, O., Kaiser, J., and Lachaux, J. (2007). Human gamma-frequency oscillations associated with attention and memory. *Trends in neurosciences*, 30(7):317–324.

Jensen, O. and Tesche, C. (2002). Frontal theta activity in humans increases with memory load in a working memory task. *European Journal of Neuroscience*, 15(8):1395–1399.

Jinpa, T. (2006). Is meditation a means of knowing our mental world? *Institute of Tibetan Classics, McGill University*.

Jirsa, V. and Haken, H. (1996). Field theory of electromagnetic brain activity. *Physical Review Letters*, 77(5):960–963.

Jokisch, D. and Jensen, O. (2007). Modulation of gamma and alpha activity during a working memory task engaging the dorsal or ventral stream. *The Journal of neuroscience*, 27(12):3244.

Jones, E. (1975). Some aspects of the organization of the thalamic reticular complex. *The Journal of Comparative Neurology*, 162(3):285–308.

Joyce, C., Gorodnitsky, I., and Kutas, M. (2004). Automatic removal of eye movement and blink artifacts from EEG data using blind component separation. *Psychophysiology*, 41(2):313–325.

Jung, K., Kooa, Y., Kim, B., Ko, D., Lee, G., Kim, K., and Im, C. (2011). Sleep medicine. *Sleep Medicine*, 12:416–421.

Kabat-Zinn, J. (1993). Mindfulness meditation: Health benefits of an ancient Buddhist practice. *Mind/body medicine*, pages 259–275.

Kabat-Zinn, J. (1994). *Wherever you go, there you are: Mindfulness meditation in everyday life*. Hyperion Books.

Kasamatsu, A. and Hirai, T. (1966). An electroencephalographic study on the zen meditation (zazen). *Psychiatry and Clinical Neurosciences*, 20(4):315–336.

Kayser, J. (2009). Current source density (csd) interpolation using spherical splines-csd toolbox (http://psychophysiology. cpmc. columbia. edu/csd toolbox. html). division of cognitive neuroscience. *New York State Psychiatric Institute*.

Kayser, J. and Tenke, C. (2006). Principal components analysis of laplacian waveforms as a generic method for identifying erp generator patterns: I. evaluation with auditory oddball tasks. *Clinical Neurophysiology*, 117(2):348–368.

Kerr, C., Kemp, A., Rennie, C., and Robinson, P. (2010a). Thalamocortical changes in major depression probed by deconvolution and physiology-based modeling. *NeuroImage*.

Kerr, C., Rennie, C., and Robinson, P. (2008). Physiology-based modeling of cortical auditory evoked potentials. *Biological cybernetics*, 98(2):171–184.

Kerr, C., Rennie, C., and Robinson, P. (2011). Model-based analysis and quantification of age trends in auditory evoked potentials. *Clinical Neurophysiology*, 122(1):134–147.

Kerr, C., van Albada, S., Rennie, C., and Robinson, P. (2010b). Age trends in auditory oddball evoked potentials via component scoring and deconvolution. *Clinical Neurophysiology*, 121(6):962–976.

Khalsa, D. and Newberg, A. (2007). P-087 stress, meditation, spect scans, and dementia prevention. *Alzheimer's & Dementia: The Journal of the Alzheimer's Association*, 3(3S):126–126.

Khushu, S., Telles, S., Kumaran, S., Naveen, K., and Tripathi, R. (2000). Frontal activation during meditation based on functional magnetic resonance imaging (fmri). *Indian journal of Physiology and Pharmacology*, 44(5):34.

Killingsworth, M. and Gilbert, D. (2010). A wandering mind is an unhappy mind. *Science*, 330(6006):932.

Kim, J., Roberts, J., and Robinson, P. (2009). Dynamics of epileptic seizures: Evolution, spreading, and suppression. *Journal of theoretical biology*, 257(4):527–532.

Kjaer, T., Nowak, M., and Lou, H. (2002). Reflective self-awareness and conscious states: Pet evidence for a common midline parietofrontal core. *Neuroimage*, 17(2):1080–1086.

Klimesch, W. (1999). EEG alpha and theta oscillations reflect cognitive and memory performance: a review and analysis. *Brain Research Reviews*, 29(2-3):169–195.

Klimesch, W., Doppelmayr, M., Pachinger, T., and Ripper, B. (1997). Brain oscillations and human memory: Eeg correlates in the upper alpha and theta band. *Neuroscience letters*, 238(1-2):9–12.

Klimesch, W., Doppelmayr, M., Schwaiger, J., Auinger, P., and Winkler, T. (1999). Paradoxical alpha synchronization in a memory task. *Cognitive Brain Research*, 7(4):493–501.

Klimesch, W., Schimke, H., Ladurner, G., and Pfurtscheller, G. (1990). Alpha frequency and memory performance. *Journal of Psychophysiology*.

Koskenniemi, K. (1984). A general computational model for word-form recognition and production. In *Proceedings of the 10th International Conference on Computational Linguistics and 22nd annual meeting on Association for Computational Linguistics*, pages 178–181. Association for Computational Linguistics.

Krishnamurti, T., Kishtawal, C., LaRow, T., Bachiochi, D., Zhang, Z., Williford, C., Gadgil, S., and Surendran, S. (1999). Improved weather and seasonal climate forecasts from multimodel superensemble. *Science*, 285(5433):1548.

LaBerge, D. (1997). Attention, awareness, and the triangular circuit* 1. *Consciousness and cognition*, 6(2-3):149–181.

LaBerge, D. (2005). Sustained attention and apical dendrite activity in recurrent circuits. *Brain research reviews*, 50(1):86–99.

Lagerlund, T. and Sharbrough, F. (1989). Computer simulation of the generation of the electroencephalogram. *Electroencephalography and clinical neurophysiology*, 72(1):31.

Lakatos, P., Karmos, G., Mehta, A., Ulbert, I., and Schroeder, C. (2008). Entrainment of neuronal oscillations as a mechanism of attentional selection. *science*, 320(5872):110.

Lam, Y. and Sherman, S. (2011). Functional organization of the thalamic input to the thalamic reticular nucleus. *The Journal of Neuroscience*, 31(18):6791.

Lansky, E. and St Louis, E. (2006). Transcendental meditation: A double-edged sword in epilepsy? *Epilepsy & Behavior*, 9(3):394–400.

Larson, C., Davidson, R., Abercrombie, H., Ward, R., Schaefer, S., Jackson, D., Holden, J., and Perlman, S. (1998). Relations between pet-derived measures of thalamic glucose metabolism and eeg alpha power. *Psychophysiology*, 35(2):162–169.

Laufs, H., Kleinschmidt, A., Beyerle, A., Eger, E., Salek-Haddadi, A., Preibisch, C., and Krakow, K. (2003). Eeg-correlated fmri of human alpha activity. *NeuroImage*, 19(4):1463–1476.

Lazar, S., Bush, G., Gollub, R., Fricchione, G., Khalsa, G., and Benson, H. (2000). Functional brain mapping of the relaxation response and meditation. *Neuroreport*, 11(7):1581.

Lazar, S., Kerr, C., Wasserman, R., Gray, J., Greve, D., Treadway, M., McGarvey, M., Quinn, B., Dusek, J., Benson, H., et al. (2005). Meditation experience is associated with increased cortical thickness. *Neuroreport*, 16(17):1893.

Lehmann, D. (1987). Principles of spatial analysis. *Handbook of electroencephalography and clinical neurophysiology*, 1:309–354.

Lehmann, D., Faber, P., Achermann, P., Jeanmonod, D., Gianotti, L., and Pizzagalli, D. (2001). Brain sources of eeg gamma frequency during volitionally meditation-induced, altered states of consciousness, and experience of the self. *Psychiatry Research: Neuroimaging*, 108(2):111–121.

Lenggenhager, B., Tadi, T., Metzinger, T., and Blanke, O. (2007). Video ergo sum: manipulating bodily self-consciousness. *Science*, 317(5841):1096.

Lesh, T., Niendam, T., Minzenberg, M., and Carter, C. (2010). Cognitive control deficits in schizophrenia: mechanisms and meaning. *Neuropsychopharmacology*.

Li, Y., Adalı, T., and Calhoun, V. (2007). Estimating the number of independent components for functional magnetic resonance imaging data. *Human brain mapping*, 28(11):1251–1266.

Liley, D. and Wright, J. (1994). Intracortical connectivity of pyramidal and stellate cells: estimates of synaptic densities and coupling symmetry. *Network: Computation in Neural Systems*, 5(2):175–189.

Logothetis, N. (2008). What we can do and what we cannot do with fMRI. *Nature*, 453(7197):869–878.

Lopes da Silva, F., Hoeks, A., Smits, H., and Zetterberg, L. (1974). Model of brain rhythmic activity. *Biological Cybernetics*, 15(1):27–37.

Lou, H., Kjaer, T., Friberg, L., Wildschiodtz, G., Holm, S., and Nowak, M. (1999). A 15o-h2o pet study of meditation and the resting state of normal consciousness. *Human Brain Mapping*, 7(2):98–105.

Lozsadi, D. (1995). Organization of connections between the thalamic reticular and the anterior thalamic nuclei in the rat. *The Journal of Comparative Neurology*, 358(2):233–246.

Luck, S. (2005). *An introduction to the event-related potential technique*. The MIT press.

Lumer, E., Edelman, G., and Tononi, G. (1997). Neural dynamics in a model of the thalamocortical system. I. Layers, loops and the emergence of fast synchronous rhythms. *Cerebral Cortex*, 7(3):207.

Lutz, A., Dunne, J., and Davidson, R. (2006). Meditation and the neuroscience of consciousness: An introduction. *The Cambridge handbook of consciousness*.

Lutz, A., Greischar, L., Rawlings, N., Ricard, M., and Davidson, R. (2004). Long-term meditators self-induce high-amplitude gamma synchrony during mental practice. *Proceedings of the National Academy of Sciences*, 101(46):16369.

Lutz, A., Slagter, H., Dunne, J., and Davidson, R. (2008a). Attention regulation and monitoring in meditation. *Trends in Cognitive Sciences*, 12(4):163–169.

Lutz, A., Slagter, H., Dunne, J., and Davidson, R. (2008b). Attention regulation and monitoring in meditation. *Trends in cognitive sciences*, 12(4):163–169.

Lutz, A., Slagter, H., Rawlings, N., Francis, A., Greischar, L., and Davidson, R. (2009). Mental Training Enhances Attentional Stability: Neural and Behavioral Evidence. *Journal of Neuroscience*, 29(42):13418.

Luu, P., Tucker, D., Derryberry, D., Reed, M., and Poulsen, C. (2003). Electrophysiological responses to errors and feedback in the process of action regulation. *Psychological Science*, 14(1):47.

MacLean, K., Ferrer, E., Aichele, S., Bridwell, D., Zanesco, A., Jacobs, T., King, B., Rosenberg, E., Sahdra, B., Shaver, P., et al. (2010). Intensive meditation training improves perceptual discrimination and sustained attention. *Psychological Science*, 21(6):829.

Makeig, S., Bell, A., Jung, T., Sejnowski, T., et al. (1996). Independent component analysis of electroencephalographic data. *Advances in neural information processing systems*, pages 145–151.

Malmivuo, J. and Suihko, V. (2004). Effect of skull resistivity on the spatial resolutions of EEG and MEG. *IEEE Transactions on Biomedical Engineering*, 51(7):1276–1280.

Maris, E. and Oostenveld, R. (2007). Nonparametric statistical testing of EEG-and MEG-data. *Journal of neuroscience methods*, 164(1):177–190.

Maris, E., Schoffelen, J., and Fries, P. (2007). Nonparametric statistical testing of coherence differences. *Journal of neuroscience methods*, 163(1):161–175.

MATLAB (2010). The mathworks inc. *Natick, MA*.

McAlonan, K., Cavanaugh, J., and Wurtz, R. (2008). Guarding the gateway to cortex with attention in visual thalamus. *Nature*, 456(7220):391–394.

McMenamin, B., Shackman, A., Maxwell, J., Bachhuber, D., Koppenhaver, A., Greischar, L., and Davidson, R. (2010). Validation of ica-based myogenic artifact correction for scalp and source-localized eeg. *Neuroimage*, 49(3):2416–2432.

M*ü*ller, M., Keil, A., Gruber, T., and Elbert, T. (1999). Processing of affective pictures modulates right-hemispheric gamma band eeg activity. *Clinical Neurophysiology*, 110(11):1913–1920.

Medendorp, W., Kramer, G., Jensen, O., Oostenveld, R., Schoffelen, J., and Fries, P. (2007). Oscillatory activity in human parietal and occipital cortex shows hemispheric lateralization and memory effects in a delayed double-step saccade task. *Cerebral Cortex*, 17(10):2364.

Melloni, L., Molina, C., Pena, M., Torres, D., Singer, W., and Rodriguez, E. (2007). Synchronization of neural activity across cortical areas correlates with conscious perception. *The Journal of Neuroscience*, 27(11):2858.

Menon, V., Freeman, W., Cutillo, B., Desmond, J., Ward, M., Bressler, S., Laxer, K., Barbaro, N., and Gevins, A. (1996). Spatio-temporal correlations in human gamma band electrocorticograms. *Electroencephalography and clinical Neurophysiology*, 98(2):89–102.

Michel, C., Murray, M., Lantz, G., Gonzalez, S., Spinelli, L., and Grave de Peralta, R. (2004). EEG source imaging. *Clinical Neurophysiology*, 115(10):2195–2222.

Miikkulainen, R. (1993). *Subsymbolic natural language processing: An integrated model of scripts, lexicon, and memory*. The MIT Press.

Minderhoud, J. (1971). An anatomical study of the efferent connections of the thalamic reticular nucleus. *Experimental Brain Research*, 12(4):435–446.

Mitra, P. and Pesaran, B. (1999). Analysis of dynamic brain imaging data. *Biophysical journal*, 76(2):691–708.

Mitrofanis, J. and Guillery, R. (1993). New views of the thalamic reticular nucleus in the adult and the developing brain. *Trends in neurosciences*, 16(6):240–245.

Moll, M. and Miikkulainen, R. (1997). Convergence-zone episodic memory: Analysis and simulations. *Neural Networks*, 10(6):1017–1036.

Montero, V. and Scott, G. (1981). Synaptic terminals in the dorsal lateral geniculate nucleus from neurons of the thalamic reticular nucleus: a light and electron microscope autoradiographic study. *Neuroscience*, 6(12):2561–2577.

Muller, K., Vigario, R., Meinecke, F., and Ziehe, A. (2004). Blind source separation techniques for decomposing event-related brain signals. *International Journal of Bifurcation and Chaos*, 14(2):773–791.

Murthy, V. and Fetz, E. (1992). Coherent 25-to 35-hz oscillations in the sensorimotor cortex of awake behaving monkeys. *Proceedings of the National Academy of Sciences of the United States of America*, 89(12):5670.

Näpflin, M., Wildi, M., and Sarnthein, J. (2007). Test-retest reliability of resting eeg spectra validates a statistical signature of persons. *Clinical Neurophysiology*, 118(11):2519–2524.

Neilson, M. and Neilson, P. (1987). Speech motor control and stuttering: A computational model of adaptive sensory-motor processing. *Speech communication*, 6(4):325–333.

Newberg, A., Alavi, A., Baime, M., Pourdehnad, M., Santanna, J., and d'Aquili, E. (2001). The measurement of regional cerebral blood flow during the complex cognitive task of meditation: a preliminary SPECT study. *Psychiatry Research: Neuroimaging*, 106(2):113–122.

Newberg, A. and Iversen, J. (2003). The neural basis of the complex mental task of meditation: neurotransmitter and neurochemical considerations. *Medical Hypotheses*, 61(2):282–291.

Niedermeyer, E. (1993). Sleep and eeg. *Electroencephalography: Basic Principles, Clinical Applications, and Related Fields, 3rd edn Williams & Wilkins: Baltimore, MD*, pages 153–166.

Nilsson, L. and Markowitsch, H. (1999). *Cognitive neuroscience of memory*. Hogrefe and Huber.

Nunez, P. (1974a). The brain wave equation: A model for the EEG. *Mathematical Biosciences*, 21:279–297.

Nunez, P. (1974b). Wavelike properties of the alpha rhythm. *IEEE Transactions on Biomedical Engineering*, pages 473–482.

Nunez, P. and Pilgreen, K. (1991). The spline-Laplacian in clinical neurophysiology: a method to improve EEG spatial resolution. *Journal of Clinical Neurophysiology*, 8(4):397.

Nunez, P. and Srinivasan, R. (2006). *Electric fields of the brain: the neurophysics of EEG*. Oxford University Press, USA.

Nunez, P. and Srinivasan, R. (2010). Scale and frequency chauvinism in brain dynamics: too much emphasis on gamma band oscillations. *Brain Structure and Function*, pages 1–5.

Nunez, P., Srinivasan, R., Westdorp, A., Wijesinghe, R., Tucker, D., Silberstein, R., and Cadusch, P. (1997). EEG coherency I: statistics, reference electrode, volume conduction, Laplacians, cortical imaging, and interpretation at multiple scales. *Electroencephalography and clinical Neurophysiology*, 103(5):499–515.

Nuwer, M., Comi, G., Emerson, R., Fuglsang-Frederiksen, A., Guerit, J., Hinrichs, H., Ikeda, A., Luccas, F., and Rappelsberger, P. (1999a). Ifcn standards for digital recording of clinical eeg. *Recommendations for the practice of clinical neurophysiology: guidelines of the International Federation of Clinical Neurophysiology*, page 11.

Nuwer, M., Lehmann, D., da Silva, F., and Vibert, J. (1999b). IFCN guidelines for topographic and frequency analysis of EEGs and EPs. *Recommendations for the Practice of Clinical Neurophysiology: Guidelines of the International Federation of Clinical Neurophysiology*, page 15.

O'Connor, S. and Robinson, P. (2004). Spatially uniform and nonuniform analyses of electroencephalographic dynamics, with application to the topography of the alpha rhythm. *Physical Review E*, 70(1):11911.

O'Connor, S. and Robinson, P. (2005). Analysis of the electroencephalographic activity associated with thalamic tumors. *Journal of theoretical biology*, 233(2):271–286.

Oertel, W., Graybiel, A., Mugnaini, E., Elde, R., Schmechel, D., and Kopin, I. (1983). Coexistence of glutamic acid decarboxylase-and somatostatin-like immunoreactivity in neurons of the feline nucleus reticularis thalami. *The Journal of Neuroscience*, 3(6):1322.

Ohara, P., Lieberman, A., Hunt, S., and Wu, J. (1983). Neural elements containing glutamic acid decarboxylase (gad) in the dorsal lateral geniculate nucleus of the rat; immunohistochemical studies by light and electron microscopy. *Neuroscience*, 8(2):189–211.

Olendzki, A. (2011). The construction of mindfulness. *Contemporary Buddhism*, 12(01):55–70.

Onton, J., Delorme, A., and Makeig, S. (2005). Frontal midline eeg dynamics during working memory. *Neuroimage*, 27(2):341–356.

Oostenveld, R., Fries, P., Maris, E., and Schoffelen, J. (2011). Fieldtrip: open source software for advanced analysis of meg, eeg, and invasive electrophysiological data. *Computational Intelligence and Neuroscience*, 2011:1.

O'Reilly, R., Braver, T., and Cohen, J. (1999). A biologically based computational model of working memory. *Models of working memory: Mechanisms of active maintenance and executive control*, pages 375–411.

O'Reilly, R., Herd, S., and Pauli, W. (2010). Computational models of cognitive control. *Current Opinion in Neurobiology*, 20(2):257–261.

O'Reilly, R. and Munakata, Y. (2000). *Computational explorations in cognitive neuroscience: Understanding the mind by simulating the brain*. The MIT Press.

Orme-Johnson, D. (2006). Evidence that the transcendental meditation program prevents or decreases diseases of the nervous system and is specifically beneficial for epilepsy. *Medical hypotheses*, 67(2):240–246.

Osaka, M. (1984). Peak alpha frequency of eeg during a mental task: Task difficulty and hemispheric differences. *Psychophysiology*, 21(1):101–105.

Osaka, M., Osaka, N., Koyama, S., Okusa, T., and Kakigi, R. (1999). Individual differences in working memory and the peak alpha frequency shift on magnetoencephalography1. *Cognitive brain research*, 8(3):365–368.

Pagano, R., Warrenburg, S., Davidson, R., Schwartz, G., and Shaphiro, D. (1983). Meditation: In search of a unique effect. *Consciousness and self-regulation*, 3:152–210.

Pardo, J., Fox, P., and Raichle, M. (1991). Localization of a human system for sustained attention by positron emission tomography. *Nature*, 349(6304):61–64.

Pearl, J. (2000). Causality. *Causality, by Judea Pearl, pp. 400. ISBN 0521773628. Cambridge, UK: Cambridge University Press, March 2000.*, 1.

Perrin, F., Pernier, J., Bertrand, O., and Echallier, J. (1989). Spherical splines for scalp potential and current density mapping. *Electroencephalography and clinical Neurophysiology*, 72(2):184–187.

Pfurtscheller, G., Stancak, A., et al. (1996). Event-related synchronization (ers) in the alpha band–an electrophysiological correlate of cortical idling: a review. *International Journal of Psychophysiology*, 24(1-2):39–46.

Pinault, D. (2011). Dysfunctional thalamus-related networks in schizophrenia. *Schizophrenia Bulletin*, 37(2):238.

Pivik, R., Broughton, R., Coppola, R., Davidson, R., Fox, N., and Nuwer, M. (1993). Guidelines for the recording and quantitative analysis of electroencephalographic activity in research contexts. *Psychophysiology*, 30:547–547.

Pizzagalli, D. (2007). Electroencephalography and high-density electrophysiological source localization. *Handbook of psychophysiology*, 3:56–84.

Polich, J. (1997). Eeg and erp assessment of normal aging. *Electroencephalography and Clinical Neurophysiology/Evoked Potentials Section*, 104(3):244–256.

Portas, C., Rees, G., Howseman, A., Josephs, O., Turner, R., and Frith, C. (1998). A specific role for the thalamus in mediating the interaction of attention and arousal in humans. *The Journal of Neuroscience*, 18(21):8979.

Posner, M. (1989). The attention system of the human brain. Technical report, DTIC Document.

Posner, M. (2004). *Cognitive neuroscience of attention*. The Guilford Press.

Posner, M. and Cohen, Y. (1984). Components of visual orienting. *Attention and performance X: Control of language processes*, 32:531–556.

Posner, M. and Dehaene, S. (1994). Attentional networks. *Trends in neurosciences*, 17(2):75–79.

Posner, M. and Fan, J. (2005). Attention as an organ system. *Topics in integrative neuroscience: From cells to cognition*, pages 1–34.

Posner, M. and Petersen, S. (1990). The attention system of the human brain. *Annual review of neuroscience*, 13(1):25–42.

Posner, M. and Rothbart, M. (2007). Research on attention networks as a model for the integration of psychological science. *Annu. Rev. Psychol.*, 58:1–23.

Posthuma, D., Neale, M., Boomsma, D., and De Geus, E. (2001). Are smarter brains running faster? heritability of alpha peak frequency, iq, and their interrelation. *Behavior Genetics*, 31(6):567–579.

Raffone, A., Manna, A., Perrucci, G., Ferretti, A., Del Gratta, C., Belardinelli, M., and Romani, G. (2007). Neural correlates of mindfulness and concentration in buddhist monks: A fmri study. In *Noninvasive Functional Source Imaging of the Brain and Heart and the International Conference on Functional Biomedical Imaging, 2007. NFSI-ICFBI 2007. Joint Meeting of the 6th International Symposium on*, pages 242–244. IEEE.

Rennie, C. (2006). *Modeling the large-scale electrical activity of the brain*. PhD thesis, University of Sydney. Physics.

Rennie, C., Robinson, P., and Wright, J. (1999). Effects of local feedback on dispersion of electrical waves in the cerebral cortex. *Physical Review E*, 59(3):3320–3329.

Rennie, C., Robinson, P., and Wright, J. (2002). Unified neurophysical model of EEG spectra and evoked potentials. *Biological Cybernetics*, 86(6):457–471.

Ritskes, R., Ritskes-Hoitinga, A., and Stødkilde-Jørgensen, A. (2004). Mri scanning during zen meditation: the picture of enlightenment? *The relevance of the wisdom traditions in contemporary society: the challenge to psychology*, page 195.

Ritter, P., Moosmann, M., and Villringer, A. (2009). Rolandic alpha and beta EEG rhythms' strengths are inversely related to fMRI-BOLD signal in primary somatosensory and motor cortex. *Hum Brain Mapp*, 30:1168–1187.

Roberts, J. and Robinson, P. (2008). Modeling absence seizure dynamics: Implications for basic mechanisms and measurement of thalamocortical and corticothalamic latencies. *Journal of theoretical biology*, 253(1):189–201.

Robertson, I., Manly, T., Andrade, J., Baddeley, B., and Yiend, J. (1997). Oops!': performance correlates of everyday attentional failures in traumatic brain injured and normal subjects. *Neuropsychologia*, 35(6):747–758.

Robinson, P. (2003). Neurophysical theory of coherence and correlations of electroencephalographic and electrocorticographic signals. *Journal of theoretical biology*, 222(2):163–175.

Robinson, P., Rennie, C., and Rowe, D. (2002). Dynamics of large-scale brain activity in normal arousal states and epileptic seizures. *Physical Review E*, 65(4):41924.

Robinson, P., Rennie, C., Rowe, D., and O'Connor, S. (2004). Estimation of multiscale neurophysiologic parameters by electroencephalographic means. *Human brain mapping*, 23(1):53–72.

Robinson, P., Rennie, C., Rowe, D., O'Connor, S., Wright, J., Gordon, E., and Whitehouse, R. (2003). Neurophysical modeling of brain dynamics. *Neuropsychopharmacology*, 28(1):74.

Robinson, P., Rennie, C., and Wright, J. (1997). Propagation and stability of waves of electrical activity in the cerebral cortex. *Physical Review E*, 56(1):826–840.

Robinson, P., Rennie, C., Wright, J., Bahramali, H., Gordon, E., and Rowe, D. (2001). Prediction of electroencephalographic spectra from neurophysiology. *Physical Review E*, 63(2):21903.

Robinson, P., Rennie, C., Wright, J., and Bourke, P. (1998). Steady states and global dynamics of electrical activity in the cerebral cortex. *Physical Review E*, 58(3):3557–3571.

Rowe, D., Robinson, P., and Gordon, E. (2005a). Stimulant drug action in attention deficit hyperactivity disorder (ADHD): inference of neurophysiological mechanisms via quantitative modelling. *Clinical Neurophysiology*, 116(2):324–335.

Rowe, D., Robinson, P., Lazzaro, I., Powles, R., Gordon, E., and Williams, L. (2005b). Biophysical modeling of tonic cortical electrical activity in attention deficit hyperactivity disorder. *International journal of neuroscience*, 115(9):1273–1305.

Rowe, D., Robinson, P., and Rennie, C. (2004a). Estimation of neurophysiological parameters from the waking EEG using a biophysical model of brain dynamics. *Journal of theoretical biology*, 231(3):413–433.

Rowe, D., Robinson, P., Rennie, C., Harris, A., Felmingham, K., Lazzaro, I., and Gordon, E. (2004b). Neurophysiologically-based mean-field modelling of tonic cortical activity in post-traumatic stress disorder (ptsd), schizophrenia, first episode schizophrenia and attention deficit hyperactivity disorder (adhd). *Journal of integrative neuroscience*, 3(4):453.

Saggar, M., Markman, A., Maddox, W., and Miikkulainen, R. (2007). A computational model of the motivation-learning interface. In *The 29th Annual Conference of the Cognitive Science Society, Nashville, TN, USA*.

Saggar, M., Miikkulainen, R., and Schnyer, D. (2010). Behavioral, neuroimaging, and computational evidence for perceptual caching in repetition priming. *Brain research*, 1315:75–91.

Sahdra, B., MacLean, K., Ferrer, E., Shaver, P., Rosenberg, E., Jacobs, T., Zanesco, A., King, B., Aichele, S., Bridwell, D., et al. (2011). Enhanced response inhibition during intensive meditation training predicts improvements in self-reported adaptive socioemotional functioning. *Emotion*, 11(2):299.

Samar, V., Bopardikar, A., Rao, R., and Swartz, K. (1999). Wavelet analysis of neuroelectric waveforms: a conceptual tutorial. *Brain and language*, 66(1):7–60.

Saron, C. D., Rivera, S. M., Beransky, M., L., M., Colombi, C., Horton, D., Riggins, T., L., D., Kenet, T., Rogers, S. J., and Saggar, M. (2008). Loudness dependency of the auditory event-related potential in autism spectrum disorders: Further investigation of initial subphenotypes. Major data presentation to consortium researchers, Autism Phenome Project.

Sauseng, P., Hoppe, J., Klimesch, W., Gerloff, C., and Hummel, F. (2007). Dissociation of sustained attention from central executive functions: local activity and interregional connectivity in the theta range. *European Journal of Neuroscience*, 25(2):587–593.

Sauseng, P., Klimesch, W., Gerloff, C., and Hummel, F. (2009). Spontaneous locally restricted eeg alpha activity determines cortical excitability in the motor cortex. *Neuropsychologia*, 47(1):284–288.

Sawada, H., Winter, S., Mukai, R., Araki, S., and Makino, S. (2004). Estimating the number of sources for frequency-domain blind source separation. *Independent Component Analysis and Blind Signal Separation*, pages 610–617.

Schacter, D. (1977). Eeg theta waves and psychological phenomena: A review and analysis. *Biological Psychology*, 5(1):47–82.

Scheeringa, R., Fries, P., Petersson, K., Oostenveld, R., Grothe, I., Norris, D., Hagoort, P., and Bastiaansen, M. (2011). Neuronal dynamics underlying high-and low-frequency eeg oscillations contribute independently to the human bold signal. *Neuron*, 69(3):572–583.

Scheibel, M. and Scheibel, A. (1966). The organization of the nucleus reticularis thalami: a golgi study. *Brain Research*, 1(1):43–62.

Schwartzman, D. and Kranczioch, C. (2010). In the blink of an eye. the contribution of microsaccadic activity to the induced gamma band response. *International Journal of Psychophysiology*.

Shamatha-Project (2007). The Shamatha Project: A longitudinal, randomized waitlist control study of cognitive, emotional, and neural effects of intensive meditation training. *http://mindbrain.ucdavis.edu/labs/Saron/shamatha-project/*.

Sherman, S. (1996). Dual response modes in lateral geniculate neurons: mechanisms and functions. *Vis Neurosci*, 13(2):205–213.

Sherman, S. and Guillery, R. (2002). The role of the thalamus in the flow of information to the cortex. *Philosophical Transactions of the Royal Society of London. Series B: Biological Sciences*, 357(1428):1695.

Sherman, S. and Guillery, R. (2006). *Exploring the thalamus and its role in cortical function*. MIT press Cambridge, MA.

Shiffrin, R. (2010). Perspectives on modeling in cognitive science. *Topics in Cognitive Science*.

Short, E., Kose, S., Mu, Q., Borckardt, J., Newberg, A., George, M., and Kozel, F. (2010). Regional brain activation during meditation shows time and practice effects: an exploratory fmri study. *Evidence-Based Complementary and Alternative Medicine*, 7(1):121–127.

Shwedyk, E., Balasubramanian, R., and Scott, R. (1977). A nonstationary model for the electromyogram. *IEEE Transactions on Biomedical Engineering*, pages 417–424.

Singer, W. (1993). Synchronization of cortical activity and its putative role in information processing and learning. *Annual Review of Physiology*, 55(1):349–374.

Singer, W. (2001). Consciousness and the binding problem. *Annals of the New York Academy of Sciences*, 929(1):123–146.

Singh, R. (1999). *Empowering your soul through meditation*. Element.

Slagter, H., Davidson, R., and Lutz, A. (2011). Mental training as a tool in the neuroscientific study of brain and cognitive plasticity. *Frontiers in Human Neuroscience*, 5.

Slagter, H., Lutz, A., Greischar, L., Francis, A., Nieuwenhuis, S., Davis, J., and Davidson, R. (2007). Mental training affects distribution of limited brain resources. *PLoS Biol*, 5(6):e138.

Speckmann, E. and Altrup, U. (1993). Generation of cortical field potentials. *Basic Mechanisms of the EEG*, pages 29–40.

Steinmetz, M., Motter, B., Duffy, C., and Mountcastle, V. (1987). Functional properties of parietal visual neurons: radial organization of directionalities within the visual field. *The Journal of neuroscience*, 7(1):177.

Steriade, M. (2000). Corticothalamic resonance, states of vigilance and mentation. *Neuroscience*, 101(2):243–276.

Steriade, M. and Amzica, F. (1998). Coalescence of sleep rhythms and their chronology in corticothalamic networks. *Sleep research online: SRO*, 1(1):1.

Steriade, M., Domich, L., and Oakson, G. (1986). Reticularis thalami neurons revisited: activity changes during shifts in states of vigilance. *The Journal of neuroscience*, 6(1):68.

Steriade, M., McCormick, D., and Sejnowski, T. (1993). Thalamocortical oscillations in the sleeping and aroused brain. *Science*, 262(5134):679.

Stigsby, B., Rodenberg, J., and Moth, H. (1981). Electroencephalographic findings during mantra mediation (transcendental meditation). a controlled, quantitative study of experienced meditators. *Electroencephalography and Clinical Neurophysiology*, 51(4):434–442.

Stroop, J. R. (1935). Studies of interference in serial verbal reactions. *Journal of Experimental Psychology*, 18:643–662.

Tabachnick, B., Fidell, L., and Osterlind, S. (2001). *Using multivariate statistics*. Allyn and Bacon Boston.

Tallon, C., Bertrand, O., Bouchet, P., and Pernier, J. (1995). Gamma-range activity evoked by coherent visual stimuli in humans. *European Journal of Neuroscience*, 7(6):1285–1291.

Tallon-Baudry, C. (2009). The roles of gamma-band oscillatory synchrony in human visual cognition. *Frontiers in bioscience: a journal and virtual library*, 14:321.

Tamura, Y., Hoshiyama, M., Nakata, H., Hiroe, N., Inui, K., Kaneoke, Y., Inoue, K., and Kakigi, R. (2005). Functional relationship between human rolandic oscillations and motor cortical excitability: an meg study. *European Journal of Neuroscience*, 21(9):2555–2562.

Tanaka, H., Hayashi, M., and Hori, T. (1997). Topographical characteristics and principal component structure of the hypnagogic eeg. *Sleep*, 20(7):523.

Taneli, B. and Krahne, W. (1987). Eeg changes of transcendental meditation practitioners. *Advances in biological psychiatry*.

Tang, A., Liu, J., and Sutherland, M. (2005). Recovery of correlated neuronal sources from EEG: The good and bad ways of using SOBI. *NeuroImage*, 28(2):507–519.

Thakor, N. and Tong, S. (2004). Advances in quantitative electroencephalogram analysis methods. *Annu. Rev. Biomed. Eng.*, 6:453–495.

Timofeev, I., Contreras, D., and Steriade, M. (1996). Synaptic responsiveness of cortical and thalamic neurones during various phases of slow sleep oscillation in cat. *Journal of Physiology*, 494(1):265–278.

Traub, R., Jefferys, J., and Whittington, M. (1997). Simulation of gamma rhythms in networks of interneurons and pyramidal cells. *Journal of Computational Neuroscience*, 4(2):141–150.

Travis, F. (1991). Eyes open and tm eeg patterns after one and eight years of tm practice. *Psychophysiology*, 28(3a):S58.

Travis, F., Haaga, D., Hagelin, J., Tanner, M., Arenander, A., Nidich, S., Gaylord-King, C., Grosswald, S., Rainforth, M., and Schneider, R. (2010). A self-referential default brain state: patterns of coherence, power, and eloreta sources during eyes-closed rest and transcendental meditation practice. *Cognitive Processing*, 11(1):21–30.

Travis, F. and Shear, J. (2010). Focused attention, open monitoring and automatic self-transcending: Categories to organize meditations from vedic, buddhist and chinese traditions. *Consciousness and cognition*, 19(4):1110–1118.

Travis, F. and Wallace, R. (1999). Autonomic and eeg patterns during eyes-closed rest and transcendental meditation (tm) practice: the basis for a neural model of tm practice. *Consciousness and cognition*, 8(3):302–318.

Tsotsos, J. (1995). Toward a computational model of visual attention.

Ulfig, N., Nickel, J., and Bohl, J. (1998). Transient features of the thalamic reticular nucleus in the human foetal brain. *European Journal of Neuroscience*, 10(12):3773–3784.

Vaidya, C., Bunge, S., Dudukovic, N., Zalecki, C., Elliott, G., and Gabrieli, J. (2005). Altered neural substrates of cognitive control in childhood adhd: evidence from functional magnetic resonance imaging. *American Journal of Psychiatry*, 162(9):1605.

van Albada, S., Kerr, C., Chiang, A., Rennie, C., and Robinson, P. (2010). Neurophysiological changes with age probed by inverse modeling of eeg spectra. *Clinical Neurophysiology*, 121(1):21–38.

Van Boxtel, A. (2001). Optimal signal bandwidth for the recording of surface EMG activity of facial, jaw, oral, and neck muscles. *Psychophysiology*, 38(01):22–34.

Van Boxtel, A., Goudswaard, P., Van der Molen, G., and Van Den Bosch, W. (1983). Changes in electromyogram power spectra of facial and jaw-elevator muscles during fatigue. *Journal of Applied Physiology*, 54(1):51.

van Ede, F., de Lange, F., Jensen, O., and Maris, E. (2011). Orienting attention to an upcoming tactile event involves a spatially and temporally specific modulation of sensorimotor alpha-and beta-band oscillations. *The Journal of Neuroscience*, 31(6):2016.

Varela, F. and Shear, J. (1999). First-person methodologies: What, why, how. *The view from within: First-person approaches to the study of consciousness*, pages 2–3.

Verbruggen, F. and Logan, G. (2008). Response inhibition in the stop-signal paradigm. *Trends in Cognitive Sciences*, 12(11):418–424.

Villringer, A., Planck, J., Hock, C., Schleinkofer, L., and Dirnagl, U. (1993). Near infrared spectroscopy (nirs): a new tool to study hemodynamic changes during activation of brain function in human adults. *Neuroscience Letters*, 154(1-2):101–104.

Vinogradova, O. (1995). Expression, control, and probable functional significance of the neuronal theta-rhythm. *Progress in Neurobiology*, 45(6):523–583.

Vogt, B., Finch, D., and Olson, C. (1992). Functional heterogeneity in cingulate cortex: the anterior executive and posterior evaluative regions. *Cerebral cortex*, 2(6):435.

Wallace, B. (1999). The Buddhist tradition of Samatha: Methods for refining and examining consciousness. *Journal of Consciousness Studies, 6*, 2(3):175–187.

Wallace, B. (2006). *The attention revolution: Unlocking the power of the focused mind*. Wisdom Pubns.

Wallace, B. and Houshmand, Z. (2004). *The four immeasurables: Cultivating a boundless heart*. Snow Lion Publications.

Wallace, R. (1970). Physiological effects of transcendental meditation. *Science*, 167(3926):1751.

Whitham, E., Pope, K., Fitzgibbon, S., Lewis, T., Clark, C., Loveless, S., Broberg, M., Wallace, A., DeLosAngeles, D., Lillie, P., et al. (2007). Scalp electrical recording during paralysis: quantitative evidence that eeg frequencies above 20 hz are contaminated by emg. *Clinical neurophysiology*, 118(8):1877–1888.

Wilson, H. and Cowan, J. (1972). Excitatory and inhibitory interactions in localized populations of model neurons. *Biophysical Journal*, 12(1):1–24.

Wilson, H. and Cowan, J. (1973). A mathematical theory of the functional dynamics of cortical and thalamic nervous tissue. *Biological Cybernetics*, 13(2):55–80.

Wilson, M. and Bower, J. (1992). Cortical oscillations and temporal interactions in a computer simulation of piriform cortex. *Journal of Neurophysiology*, 67(4):981.

Winter, W., Nunez, P., Ding, J., and Srinivasan, R. (2007). Comparison of the effect of volume conduction on eeg coherence with the effect of field spread on meg coherence. *Statistics in medicine*, 26(21):3946–3957.

Wright, J., Kydd, R., and Sergejew, A. (1990). Autoregression models of eeg. *Biological cybernetics*, 62(3):201–210.

Yuan, H., Liu, T., Szarkowski, R., Rios, C., Ashe, J., and He, B. (2010). Negative covariation between task-related responses in alpha/beta-band activity and bold in human sensorimotor cortex: an eeg and fmri study of motor imagery and movements. *Neuroimage*, 49(3):2596–2606.

Yuval-Greenberg, S., Tomer, O., Keren, A., Nelken, I., and Deouell, L. (2008). Transient induced gamma-band response in eeg as a manifestation of miniature saccades. *Neuron*, 58(3):429–441.

Zeigler, B., Praehofer, H., and Kim, T. (2000). *Theory of modeling and simulation*, volume 100. Academic press.

Zhang, J. et al. (1988). Eeg findings during special psychical state (qi gong state) by means of compressed spectral array and topographic mapping. *Computers in Biology and Medicine*, 18(6):455–463.

Ziehe, A. and Muller, K. (1998). TDSEP–an efficient algorithm for blind separation using time structure. In *Proc. Int. Conf. on Artificial Neural Networks (ICANN'98)*, pages 675–680.

Zikopoulos, B. and Barbas, H. (2007). Circuits for multisensory integration and attentional modulation through the prefrontal cortex and the thalamic reticular nucleus in primates. *Reviews in the Neurosciences*, 18(6):417.

Vita

Manish Saggar attended the Indian Institute of Information Technology (Allahabad, India) and graduated in 2005 with B.Tech. (Honors), before enrolling in the graduate school at the University of Texas at Austin.

Permanent Address: Department of Computer Science,
1 University Station, D9500,
Austin, Texas 78712 USA

This dissertation was typeset with LaTeX 2_ε[1] by the author.

[1] LaTeX 2_ε is an extension of LaTeX. LaTeX is a collection of macros for TeX. TeX is a trademark of the American Mathematical Society. The macros used in formatting this dissertation were written by Dinesh Das, Department of Computer Sciences, The University of Texas at Austin, and extended by Bert Kay and James A. Bednar.